Sensitivity Analysis of Variable-Density Groundwater Models

Case study of the Braakman South region, Zeeland, The Netherlands

ALI AHMED ABDALLAH OBEID

MSc Thesis Identifier: WSE-HWR.20-13

23 April 2020

Sensitivity Analysis of Variable-Density Groundwater Models

Case study of the Braakman South region, Zeeland, The Netherlands

Master of Science Thesis

by

ALI AHMED ABDALLAH OBEID

Supervisor

Prof. Michael McClain

Mentors

Dr. Yangxiao Zhou

Examination Committee
Prof. Michael McClain
Dr. Gualbert Oude Essink
Dr. Yangxiao Zhou

This research is done for the partial fulfilment of requirements for the Master of Science degree at the
IHE Delft Institute for Water Education, Delft, the Netherlands.

Delft

23/04/2020

Although the author and IHE Delft Institute for Water Education have made every effort to ensure that the information in this thesis was correct at press time, the author and IHE Delft do not assume and hereby disclaim any liability to any party for any loss, damage, or disruption caused by errors or omissions, whether such errors or omissions result from negligence, accident, or any other cause.

Abstract

Groundwater represents an important source of water supply especially in the coastal areas where the population is denser. The shortage of freshwater supply during the summer period affects the agriculture and the industrial sections in the study area. Therefore, this study aims to evaluate the existing 3D model and assess the potential for aquifer storage and recovery system in Braakman South Region, Netherlands. To achieve that the effect of model discretization, numerical solutions and model settings on the accuracy of the results need to be examined with the help of benchmarks cases to come up with a reliable model to be used as an assessment tool. Then with this tool, the effects on the aquifer from recharge and extraction processes will be assessed.

Freshwater Lens, Henry case and Saltwater Pocket benchmarks were examined for the effect on the grid sizes by varying the cell size and the layer thickness. After that, a reference model from each case was simulated with all the available solvers in SEAWAT model. In addition to that, the effect of the courant number, convergence criteria, the solvers setting for the advection packages and the dispersivity length were tested as well on that reference case. The results were compared to the available analytical solutions taking into consideration the computational time and the accuracy of the obtained results. The case study model was studied for the effect of the cell size by changing the cell sizes and the layer thickness. Then the effects of solvers and important parameters gained from the benchmark's tests were assessed as well. A compromised model was used for the assessment of the aquifer recharge system by doubling the recharge during the winter period under the areas of creek ridges and then extracting half and three-quarters of what being added during the summer period.

The model discretization has a significant influence on the size of the numerical errors associated with the numerical schemes in the transport models, with finer grids I obtained accurate results but at the same time longer computational time, therefore, I always need to compromise depending on the intended purpose of the model. The length of the transport step in case of using a relatively coarser model needs to be adjusted manually. Each of the solvers gave different results under different situations, therefore for each case I need to test all the solvers to see which one is suitable to be used as well as the solver's settings, taking into consideration the groundwater characteristic.

In the aquifer storage and recovery system, doubling the recharge under the creek ridges area led to an increase in the groundwater table, which in turn resulted in growth in the thickness of

ii

the freshwater lens under that area. By extracting half of the water added to the system, the water budget influence as the outflow to the rivers and drains reduced to balance the new extraction. This reduction has led to minimization in the chloride movement under the rivers. However, the extraction started saline water up-coning under the areas of creek ridge, but the effect is not big. While extracting three-quarter has more or less similar results but at a level more than the case of extracting half. Therefore, first, a replacement of the well package by the other package is needed to see the real influence. Furthermore, assessment of the influence of the drawdown on the area needs to be studied.

Acknowledgements

Table of Contents

List of Figures

ix

List of Tables

Chapter 1   Introduction

1.1 General overview

Groundwater represents a significant source of fresh water in various parts of the world as it supports economic development, water supply, and ecosystem stability. Groundwater has some general positive characteristics such as: relatively big storage, good quality, consistency of temperature, relatively cheap and water availability in dry periods (Jha, et al., 2006). But with the increase in population, economic growth and human intervention, more stress has been put on groundwater resources which can lead to both depletion in storages and deterioration in the water quality.

Appropriate groundwater resources management is essential for guaranteeing the sustainability of the water storage yield and the environment. For examples, regulating the pumping rates, artificial recharge of excess in surface water and measures to reduce the effect of saltwater intrusion or any other contaminants will lead to sustainable storage. However, as groundwater is an invisible source and slowly flows, we cannot immediately feel the responses upon other activities in the groundwater system. This makes it challenging to manage and to predict the effects of future stresses without modelling tools. Therefore, the need for better mathematical models for better water management is necessary to simulate all the processes and assess what will happen. With the technological revolution, groundwater modelling has become an important tool in the field of hydro(geo)logy and has been used for many purposes. For example, modelling groundwater system dynamics and flow patterns response of groundwater systems to hydro(geo)logical stresses. This can lead to better assessment tools for aquifer storage and recovery (ASR) systems (Zhou and Li, 2011).

When focusing on the coastal parts in the world, additional stresses are threating the fresh groundwater resources. Three-quarter of the world population lives nearby the coasts (Ramkumar, et al., 2019), leading to an increase in fresh groundwater exploitations. In addition, the presence of saline groundwater, climate change, and sea level rise will cause to saltwater intrusion more inland and threatening fresh groundwater resource. As such variable-density

groundwater flow and coupled salt transport modelling is required to simulate the dynamics of fresh, brackish and saline groundwater.

1.2 Study area

The Braakman South region falls within the municipality of Terneuzen, Province of Zeeland, The Netherlands. The area was a large tidal inlet in Zeeuws-Vlaanderen. It is formed as a result of large storm surges in the 14th and 15th centuries. Over the years, the land steadily extended and attracted people to settle. People also started to reclaim the land from the sea (Wikipedia, 2005). Figure 1-1 shows the study area extent. As can be seen, a part of the groundwater system falls within Belgium.
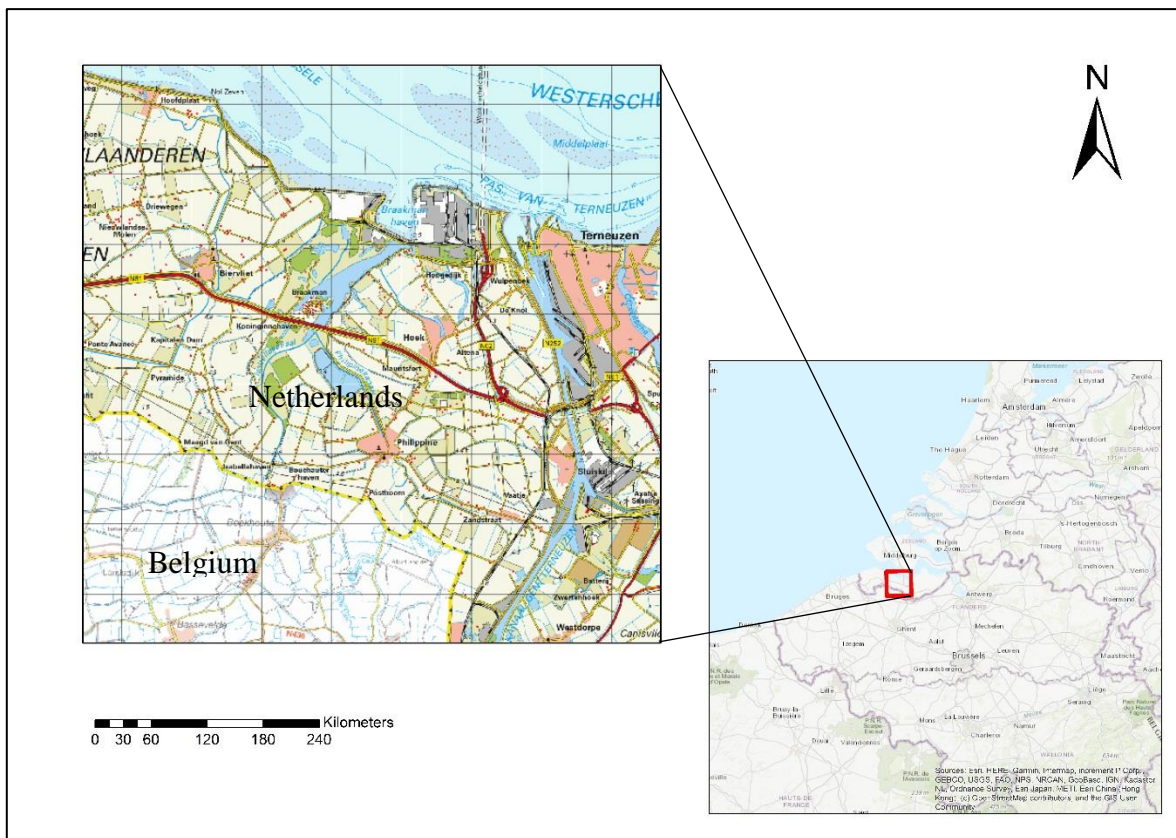
Figure 1-1: Study Area, part of the groundwater system falls within Belgium while the rest in the Netherlands

During the dry periods, farmers experience a shortage in the fresh water supply and in turn a reduction in their crop productivity (note that about 60% of the polder area is set for agriculture (Wikipedia, 2011)). DOW Chemicals (chemical company) is also experiencing the same water shortage issue though they want to reduce their water footprint. Therefore, a solution is proposed to solve this water problem by storing the excess surface water and rainwater to be used whenever there is shortage. Subsurface storage can be used to store this water due to the

2

huge vertical extent and relatively of good quality. This solution can equip the area against the challenges of accelerated urbanisation and increase in water demand, while on top, climate change effecting a sustainable fresh water supply in the future is also pressing.

Braakman in a low-lying coastal region, meaning not the entire groundwater system is composed of freshwater. Instead, there is also saline groundwater present in the groundwater system, which will complicate the use of fresh groundwater system. Also sea-level rise can influence the fresh water availability in the future. Some of the projects that have been implemented like GO-FRESH (Oude Essink et al, 2018) in Zeeland for the farmers to store the water through subsurface drainage and create a freshwater lens above the saline groundwater in order to pump it in the dry season (Zuidwestelijke Delta, 2018). But these projects are small scale projects and the application of these projects on a large scale is still not present.

1.2.1 Geological settings

The Province of Zeeland is not like other provinces along the Dutch shoreline where the Tertiary deposits are too deep to be affected by the recent coastal evolution. In Zeeland, the Tertiary deposits lie directly under the Holocene deposits or only a thin Pleistocene layer. It is also characterized by strong elevation gradient over short distances (Deltares, 2015). The older Pleistocene deposits (before Holocene) show a general dip in the direction of Northeast. The upper part of these deposits composes of periglacial and Aeolian sands plus silts of the Boxtel Formation. The lower part includes fine to medium grained marine sands and shell fragments, and fine to medium grained estuarine sands and clay layers (Stafleu, et al., 2014). They all have a low conductivity.

The shallow subsurface is formed as a result of the tidal canal, flat tide and lagoonal deposits in rotation with peat beds, coastal shoreline and dune deposits in the Holocene period (Stafleu, et al., 2014).

Between 10000 and 8000 BC, the deeper parts of the North Sea were flooded, but the area of Zeeland was not flooded. This rise in sea-level, however, induce the groundwater level to increase which lead to the growth of the peat bogs in the lower parts of Zeeland. At 4500 BC, there was a change in the tidal areas due to the blocking in the tidal inlets by the barrier beaches and low dunes. The area behind these barriers were sedimented for the next 500 years. Meanwhile, peat bogs were formed on the higher Pleistocene to the south and east. These processes were also influenced by the reduction in sea level-rise. About 2500 BC, the barrier was breached by storm surges, these processes led to the enhancement of peat drainage,

3

oxidation of peats and lowered surface elevation. At 1000 BC, the tidal channels were eroded deep into the already existing sediments (Deltares, 2019).

1.2.2 Hydrogeology

Figure 1-2 indicates the regional cross-section from Zeeuws-Vlaanderen to Zuid-Beveland: the clay forms confining layers and the sand forms confined aquifers.
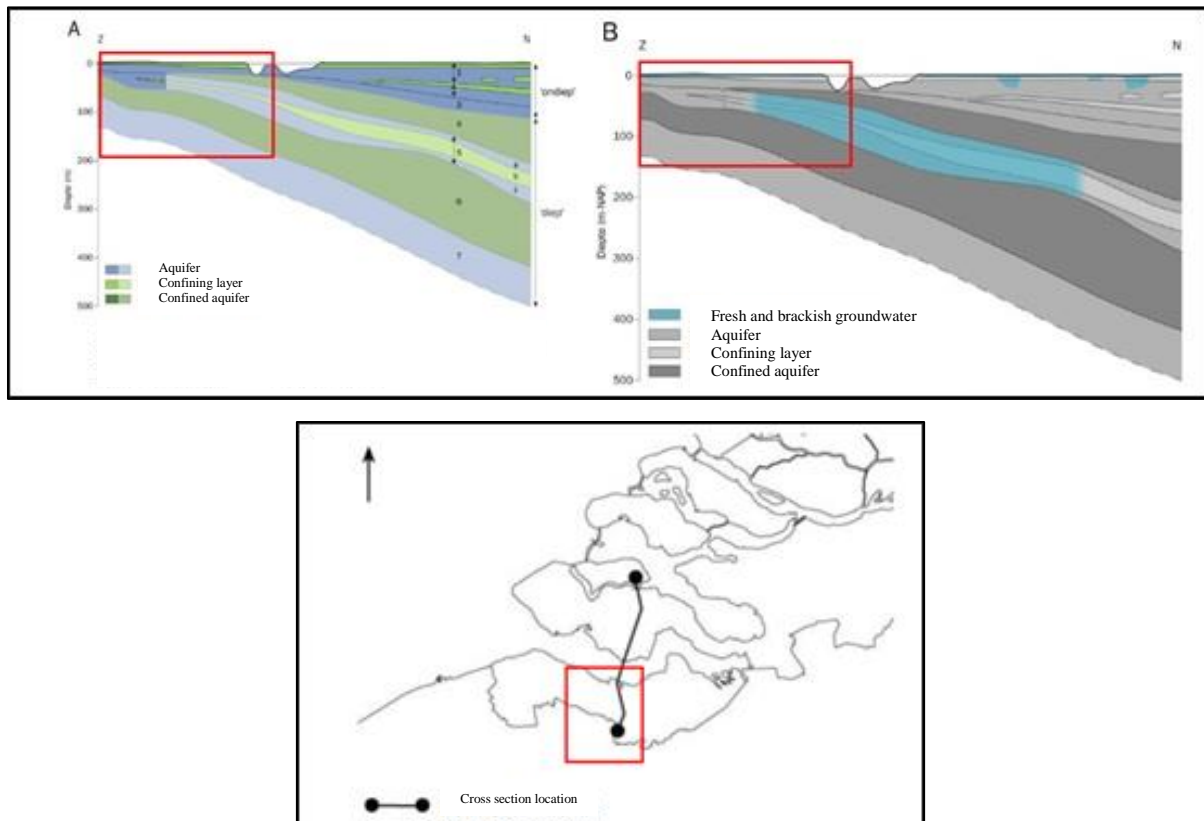
Figure 1-2: Regional cross-section from Zeeuws-Vlaanderen (left) to Zuid-Beveland (right), the red box is the study area. Source: (Deltares, 2019)

A regional flow of fresh, brackish and saline groundwater can be found within the confining aquifer from South to North. Shallower groundwater flow of fresh and saline groundwater is present on top of the dipping layers. Saline groundwater is deposited as a result of the Holocene transgressions. The geological formation along the time as well as the land reclamation have influenced the spreading of the fresh and saline groundwater distribution in Zeeland and became complex distribution.

Regard the distribution of fresh and saline groundwater, the FRESHEM Zeeland project (Delsman, et al., 2018) has been used, where a device throughout Zeeland has been carried using a helicopter flying on 40 meters above the ground sending electro-magnetic waves penetrating the soil every 4 meters. Using the reflected signals, the conductivity of the substrata

4

has been estimated and hence with the corrections for the subsurface formation the groundwater was identified either fresh, brackish or saline (Zuidwestelijke Delta, 2017). The results showed that almost everywhere the deep groundwater is brackish to saline, except in parts of Zeeuws-Vlaanderen and the so-called Kop van Schouwen. In the shallow aquifer system, fresh groundwater was found in top of saline groundwater. However, the thickness of the freshwater lens varies with elevation as indicated in Figure 1-3. In addition to that, from the results we can find sometimes fresh groundwater present below saline groundwater at different locations as a result of the geological formation of the strata (Deltares, 2019).
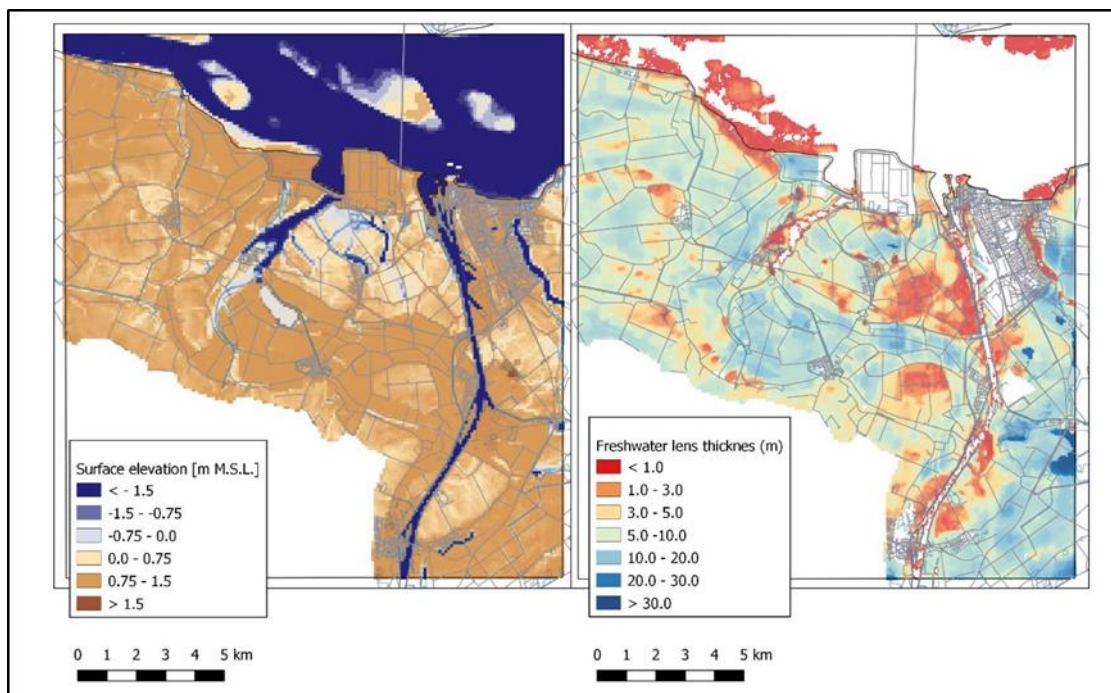
Figure 1-3: left. Elevation map; right thickness of the freshwater lens (source: (Deltares, 2019)).

1.3 Problem definition

The Braakman South region is suffering from a shortage in the freshwater supply during the dry period. Additional freshwater storages are needed to supply both industrial and agricultural demand. The proposed solution here is to store the excess in surface and rainfall water during the wet season into the groundwater system. The problem is that here, the groundwater system is not completely fresh. The system contains a complex distribution of fresh and saline groundwater. Modelling tools are needed to investigate where to store the water, keep the water fresh and extract it without big effects like mixing with saline groundwater. However, in these coastal areas, this spatial variation in fluid densies can considerably affect the groundwater flow patterns and require accurate models to represent the situation.

Computer codes like SEAWAT (Guo and Langevin, 2002) can be used to simulate fresh and saline groundwater dynamics in the groundwater system. These computer codes have different numerical approximations and many model parameters (dispersivity, particles number, etc). The effects of these numerical solutions, model parameters and discretisation on model performance is still not completely clear as every model representing a case-study, is different (Al-Maktoumi, et al., 2007, Goswami, et al., 2012, Graf and Degener, 2011) .Therefore, a sensitivity analysis for the above-mentioned factors must to be conducted to improve the model, and in turn, investigate what is the best ASR solution for reducing water shortage at the case study Braakman South.

1.4 Objectives

The overall objectives of this study are to evaluate the existing 3D model for variable-density groundwater flow and coupled salt transport and to assess the potential for groundwater storage and recovery system in the Braakman South region using complex modelling tools.

Specific objectives:

- Review the existing model setup for the variable-density groundwater flow and salt transport for the study area.
- Sensitivity analysis for three benchmarks for better understanding of the influence of the model discretization, solvers and other model settings.
- Sensitivity analysis for the case study to examine the influence of model discretization, solvers and other model settings to create a workable assessment modelling tool.
- Studying the growth of freshwater lens within the physical boundaries of the system.

1.5 Research questions

- What is the influence of model discretization on the accuracy of the results in the benchmarks cases and the case study model?
- Which solute transport model parameters and settings are more sensitive than others and how are they influencing the model results in both benchmarks models and case study model?

- Which numerical solution is suitable for the study area taking into consideration the model cell size and the solute transport step to obtain accurate model results in acceptable run times?
- How does the subsurface system respond to the processes of storing and recovering freshwater at different locations considering suitable ways of storing and extracting?

Chapter 2   Background Information

2.1 Application of groundwater models

The model is a simplified representation of reality. In groundwater, models can be conceptual, physical and mathematical (Anderson, et al., 2015). Conceptual models are simplified and summing up the hydrogeological process in terms of cross-section, text, tables, and diagrams. The physical model is an experimental work in laboratory involve water containers and columns with porous materials in which the flow and the head can be measured. The mathematical models are divided into data-driven models and process-based models. Data-driven models are simply using empirical and statistical equations to obtained variables based on measured ones. The process-based models are using the principles of physics to represent groundwater system, it can be either stochastic or deterministic. These physical models can be solved either analytically or numerically.

Anderson, et al. (2015) classified the modelling purposes into two main categories, the forecasting/hindcasting models and the interpretative models. The first type is used to predict what will happen in the future when we did a certain action or we did not do anything, but it can also be used to represent a past situation. It is named forecasting and not predicting due to the uncertainties accompanied with the results.

The interpretative models are the types used for engineering calculations to obtain specifically required variable like the drawdown.

2.2 SEAWAT

Guo and Bennett (1998) indicated what made them to develop SEAWAT as they wanted to produce a conventional tool for studying the groundwater flow of variant density by coupling two software packages, MODFLOW and MT3D. They modified MODFLOW to conserve fluid mass instead of fluid volume. They also included the density terms in the governing flow equations for simulating the flow, and hence the flow being calculated using the head difference and the density variation. Then the resulted flow is given to MT3D for solving the solute
8

transport equation. The calculated solute concentration is used for updating the fluid density, before passing it back to MODFLOW. From then, SEAWAT has been developed to meet the needs, along with development in MODFLOW and MT3D.

The new flow governing equation is based on the concept of equivalent freshwater head. The equivalent freshwater head is calculated from the measured head of the saline water and then based on the density difference the head is converted to freshwater head. This means the heads calculated from SEAWAT is not the actual level in the field and needs to be converted back based on the density difference. The equation adopted by SEAWAT (Guo and Langevin, 2002) for the flow can be seen below:

$$\frac{\partial}{\partial \alpha}\left(\rho K_{f\alpha}\left[\frac{\partial h_f}{\partial \alpha} + \frac{\rho - \rho_f}{\rho_f}\frac{\partial Z}{\partial \alpha}\right]\right) + \frac{\partial}{\partial \beta}\left(\rho K_{f\beta}\left[\frac{\partial h_f}{\partial \beta} + \frac{\rho - \rho_f}{\rho_f}\frac{\partial Z}{\partial \beta}\right]\right)$$
$$+ \frac{\partial}{\partial \gamma}\left(\rho K_{f\gamma}\left[\frac{\partial h_f}{\partial \gamma} + \frac{\rho - \rho_f}{\rho_f}\frac{\partial Z}{\partial \gamma}\right]\right) = \rho S_p g \rho_f \frac{\partial h_f}{\partial t} + \theta \frac{\partial \rho}{\partial C}\frac{\partial C}{\partial t} - \bar{\rho} q_s. \qquad \text{(Equation 2-1)}$$

Where, α, β, and γ are the directions, K_f is the freshwater hydraulic conductivity, ρ is the water density, h_f is the freshwater head, ρ_f is the freshwater density, Z is the elevation above the datum, g is the gravitational acceleration, S_p is the specific storage, t is the time, C is the solute concentration, θ is the porosity, $\bar{\rho}$ is the density of water entering from source or leaving through source, and q_s is the volumetric flow rate per volume representing source and sink,

For the solute transport equation, no changes have been carried on it. Therefore the same equation in MT3D (Zheng and Wang, 1999) was used in SEAWAT.

$$R\theta \frac{\partial C}{\partial t} = \frac{\partial}{\partial x_i}\left(\theta D_{ij}\frac{\partial C}{\partial x_j}\right) - \frac{\partial}{\partial x_i}(\theta v_i C) + q_s C_s - q'_s C - \lambda_1 \theta C - \lambda_2 P_b \bar{C} \qquad \text{(Equation 2-2)}$$

Where, θ is the porosity, R is the retardation factor, t is time, D is hydrodynamic dispersion coefficient tensor, C species concentration, v is liner water velocity, q_s is the volumetric flow rate per volume representing source and sink, C_s is the concentration of source and sink, λ_1 & λ_2 are the first and second order reaction rate, P_b is the bulk density of subsurface medium and $\bar{C}$ is the concentration of species sorbed by the subsurface.

As stated above, SEAWAT couples these two equations in synchronised time step. Which means that for the same time step both equations being solved. There are two ways of coupling the flow and the solute transport, implicit and explicit. In the implicit method the groundwater flow and solute transport equation are being calculated in an iterative way till the difference

9

between the densities is smaller than a specified value. In the explicit, the flow and transport equation just solved once. Another difference is that, using the implicit solution we can specify the length of the time step for the calculation but in the explicit the time step is calculated from stability criteria, for advection, dispersion and sink and source, before each step. In the current versions of SEAWAT only the Finite difference solution option can be used with implicit method. The general systematic way of solving the two-equation adopted by SEAWAT can be seen in Figure 2-1.
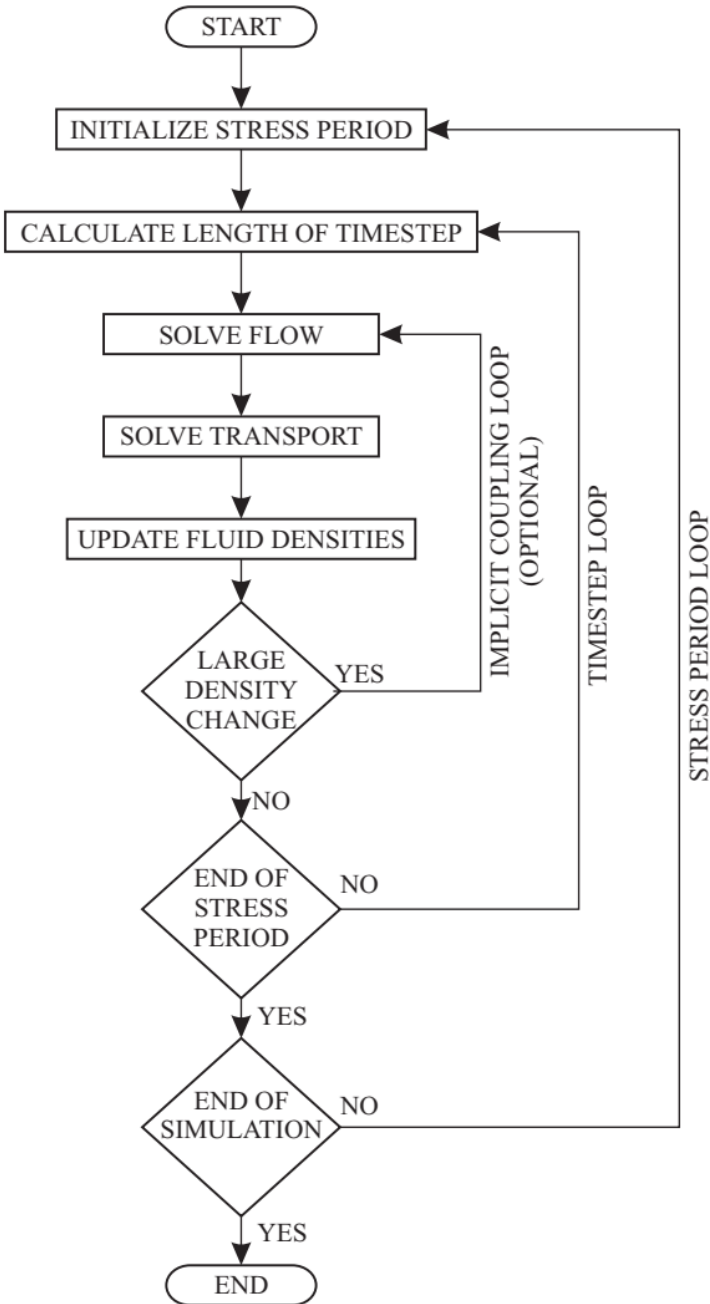
Figure 2-1: SEAWAT general scheme for solving the variable density problems (Guo and Langevin, 2002)

2.3 Numerical solution for solute transport

The difficulty in numerical solution for the transport equation comes from the co-exist of both advection and hydrodynamic dispersion together in the equation. Although numerical solution has been developed during the last three decades but still there is no single solution for the solute transport can give satisfactory results under all hydrogeological situations (Zheng and Wang, 1999).

A full description about the numerical solutions used for the solute transport can be found in (Zheng and Wang, 1999), however, main highlights will be given here. The numerical solutions to solve the transport equation can be categorized as Eulerian, Lagrangian and mixed Eulerian-Lagrangian. Eulerian method is a mass conservative approach using a fixed grid size, like the finite difference and the finite element. Two methods available within MT3DMS to solve the solute transport equation are based on this concept: Finite Difference (FD) and Third Order Method (TVD). The Lagrangian method uses the particle tracking approach by applying a number of particles in the cell and track them. This method can be used in a fixed or deformed cell size like the random walk method. The mixed Eulerian-Lagrangian is using both method's advantages to solve the solute transport equation but cannot assure mass conservation while it is computationally not efficient. Examples of solvers using this method are, the method of characteristics (MOC), backward tracking modified method of characteristics (MMOC) and hybrid of these both (HMOC).

The main difference between the five methods adopted by MT3DMS is in the way of solving the advection term, as the other terms (dispersion, sinks and sources, and chemical reactions) are solved with the Finite Difference method. A general description of how these methods treat the advection part will be given in next paragraph, but first, the numerical errors associated with these methods will be addressed. There are two main numerical errors, numerical dispersion and artificial oscillation. In numerical dispersion, an additional dispersion-like term will appear and induce more mixing of the saline and fresh groundwater. This type of error resulted from the truncation error of the differential equation. Oscillation is happened in the solution due to under- and overshooting of the concentration values and can lead to an unstable solution. The numerical dispersion error can be overcome with adapting the spatial and temporal discretization of the numerical scheme, but at the same time this can amplify the oscillation; so one has to treat this possibility to change the discretization with great care.

11

The Eulerian methods uses the finite difference algorithm for each node to solve the advection term and approximated to the concentration difference between the cell interfaces. However, the difference between the FD and TVD is in the way how the interface concentration being calculated. In the FD method, the interface concentration is either used as the upstream cell concentration, named as upstream weighting, or a weighted average of the two nodes where the interface in between, named as central in space weighting. The upstream approach can lead to solution suffering from the numerical dispersion errors while the central in space approach can has significant artificial oscillation problems. The other method, TVD, uses the upstream concentration over a distance (velocity of the flow in the cell multiplied by the transport step) as the interface concertation. This way can lead to artificial oscillation, but TVD has a scheme of checking the concentration with the adjacent cells and adjust it to eliminate the oscillation.

The other three methods, viz. MOC, MMOC and HMOC, are based on the concept of the particles tracking. MOC approach is based on placing number of particles in a cell and then track them forward. The concentration after time step for each cell in the average concentration of the particles landed in that cell where each particle has the concentration of the cell where it's originated. On the other hand, MMOC uses only one particle for each cell and track it backward in time. In this manner, MOC is computationally demanding as the information of all the particles is being recorded, while in MMOC each time step new particle is placed in the cells. However, MMOC is suffering from the numerical dispersion errors while MOC can have problems with instabilities and the concentration is not smooth. The last method, HMOC is a mix between the MOC and MMOC. A switch between both MOC and MMOC is being done based about the flow.

Table 2-1: available solution in MT3dMS for contaminant transport groundwater simulation (source: (Zheng and Wang, 1999)

Group	Solution Options for Advection[1]	Solution Options for Dispersion, Sink/Source, and Reaction[1]
A	Particle-tracking-based Eulerian-Lagrangian methods • MOC • MMOC • HMOC	Explicit finite-difference method
B	Particle Tracking Based Eulerian-Lagrangian Methods • MOC • MMOC • HMOC	Implicit finite-difference method
C	Explicit Finite-Difference Method • Upstream weighting	Explicit finite-difference method
D	Implicit Finite-Difference Method • Upstream weighting • Central-in-space weighting	Implicit finite-difference method
E	Explicit 3rd-order TVD (ULTIMATE)	Explicit finite-difference method
F	Explicit 3rd-order TVD (ULTIMATE)	Implicit finite-difference method

12

2.4 Stability criteria

The different proposed numerical solutions for the governing equations are approximations of the exact solution. Replacing the derivatives by finite difference can lead to truncation errors and at the end lead to instability of the algorithm (Holzbecher and Sorek, 2006). Therefore, three dimensionless numbers are significant for the stability and accuracy of the model. These numbers are: Courant number (Cou), Grid-Peclet number (Pe) and Neumann number (Neu).

The Grid-Peclet number is relevant for all numerical solutions, violating this number can be seen in the numerical dispersion error. It is given by the following formula:

$$Pe = \frac{v \, \Delta x}{D} \leq 2 \qquad \text{(Equation 2-3)}$$

Both Courant number and Neumann number are mainly for the explicit algorithm and given by:

$$Cou = \frac{v \, \Delta t}{\Delta x} \leq 1 \qquad \text{(Equation 2-4)}$$

$$Neu = \frac{D \Delta t}{\Delta x^2} \leq \frac{1}{2} \qquad \text{(Equation 2-5)}$$

Where, v is the linear flow velocity, Δx is the cell size in x direction, Δt is the transport step, and D is the hydrodynamic dispersion coefficient. All of these numbers can be met by using a smaller time step when the used grid size is small to obtain reasonable resolution, but this can lead to long computational times.

2.5 Sensitivity analysis

A sensitivity analysis is often used to evaluate the effect of model parameters as well as different numerical solutions and model discretisation on the model output as a part of the model calibration process. Al-Maktoumi, et al. (2007) stated that a comprehensive study for the effect of the cell size and time step for unstable flow situation has not been carried out.

Carrera (1993) pointed out that the two main factors which make the solute equation fail to simulate the problem. The first one is that the dispersion can no longer be represented by Fick's law, the second one is the numerical errors pointed above. However, these numerical problems can partly be overcome nowadays with the increase in computational powers. This leaves us with the conceptual errors which are related to features observed in the field and badly represented in the models. Carrera stated that there are many uncertainties related to the

13

conceptual difficulties. These include: 1) scale dependency of dispersivity, 2) influence of flow direction on the estimated arrival time and dispersivity in the lap, 3) lack of movement of pollution in upstream of the source, 4) different in breakthrough tails from the observed data, and 5) the skewed pattern of plumes. All these difficulties are linked to the spatially heterogeneity in hydraulic conductivities.

Ibaraki (1998) conducted a sensitivity analysis for MITSU3D in simulating variable density-dependent flow by comparing the results to known analytical solutions and other numerical solutions. He found that when using very small discretisation, MITSU3D and SUTRA were performing fine, but at larger discretisation MITSU3D was more stable than SUTRA.

Al-Maktoumi, et al. (2007) represent a sensitivity analysis for SEAWAT using the Elder problem. They analysed the simulation results using qualitative and quantitative methods. In the qualitative method, they compared the results to other codes, while in quantitative they analysed issues like penetration depth and total mass of contaminant. They found that SEAWAT is sensitive to the grid size and transport step. For the same transport step and time step, different solvers like MMOC, TVD and FD can give different results which clearly indicates that the solver type can also influence the results. They also found out that comparing quantitative methods is very useful.

Goswami, et al. (2012) tested three of the numerical solutions used in SEAWAT (MOC, FD, and TVD) by simulating two experiments in a (supposing) first completed analysis for problems regarding the unstable variable-density groundwater flow. They tried two setups, rising and sinking transport conditions and found out that none of the numerical solutions was capable to simulate both of them at same model parameters without stabilities. Al-Maktoumi, et al. (2007) has studied the sensitivity of SEAWAT to the spatial resolution for the unstable Elder problem and found that SEAWAT is sensitive to the cell.

Park and Aral (2007) have found that the variation in velocity can lead to significant differences in the obtained results. They also found that the physical instabilities in terms of the percentage of density difference can influence the results. In addition to that when using irregular grids, the pattern of the results can be affected.

Graf and Degener (2011) studied the effect of discretisation on the grid convergence in fractured-porous media for variable-density groundwater flow. They found that the solution,

patterns and penetration depth of plumes are affected by the adopted transport step and grid size.

2.6 Some benchmarks

2.6.1 Freshwater lens

The case is a 2D profile of a sandy aquifer in a coastal area. The freshwater lens is developing under the effects of the natural recharge. An analytical solution for this case does exist and can be used for comparing with the numerical solution. The analytical solution is just a good approximation for the actual position of the fresh-salt interface, however, there are some assumption need to be taken under consideration to compare the numerical with the analytical solution (Oude Essink, 2001). These assumptions are:

1. The aquifer is homogeneous and isotropic
2. The transition zone from fresh to saline water is assumed to be sharp and no brackish transition zone, which means the dispersion is neglected.
3. The saline water is stagnant which mean the situation is stable.
4. The Dupiut-Forcheimer assumption is used, this means there is only vertical flow in the aquitards and horizontal flow only in the aquifer.

There are few mismatches with these assumptions, for example the vertical flow in the aquifer cannot be neglected. The outflow point to the sea is not coinciding with the phreatic groundwater line. And the last one is the assumption of the hydrostatic balance between the fresh and saline water.

The analytical solution gives the approximate depth of the interface, the volume of the freshwater lens that has been developed under the natural recharge and the time of residence of the groundwater in the aquifer. The formulas used are taken from (Oude Essink, 2001). The depth of the interface is given with the following formula:

$$H = \sqrt{\frac{f(0.25\,B^2 - x^2)}{k\,(1+\alpha)\,\alpha}} \qquad \text{(Equation 2-6)}$$

Where, f is the recharge rate, B is the width of the island, k is the hydraulic conductivity, and α is the buoyancy factor which is the ratio between the phreatic groundwater head to the depth of the interface.

Volume of the freshwater is given by:

$$V = \frac{1}{4}\pi(1+\alpha)H_{max}Bn_e \qquad \text{(Equation 2-7)}$$

Where n_e is the effective porosity.

The characteristic time of the groundwater is defined by:

$$T = \frac{\pi n_e B}{8}\sqrt{\frac{(1+\alpha)}{k f \alpha}} \qquad \text{(Equation 2-8)}$$

2.6.2 Modified Henry case

The original Henry case (Henry, 1964) has been used numerous times as a benchmark for the variable density groundwater flow models. The case represents a part of a homogenous, isotropic confined aquifer. Where a fresh groundwater flux comes from landward boundary flowing in the direction of the seaward boundary which consist of higher density sea water. The seawater starts to intrude as a result of the diffusivity until the steady state is reached. Henry (1964) developed a semi-analytical solution for the problem, and hence, this semi-analytical solution is (always) being used for comparison.

Simpson and Clement (2004) modified the original case by reducing the amount of freshwater flux to allow more density dependent movement. They tested the Henry case for coupled and uncoupled groundwater models to check the worthlessness of Henry case to be used as a variable density benchmark and found out that there was no much significant difference between both of them (Simpson and Clement, 2003) and therefore they proposed this adjustment in the value of the freshwater flux to add more influence from the density variation in the groundwater flow patterns. Finally, they found that their adjustments will add more value to original Henry case to be used as a benchmark.

Henry (1964) used three dimensionless parameters in the solution of the problem, these parameters are:

$$\xi = l/d, \qquad a = Q/k_1 d \qquad \text{and} \qquad b = D_h/Q \qquad \text{(Equation 2-9)}$$

Where, l is the length of the domain, d is the depth Q is the freshwater flux from the inland boundary as recharge, k is the hydraulic conductivity, D is the hydrodynamic dispersion coefficient.

Then the concentration distribution and the stream function has been solved by introducing both in a shape of double Fourier series:

$$\bar{\Psi} = \sum_{m=1}^{\infty} \sum_{n=0}^{\infty} A_{m,n} \sin(m\pi z) \cos\left(n\pi \frac{x}{\xi}\right)$$

$$\bar{C} = \sum_{r=0}^{\infty} \sum_{s=1}^{\infty} B_{r,s} \cos(r\pi z) \sin\left(s\pi \frac{x}{\xi}\right)$$

(Equation 2-10)

The modified solution differs in the values of *a* and *b*, they are half the original value since the flux was reduced by half.

2.7 Managed aquifer recharge

Managed aquifer recharge (MAR) is used broadly in many regions for water storing and treatment (Dillon, et al., 2010). It serves as a solution to meet the increased demands on the water supply resulted from population growth and economic development. There are many types of managed aquifer recharge systems. In the Netherlands, some of the used types are Artificial Recharge through Basin (BAR), Aquifer Storage and Recovery (ASR), Aquifer Transfer Recovery (ATR) and River Bank Infiltration (RBF) (Stuyfzand, 2016). Factors that determine what type of MAR should to be used for recharging water to the groundwater system are, among others: the quality and source of water, the geology of the area, the soil types, the topography and surface conditions, and the hydrogeology of the area (UNESCO, 2005). Rahman, et al. (2013) mentioned that hydrogeological conditions play a significant role in determining the success of the MAR system, because the applicability differs from location to location, while it also depends on the groundwater flow and transport processes along with the dynamics of regional groundwater flow. Moreover, the increase of the groundwater head due to the recharge can also change the direction of groundwater flow.

MAR systems have many advantages as it needs less space on the surface, fewer water losses through evaporation and less vulnerable to be contaminated. However, in the coastal zone where the groundwater system consists of fresh, brackish and saline groundwater, the recovery efficiency is reduced by the effect of mixing with the saline water (Ward, et al., 2007). Fresh groundwater is lighter than saline groundwater and it will float and rise while denser water (saline groundwater) is reaching the lower part of the groundwater system. In addition to that, some of the fresh groundwater is lost through the horizontal flow of groundwater (Zuurbier, 2016). Zuurbier (2016) proposed a solution with multiple penetration wells to improve the

17

efficiency of recovery in ASR systems. It was efficient for the ASR system to be used in fresh-saline groundwater system where the normal way of extraction groundwater is inefficient.

Pauw, et al. (2015) used a small-scale ASR system in a case study in the Netherlands but instead of using wells, they used agricultural drains. The aim was to increase the groundwater table under the areas with higher elevation, called creek ridges, to have a thicker freshwater lens. The main concept was based on the relation between the groundwater phreatic table and the lens thickness developed by the Badon Ghijben-Herzberg principle. It was found that an average increase of the groundwater table by 0.5 m can lead to an increase in the thickness of the freshwater lens by 6-8 m in ten years; this is less than the 1 over 40 factor as given by the Badon Ghijben-Herzberg principle, but resistance layers limited the full growth of the lens over time.

Chapter 3   Methodology

An overview of the steps that have been followed to obtain an assessment of the potentiality of groundwater storage and recovery system is given in Figure 3-1. A variable-density groundwater flow model has been used as an interpretation tool in our study. Effects of different numerical solutions, model criteria and model discretisation in model results have been examined to acquire a reliable model.
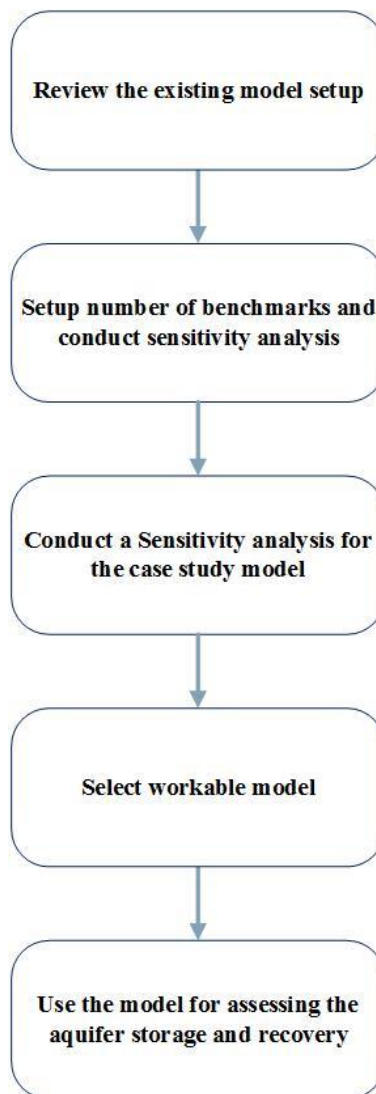
Figure 3-1: Research Methodology flow chart

3.1 Benchmark models

3.1.1 Freshwater lens

The benchmark simulates development of a freshwater lens in an island. The island length is 4 km, located in the middle of the model surrounded with the sea. Model profile is two dimensional with total length of 10 km and depth of 150 m. The spatial discretization is 100 m in the horizontal direction and 10 m in the vertical direction. It has been run for 1000 year with stress periods of 25 years, the simulation time was set to be long to assure that the lens has fully developed. Homogeneous and isotropic situation was assumed to match the analytical solution. Boundary condition as no flow from all the sides except the top where there is coming inflow from the recharge rainwater and a fixed head between the sea and the aquifer. The recharge was distributed over the island and simulated through recharge package.
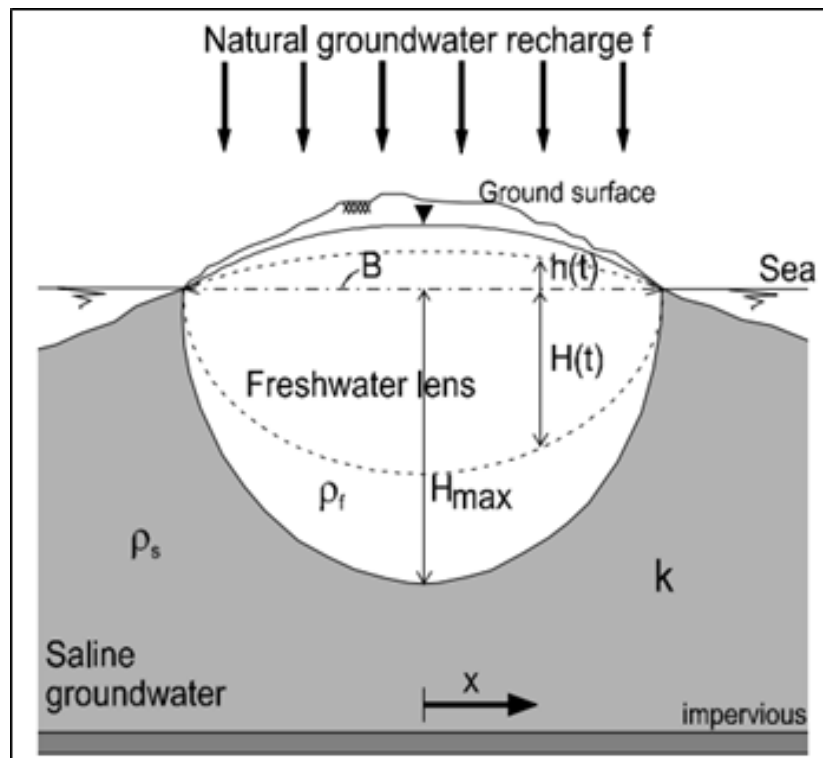
Figure 3-2: Conceptual model of the freshwater lens benchmark (Oude Essink, 2001)

For the transport model, the initial concentration all over the model was set to a value of TDS of 35 g/l, which is the seawater. Only advection and source and sinks package were used for the transport of the seawater, there was no dispersion due to the assumption of the sharp interface in the analytical solution and no mixing.

Table 3-1: freshwater lens model properties used in the numerical simulation

Horizontal cell size (m)	100	K_{hor} (m/day)	20
vertical cell size (m)	10	anisotropy	1
layers	16	ne	0.35
number of rows	1	Al	0
number of columns	100	recharge (mm/day)	1
initial concentration (TDS g/l)	35	recharge concentration (TDS g/l)	0
buoyancy	0.025	courant	0.95

3.1.2 Henry's case

Henry's case represents an intrusion of seawater to a (conceptual) rectangular confined aquifer, and due the dispersion, the saline water merges with the freshwater. The geometry of the case can be seen in Figure 3-10, the total length is 2 m and the depth is 1 m. The spatial discretization was set to be 0.05 in both horizontal and vertical directions.

The boundary condition of the model is no flow boundaries in the top and the bottom, the left side is a flow boundary of constant freshwater flux while the right side is a constant saltwater head boundary.
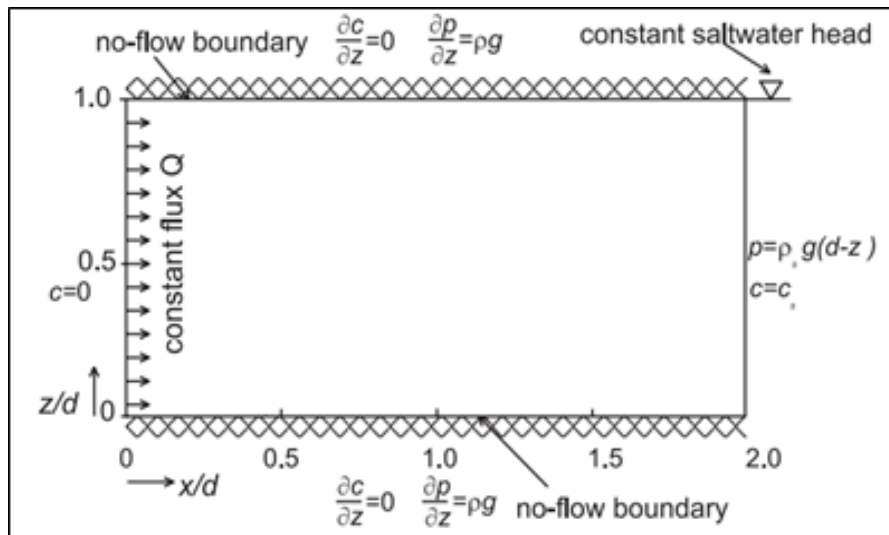
Figure 3-3: Henry problem conceptual model (Oude Essink, 2001)

The freshwater flux was simulated by putting wells in each cell in the first column and the summation of these injection rates sum up the total flux. For the transport model, all the model

domain was freshwater except the constant boundary was a saline water of concentration of 35 g/l TDS. Summary of the parameters used in the numerical scheme can be found in Table 3-3.

Table 3-2: Modified Henry case aquifer properties used in the numerical simulation.

horizontal cell size (m)	0.05	K_{hor} (m/day)	864
vertical cell size (m)	0.05	anisotropy	1
layers	20	effective porosity (ne)	0.35
number of rows	1	longitudinal dispersivity (m)	0
number of columns	40	recharge per unit width (m^2/day)	2.85
seawater salinity (TDS g/l)	35	recharge concentration (TDS g/l)	0
buoyancy (-)	0.025	molecular diffusion (m^2/day)	1.63

3.1.3 Saltwater pocket

This case simulates the presence of saline water pocket within a fresh groundwater, the model is a rectangular with length of 1 m and depth of 0.5 m. The spatial discretization of the model is 0.025 m in both horizontal and vertical directions. The boundary conditions are no flow boundary from all the sides, with one cell in the middle of the first column as a constant head to be as a reference for the groundwater head simulation as can be seen in Figure 3-11.
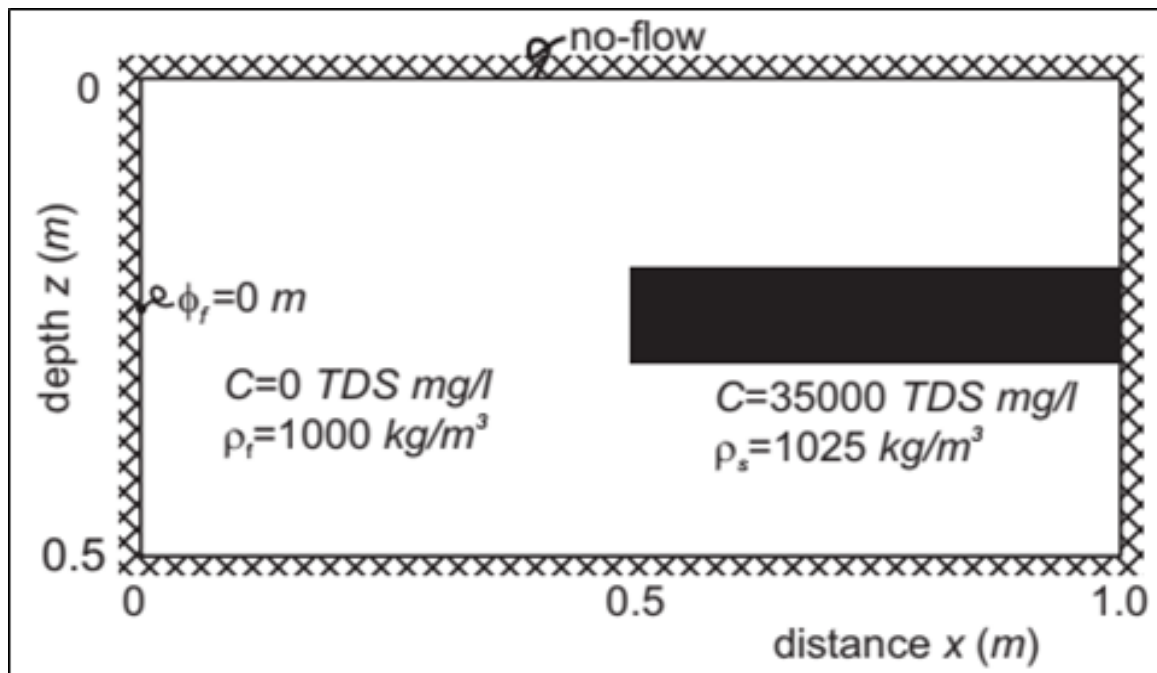
Figure 3-4: Saltwater pocket conceptual model (Oude Essink, 2001)

At the beginning the pocket has a concentration of saline water, 35000 mg/l TDS, while elsewhere is zero. As a result of the gravity force the saline water start to sink and fingering occurs due to mixing resulted from the dispersion. Summary of the parameters used in the simulation can be found in Table 3-4.

Table 3-3: Saltwater pocket case aquifer properties used in the simulation.

horizontal cell size (m)	1.0	K_{hor} (m/day)	86.4
vertical cell size (m)	1.0	anisotropy	1
Layers	40	effective porosity (ne)	0.1
number of rows	1	longitudinal dispersivity (m)	0.001
number of columns	80	molecular diffusion (m^2/day)	8.64E-05
seawater salinity (TDS g/l)	35		

3.2 Existing model setup of the DOW case study

The base model for the case study has been developed by Deltares, we will refer to the case study model in the rest of this report as the DOW model. It was implemented in the SEAWAT code to account for the variable-density groundwater flow and coupled salt transport.

3.2.1 Model discretization

The model has a spatial discretization of 25 meters by 25 meters cell size in the horizontal direction, while in the vertical direction number of 47 model layers were used for the different subsurface strata. The layers thickness varies between 1 meter in the first 26 model layers, and 2 meters for the next 15 model layers, while the last 6 model layers has thickness of 5 meters. For the temporal discretization, the model has been run for a total period of 50 years. To include the effects of changes in hydrological factors, like water levels in (river) water bodies and groundwater recharge, a transient run with monthly stress periods was adopted. The year was divided between summer (form April to September) and winter (from October to March) for the river stages. Summary for the spatial and temporal discretization can be seen in Table 3-1.

Table 3-4: DOW Model discretization

Cell size (m)	25×25
number of rows	244
number of columns	264
number of layers	47
layer thickness in top 26 layer (m)	1
layer thickness in layer 27 to 41 (m)	2
layer thickness in last layers (m)	5
run time (years)	50
stress period length (month)	1
top elevation (m NAP)	6
bottom elevation (m NAP)	-80

3.2.2 Boundary condition

There are two boundary condition presents in the model, no flow boundary and head dependant boundary (Cauchy Boundary). The bottom side of the model is no flow boundary where a layer of impermeable clay is present. Northern, Southern, Eastern and Western boundaries are head dependent boundaries. These boundaries are simulated using the General Head Boundary package (GHB). The values for the head assigned in the GHB package are from another larger 3D regional model, which is Zeeland model (Van Baaren, et al., 2016).

3.2.3 Hydrogeological parameters

A subsurface lithology parameter dataset was used for the values of hydraulic conductivities. For the Netherlands part, GeoTOP and REGIS datasets were used, GeoTOP was used for the top 50 meters and REGIS was used from -50 meters to -80 meters. For the Belgium part of the groundwater system in the model, the so-called HKOV dataset was used for values of the hydraulic conductivities. These datasets for hydraulic conductivity in the horizontal and vertical direction can be seen in Figure 3-2 and Figure 3-3, respectively.
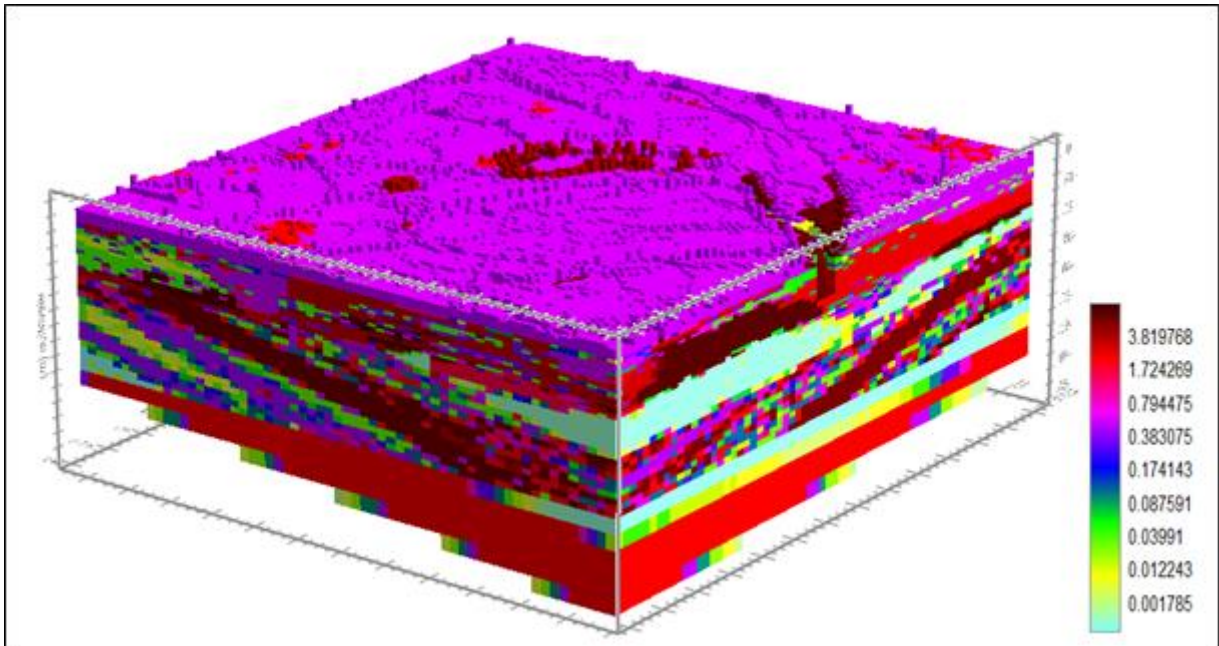
Figure 3-5: Horizontal hydraulic conductivity interpreted from GEOTOP and REGIS for Netherlands and HKOV for Belgium
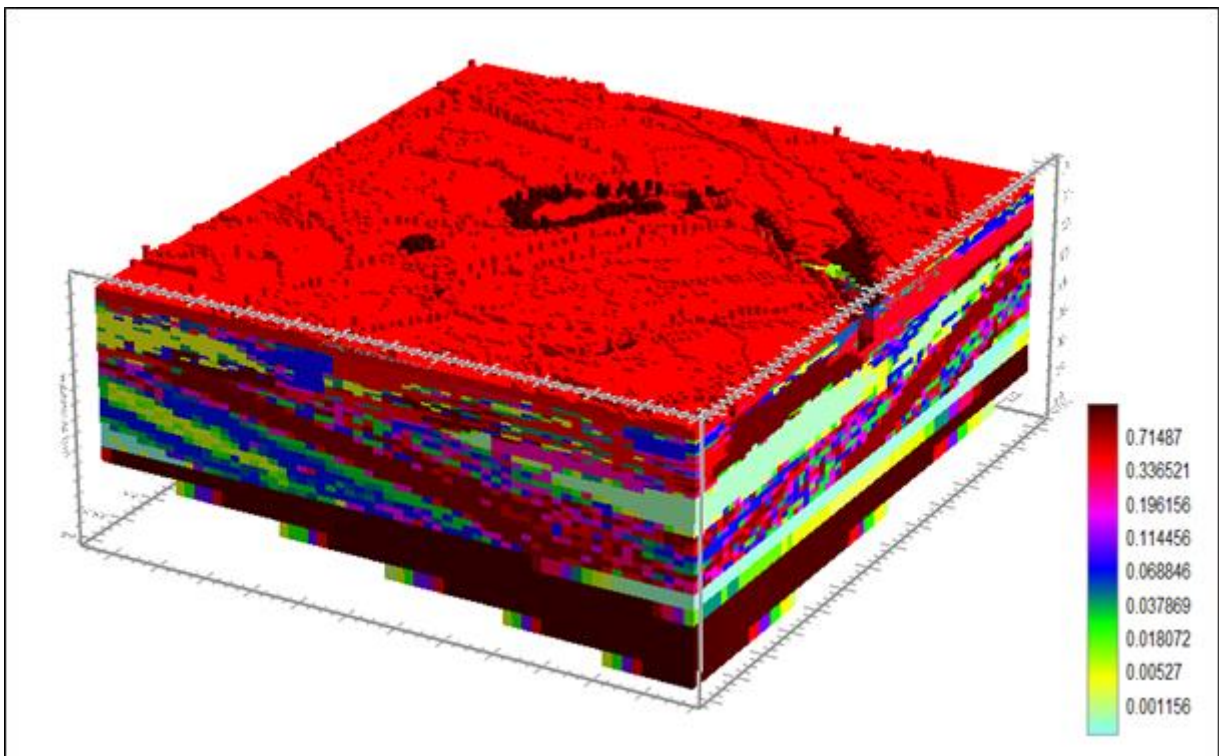
Figure 3-6: Vertical hydraulic conductivity interpreted from GEOTOP and REGIS for Netherlands and HKOV for Belgium

3.2.4 Surface water

The surface water bodies within the model domain are ditches, drainage systems and rivers. The water level in the ditches and rivers varies from the summer and the winter. These two stages are controlled by the Scheldestromen waterboard. The smallest rivers were simulated in the model using the river package, and the values of the stage, conductance and bottom were obtained from the national hydrological model of the Netherlands (LHM) (De Lange, et al., 2014). These input values were corrected for the difference in discretization between the National and DOW models. These small rivers can be seen in Figure 3-5.

The drainage system was simulated using the drains package. The input values for the drain package, drains bottom and conductance, were obtained from LHM. However, the data from LHM only covers the Dutch part of the model, the other part was given an average values of -1.1 m NAP and 160 m^2/day for the bottom and conductance respectively, because it is likely that drainage in happening within these areas. The layout of the drains is depicted in Figure 3-4.

Some of the largest rivers within the area are simulated with the GHB for better interaction within the aquifer as shown in Figure 3-6. The values of the head and conductance are obtained and rescaled for this model using the LHM model.
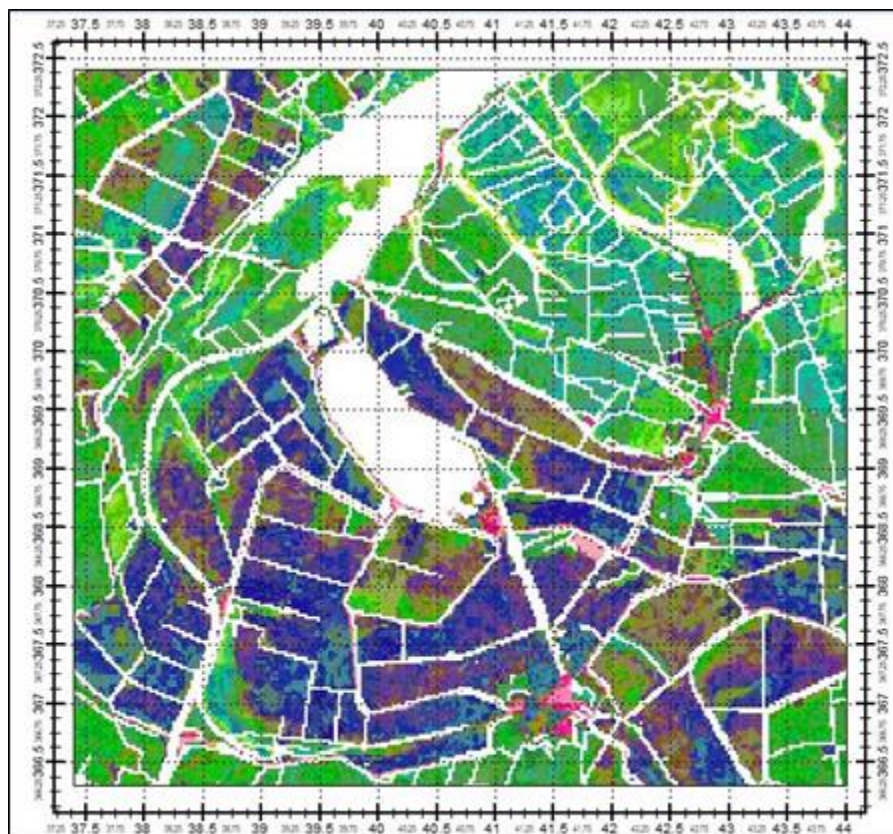
Figure 3-7: The distribution of the drainage network within the model domain simulated with the drain package
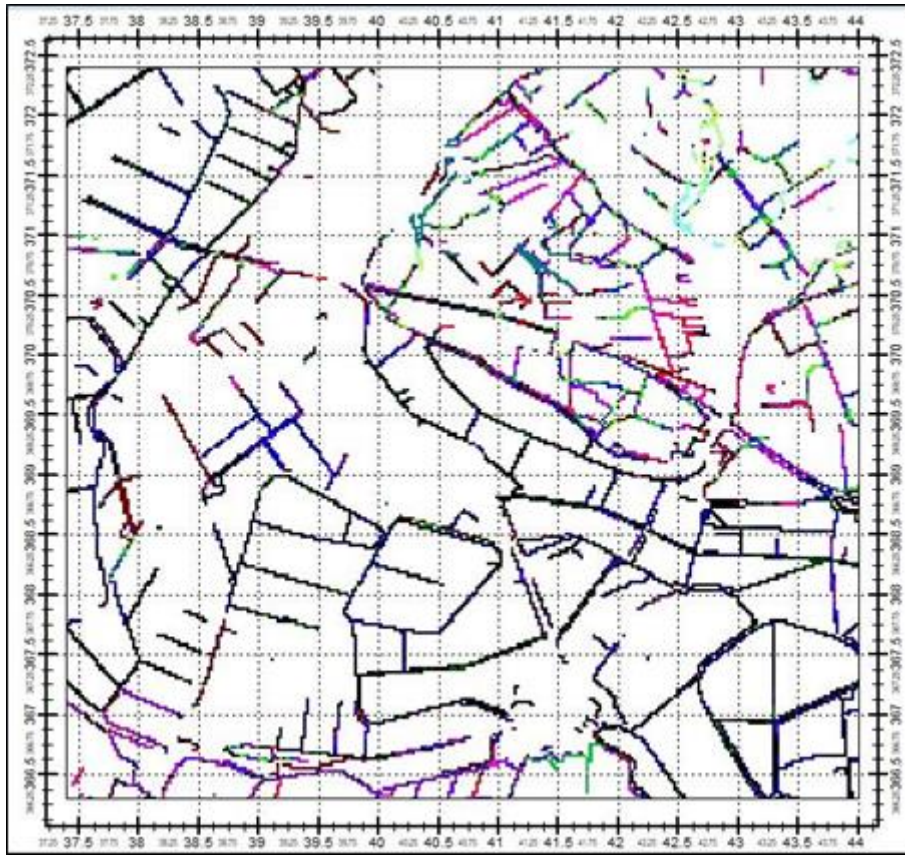
Figure 3-8: The layout of the smallest rivers which simulated with the river package
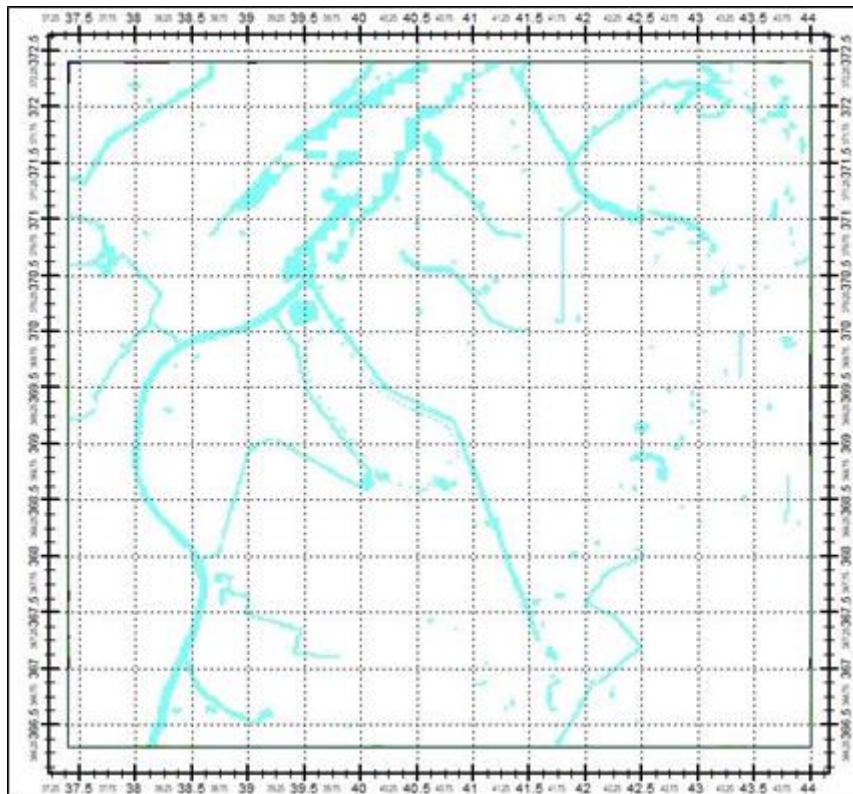
Figure 3-9: The largest rivers within the model domain simulated with the GHB as well as the boundary

3.2.5 Recharge

The natural groundwater recharge from rainfall was obtained by subtracting the evapotranspiration from the precipitation. Data from Westendorpe weather station were used in the calculation. Records of data within the period from 1988 to 2018 was obtained and then the average monthly recharge was calculated as shown in Figure 3-7.
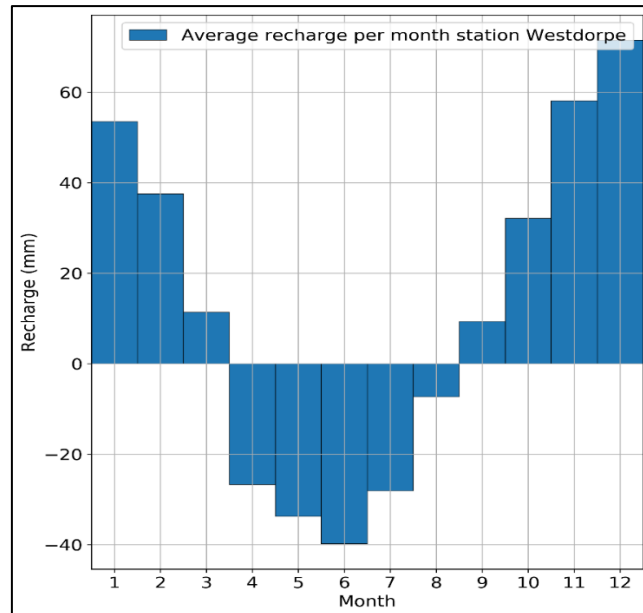
Figure 3-10: Average monthly recharge (Deltares, 2019)

3.2.6 Salt transport model

Data from FRESHEM project (Delsman, et al., 2018) were used for the distribution of the saline and fresh groundwater, and the initial concentration of chloride in the model domain was interpreted from the project data. Figure 3-4 illustrate the starting concentration along the model.
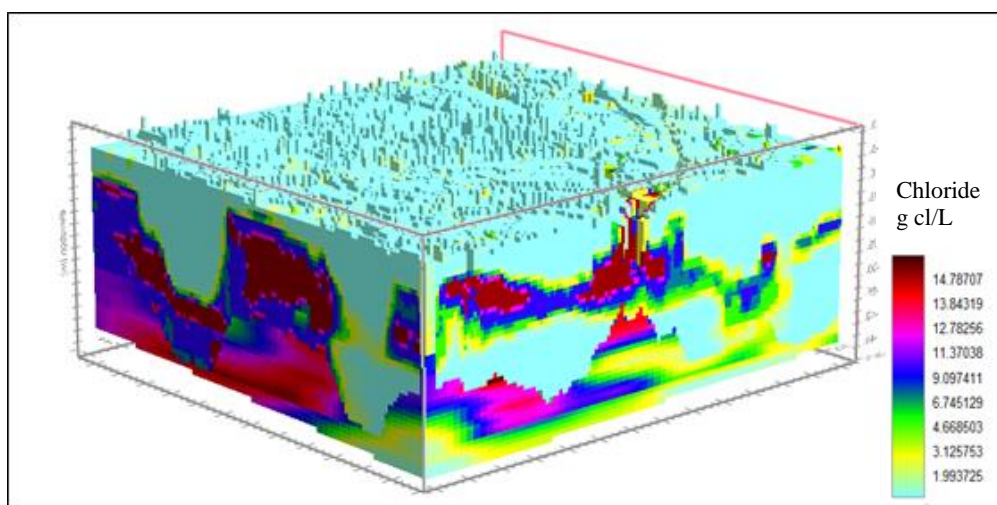
Figure 3-11: Initial Chloride concentration in the Model

Advection, dispersion and sinks and sources packages were used for the transport of the chloride. For the advection package, TVD was used with courant number of 1.0. In the dispersion package, the longitudinal dispersivity (al) was set to be 0.1 m, the ratio of the horizontal dispersivity and the vertical dispersivity to the longitudinal dispersivity were set equal to 0.1. The molecular diffusion coefficient used is 0.0001 m^2/day.

The source and sink package was used to account for any additional values of Chloride from the rainfall in the recharge or from the ditches, rivers and the boundary of the model domain. Measurements of the chloride in these three sources were implemented in the model through the source and sink (SSM) package.

3.3 Sensitivity analysis

The sensitivity analysis is required to understand how each of the parameters, different solvers and model discretisation can influence the model results. In this process, first of all, some of the benchmarks has been used to understand the influence of the above-mentioned factors because of the availability of the analytical solution for some of them and the short calculation time in compared with the real case study model. As a result, better understanding of these factors will be gained in less time. All the cases are summarized in Appendix D.

For the freshwater lens, the process started with the grid discretization by changing the horizontal cell size from 100 m up to 250 m and then reducing it down to 50,25 and 10 m. for each of the horizontal cell size three vertical discretization has been used, which are 10, 5, and 1m. So, 15 different models have been created to test the influence of the grid size. In addition, all the five solvers were used to see how each solver is influenced by the degree of discretization. After that, one model with accurate results and acceptable run time has been selected for further tests, named the reference model. This reference model was tested for the convergence criteria for the head and the flow. The head convergence (HCLOSE) was changed between 0.1, 0.01, 0.001 and 0.0001, and the flow convergence (RCLOSE) was tested for 0.1, 1 and 5.

Then the solute transport step was tested by varying courant number from 1 down to 0.75, 0.5 and 0.25, as with the reduction of the courant number the length of the transport step will be reduced. The last thing was changing some of the settings within the solvers themselves. For FD, the change between the upstream weighting and the central in space methods. For MOC, the itrack, which is the particle tracking algorithm, was changed between the three available

methods. Also, the number of particles to be placed in one cell in increased from 16 to 32 particles, besides changing the weighting ratio of the concentration (WD) from 0.5 to 0.75 and 1.

For the Henry case, the interest was about the behaviour of the solvers in such a case, so for the same original case we just changed between the solvers. No further tests have been carried for the case as there was no significant difference between the solvers.

For the last case, the saltwater pocket, the influence of the grid discretizing was tested by varying the horizontal and the vertical cell size from 1 m to 0.5, 0.25 and 0.125m. Then the finer model of cell size of 0.125m was selected of the tests. The models were compared for different solvers to see the differences among the solvers. Then the values of the longitudinal dispersivity was varied between 0.001, 0.01 and 0.1, in order to examine the influence of the dispersivity in the model results.

The last thing was the sensitivity analysis for the case study model using the ideas gained from the benchmarks. Starting with the existing model spatial discretisation, the adopted discretization by Deltares was changed. The cell size was changed from 25 up to 50 and 100m, while the layer thickness was kept constant at 2m. Furthermore, setting the cell size at 25 and changing the layer thickness with three values, 1, 2 and 5m. Then, a reference model was tested for different solvers and some of the known influenced settings within the solvers. Different simulation results will be analysed to address the sensitivity of these factors, as will be seen in chapter 4 'Results and Analysis'.

3.4 Selection of workable model

The results obtained from different simulations, when trying a different range of parameters with different solvers, will be analysed and compared to obtain a model with good accuracy and reliable results but at the same considering acceptable run times to be used for the assessment of the aquifer storage and recovery in the groundwater system.

3.5 Aquifer storage and recovery

The model will be used to investigate of the potential groundwater storage and recovery. The dynamics of fresh, brackish and saline groundwater will be visualized. This process will be carried out by doubling the recharge in areas which are favourable for water to be infiltrated. These areas are called the creek ridges and they are formed with sandy deposits (Pauw, et al.,

2015). Below these areas the thickness of the freshwater lens is higher as can be seen in Figure 1-3, which shows the relation between the elevation and the lens thickness. In our model, the areas with elevation higher than 1.2 m NAP were taken as a creek ridge places, but also an additional condition was added by putting the limits up to 2.2 m NAP to exclude areas which are not part of these creek ridges (e.g. bigger dune or industrial areas). The areas with pinkish colour in Figure 3-12 are the areas where the recharge has been doubled during the winter period (from October up to March). This infiltrated water will make a rise in the groundwater heads and, in turn, will increase the growth of the freshwater lens. As from the Badon Ghijben-Herzberg relation, an increase in the phreatic head will lead to an additional growth of the freshwater lens.

During the summer period (from April to September) extraction of half of the infiltrated water will take place through many wells distributed around the creek ridge area, as indicated in Figure 3-12, in model layer 10 with small extraction rates of 50 m^3/day. An additional scenario with extracting three-quarter of infiltrated water has also been simulated. The influence of these process on the fresh, brackish and saline ground water distribution will be examined to make sure that no serious up-coning of saline water will take place.

Finally, from the simulation results, conclusions on how and where to implement the ASR systems will be given. Recommendations for further investigation will be given too.
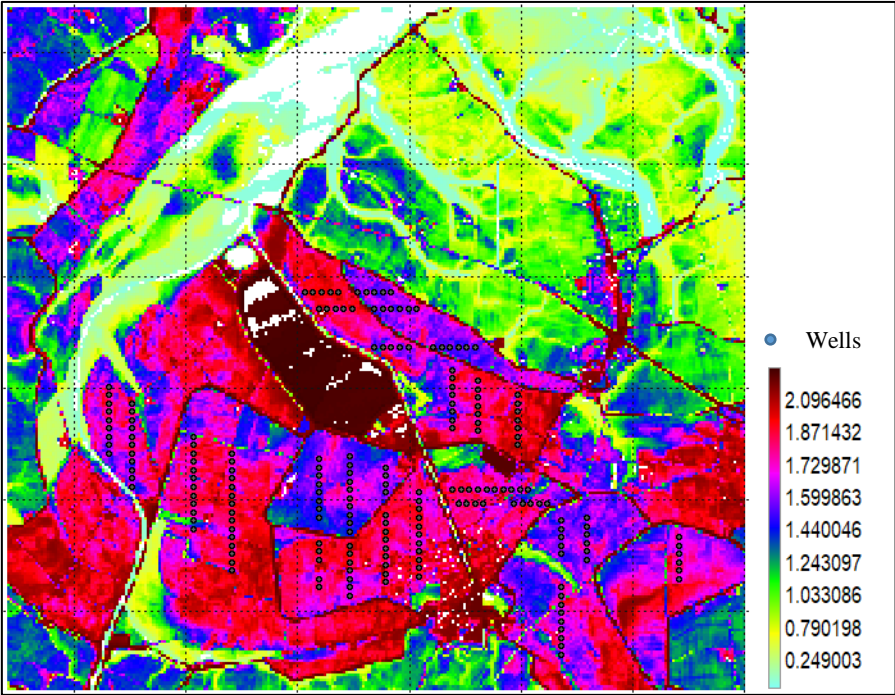
Figure 3-12: Elevation map of the model domain with the extraction wells in small points.

31

Chapter 4   Results and Analysis

4.1 Freshwater lens

4.1.1 Sensitivity of the sharp interface to the model cell size

Creating finer model grids helps to eliminate the numerical errors associated with the numerical approaches to solving the transport equation, such as numerical dispersion and artificial oscillation. In this section 4.1, the effects of adopting different cell sizes on the accuracy of the results are shown. In addition, the run time is considered to obtain an accurate model with acceptable computational time, to which other models are compared. The accuracy of the results is measured by the degree of how sharp the interface is between the fresh and saline groundwater. This measure was adopted since only advection is used. Thus, no hydrodynamic dispersion is modelled and a mixing zone of brackish groundwater should be absent; if any this would be numerical dispersion.

All results for different cell sizes using different solvers for the advection part of the solute transport are available in Appendix B. Here, only the obvious differences are presented. The main outcome is that with the reduction of the cell sizes, the interface becomes sharper as the case in the analytical solution as can be seen in Figure 4-1 and Figure 4-2. In this example, TVD was used for the advection package and can be seen that the bigger size model produces larger mixing zone as induced from the numerical dispersion error.
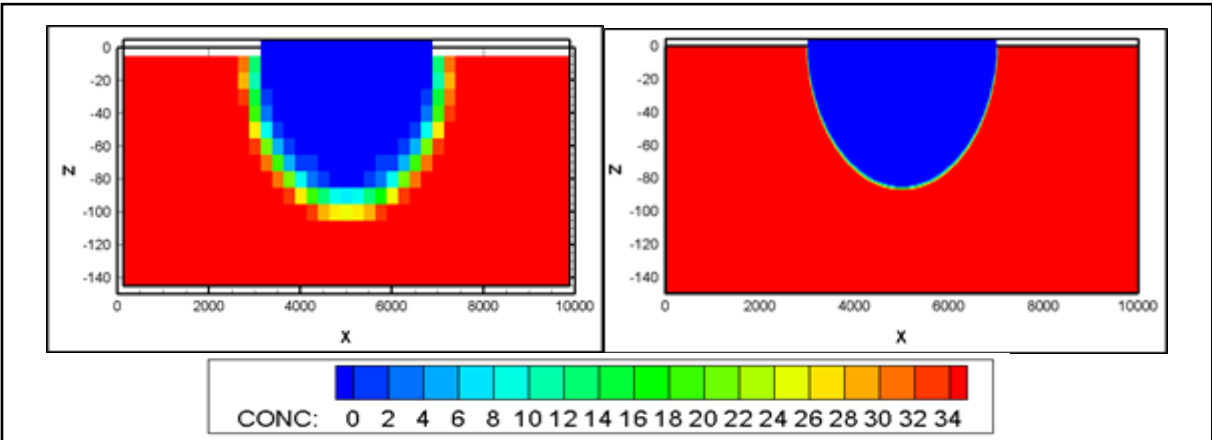
Figure 4-1: Shape of freshwater lens obtained from two models with different spatial resolution, left: 250m horizontal and 10 m thickness (case F_TVD001), right:10m horizontal and 1 m thickness (case F_TVD015)
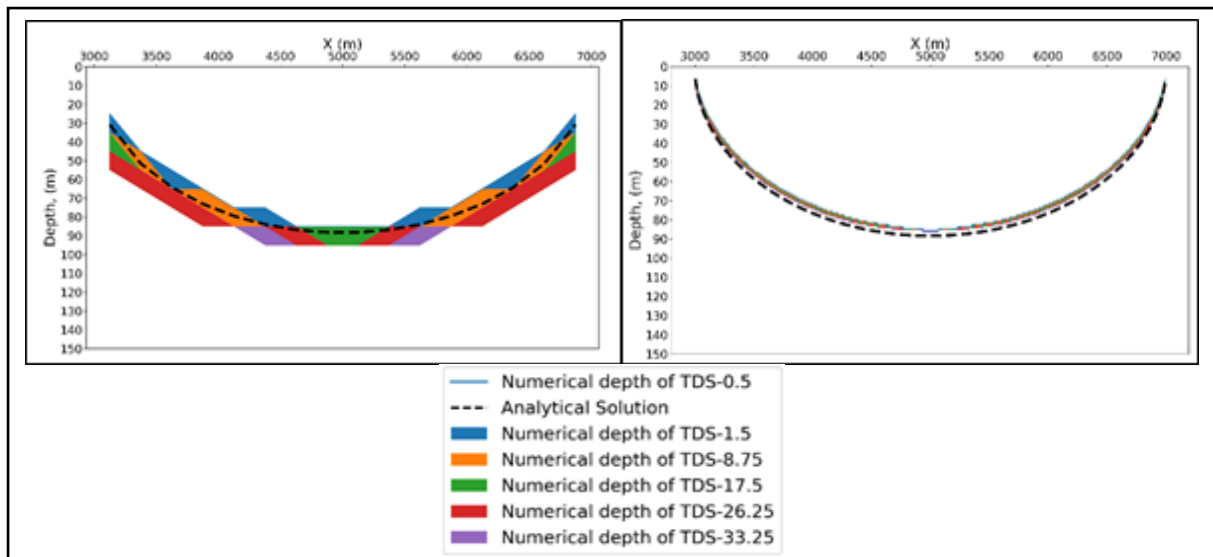
Figure 4-2: Shape of the interface obtained from two models with different spatial resolution, left: 250m horizontal and 10 m thickness (case F_TVD001), right:10m horizontal and 1 m thickness (case F_TVD015)

For TVD, FD, and MMOC, the bigger cell size causes numerical dispersion, it can be seen in Figure 4-1 and Figure 4-2 left. The results of FD and MMOC can be seen in Figure 4-3 and Figure 4-4. Even for the very fine cell size model, FD and MMOC cannot produce results free from numerical dispersion as the other three solvers (TVD, MOC and HMOC with the same spatial resolution). In FD and MMOC, the size of the interface is small but not as small as with TVD in Figure 4-1 right and Figure 4-2 right. Also, we can see that FD has problems at the centre of the model under the interface. Here the groundwater should be completely saline (with a concentration of 35 g/l TDS), but in FD the concentration is smaller than 34 g/l TDS. So, in the dominant advection transport the FD method can give relatively good results but it is not as accurate as TVD, MOC and HMOC; it has more or less the same result as MMOC which even appears to be a degree better.
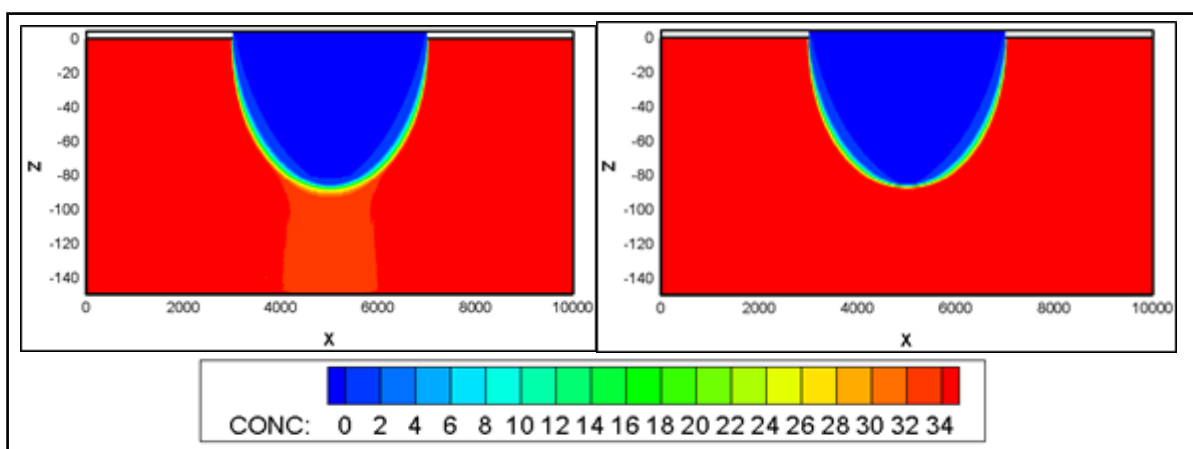
Figure 4-3: Shape of freshwater lens obtained from two models with same spatial resolution, 10m horizontal and 1 m thickness, but using FD (left) case F_FD015 and MMOC (right) case F_MMOC015
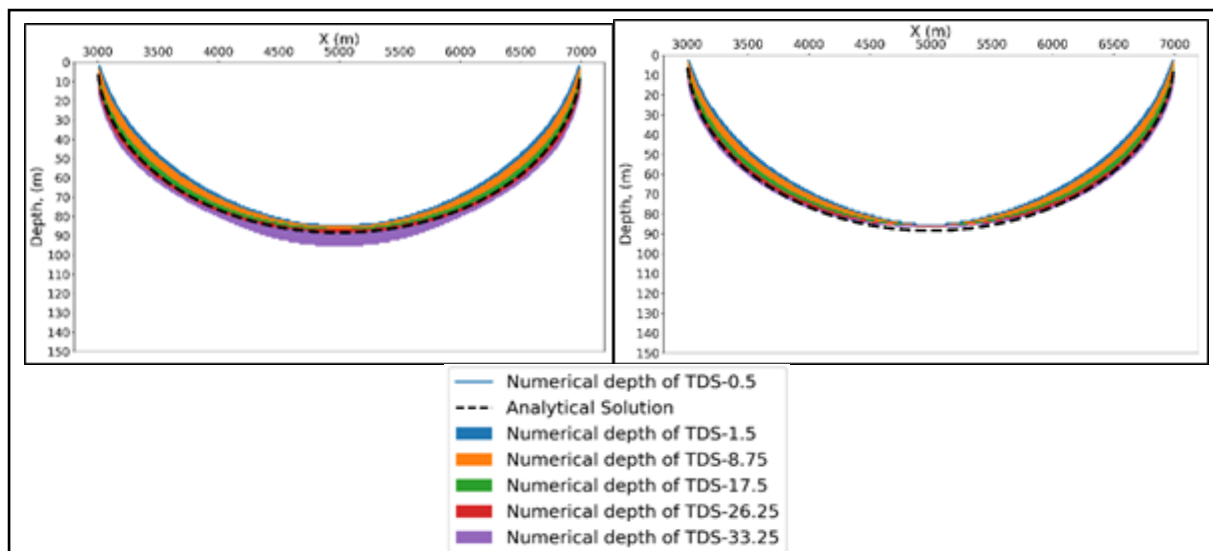
Figure 4-4: Shape of the interface obtained from two models with same spatial resolution, 10m horizontal and 1 m thickness, but using FD (left) case F_FD015 and MMOC (right) case F_MMOC015

On the other hand, MOC and HMOC have problems with coarser models. Figure 4-5 and Figure 4-6 show that the values of the interface are not as smooth as the other three solvers (Appendix B) and interface is very large. The observed relatively large thicknesses of the mixing zone in Figure 4-6 for MOC and HMOC are even coarser than the TVD solution (Figure 4-1 left). This is due to the fact that the large cell size in especially the vertical direction leads to larger transport step and therefore the particles move long distances carrying the concentration. For HMOC, which is switching between MOC and MMOC, in cases where advection is dominant, HMOC is more likely following the same behavior as MOC. However, there is also an extra though small additional numerical dispersion issue in HMOC in comparison with MMOC (Appendix B).
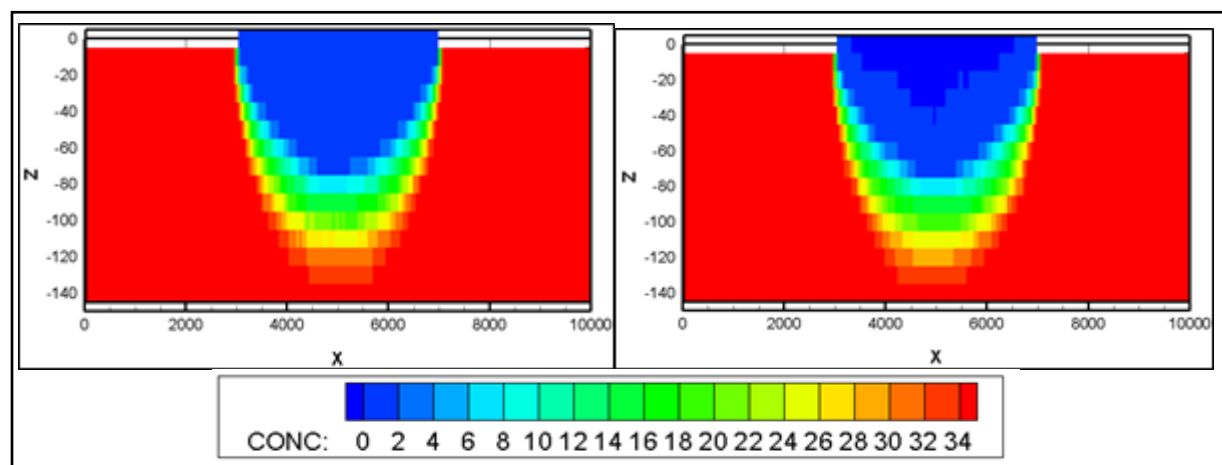
Figure 4-5: Shape of freshwater lens obtained from two models with same spatial resolution, 50m horizontal and 10 m thickness, but using MOC (left) case F_MOC003 and HMOC (right) case F_HMOC_003
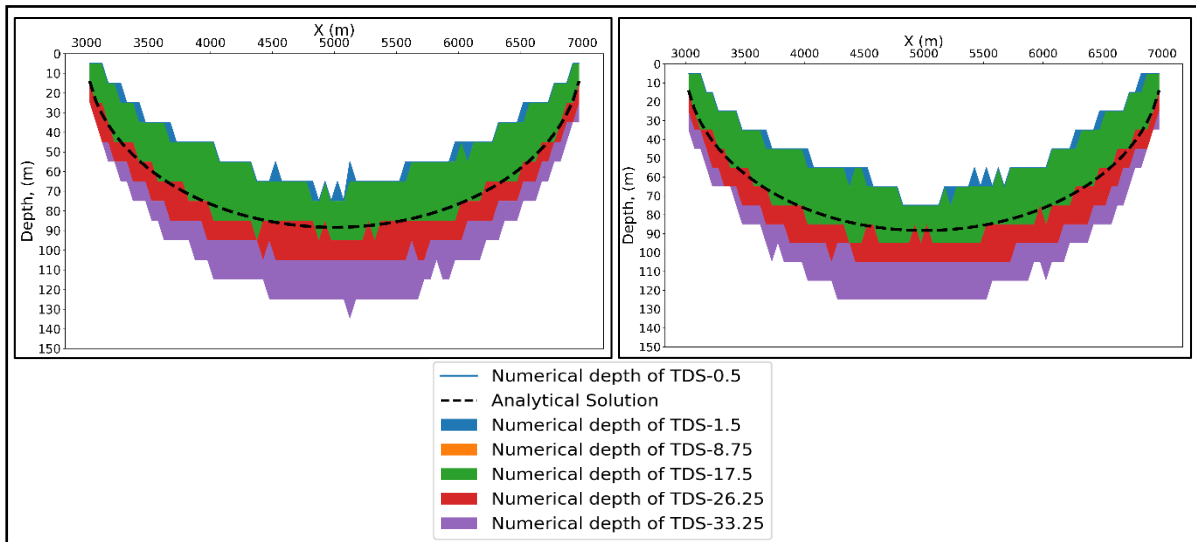
Figure 4-6: Shape of the interface obtained from two models with same spatial resolution, 50 m horizontal and 1 m thickness, but using MOC (left) case F_MOC003 and HMOC (right) case F_HMOC_003

The above-mentioned was about the accuracy of the model, but now the computational time is considered. Figure 4-7 illustrate the variation of the run time with the changes in the model grid sizes. We can observe that with the increase in horizontal resolution for the same model layer thickness run time increases. Especially when cell sizes smaller than 50 m are used, the run time increases significantly. Also, we can see that the increase in vertical resolution leads to a huge increase in the run time for the finer horizontal cell sizes. One more thing is that we can see FD always has the lower run time for all the cases while TVD and MMOC have relatively faster run time in comparison to HMOC and MOC but not faster than FD. Both MOC and HMOC always have higher run time. For the model layer thickness of 5 m, we can see that MOC has the highest run time of all solvers.

Another way to look at it is through the number of transport steps that the model adopted for calculating the concentration at each stress period. Figure 4-8 shows the number of solute transport steps SEAWAT has used for the whole simulation period. With the increase in the horizontal resolution the number of transport steps increases, as in the run time going finer than 50m increases the number of transport steps significantly. One important thing we can observe is that the vertical thickness has more effect than the horizontal cell sizes for the finer horizontal cell sizes. Since the stability criteria for defining the transport step size is a function of both directions, therefore for the smaller horizontal cell sizes the vertical does control the length of the transport step more. In addition to that, it can be said that TVD always has a higher number of transport steps compared to the other solvers. This is due to a slightly lower flow velocity estimated with the TVD compared to the other solvers.

35
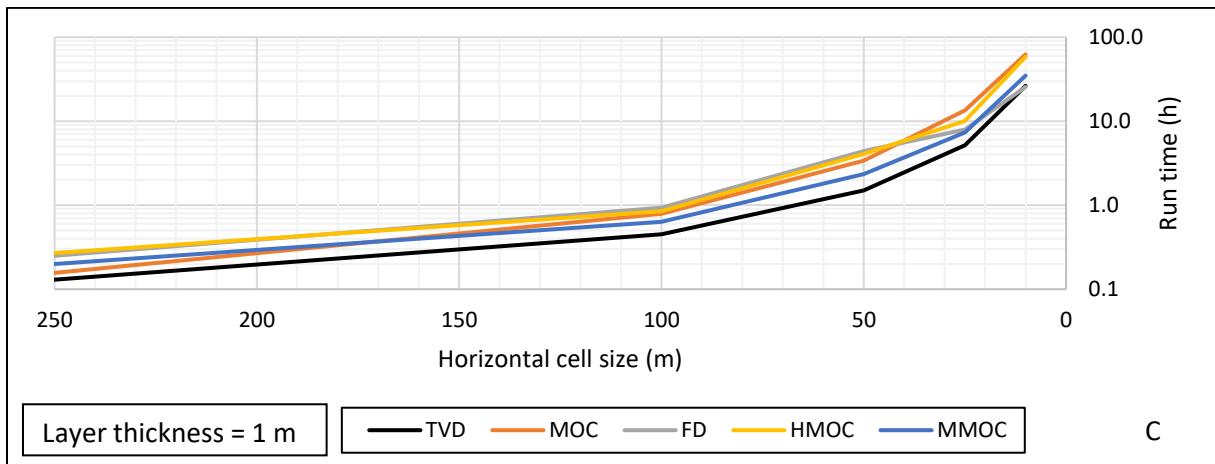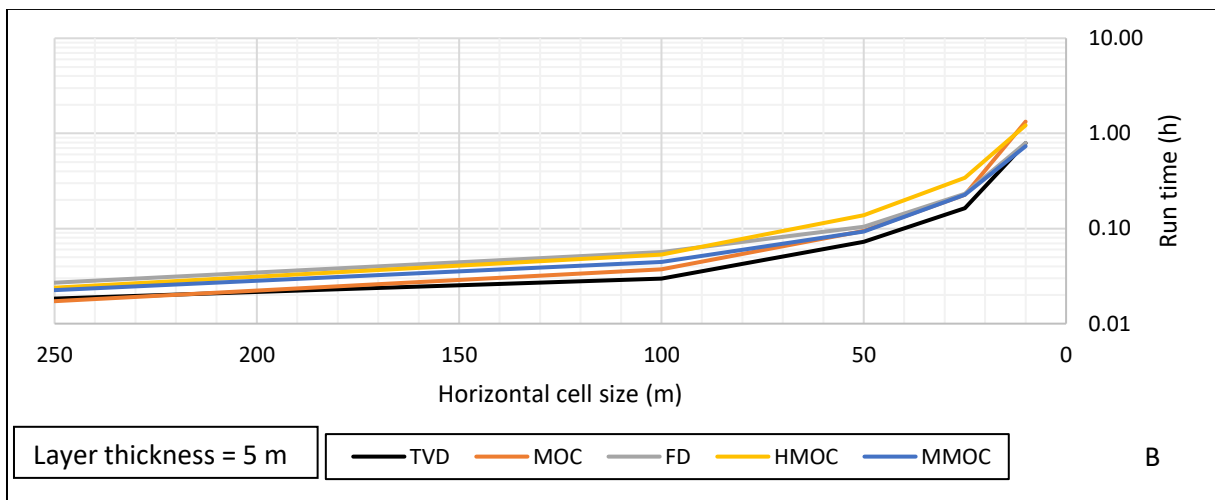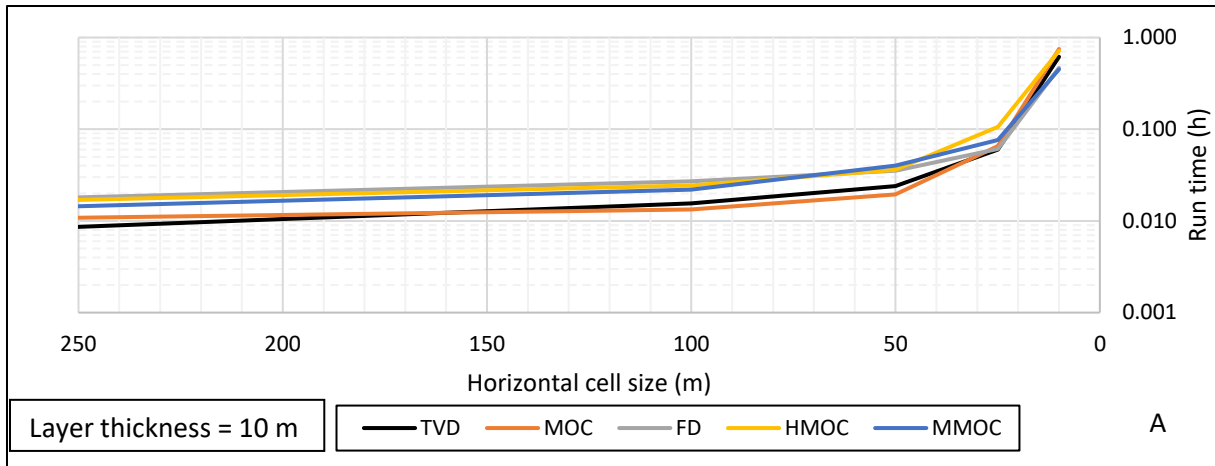
Figure 4-7: The computational time (in log scale) with change in the horizontal cell size for the same layer thickness for different solvers. A: layer thickness of 10 m. B: layer thickness of 5 m. C: layer thickness of 1 m.
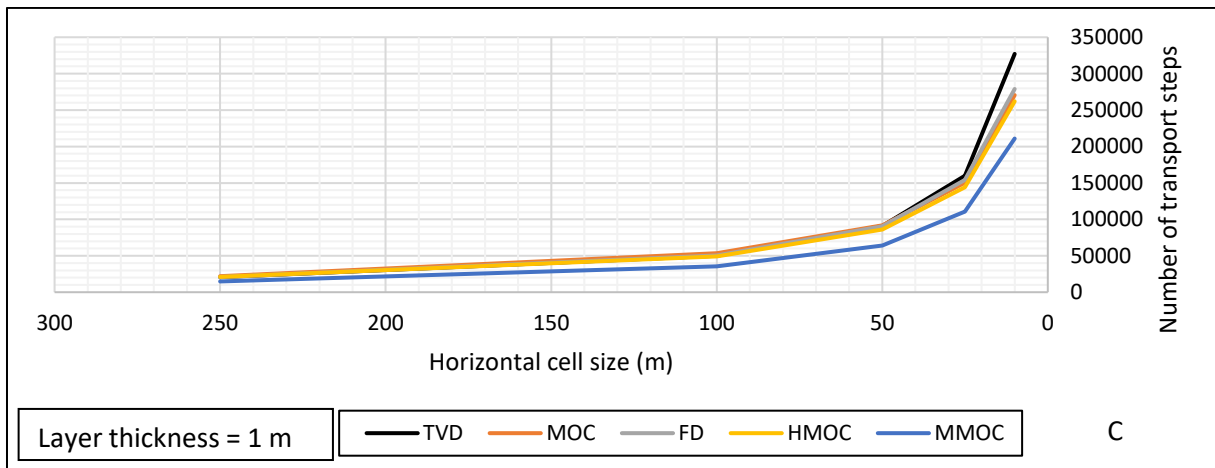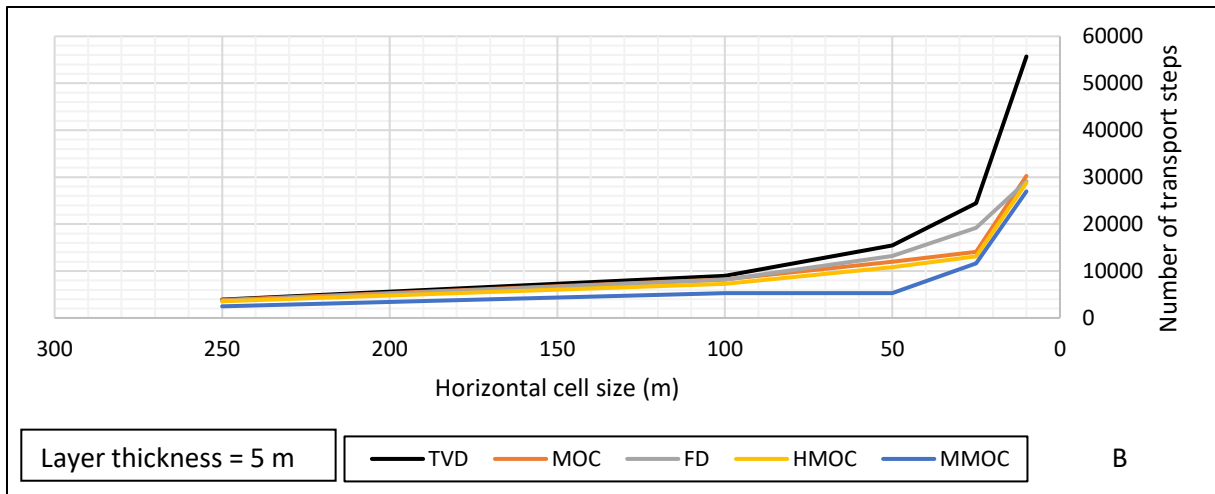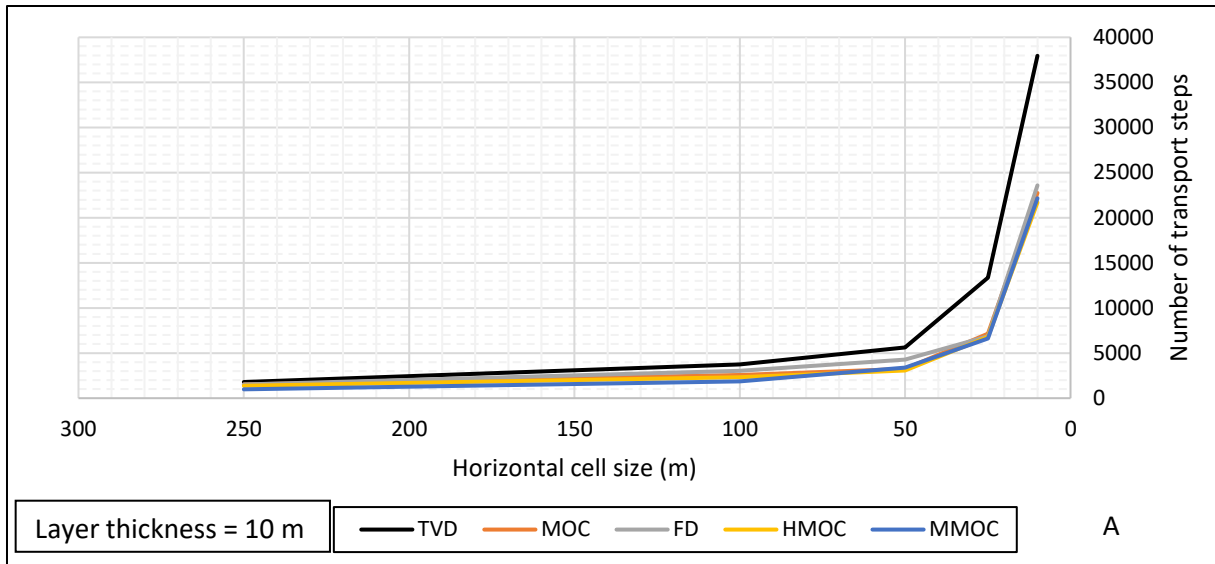
Figure 4-8: The number of transport step for different cell horizontal cell size with the same layer thickness using different solvers. A: layer thickness of 10 m. B: layer thickness of 5 m. C: layer thickness of 1 m.

The freshwater volume for the different model simulations has been compared to the analytical volume from the analytical equation. The results are presented in Figure 4-9. The bigger horizontal cell sizes (coarser models) give a bigger volume and seem to be more accurate as it is closer to the analytical solution volume. However, the fact is that this volume has been calculated by counting the number of cells that have a concentration equal or lower than 1.5 g/l TDS, and then this number of cells is multiplied by the volume of each cell including effective porosity. In the numerical solution, the concentration at the node is the same for the whole cells. So, for the bigger cell sizes, the volume of freshwater is apparently exaggerated. This is shown in the Figures 4-2 and 4-6, and checking the shape of the interface for the coarser models. As can be seen, the line of the analytical solution falls within the thick interface (brackish water) and therefore the actual freshwater volume is less. It can be notices from the figures as well that in terms of freshwater volume accuracy, the vertical cell sizes are important. By comparing the solvers with each other, MOC and TVD have the largest freshwater volumes as they act free of numerical dispersion. At the same time, we can see that FD and MMOC have less water volume due to the numerical dispersion which leads to more brackish groundwater.

4.1.2 Sensitivity of mass budget to the model cell size

We considered the mass balance since SEAWAT is based on mass conservation, not water volume. Before we start comparing the values of the mass budget, we would like to see what terms are considered in the mass balance. There are no sources or sinks within the model of this benchmark, so we have mass entering and mass leaving the model. Mass entering the system will be expressed in terms of recharge from rain and constant head which is the sea and later it will be explained why we have (some) groundwater coming from the sea since the groundwater head is higher than the sea level which means that conceptually, groundwater should only flow from the groundwater system to the sea. Additional terms included in SEAWAT in the mass balance denoted by (DCDT) which is used for the rate of change in the volume due to the change in the solute concentration. As said earlier, there is groundwater entering the model from the sea although the groundwater head is higher, and the groundwater is flowing from the higher head to the lower head. The reason for that is, when the freshwater exiting the model to sea it induces a counter-movement by the friction of different in densities and then creates flow lines from the sea entering into the model and flow to the mixing zone and then flow back to the sea. This can be seen clearly in Figure 4-10, where in the figure to the right, we see the flow lines from the sea to the mixing zone and this is supported by the left graph of the Figure 4-10.
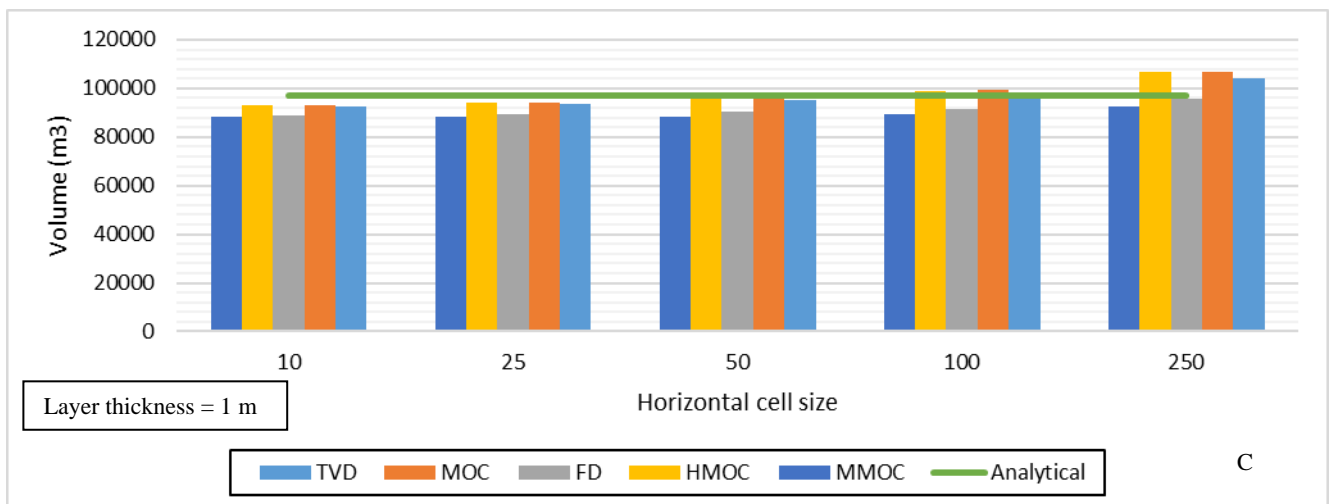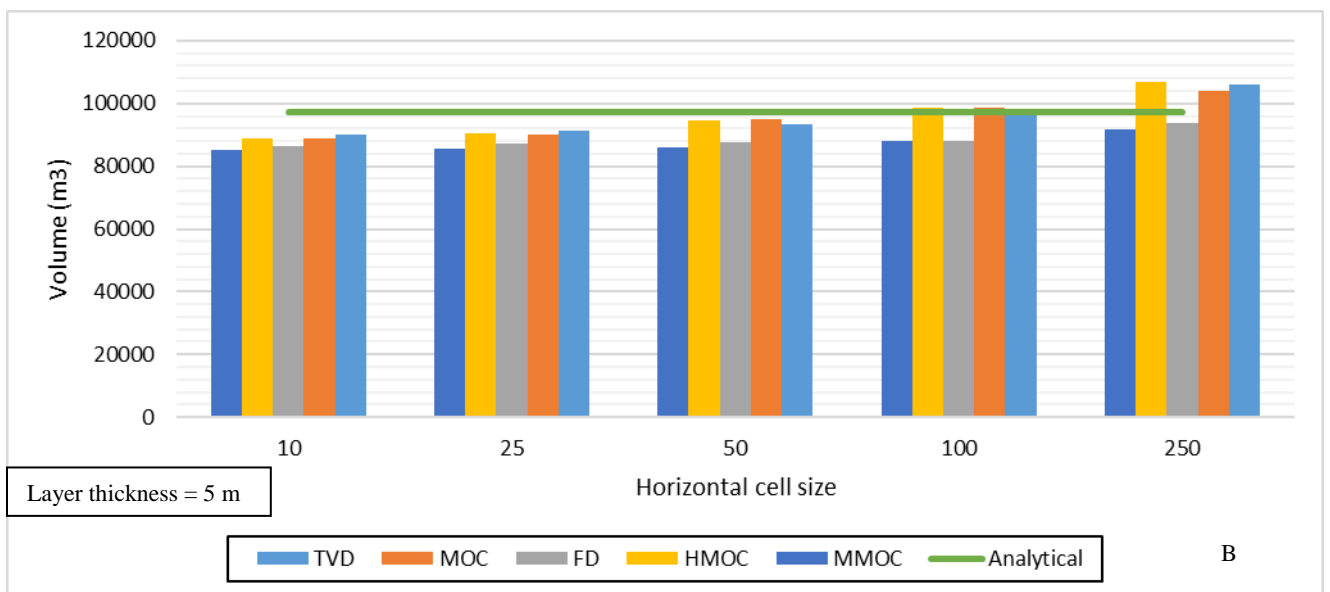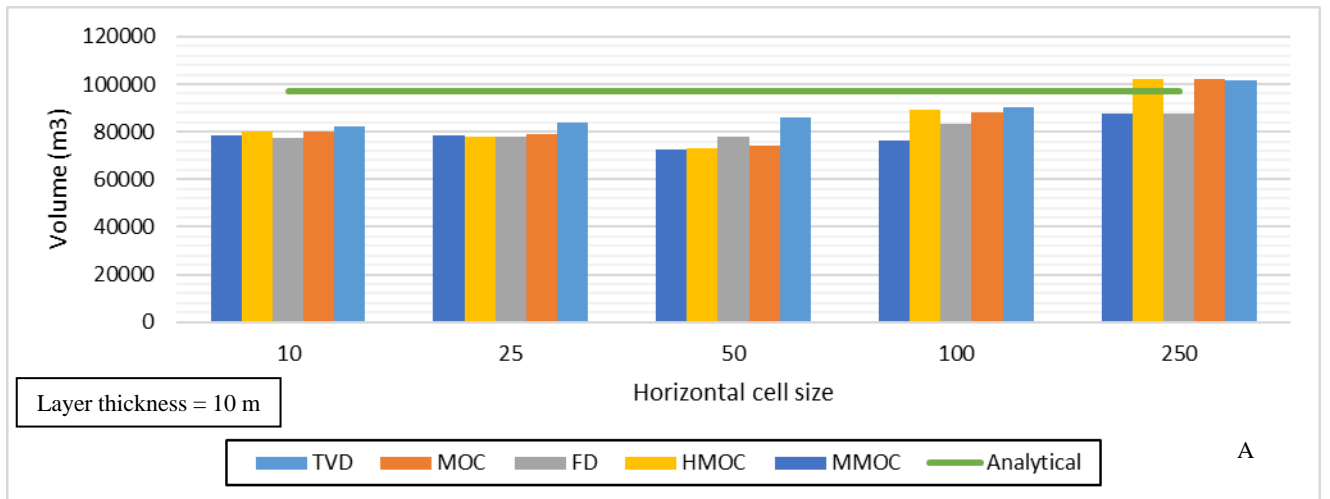
Figure 4-9: Freshwater volume for different horizontal cell sizes using different solvers. A: layer thickness of 10 m. B: layer thickness of 5 m. C: layer thickness of 1 m.
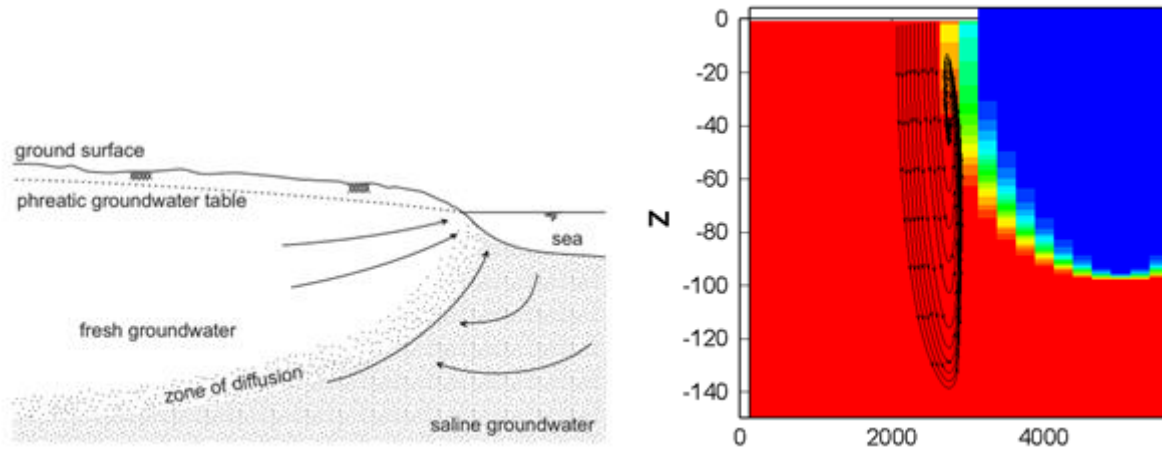
Figure 4-10: circulation of the water from sea to mixing zone and then existing to the sea

Table 4-1, Table 4-2 and Table 4-3 summarise the mass budget for the simulations. For the sake of brevity, only three solvers were included: TVD, MOC, and FD. There is a fixed value for the recharge for all the simulations. The amount of water entering from the sea (called 'constant head') reduces with the increase in the model grid resolutions. This can be related to the size of the horizontal cell, when reducing the size, the outlet becomes closer to the point where the freshwater and seawater meet (which is brackish water) and less circulation occurs as in the right figure in Figure 4-11. In contrast, the bigger cell size leads to outlet point more in the sea and more circulation occurs as in the figure to the left.
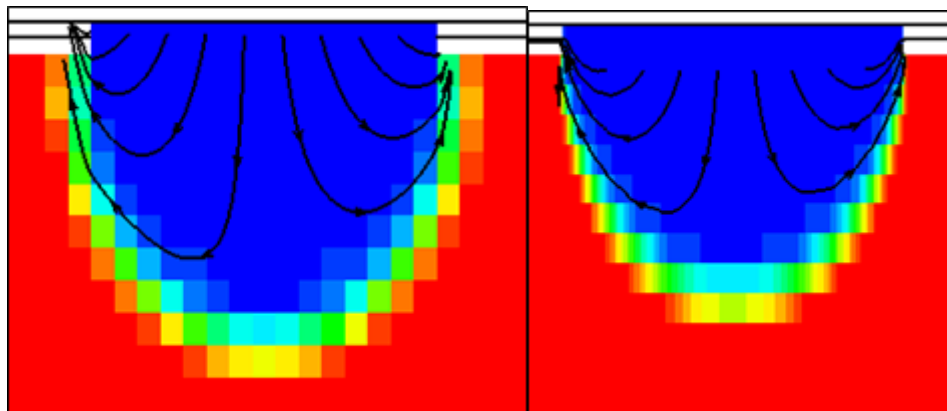
Figure 4-11: Flow lines for freshwater existing the model to the sea.

By comparing the three solvers, we can see that in general FD has the smallest mass error, directly followed by TVD. MOC has a higher mass error in comparison to them (this is known for MOC). The value of DCDT is higher for MOC due to fluctuation in maximum head value with time as a result of the unsmoothed concentration obtained by MOC, unlike the other two solvers.

40

Table 4-1: Mass budget for different spatial discretization using TVD as numerical solver

Horizontal cell size	layer thickness	constant head	recharge	DCDT	total in	constant head	DCDT	total out	in -out
250	10	3328.2	4000.0	0.049	7328.3	7328.2	0.048	7328.3	0.014
100	10	2829.7	4000.0	0.074	6829.8	6829.8	0.075	6829.9	-0.055
50	10	2231.6	4000.0	0.108	6231.7	6231.6	0.106	6231.7	0.038
25	10	1406.6	4000.0	0.222	5406.8	5406.3	0.237	5406.5	0.230
10	10	613.2	4000.0	0.213	4613.4	4613.1	0.243	4613.3	0.079
250	5	3845.9	4000.0	0.089	7846.0	7845.8	0.093	7845.9	0.057
100	5	3396.5	4000.0	0.174	7396.7	7396.4	0.176	7396.6	0.062
50	5	2623.9	4000.0	0.230	6624.1	6623.9	0.238	6624.1	-0.022
25	5	1847.6	4000.0	0.389	5848.0	5847.7	0.401	5848.1	-0.116
10	5	1130.7	4000.0	0.659	5131.4	5130.7	0.688	5131.4	-0.077
250	1	4301.5	4000.0	0.540	8302.1	8301.5	0.584	8302.0	0.027
100	1	4049.4	4000.0	0.657	8050.1	8049.7	0.585	8050.3	-0.174
50	1	3378.0	4000.0	0.870	7378.9	7378.0	0.908	7378.9	-0.025
25	1	2526.8	4000.0	1.721	6528.6	6526.9	1.698	6528.6	-0.061
10	1	1505.1	4000.0	1.857	5507.0	5505.0	1.981	5507.0	-0.040

Table 4-2: Mass budget for different spatial discretization using MOC as numerical solver

Horizontal cell size	layer thickness	constant head	recharge	DCDT	total in	constant head	DCDT	total out	in -out
250	10	3576.1	4000.0	70.141	7646.2	7587.3	59.560	7646.9	-0.627
100	10	3347.7	4000.0	179.749	7527.4	7354.5	173.071	7527.6	-0.153
50	10	1906.4	4000.0	280.640	6187.1	5908.7	279.357	6188.0	-0.934
25	10	1367.8	4000.0	317.810	5685.6	5349.5	337.427	5686.9	-1.294
10	10	630.7	4000.0	549.760	5180.7	4635.3	542.639	5177.9	2.543
250	5	4207.3	4000.0	96.550	8303.8	8221.0	82.914	8303.9	-0.106
100	5	3307.5	4000.0	102.978	7410.5	7295.7	116.062	7411.7	-1.253
50	5	2154.6	4000.0	202.872	6357.5	6150.9	206.377	6357.3	0.205
25	5	1726.2	4000.0	284.698	6010.9	5704.9	304.683	6009.5	1.376
10	5	748.6	4000.0	424.198	5172.8	4785.8	381.134	5167.0	5.810
250	1	4932.0	4000.0	514.392	9446.4	8902.1	544.355	9446.5	-0.126
100	1	5091.7	4000.0	325.433	9417.1	9051.3	365.810	9417.2	-0.061
50	1	3898.2	4000.0	334.743	8233.0	7980.0	253.662	8233.6	-0.647
25	1	2529.2	4000.0	244.257	6773.5	6532.1	262.327	6794.4	-20.896
10	1	1453.2	4000.0	296.680	5749.9	5439.0	303.619	5742.6	7.300

'

Table 4-3: Mass budget for different spatial discretization using FD as numerical solver

250	10	4004.4	4000.0	0.043	8004.5	8004.4	0.061	8004.5	0.008
100	10	3752.3	4000.0	0.117	7752.4	7752.4	7752.255	0.1	-0.003
50	10	3098.8	4000.0	0.692	7099.5	7098.8	0.662	7099.5	0.019
25	10	2456.4	4000.0	0.504	6456.9	6456.4	0.515	6456.9	-0.008
10	10	2098.0	4000.0	0.445	6098.4	6098.0	0.484	6098.5	-0.033
250	5	4367.7	4000.0	0.082	8367.8	8367.6	0.104	8367.7	0.000
100	5	4219.9	4000.0	0.425	8220.4	8220.0	0.426	8220.4	-0.044
50	5	3556.1	4000.0	0.356	7556.5	7556.1	0.362	7556.4	0.033
25	5	2771.8	4000.0	0.637	6772.4	6771.7	0.684	6772.4	0.083
10	5	2116.9	4000.0	0.457	6117.3	6117.0	0.453	617.5	-0.118
250	1	4611.9	4000.0	0.561	8612.5	8611.8	0.569	8612.4	0.060
100	1	4477.3	4000.0	1.796	8479.1	8477.3	1.862	8479.2	-0.046
50	1	3787.0	4000.0	0.000	7787.0	7787.0	0.000	7787.0	0.000
25	1	2916.8	4000.0	0.000	6916.8	6916.8	0.000	6916.8	0.000
10	1	1828.1	4000.0	0.000	5828.1	5828.1	0.000	5828.1	-0.026

4.1.3 Sensitivity of the sharp interface to the convergence criteria and courant number

Both head and flow convergence criteria have no much influence in this case in terms of the shape of the interface. The shape of the interface has not changed significantly. However, these criteria have some influences regards the mass budget. For example, increasing the flow convergence criteria from 0.1 to 1 has led to mass balance error increasing from 4.59E-02 to 0.157 for the FD and from 6.05E-2 to 4.55 for MOC. However, setting the convergence criteria very small can lead to an increase in the run time by increasing the number of iterations required, therefore in real cases setting these criteria should consider both acceptable runtime and small mass error.

Reducing the courant number leads to a reduction in a part of the cell that the particles can move in one transport step, which put restriction on the length of the transport step by making it shorter. In terms of the interface in this benchmark, the courant number has not much influence on the shape of the interface which remains the same.

4.1.4 Sensitivity of sharp interface to solvers and solver's settings

First, the differences between the solvers themselves will be addressed and then some solvers' settings that might influence the results will be high lightened.

Some differences were already addressed in the above-mentioned sections in terms of mass balance errors, runtime, freshwater volume and the shape of the interface. Considering the finer model grid, FD and MMOC have a wider transition zone in comparison to the other three solvers due to the influence of the numerical dispersion (see Appendix B). Looking closely at the shape of the interface as shown in Figure 4-12, MMOC and FD have a smoother pattern while TVD, MOC, and HMOC have a sharp interface.
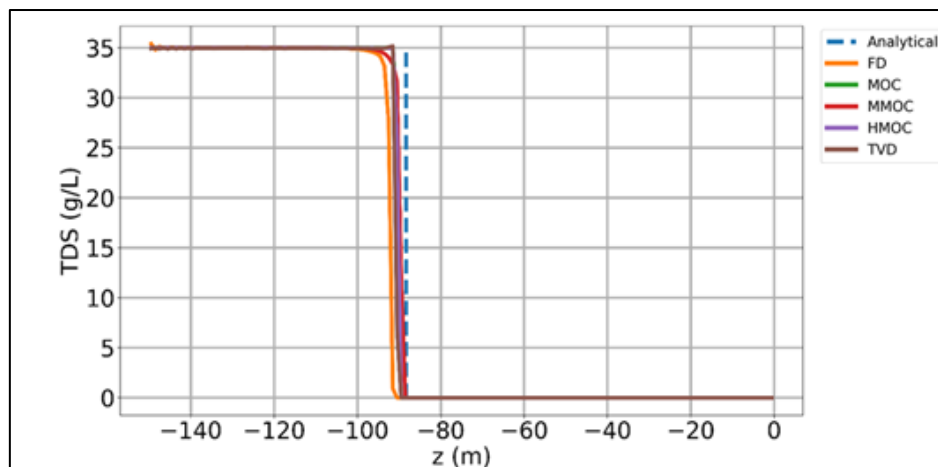
Figure 4-12: shape of the interface at the centre of the model

Moving to the second part in which some solver's settings are changed. For the FD method, results for simulating the case with upstream weighting and central in space methods are presented in Figure 4-13.
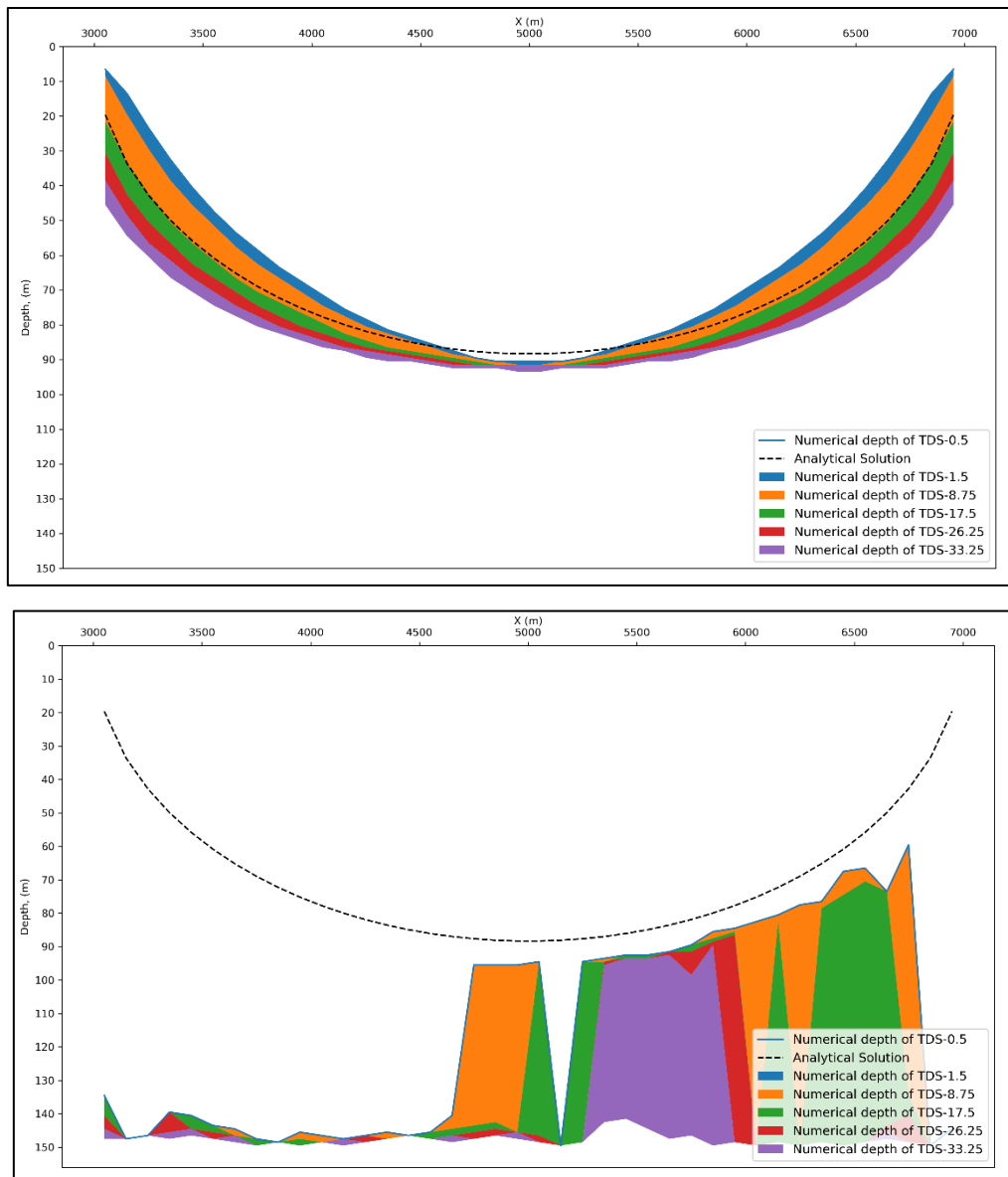
Figure 4-13: Shape of the interface: FD method, cell sizes are X Y: changes between upstream weighting (top) case F_FD012 and central in space (bottom) Case F_FD0026

For MOC changing the weighting factor between 0.5 and 1 has no big differences. Another interesting parameter in the MOC solver is DCEPS. This threshold values means that when the concentration gradient in a cell is higher than that value, more particles are placed per cell (viz NPH). The effect of increasing the value means the shape of the interface is less accurate, as can be seen in Figure 4-14. The increase in the value of DCEPS to 1E-1 has led to a change in the position of the isochore of 0.5 and 1.5 g/l TDS lines due to the change in number of particles

45

per cell if the concentration gradient is lower than DCEPS (there are now more cells with less particles (equal to NPL).
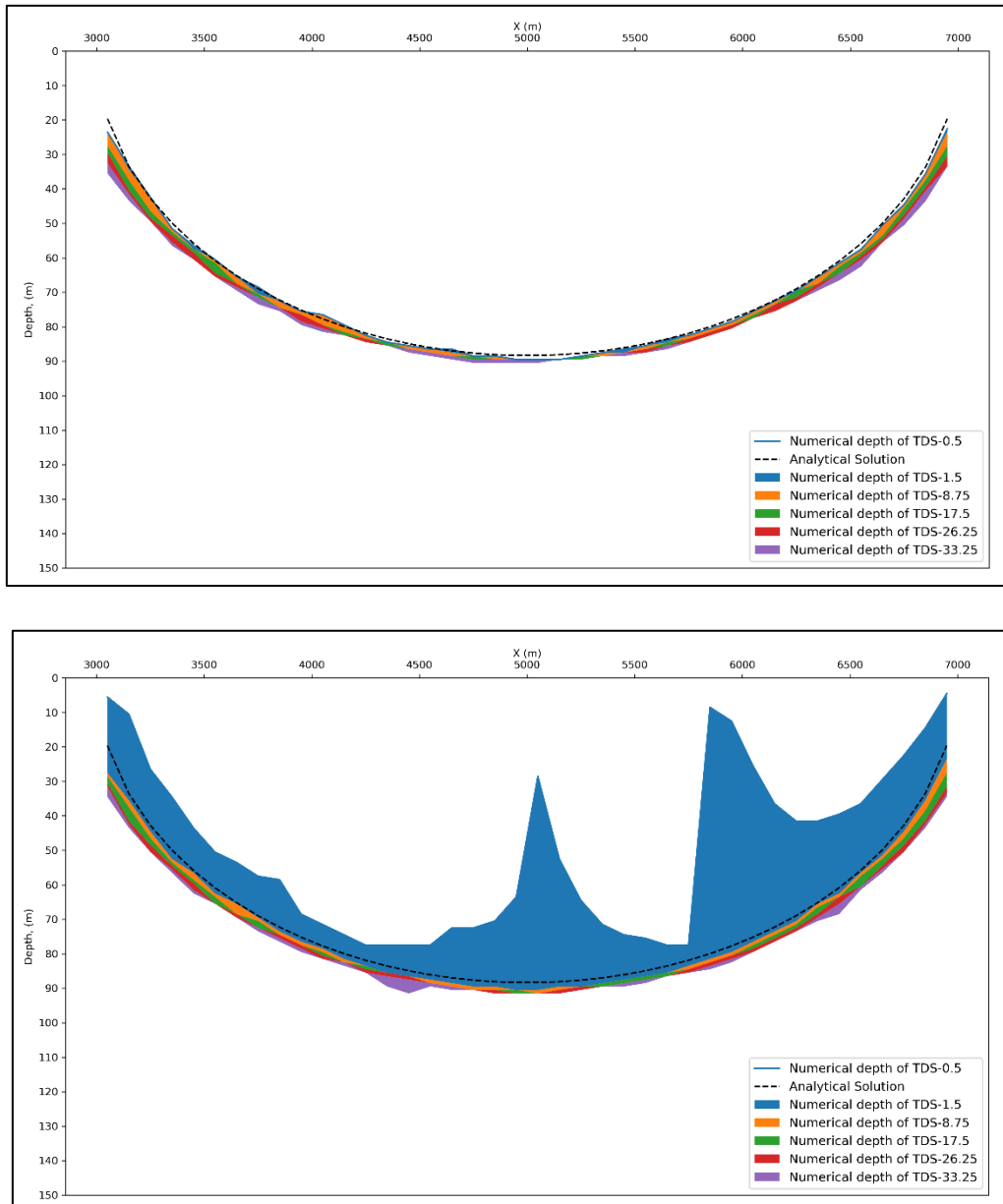
Figure 4-14: Shape of the interface: effect of changing DCEPS from 1E-5 to 1E-1 case F_MOC032

4.2 Henry

4.2.1 Sensitivity of Henry case to model discretization

Results for two different model discretization is shown in Figure 4-15. Reducing the cell size has resulted in a more accurate result where the locations of the lines for the salinity distribution are closer to the semi-analytical solution of the modified Henry case. One change has been done

since the coarser model was already close to the semi-analytical solution, viz. decreasing the grid cell dimension in order to make the results more accurate.
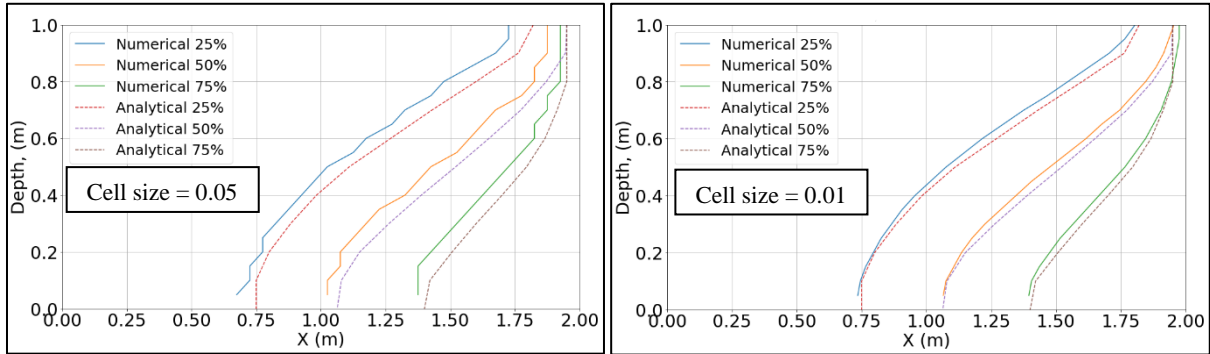
Figure 4-15: The 25%, 50% and 75% isochore lines for two model discretization against the semi-analytical solution (Simpson and Clement, 2004).

4.2.2 Sensitivity of Henry case to solvers

The model simulation results were compared to the semi-analytical solution of the modified Henry case. The positions of the 25%, 50% and 75% isochores lines were taken from (Simpson and Clement, 2004). The same case was with the same discretization in the paper, but with different solvers to examine the effect of the solvers. A comparison of different solvers can be seen in Figure 4-16.
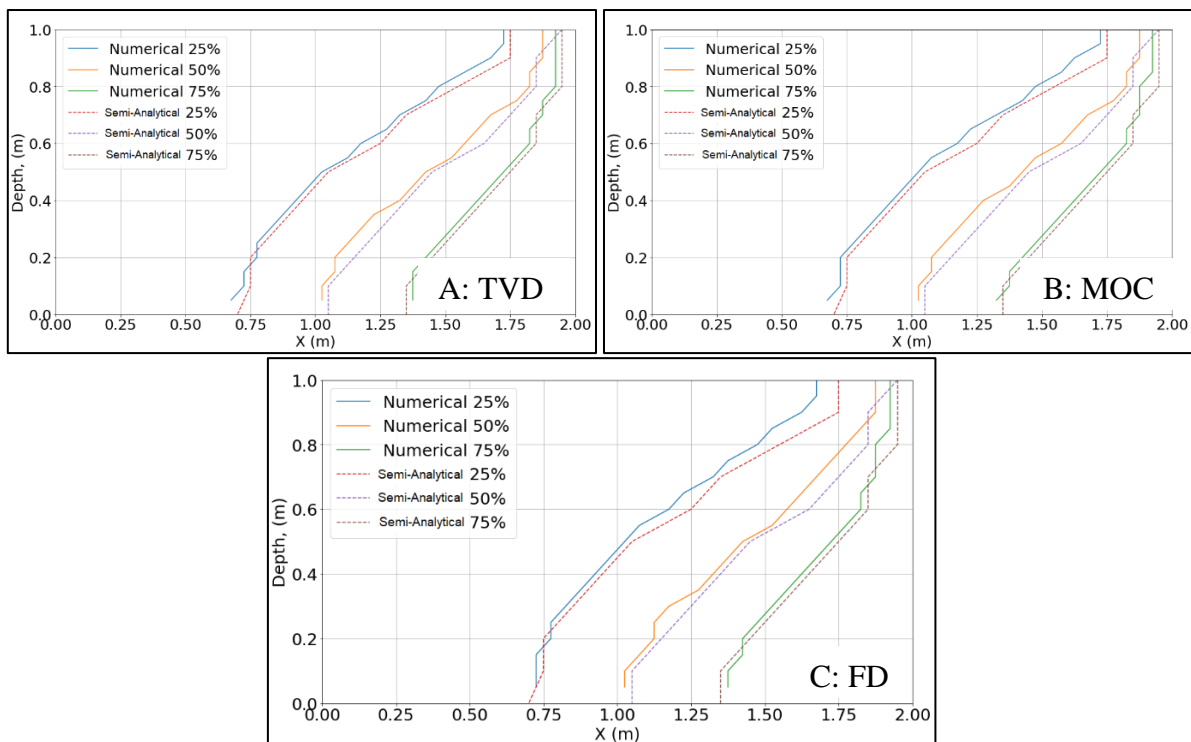
Figure 4-16: Comparison between the model simulation and the semi-analytical solution of the modified henry case using three solvers. A: TVD, B: MOC, C: FD. For cell size of 0.05

From the figure, it can be seen that there is no significant difference between the solvers in simulating the case. However, the solvers do not match 100% with the semi-analytical solution as the values of the position of isochore were approximated from the paper and the coarser grid was used for the comparison. In this case, the process was controlled by the molecular diffusion and not the advection process, which is why the solvers have the same results. As it is known that in the solute transport equation the advection term is only solved with different numerical schemes while the other terms are solved using the finite difference approach.

In terms of mass budget, as in Table 4-4, we have saline groundwater entering from the sea and which circulates within the mixing zone before existing to the sea with the freshwater flux. Regards the solvers: TVD and FD have lower mass balance error while the MOC has the higher rate of change in volume with change in concentration, as also observed above in Section 4.1 in the freshwater lens case.

In general, the Henry case that is tested is a widely used case for testing variable-density groundwater flow and coupled salt transport models because it simulates the process of seawater intruding a coastal aquifer. Besides that, the modified case by (Simpson and Clement, 2004) was used because reducing the amount of the freshwater fluxes makes the case more worthiness. Since our interest was mainly about the difference between the solvers and some settings, the results showed no noticeable differences. Therefore, we did not carry out other tests.

Table 4-4: Mass budget for the modified Henry case simulation.

		TVD	MOC	FD
In	Sea	1365.5	1351.7	1379.7
	Freshwater flux	2840.0	2840.0	2840.0
	DCDT	0.010	6.658	0.007
	Total in	4205.5	4198.4	4219.7
Out	Sea	4206.0	4188.1	4219.1
	DCDT	0.700	12.770	0.717
	Total out	4205.7	4200.9	4219.8
	In - out	-0.169	-2.543	-0.106

4.3 Saltwater pocket

4.3.1 Sensitivity of the case to changes in grid size

The number of cells used in the case has a big influence on the model results and the number of fingers formed. In Figure 4-17, the difference between the coarser and the finer gird is clear, and it can be seen that the fingering process of the saltwater going down will the freshwater trapped under the saltwater pocket moving upwards in between the saltwater. There is no fixed number of fingers that have to develop but we can see with the increase in model discretization the number of fingers is increasing.
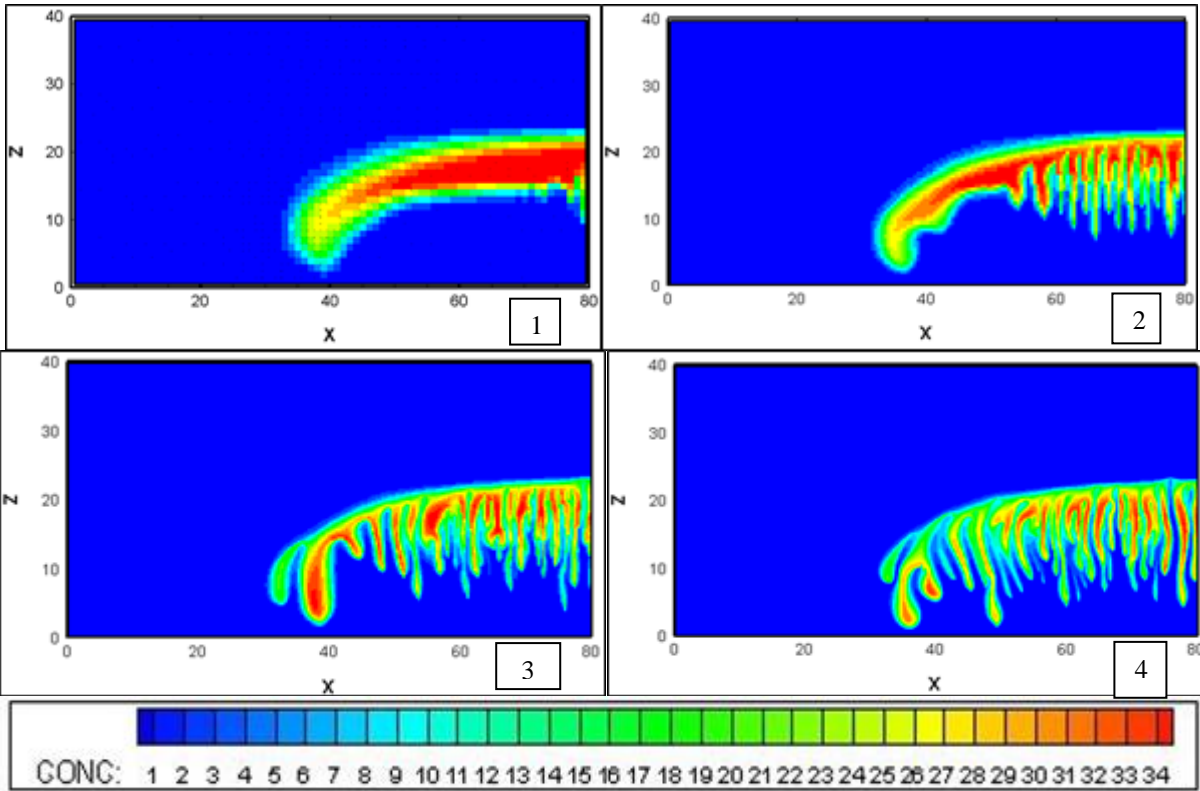
Figure 4-17: effect of grid size of the formation of the fingers. [1]:dx, dz = 1.0 m, [2]: dx,dz = 0.5m [3]: dx,dz = 0.25 m   [4] dx,dz = 0.125 m after 3600 min using FD

4.3.2 Sensitivity of the case to the solvers

The effect of different solvers on the results is depicted in Figure 4-18, the results are for the fine model grid. The fingers have developed when FD and MMOC are used, also to some extend TVD has formed some of the fingers but the salt concentration is distributed. While for the MOC and HMOC, no fingers have formed even in the finer grid. This can be related to the addition of the numerical dispersion error by the FD and MMOC where both solvers suffer from this error and add more dispersion to the actual hydrodynamic dispersion terms. On the

49

other hand, MOC and HMOC are free from numerical dispersion and on top of that, the nature of the particle tracking scheme in solving the advection terms has led to the distribution of the salt concentration.
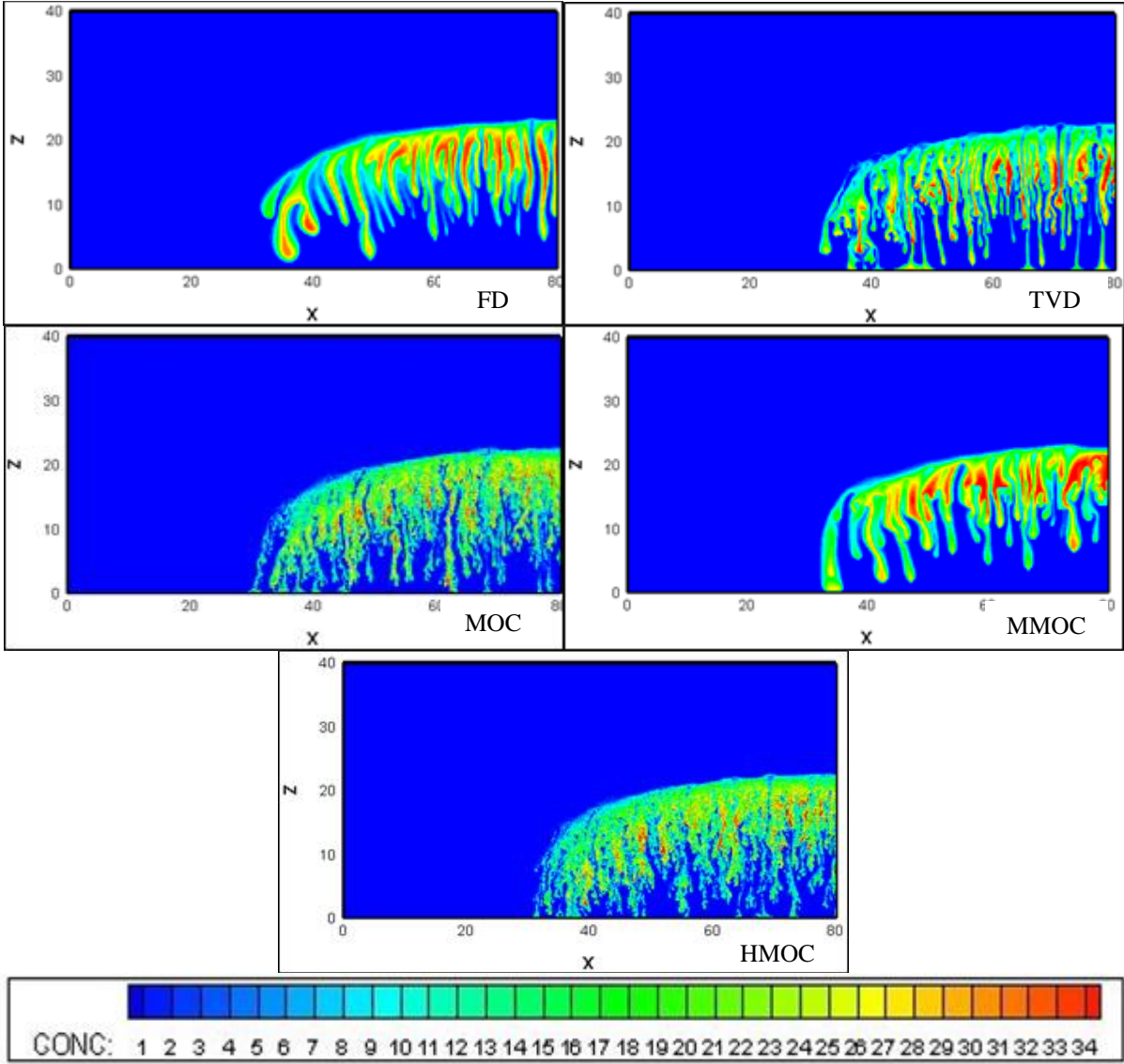
Figure 4-18: Effect of solvers on the formation of the salt fingers after 3600 min for cell size of 0.125 m

The effects of the mechanical dispersion of the development of the salt fingers are examined for different solvers and the influence is presented in Figure 4-19. It is obvious that increasing the mechanical dispersivity (as I increased the value of longitudinal dispersivity al) helped MOC and TVD to form clear and thicker fingers, At the same time, FD still faces problems due to numerical dispersion; on top the movement of the fingers in the medium slowed down; as if small fingers can reach the bottom earlier. However, there is no reference to compare all of these results to but in overall it can be said that the discretization of the model has significant influence in the formation for of the fingers, and for MOC and TVD, the value of the mechanical
50

dispersion is of an important matter and need to be examined carefully in such as cases where salt groundwater lays on top of fresh groundwater.
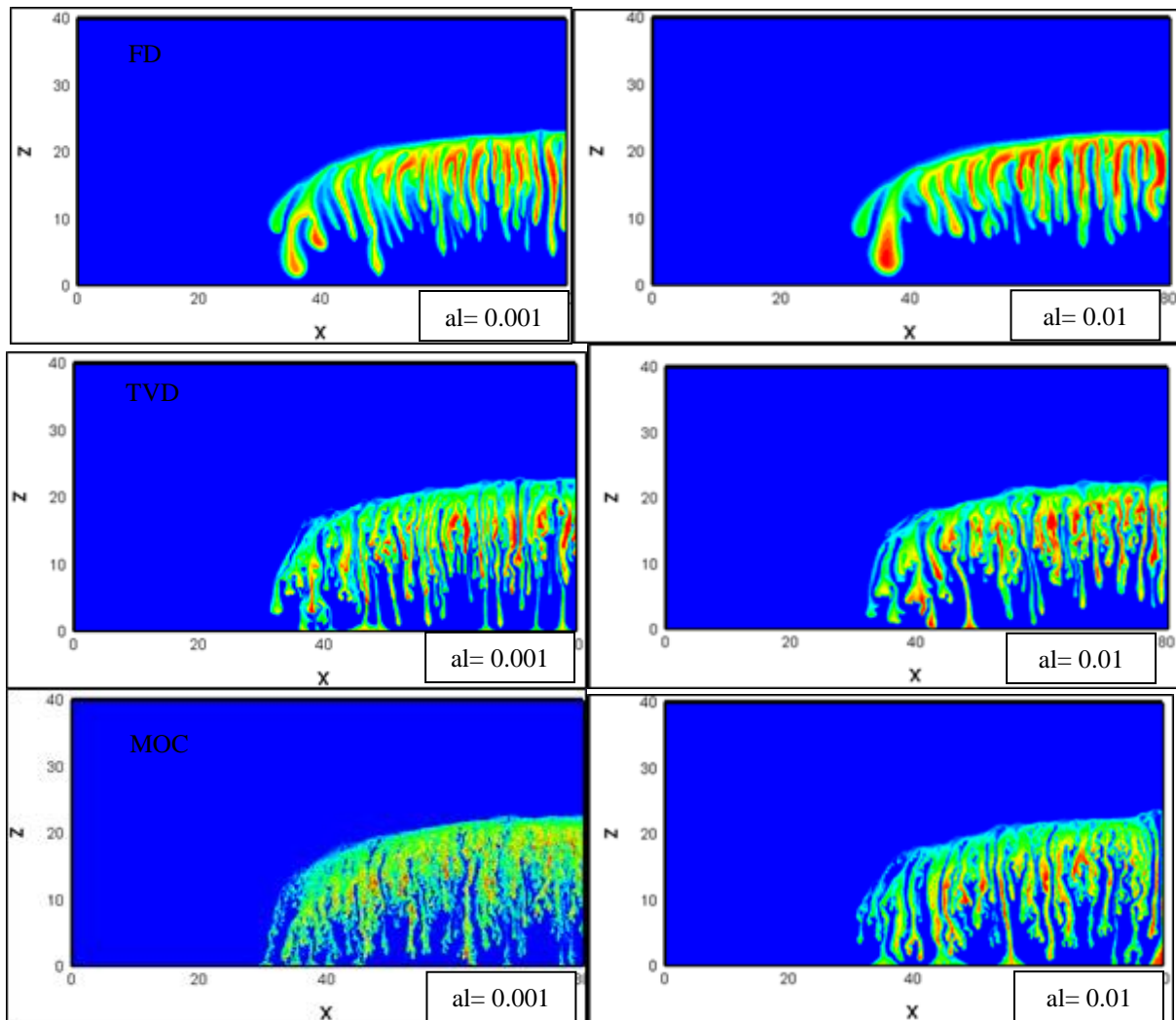
Figure 4-19: Effect of changing the mechanical dispersion on the formation of the fingers using cell size 0.125m

The additional test has been carried out for MOC to see the influence of the number of particles used. The number of particles used for the cells which has a small concentration gradient was set to zero (NPL = 0) as these cells considered negligible. This number was set equal to the number of particles used in other cells (16 particles) which are considered due to the higher concentration gradient (NPL = NPH = 16). The results for this simulation are shown in Figure 4-20. By comparing this figure with the results obtained by MOC in Figure 4-18, it can be seen that by setting the number of particles equal in all the cells some of the fingers have formed. By doing that a uniform situation is created and this led to results also closer to the results obtained by increasing the value of the mechanical dispersion.
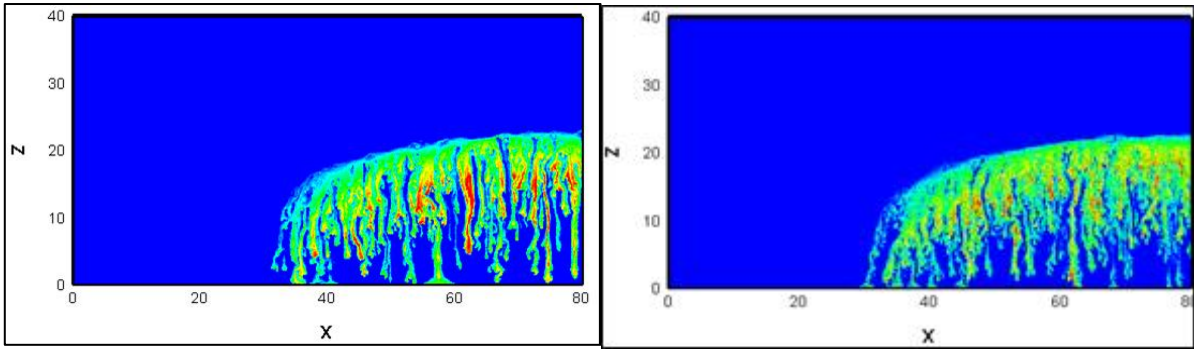
Figure 4-20: Effect of making NPL equal to NPH with 16 particles each on the formation of the salt fingers;
MOC solver, al=0.001, cell size of 0.125 m

4.4 DOW model

4.4.1 Results of groundwater flow

A comparison between the available observation and simulated groundwater heads is depicted in Figure 4-21 and Figure 4-22. The measured values are available for the period between 1959 and 1978. Averaged values for these locations are compared to the averaged values for the groundwater heads resulted from the model as can be seen in Figure 4-21. The correlation (R^2) is 0.792 which shows for a 3D dynamic model a plausible good correlation. However, the transient comparison (Figure 4-22) is not matching exactly but is fluctuating within the range of the observed values. Many factors can influence the mismatch. For instance, the recharge values are averaged over the period for each month, and therefore, the actual fluctuation of the values cannot be seen. In addition, also the dynamic influences from humans (not modelled as the input data are not known) in the area can led to changes in the groundwater flow regime which is not modelled. Finally, changes in the topography of the area also could cause some mismatch between observation and modelling results.
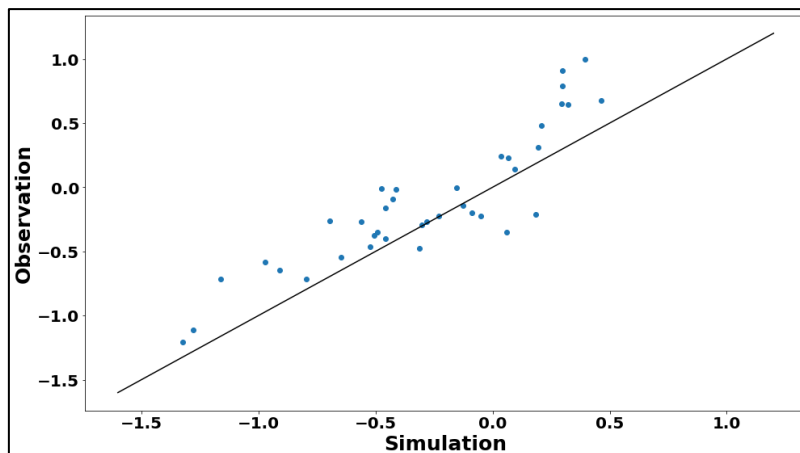
Figure 4-21: Comparison between the observed and the simulated groundwater head in the DOW model area.
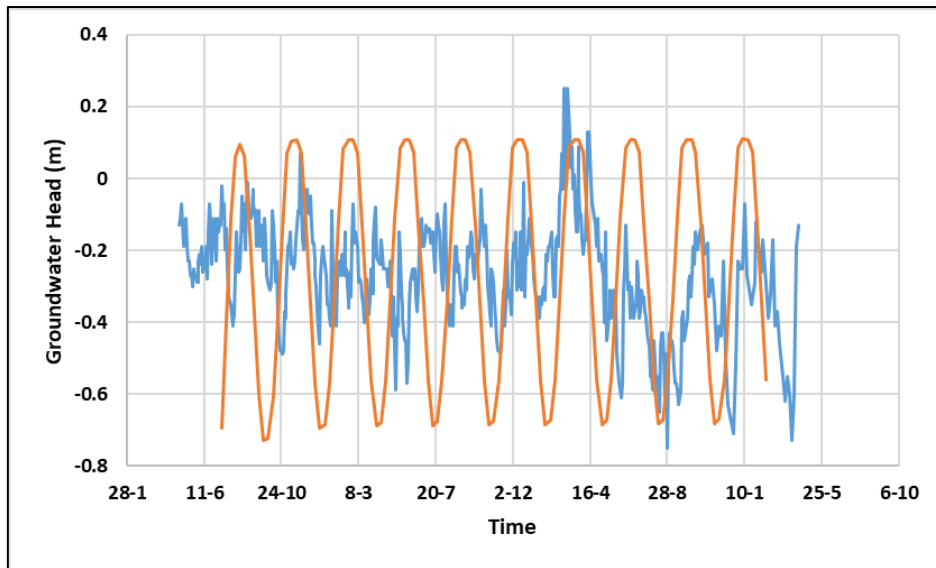
Figure 4-22: Transient comparison between the observed (blue) and the simulated (orange) groundwater heads.

4.4.2 Water budget

The summary of the water budget rates in m^3/day for the last simulation year is presented in Table 4-5. The drainage system drains more water during the winter period as the groundwater table is higher. At the same time the rivers, either in river package or GHB, give water to the aquifer during the summer period. But during the winter, the rivers and GHB drain more water out of the system. This is due to the control of the river stages by the waterboarded. The river stages are kept lower during the winter period which allows more water to drain out from the groundwater system. During the summer the water level in these rivers is kept higher which leads to more recharge induced to the groundwater system. In the GHB, some of the water is entering or leaving through the model sides as it is head-dependent boundaries, but the ratio of the vertical fluxes to the horizontal fluxes is higher.

The recharge is the net recharge which is the difference between the precipitation and the evapotranspiration. During the winter periods, the water appears as a recharge to the groundwater system but during the summer the water is taken out as an influence of a larger average evapotranspiration. The dynamics between the rivers, drains and recharge is what mainly controls the groundwater in the groundwater system. It results generally in more water leaving the storage during the summer than it is entering during the winter period.

4.4.3 Chloride distribution

Contour maps for the distribution of the chloride distributions are presented in Figure 4-23 and Figure 4-24. These maps presented here are just an example of the chloride distribution and shows the different distribution for different model layers.

53

Table 4-5: Water budget for the DOW model in m^3/day for year 2050

MONTH	DRAINS	GHB (BIG RIVERS +BOUNDARIES)	RECHARGE	SMALL RIVERS	STORAGE	DCDT	TOTAL IN	DRAINS	GHB (BIG RIVERS +BOUNDARIES)	RECHARGE	SMALL RIVERS	STORAGE	DCDT	TOTAL OUT	CHANGE IN STORAGE
AUG	0.00	4366.93	0.00	9368.61	22029.33	847.98	36612.86	-165.73	-594.47	-33957.00	-1047.25	-1.54	-822.82	-36588.81	24.05
SEP	0.00	3406.48	0.00	8767.99	1952.88	955.89	15083.24	-231.54	-879.69	-9432.50	-1147.33	-2436.71	-914.03	-15041.80	41.43
OCT	0.00	2173.31	11319.00	7274.41	106.23	733.33	21606.28	-467.47	-1831.60	0.00	-1459.43	-17113.49	-660.03	-21532.02	74.25
NOV	0.00	4229.41	34550.00	2653.29	590.04	285.32	42308.06	-2297.75	-3562.97	0.00	-2929.34	-33230.73	-236.75	-42257.53	50.53
DEC	0.00	1741.03	67539.51	933.28	41.26	162.74	70417.81	-6918.52	-5554.40	0.00	-6743.52	-51037.87	-107.50	-70361.81	56.00
JAN	0.00	1216.67	67714.62	480.84	40.27	320.58	69772.99	-22614.35	-7341.98	0.00	-10220.89	-29273.83	-198.87	-69649.92	123.07
FEB	0.00	1333.46	52407.87	380.48	101.47	295.48	54518.76	-25367.44	-7532.77	0.00	-11196.68	-10126.45	-193.06	-54416.40	102.37
MAR	0.00	1509.19	42203.37	354.49	929.47	101.55	45098.06	-22811.52	-7329.01	0.00	-11151.55	-3704.29	-68.78	-45065.15	32.91
APR	0.00	2224.10	13205.50	423.66	9809.20	347.23	26009.70	-10319.71	-6077.01	0.00	-9051.20	-215.38	-255.85	-25919.15	90.55
MAY	0.00	1265.19	0.00	3147.33	39874.46	657.84	44944.82	-1321.87	-4864.34	-33957.00	-3761.24	-386.16	-520.49	-44811.10	133.72
JUN	0.00	2180.11	0.00	5995.02	38090.94	424.67	46690.74	-509.94	-2215.12	-41503.00	-1990.65	-47.61	-366.89	-46633.21	57.53
JUL	0.00	3841.47	0.00	8477.46	39063.91	817.70	52200.54	-224.98	-890.78	-49049.01	-1217.68	-1.96	-765.06	-52149.46	51.07
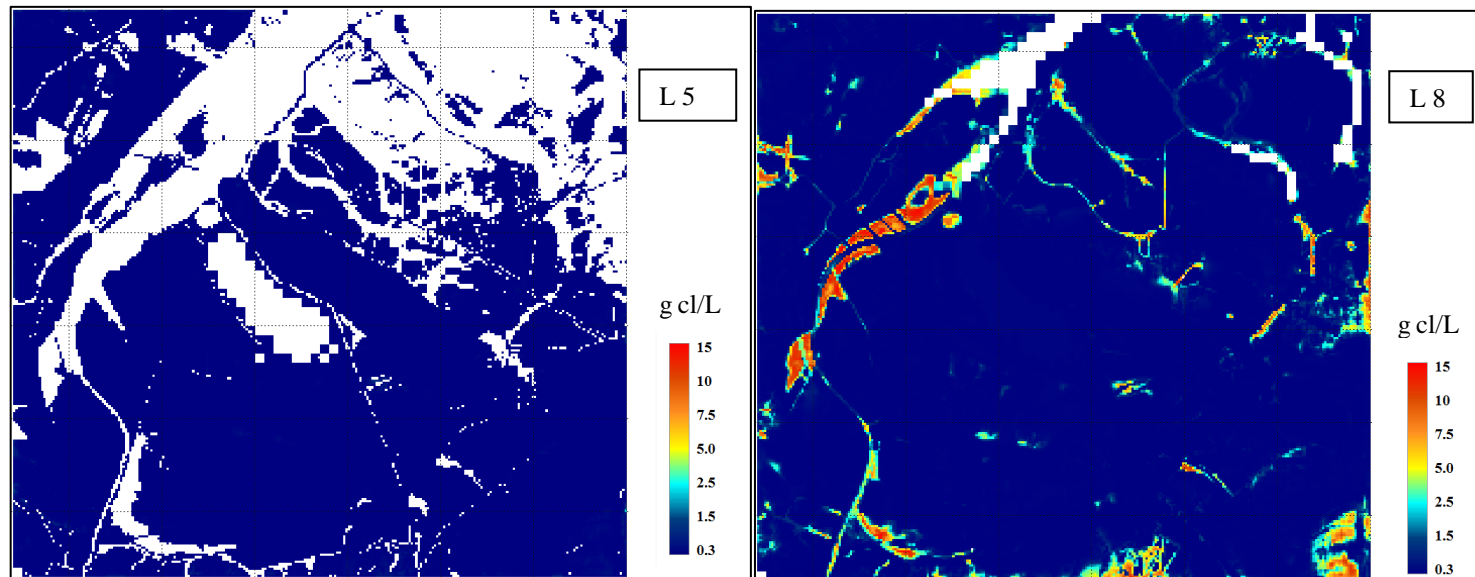
Figure 4-23: Chloride distribution in the model domain for the model layers 5 and 8.
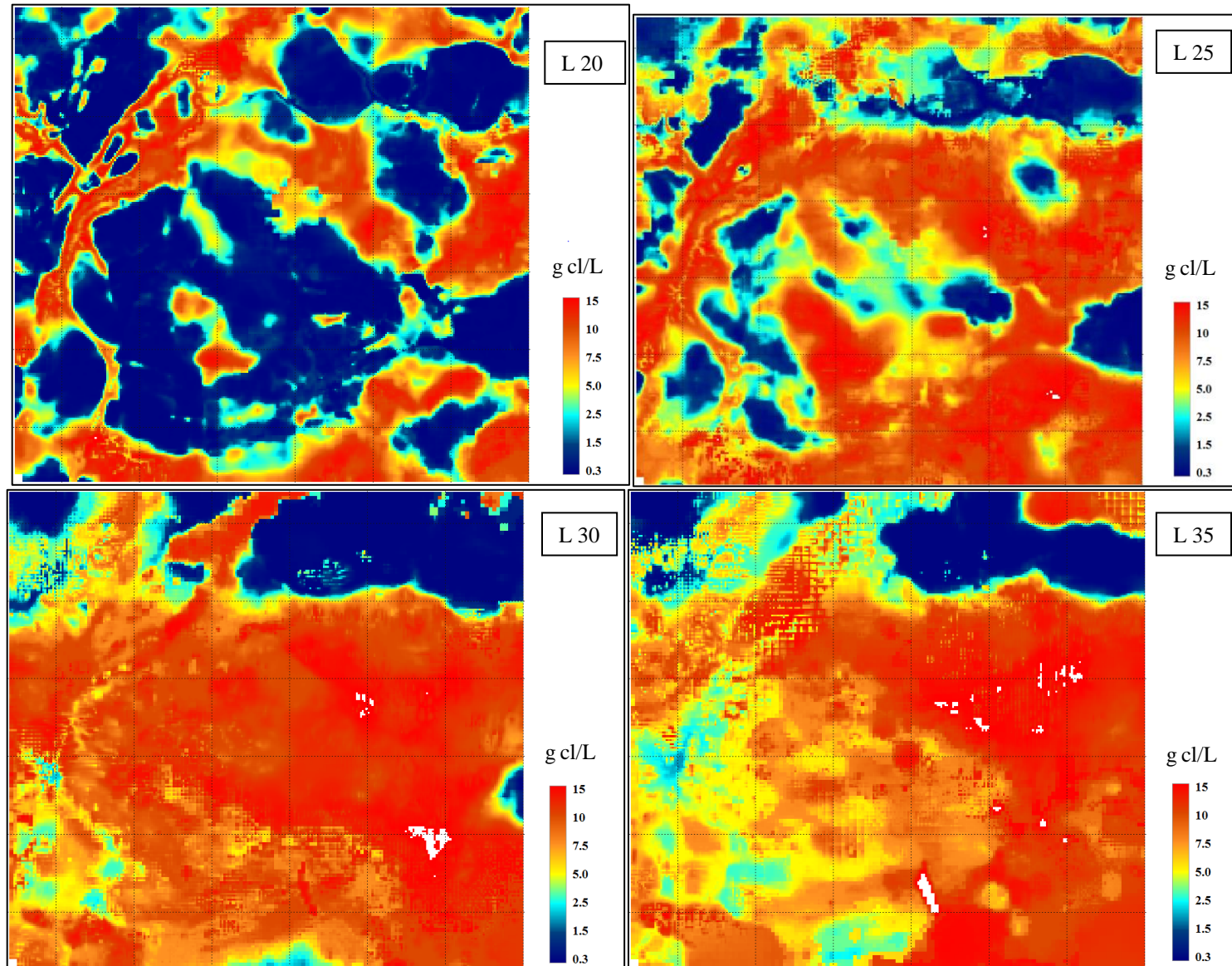
Figure 4-24: Chloride distribution in the model domain for different layers.

The first four model layers are not presented above because these layers have few active cells and the chloride concentration is mainly less than 0.1 g/l which is freshwater. In model layer 5 (1 m NAP), it is the same situation as most of the model domain is freshwater with a concentration lower than 0.2 g/l, except for few spots.

In model layer 8 (-1 m NAP), the chloride starts to cone up under the rivers due to the higher vertical velocity due to the exchange with the bigger river system. This causes some saline water to seep into the rivers. Moving downwards in depth, the up-coning is increasing and other areas with saline groundwater start to appear, as can be seen in model layer 20 (-13 m NAP). In the same model layer 20, the area in the middle of the model is still fresh which corresponds to higher elevation, and therefore, the freshwater lens is thicker in this location. Then, these areas become more brackish while going down as more saline water is present in the lower model layers.

Reaching model layer 30 (-23 m NAP), most of the groundwater in the model domain is saline except small part in the northern side, where fresh water is presence under saline groundwater in the top model layers (here an inversion of saline-fresh groundwater is existing and only can happen as the in between geology consists of a very low hydraulic conductivity). In deepest model layers, the eastern side remains saline and some areas in the western side start to become brackish with very small spots of fresh groundwater.

4.4.4 Sensitivity of the model to grid size

The cell sizes have been changed from 25 to 50 and 100 m while keeping the layer thickness constant at 2m. Then keeping the same cell size at 25 m but changing the layer thickness between 1, 2, 5 and 10 m. A comparison between these models is in the bases of differences in the cross-sections of the chloride distribution and run time.

Results for changing the cell size for the same layer thickness is depicted in Figure 4-25. With the increase in the cell sizes, more brackish water in the transition zone is present as a result of the numerical dispersion. In addition to that, the presence of the higher chloride concentration (dark brown color) is sharper in the smaller cell size but in the bigger cell sizes, the concentration is distributed and less severe. Furthermore, at Y = 371300, the cell size 100 m gives serious up-coning but not in the other two cell sizes. The effect of the vertical discretization is shown in Figure 4-26. The vertical discretization has more influence on the accuracy of the results obtained. When using cell sizes of 5 m for the vertical discretization, more brackish water is present as a result of numerical dispersion and the distribution of higher

56

concentration is not as sharp as in 1 m model layer thickness which has accurate results based on what is known from testing the benchmarks. Using a model layer thickness of 2 m has satisfied results to some extent and can be acceptable when considering the computational time for carrying out the rest of the analysis. Generally, we can say that the model smooths up salinities due to reducing the layer thickness.
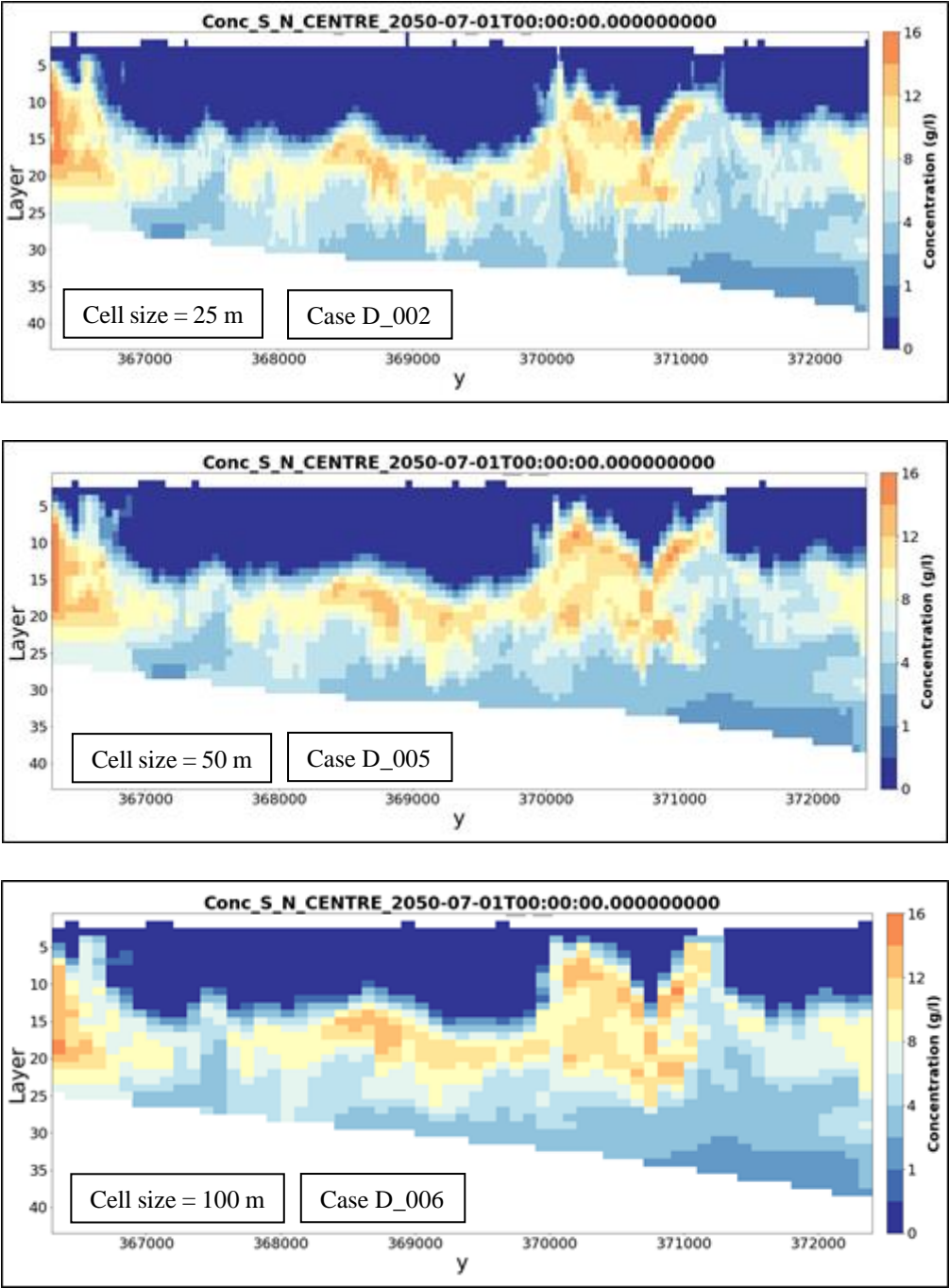
Figure 4-25: Cross section for chloride distribution after 50 years using different cell sizes but same layer thickness, 2m, using TVD
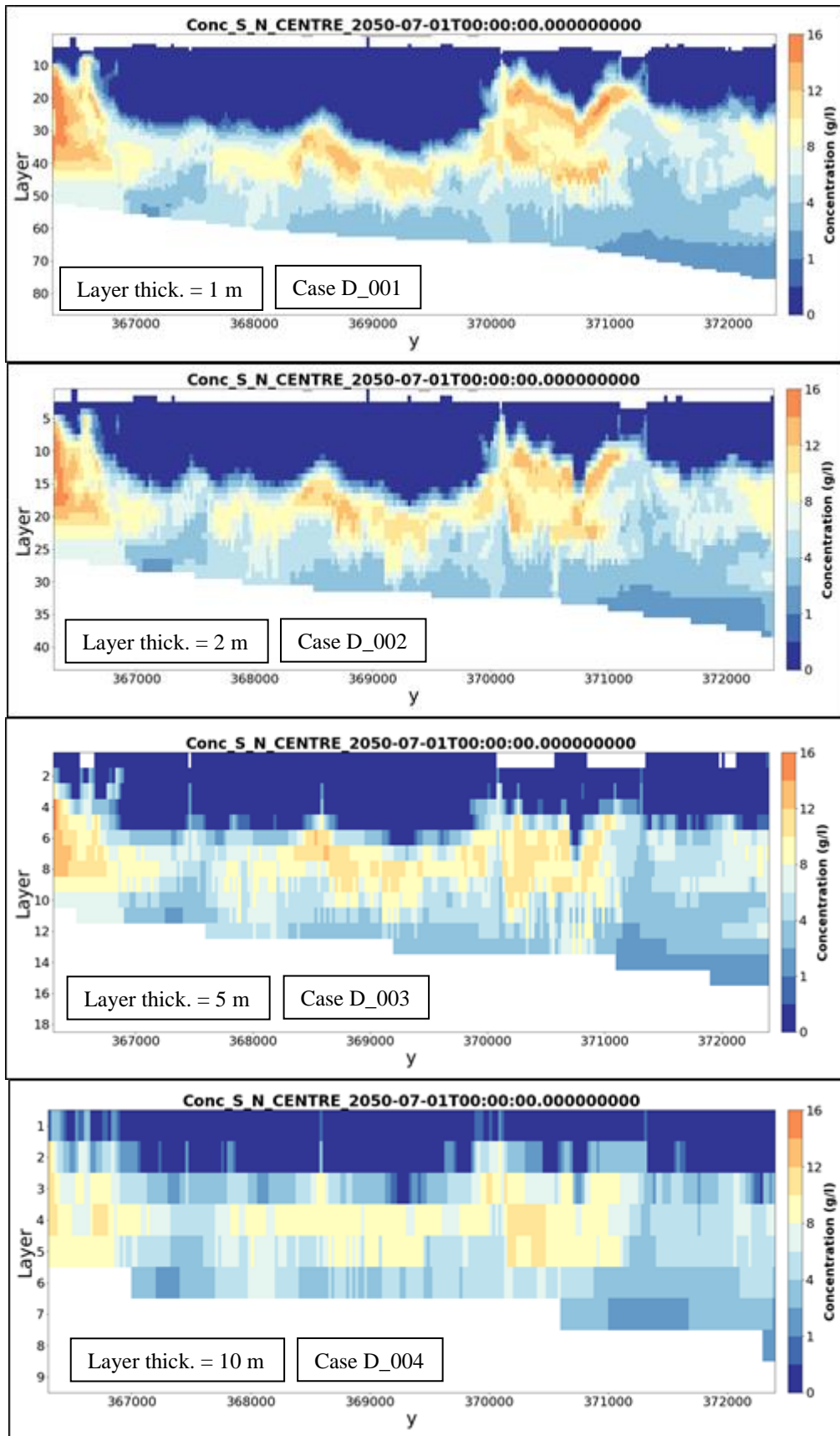
Figure 4-26: Cross section of chloride distribution after 50 years using same cell size (25 m) but different layer thicknesses. Using TVD.

By looking at Figure 4-27 it can be seen that while using finer grids the computational time is long and can reach almost three days for the cell size of 25 m and layer thickness of 1m. By just increasing the layer thickness from 1 to 2 m the run time reduced to less than a day, being a factor 3.6. The thinner cells cause larger head differenced and so large velocity which in turn reduce the transport step length, beside the increased number of cells required longer iteration. A combination of different model layer thicknesses can be used to obtain acceptable results at a reasonable run time based on the required accuracy.
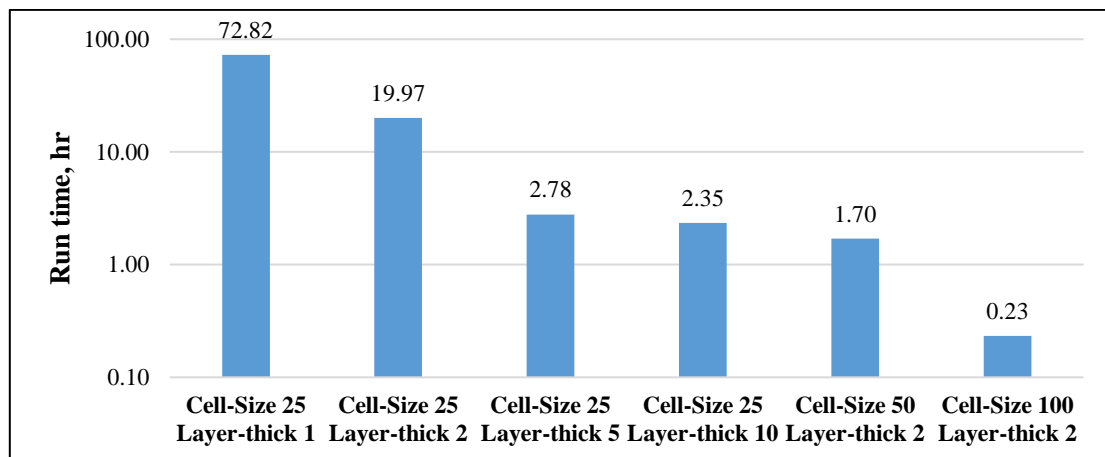
Figure 4-27: Run time (in log scale) for different model discretization. Using TVD

4.4.5 Sensitivity of the model to solver

The model developed by Deltares has been used for comparison due to the acceptable run time, 6 hours and accurate results. The vertical grid resolution is as follows: model layer thicknesses of 1 m for the top 26 m; model layer thicknesses of 2 m for the next 30 m; and finally, for the deeper last 30 m model layers thicknesses of 5 m. However, the last 30 m of the groundwater system has a very small number of active cells (as an impervious clay is present there) and is thus insignificantly affecting the accuracy of the chloride distribution. The difference between TVD, FD, and MOC is significant, as can be seen in the cross-sections in Figure 4-28 as well as in the breakthrough curves in Appendix C. In Figure 4-28 we can see the movement of chloride upwards under the effects of the discharge to the river is simulated with TVD and FD, while in contrast, MOC could not be able to simulate it. With TVD and FD, freshening in some areas in taking place and the freshwater lens is developing while in MOC the chloride is scattered as a result of the dispersion movement. Another difference between MOC and the two others is about the distribution of the chloride in the first four model layers. In MOC very high values are observed for the chloride concentration can reach 10 g/l and it is not the case for the other two where the water is fresh. The possible reason for this is the dominant vertical

59

movement of the groundwater flow. Furthermore, this movement is not only in one direction but rather upwards in some places and downwards in adjacent places due to the interaction between the aquifer and the rivers, drains and ditches all over the area.
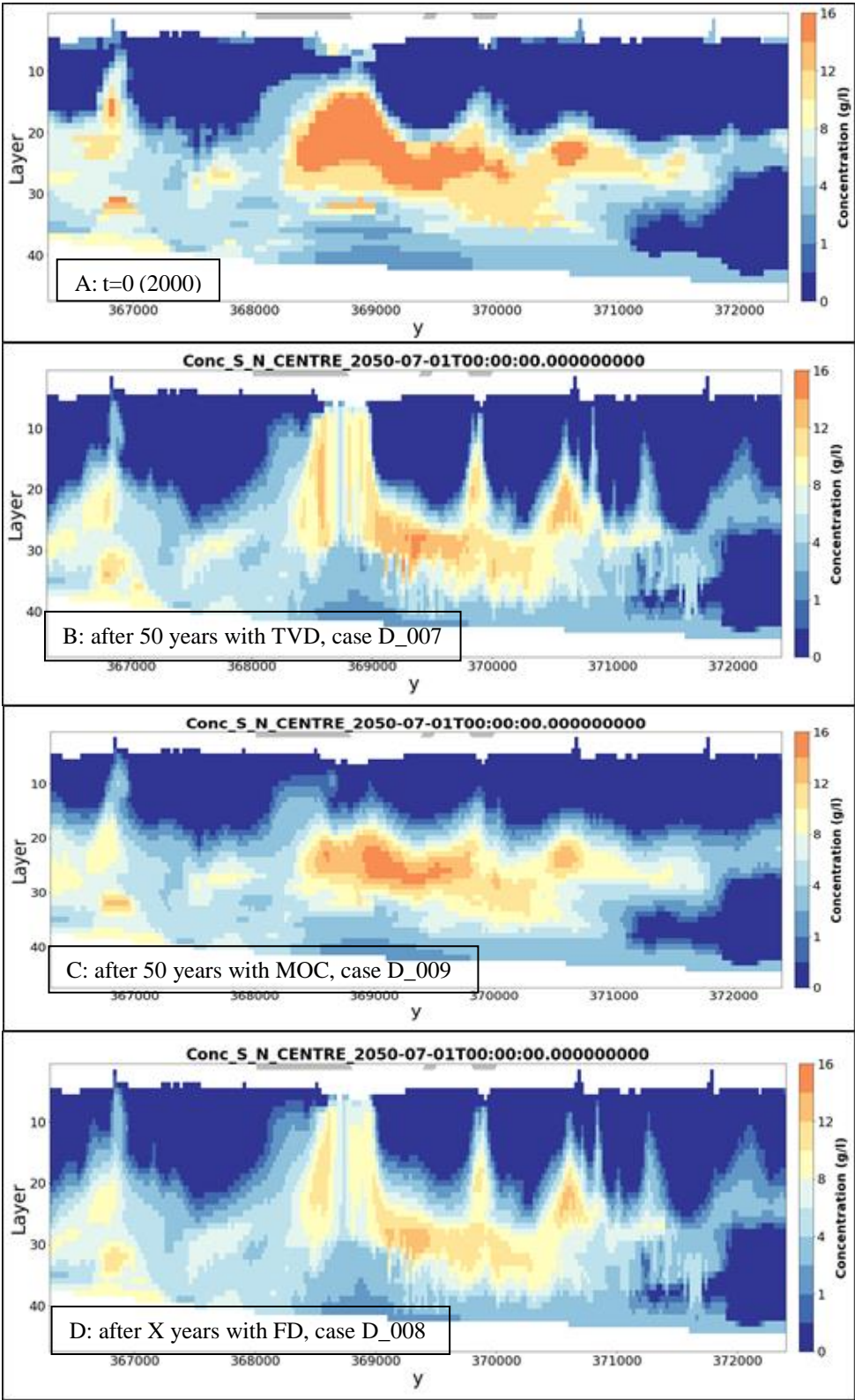
Figure 4-28: Cross section for chloride distribution before (A), and after the simulation using different solvers for same model discretization. (B) TVD, (C) MOC, (D) FD.

4.4.6 Sensitivity of parameters Courant, mechanical dispersion and particles

Since MOC could not produce similar results to what TVD and FD did, additional tests have been carried out. The length of transport steps was reduced by setting the courant number to be 0.1 so that the particles cannot move large distances in one transport step. The mechanical dispersivity was increased by increasing the longitudinal dispersivity from 0.1 to 1 and 10 m. In addition to that, the value of the number of particles for NPL and NPH was set to be equal which is 16 particles.

Figure 4-29, Figure 4-30 and Figure 4-31 illustrate the effects of the above-mentioned changes in MOC settings. By comparing these figures with graph C in Figure 4-28, clear differences induced by these changes can be seen. Reducing the courant number has shortened the transport time step and in turn, the length of the distance which particles can move. It can be seen that the concentration distribution has not changed much from the starting point shown by graph A, only a few changes due to hydrodynamical dispersion. Increasing the mechanical dispersion shows that this just increases a bit more brackish groundwater but not much mixing. For the rest no major changes from graph C. At last, making the number of NPH and NPL the same (more particles in areas of small concentration gradient over time) has created a uniform situation and resulted in results closer to the effect of changing courant number to 0.1 in terms of the pattern of the chloride distribution. Possible reasons for the behaviour of MOC in this situation is related to the mixed direction of groundwater flow in the vertical direction as a result of the interaction between different rivers and drains. This interaction has created vertical flow in both directions, upward and downward, in adjacent areas. Worth mentions that the groundwater flow is more in the vertical direction than horizontal direction to the boundaries.

For TVD, reducing the transport step to one day or increasing the dispersivity have not affected the results much and therefore the result for that simulation has not presented here.
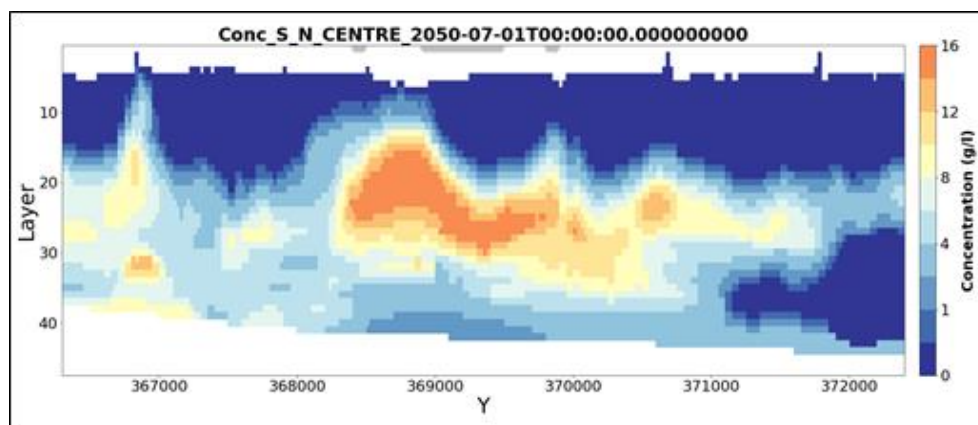
Figure 4-29: Cross section for chloride distribution using MOC with courant number of 0.1, case D_018

61
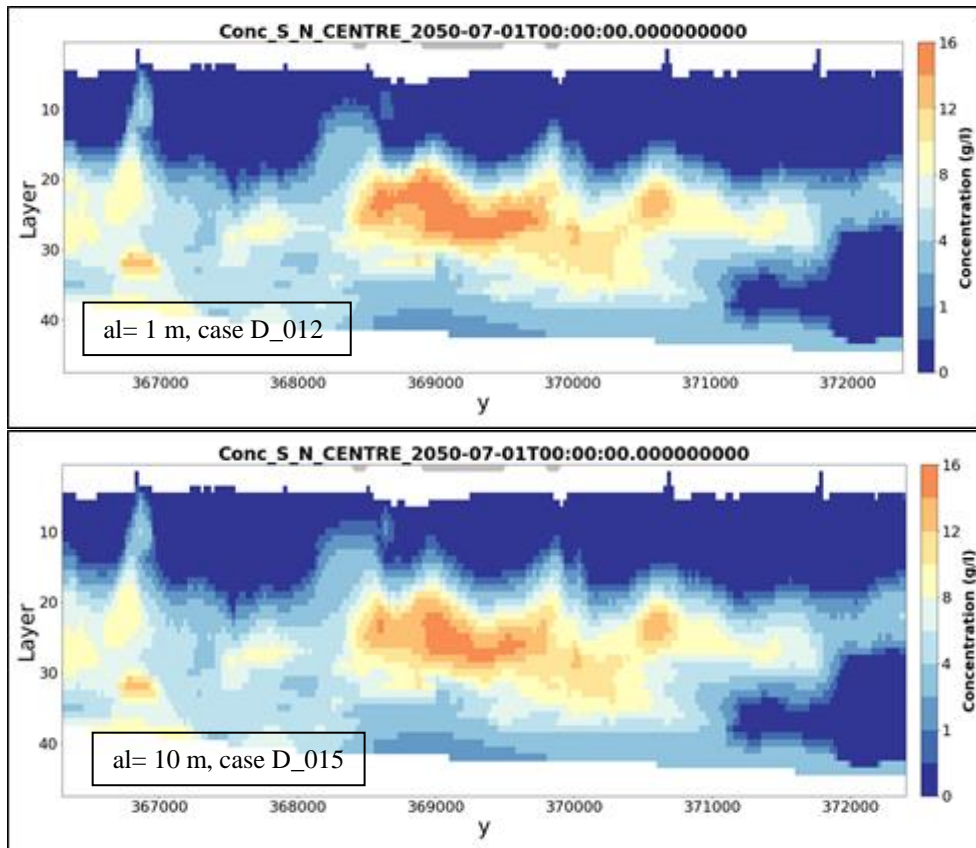
Figure 4-30: Cross section for chloride distribution using MOC with different mechanical dispersion values.
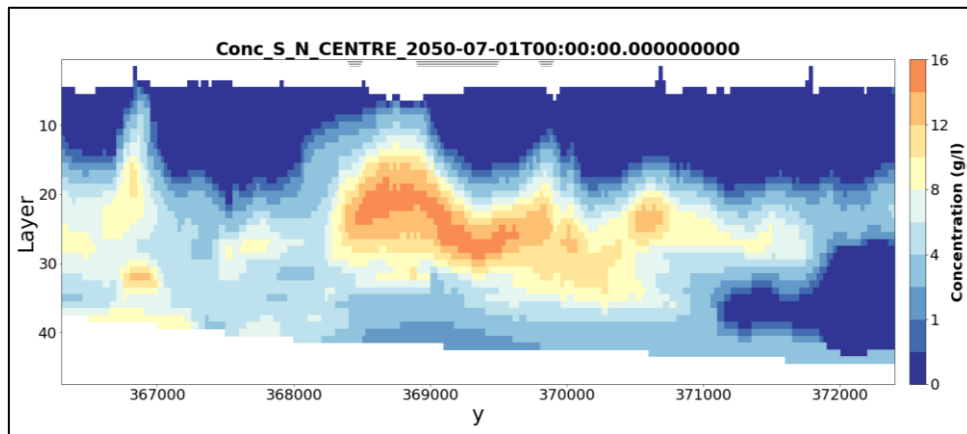
Figure 4-31: Cross section for chloride distribution using MOC with NBH = 16, NPL = 16, case D_020

4.4.7 Results of aquifer recharge

In this activity, the recharge values have been doubled in the areas of the creek ridges during the winter period. The amount of extra fresh water added to the system after increasing the recharge is 3.6 million cubic meters per year. This water has led to a rise in the groundwater table and an increment in the fresh groundwater volume. The influence on groundwater head, water budget, and chloride distribution are presented here. Case D_021 is used here.

Figure 4-32 illustrates the incensement in the average groundwater head in comparison to the situation before the recharge. Many points in the area of the creek ridge were taken. The mean for each point was calculated during the entire period. As can be seen, all the values fall above the 45° line which means the groundwater head after increasing the recharge is now higher as expected.
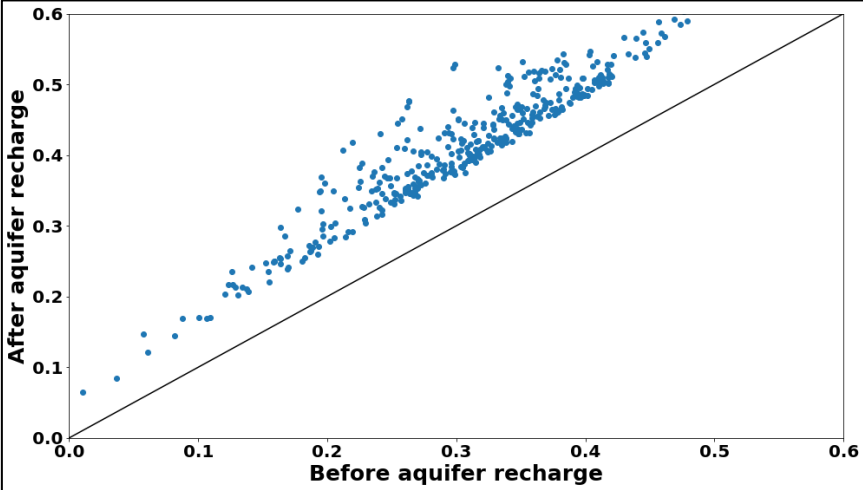
Figure 4-32: Comparison between the average head before and after doubling the recharge at a selected number of locations at eth creek ridge

The new values for the water budget are presented in Table 4-6. To better compare the two water budgets (before and after), the differences in the water budget are summarized in Table 4-7. The new water budget after increasing the recharge is subtracted from the original one, positive values mean the values were higher before and negative means the opposite. So, by looking at the difference, apart that of course must more recharge is inserted into the groundwater system, it can be seen that more water is now drained out of the aquifer through the drainage system during entire the year due to the higher groundwater heads. Less water is entering the system from the rivers as can be seen in both rivers and general head boundary packages, and more water is leaving the system through the rivers as well.

A cross-section at the location in the area where the recharge is doubled is shown in Figure 4-33. By comparing the top and bottom graphs, it can be seen that at the interface between the fresh and saline groundwater, the bottom graph of increasing the recharge shows more freshwater lens at the middle of the cross-section under the area of the creek ridge as result of more fresh surface water in now entering the system. Also can clearly be seen that due to that increase in the water discharging to the rivers and drains, the up-coning of the brackish water is higher at some places in compare to the situation before.

63

Table 4-6: water budget for DOW model after doubling the recharge in the creek ridge area

MONTH	DRAINS	GHB (BIG RIVERS +BOUNDARIES)	RECHARGE	SMALL RIVERS	STORAGE	DCDT	TOTAL IN	DRAINS	GHB (BIG RIVERS +BOUNDARIES)	RECHARGE	SMALL RIVERS	STORAGE	DCDT	TOTAL OUT	CHANGE IN STORAGE
AUG	0.00	4176.85	0.00	9134.76	22548.12	861.87	36721.60	-173.72	-634.14	-33957.00	-1094.65	-1.38	-831.22	-36692.11	29.49
SEP	0.00	3244.88	0.00	8552.84	2231.77	970.09	14999.57	-245.71	-922.02	-9432.50	-1192.22	-2237.58	-922.51	-14952.54	47.02
OCT	0.00	2056.94	11319.00	7062.62	148.20	745.39	21332.15	-498.10	-1895.05	0.00	-1521.23	-16672.21	-664.74	-21251.34	80.81
NOV	0.00	3852.32	49742.03	2056.18	531.05	310.29	56491.87	-2674.83	-3957.89	0.00	-3982.16	-45565.10	-251.72	-56431.71	60.16
DEC	0.00	1363.30	96388.19	693.26	35.28	194.96	98674.98	-27553.04	-6582.59	0.00	-10463.14	-53879.70	-127.76	-98606.23	68.75
JAN	0.00	981.74	96464.03	383.23	180.21	383.68	98392.89	-54257.20	-8451.70	0.00	-13768.16	-21530.85	-228.96	-98236.87	156.01
FEB	0.00	1112.85	74900.04	321.69	905.19	334.52	77574.30	-48909.92	-8362.64	0.00	-13939.80	-6027.58	-206.71	-77446.65	127.65
MAR	0.00	1296.81	60524.03	309.78	2008.40	120.62	64259.65	-40882.52	-7969.39	0.00	-13367.78	-1919.30	-77.17	-64216.16	43.49
APR	0.00	2096.62	19017.47	374.30	11157.58	393.05	33039.02	-15641.95	-6453.22	0.00	-10443.15	-109.05	-277.38	-32924.76	114.27
MAY	0.00	1104.00	0.00	2684.15	41420.17	728.73	45937.05	-1514.39	-5107.19	-33957.00	-4263.87	-370.47	-561.15	-45774.07	162.99
JUN	0.00	2002.06	0.00	5553.99	39042.65	445.85	47044.55	-552.80	-2342.48	-41503.00	-2156.42	-45.05	-378.13	-46977.87	66.68
JUL	0.00	3639.00	0.00	8176.49	39708.37	847.11	52370.96	-235.06	-949.22	-49049.01	-1290.50	-1.78	-784.43	-52310.00	60.96

Table 4-7: Difference in water budget in the aquifer before minus after increasing the recharge values.

MONTH	DRAINS	GHB (BIG RIVERS +BOUNDARIES)	RECHARGE	SMALL RIVERS	STORAGE	DCDT	TOTAL IN	DRAINS	GHB (BIG RIVERS +BOUNDARIES)	RECHARGE	SMALL RIVERS	STORAGE	DCDT	TOTAL OUT	CHANGE IN STORAGE
AUG	0.00	190.08	0.00	233.85	-518.79	-13.89	-108.74	-7.99	-39.67	0.00	-47.40	0.16	-8.39	-103.30	-5.45
SEP	0.00	161.61	0.00	215.15	-278.89	-14.20	83.67	-14.17	-42.33	0.00	-44.89	199.13	-8.48	89.26	-5.59
OCT	0.00	116.37	0.00	211.79	-41.96	-12.07	274.13	-30.63	-63.45	0.00	-61.80	441.28	-4.71	280.68	-6.56
NOV	0.00	377.09	-15192.03	597.10	58.99	-24.97	-14183.81	-377.09	-394.93	0.00	-1052.82	-12334.37	-14.97	-14174.17	-9.63
DEC	0.00	377.72	-28848.68	240.02	5.99	-32.23	-28257.17	-20634.52	-1028.19	0.00	-3719.62	-2841.83	-20.27	-28244.43	-12.75
JAN	0.00	234.93	-28749.41	97.62	-139.94	-63.10	-28619.90	-31642.85	-1109.72	0.00	-3547.27	7742.98	-30.09	-28586.95	-32.95
FEB	0.00	220.61	-22492.17	58.79	-803.72	-39.04	-23055.53	-23542.48	-829.88	0.00	-2743.12	4098.87	-13.65	-23030.25	-25.28
MAR	0.00	212.37	-18320.66	44.70	-1078.93	-19.08	-19161.59	-18071.00	-640.38	0.00	-2216.23	1784.99	-8.39	-19151.01	-10.58
APR	0.00	127.48	-5811.97	49.37	-1348.38	-45.82	-7029.32	-5322.24	-376.21	0.00	-1391.96	106.32	-21.52	-7005.61	-23.72
MAY	0.00	161.19	0.00	463.18	-1545.71	-70.89	-992.23	-192.52	-242.85	0.00	-502.62	15.69	-40.66	-962.96	-29.27
JUN	0.00	178.05	0.00	441.03	-951.71	-21.18	-353.81	-42.86	-127.36	0.00	-165.77	2.57	-11.24	-344.66	-9.15
JUL	0.00	202.47	0.00	300.97	-644.46	-29.41	-170.42	-10.08	-58.44	0.00	-72.82	0.17	-19.37	-160.54	-9.88
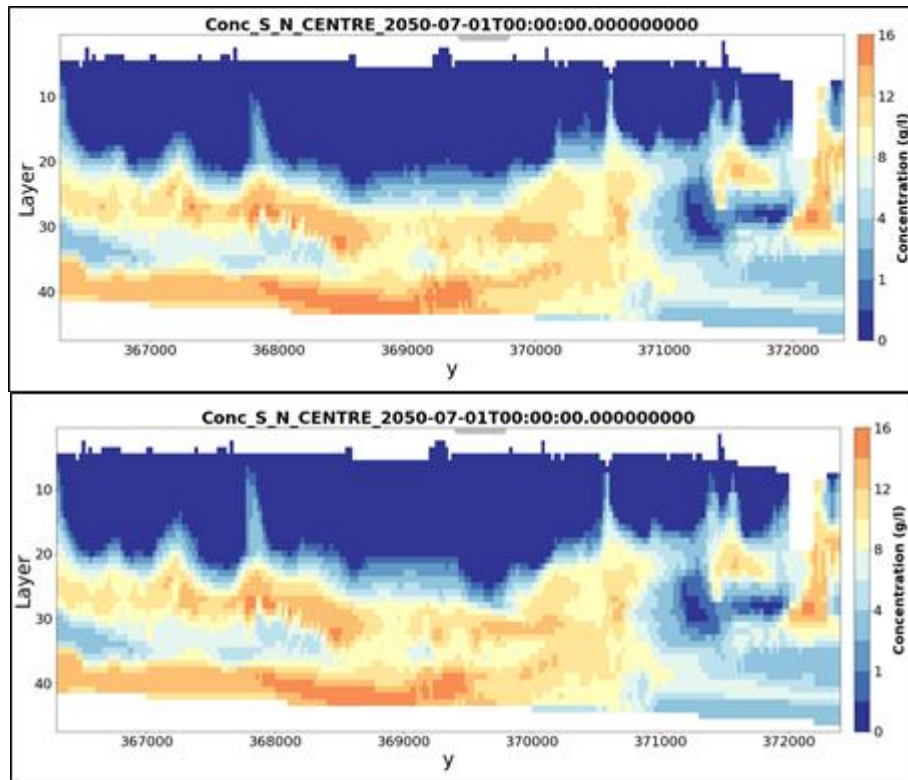
Figure 4-33: Cross section for chloride distribution before (top) and after (bottom) increasing the recharge.

During the summer period, a shortage in water supply normally takes place. Therefore, extraction of half of the water (1.8 million cubic meters) during the summer period is tested to see the influence on the groundwater system.

The groundwater heads are influenced by the extraction process, as can be seen in Figure 4-34. In a few places, the groundwater heads are higher even after the extraction took place, however, in many other places the groundwater head is dropped and even in some spots the drawdown is the magnitude of meter. Although the extraction rate is kept small and the wells are distributed at a distance of 75 m from each other, the influence of using the wells package on the groundwater drawdown is still significant.

The water budget within the aquifer is presented in Table 4-8. The difference between the original situation and the water budget after recharge and extraction is presented as well in Table 4-9. In general, the extraction process during the summer period has led to a reduction in the discharge from the aquifer through drains and rivers, and at the same time, more water is entering the system from the river. These dynamic changes result from the extraction process to maintain the balance between the inflow and outflow within the aquifer.

65
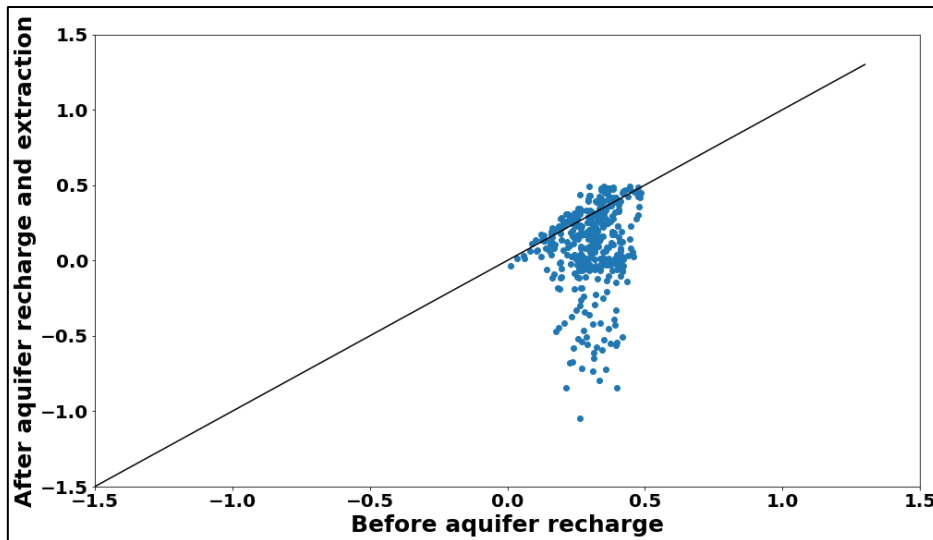
Figure 4-34: Comparison between the average head during normal situation and the doubled recharge with 50% extraction in the area of the creek ridge.

By looking at the cross-section in Figure 4-35 and compare it to the cross-sections in Figure 4-33, it can be seen that under the influence of extraction saline groundwater is started to up-coning in the middle of the cross-section under the area where the pumps are working (indicated by the black circle).

At the same time, the reduction in the discharge of water to rivers and drains has resulted in reducing in the up-coning of the brackish water under the influence of the vertical velocity under the rivers, but more brackish water is now present at the interface as the reduction led to mxing of the salinity. It also led to additional growth of the freshwater lens in the middle of the cross-section.

Figure 4-35: cross section for chloride distribution after doubling the recharge with 50% extraction

Table 4-8: water budget for DOW model after doubling the recharge in the creek ridge area with extraction half during summer

MONTH	DRAINS	GHB (BIG RIVERS +BOUNDARIES)	RECHARGE	SMALL RIVERS	WELLS	STORAGE	DCDT	TOTAL IN	DRAINS	GHB (BIG RIVERS +BOUNDARIES)	RECHARGE	SMALL RIVERS	WELLS	STORAGE	DCDT	TOTAL OUT	CHANGE IN STORAGE
AUG	0.00	5204.95	0.00	10513.42	0.00	29726.89	14.98	45460.24	-145.66	-495.12	-33957.00	-847.95	-10000.00	-0.19	-10.72	-45456.64	3.60
SEP	0.00	4368.02	0.00	10172.44	0.00	8044.49	15.25	22600.19	-202.97	-753.06	-9432.50	-890.67	-10000.00	-1306.16	-10.65	-22596.01	4.18
OCT	0.00	3231.99	11319.00	9114.89	0.00	1253.29	240.43	25159.61	-410.47	-1677.17	0.00	-1066.64	-10000.00	-11764.60	-157.00	-25075.88	83.73
NOV	0.00	3843.94	49742.03	3362.59	0.00	403.81	500.06	57852.44	-2251.26	-3165.43	0.00	-2592.30	0.00	-49343.11	-443.43	-57795.53	56.91
DEC	0.00	1379.74	96388.19	1256.87	0.00	25.42	77.64	99127.85	-12661.18	-5844.55	0.00	-7745.41	0.00	-72799.44	-55.38	-99105.97	21.89
JAN	0.00	987.20	96464.03	549.11	0.00	104.07	306.65	98411.06	-41427.49	-8034.46	0.00	-12102.29	0.00	-36539.81	-206.20	-98310.25	100.81
FEB	0.00	1114.24	74900.04	385.72	0.00	405.33	267.24	77072.57	-44411.11	-8145.10	0.00	-13122.58	0.00	-11126.55	-186.90	-76992.24	80.33
MAR	0.00	1295.56	60524.03	345.48	0.00	1551.32	73.71	63790.10	-38798.35	-7844.08	0.00	-12943.15	0.00	-4130.75	-53.00	-63769.32	20.78
APR	0.00	2094.88	19017.47	399.06	0.00	10460.51	371.67	32343.58	-14997.08	-6380.38	0.00	-10213.29	0.00	-381.58	-288.44	-32260.77	82.81
MAY	0.00	1246.56	0.00	3438.73	0.00	49563.55	76.79	54325.62	-1313.26	-4839.50	-33957.00	-3818.53	-10000.00	-322.19	-47.46	-54297.93	27.69
JUN	0.00	2470.86	0.00	6816.34	0.00	46540.91	7.05	55835.16	-463.69	-2125.34	-41503.00	-1708.55	-10000.00	-27.53	-4.51	-55832.62	2.54
JUL	0.00	4467.09	0.00	9525.69	0.00	47045.55	214.69	61253.02	-199.99	-792.89	-49049.01	-996.13	-10000.00	-0.67	-148.67	-61187.36	65.65

Table 4-9: difference in water budget in the aquifer before and after increasing the recharge values with the 50% extraction

MONTH	DRAINS	GHB (BIG RIVERS +BOUNDARIES)	RECHARGE	SMALL RIVERS	STORAGE	DCDT	TOTAL IN	DRAINS	GHB (BIG RIVERS +BOUNDARIES)	RECHARGE	SMALL RIVERS	STORAGE	DCDT	TOTAL OUT	CHANGE IN STORAGE
AUG	0.00	-838.02	0.00	-1144.81	-7697.56	833.01	-8847.38	20.07	99.35	0.00	199.29	1.35	812.10	-8867.83	20.45
SEP	0.00	-961.53	0.00	-1404.45	-6091.61	940.64	-7516.95	28.58	126.63	0.00	256.66	1130.55	903.38	-7554.21	37.25
OCT	0.00	-1058.68	0.00	-1840.48	-1147.06	492.90	-3553.33	57.00	154.44	0.00	392.79	5348.89	503.03	-3543.86	-9.47
NOV	0.00	385.47	-15192.03	-709.30	186.23	-214.74	-15544.38	46.49	397.54	0.00	337.04	-16112.38	-206.68	-15538.00	-6.38
DEC	0.00	361.29	-28848.68	-323.59	15.84	85.10	-28710.04	-5742.66	-290.15	0.00	-1001.89	-21761.57	52.12	-28744.16	34.12
JAN	0.00	229.48	-28749.41	-68.27	-63.80	13.93	-28638.07	-18813.14	-692.48	0.00	-1881.40	-7265.98	-7.33	-28660.33	22.25
FEB	0.00	219.22	-22492.17	-5.23	-303.86	28.24	-22553.80	-19043.67	-612.34	0.00	-1925.90	-1000.10	6.16	-22575.84	22.04
MAR	0.00	213.62	-18320.66	9.01	-621.85	27.84	-18692.04	-15986.83	-515.07	0.00	-1791.60	-426.46	15.79	-18704.17	12.13
APR	0.00	129.22	-5811.97	24.61	-651.31	-24.44	-6333.88	-4677.37	-303.37	0.00	-1162.10	-166.20	-32.59	-6341.62	7.74
MAY	0.00	18.63	0.00	-291.39	-9689.09	581.05	-9380.80	8.61	24.84	0.00	-57.29	63.97	473.03	-9486.83	106.03
JUN	0.00	-290.75	0.00	-821.32	-8449.97	417.62	-9144.41	46.26	89.78	0.00	282.11	20.08	362.38	-9199.41	54.99
JUL	0.00	-625.62	0.00	-1048.23	-7981.64	603.01	-9052.48	24.99	97.89	0.00	221.55	1.28	616.39	-9037.90	-14.58

The second scenario of extracting three-quarter (2.7 million cubic meters) of the amount of water being added to the system. The effect on the groundwater head is shown in Figure 4-36. As can be seen, there are some places still with higher head due to the recharge but in many other places there is more drawdown is induced compared to only 50 % extraction.
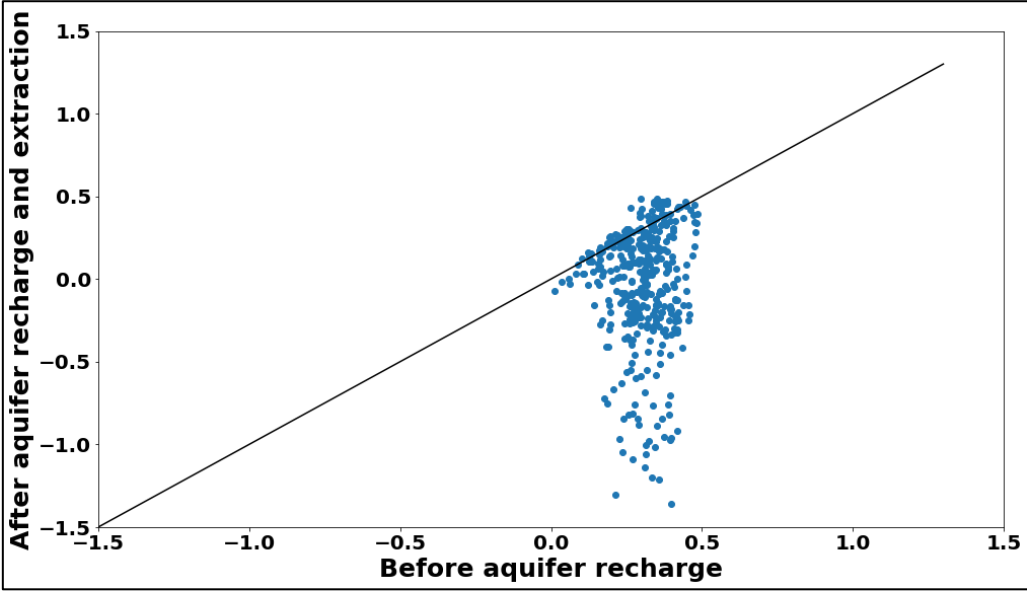
Figure 4-36: Comparison between the average head during normal situation and the doubled recharge with 75% extraction in the area of the creek ridge.

The summary of the water budget is depicted in Table 4-10, and the difference between the normal situation and the new scenario in terms of water budget is also summarised in Table 4-11. The same effects from the implementation of the extraction process as in the last scenario are presents here as well. Less water is discharging to the rivers and the drains, while at the same time more water is induced by the bigger rivers. If Table 4-9 and Table 4-11 are compared (extracting half versus three-quarter), it can be seen that in the last one more water is induced from the rivers as the extraction rates are higher. At the same time, less water is discharged to the rivers and drains. However, the difference between the two of them is not large.

The last thing is to look at the cross section of chloride distribution in Figure 4-37. Comparing this cross section to Figure 4-33b and Figure 4-35, we can see that under the effect of extraction, more up-coning is now presence under the area as indicated by the black circle after period of 50 years.

The reduction in the discharge to the rivers has led to reduction in up-coning in the areas under the large rivers, same as what happened with the extraction of 50%. We can also see in some areas the freshwater lens has grown more in compare to the normal situation.

68
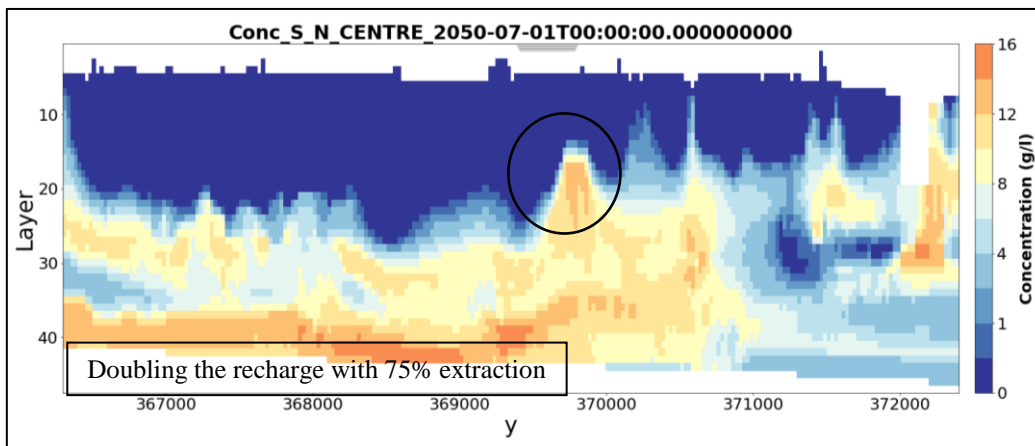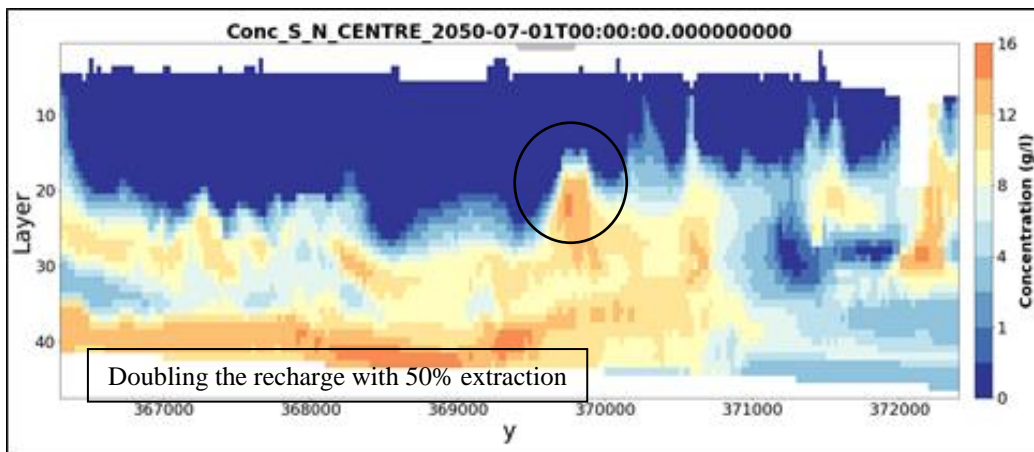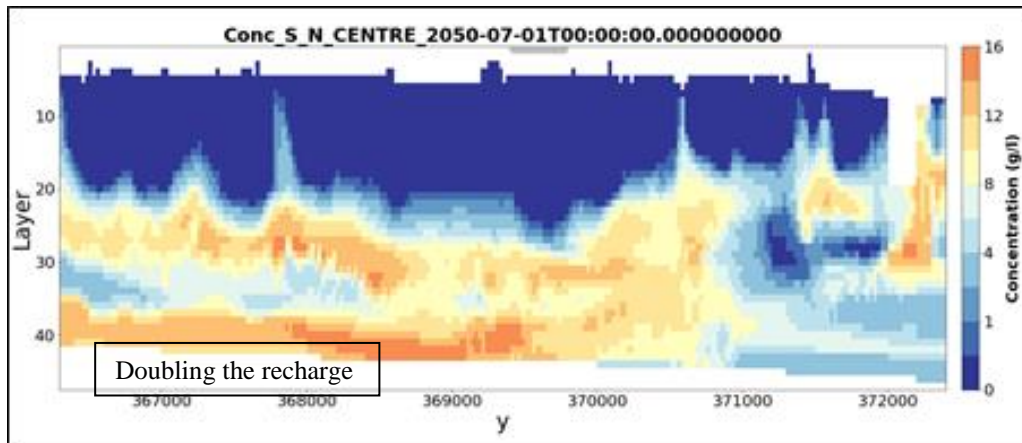
Figure 4-37: cross section for chloride distribution after doubling the recharge with 75 % extraction

Table 4-10: water budget for DOW model after doubling the recharge in the creek ridge area with extraction three-quarter during summer

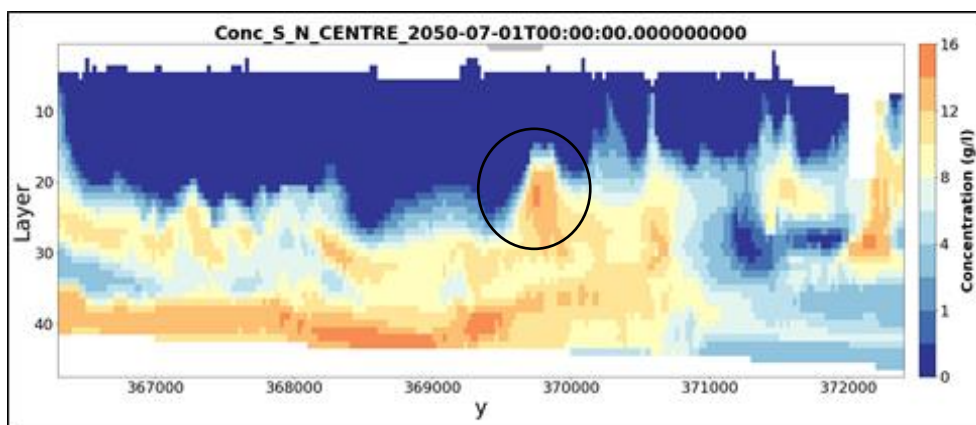| MONTH	DRAINS	GHB (BIG RIVERS +BOUNDARIES)	RECHARGE	SMALL RIVERS	WELLS	STORAGE	DCDT	TOTAL IN	DRAINS	GHB (BIG RIVERS +BOUNDARIES)	RECHARGE	SMALL RIVERS	WELLS	STORAGE	DCDT	TOTAL OUT	CHANGE IN STORAGE
AUG	0.00	5505.53	0.00	10724.43	0.00	31947.93	224.84	48402.73	-140.66	-463.69	-33957.00	-816.92	-12800.00	-0.14	-150.02	-48328.43	74.30
SEP	0.00	4724.70	0.00	10410.53	0.00	10093.72	232.44	25461.38	-195.44	-712.50	-9432.50	-853.42	-12800.00	-1235.27	-151.99	-25381.11	80.27
OCT	0.00	3625.88	11319.00	9433.83	0.00	2408.86	119.72	26907.29	-392.40	-1616.94	0.00	-1010.96	-12800.00	-10966.53	-73.53	-26860.35	46.94
NOV	0.00	4023.63	49742.03	3667.40	0.00	421.70	64.91	57919.67	-2193.53	-3030.91	0.00	-2440.88	0.00	-50188.19	-57.56	-57911.06	8.61
DEC	0.00	1430.31	96388.19	1625.77	0.00	25.64	78.56	99548.48	-11381.94	-5614.79	0.00	-7146.13	0.00	-75327.52	-57.26	-99527.63	20.85
JAN	0.00	990.81	96464.03	691.52	0.00	98.05	299.84	98544.26	-37153.39	-7850.66	0.00	-11422.54	0.00	-41817.11	-204.59	-98448.29	95.97
FEB	0.00	1115.79	74900.04	437.47	0.00	343.30	234.04	77030.64	-41880.05	-8037.20	0.00	-12686.80	0.00	-14192.72	-166.07	-76962.84	67.80
MAR	0.00	1296.19	60524.03	367.95	0.00	1405.24	51.97	63645.37	-37694.03	-7776.56	0.00	-12678.85	0.00	-5443.93	-37.98	-63631.35	14.02
APR	0.00	2095.06	19017.47	415.98	0.00	10124.50	340.34	31993.34	-14685.00	-6336.50	0.00	-10054.75	0.00	-577.30	-268.14	-31921.69	71.66
MAY	0.00	1313.41	0.00	3667.87	0.00	51840.84	176.22	56998.33	-1263.39	-4784.97	-33957.00	-3696.32	-12800.00	-321.03	-104.08	-56926.78	71.55
JUN	0.00	2618.49	0.00	7089.86	0.00	48777.43	195.56	58681.35	-450.05	-2081.31	-41503.00	-1626.07	-12800.00	-26.05	-116.44	-58602.93	78.42
JUL	0.00	4695.03	0.00	9774.93	0.00	49287.09	105.65	63862.69	-194.19	-758.78	-49049.01	-953.49	-12800.00	-0.65	-68.26	-63824.39	38.31

Table 4-11: difference in water budget in the aquifer before and after increasing the recharge values with the 75% extraction

MONTH	DRAINS	GHB (BIG RIVERS +BOUNDARIES)	RECHARGE	SMALL RIVERS	STORAGE	DCDT	TOTAL IN	DRAINS	GHB (BIG RIVERS +BOUNDARIES)	RECHARGE	SMALL RIVERS	STORAGE	DCDT	TOTAL OUT	CHANGE IN STORAGE
AUG	0.00	-1138.59	0.00	-1355.82	-9918.60	623.14	-11789.87	25.07	130.79	0.00	230.32	1.40	672.81	-11739.62	-50.25
SEP	0.00	-1318.21	0.00	-1642.54	-8140.84	723.45	-10378.14	36.10	167.19	0.00	293.91	1201.45	762.04	-10339.31	-38.84
OCT	0.00	-1452.58	0.00	-2159.43	-2302.62	613.61	-5301.02	75.07	214.67	0.00	448.47	6146.96	586.50	-5328.33	27.31
NOV	0.00	205.78	-15192.03	-1014.11	168.35	220.41	-15611.61	104.22	532.06	0.00	488.46	-16957.46	179.19	-15653.53	41.93
DEC	0.00	310.71	-28848.68	-692.50	15.62	84.17	-29130.67	-4463.42	-60.38	0.00	-402.61	-24289.65	50.24	-29165.82	35.15
JAN	0.00	225.86	-28749.41	-210.68	-57.78	20.74	-28771.27	-14539.04	-508.68	0.00	-1201.65	-12543.28	-5.72	-28798.37	27.10
FEB	0.00	217.67	-22492.17	-56.98	-241.83	61.44	-22511.87	-16512.61	-504.43	0.00	-1490.12	-4066.27	26.99	-22546.44	34.57
MAR	0.00	213.00	-18320.66	-13.46	-475.76	49.58	-18547.31	-14882.51	-447.55	0.00	-1527.30	-1739.65	30.81	-18566.20	18.89
APR	0.00	129.04	-5811.97	7.69	-315.30	6.90	-5983.64	-4365.29	-259.48	0.00	-1003.56	-361.92	-12.29	-6002.54	18.89
MAY	0.00	-48.22	0.00	-520.54	-11966.38	481.63	-12053.51	58.48	79.37	0.00	64.92	65.13	416.41	-12115.68	62.17
JUN	0.00	-438.38	0.00	-1094.84	-10686.49	229.11	-11990.61	59.89	133.80	0.00	364.58	21.57	250.45	-11969.71	-20.89
JUL	0.00	-853.56	0.00	-1297.47	-10223.18	712.05	-11662.16	30.79	132.00	0.00	264.19	1.31	696.79	-11674.92	12.77

Chapter 5   Discussion

5.1 Model discretization

In results chapter 4, it is shown that by adopting finer grids, the obtained results in terms of salinity distribution and mass budget become more accurate. Since in the numerical schemes the concentration all over the cell is represented by the concentration at the node, this can lead to errors when a coarse grid is used. In particular, where the change in concentration in transition zones between fresh, brackish and saline water is big over a small distance, bigger cell sizes cause a larger error in the salinity distribution. Here, examples of errors, viz. the numerical dispersion errors and instabilities are demonstrated in results of the benchmark freshwater lens, especially when larger cell sizes are used. Oude Essink (2001) already mentioned that to overcome the numerical errors associated with the numerical solution, the model discretization needs to be fine enough. However, it is not easy to say when a certain model is good enough and its discretization is adequate, as this depends on the purpose of the model and the complexity of the hydraulic properties. Reilly and Harbaugh (2004) stated that the intended use of the modelling results determine whether the model discretization is adequate or not and whether the missed details with the adopted discretization can lead to big error or not in the simulation results. Moreover, the resolution of the collected data to represent the relevant hydrogeological features play an important role in determining the degree of discretization along with the available computational resources. Given the above-mentioned reasons, it is clear to understand that the accuracy of model is generally still a compromise.

Findings from (Al-Maktoumi, et al., 2007) and (Graf and Degener, 2011) on the influence of the degree of the discretization on the accuracy of the results obtained by the numerical schemes provided similar results. Both studies showed that to achieved accurate results only a fine model's discretization is adequate enough.

The solute transport time step is controlled by stability criteria (Zheng and Wang, 1999). These criteria are mainly functions of the three-dimensional groundwater flow velocity and the cell size in the three dimensions. By reducing the cell size, the transport step length is reduced. On

71

top, it is very important to understand too, that with smaller cell sizes, hydraulic gradients are more profound, nearly always leading to a much larger groundwater flow velocities in the modelling domain. So, apart from more cells, also much larger velocities are calculated in a model with a refined grid. This combination means the number of transport steps will seriously be increased; the overall computational time as well; this increase of overall computational time is nearly always much larger than you expect when only more modelling cells are accounted for. In SEAWAT, the program cannot be forced to adopt a transport step larger than the one determined by the stability criteria, but we can use a smaller transport step. In terms of model results accuracy, having small transport steps can lead to more accurate results, even to some degree when still coarser grids are used. As in many of the numerical schemes the distance over which a solute is transported, it depends on the length of the transport step; so larger steps can lead to numerical errors. In the end, a combination of model discretization and transport steps can be used to obtain accurate model results while maintaining less computational time. As indicated above, the resolution of the spatial resolution as well as the run time depends, among others, on the purpose of the model where it is used for.

5.2 Numerical solvers

For the freshwater lens benchmark, t can be seen that MOC and HMOC have performed better in terms of a sharp interface if small cell sizes are used. At the same time, FD and MMOC have some numerical dispersion errors. Meanwhile TVD has managed to develop a solution free of numerical dispersion with the finest grid only. Since this benchmark represents only a dominant advection transport (dispersion is excluded as a process), MOC has resulted in very accurate results. (Zheng and Wang, 1999) stated that for the advection dominant situations, Lagrangian schemes lead to a good solution free of numerical dispersion. The coarser grids in the vertical direction have led to instabilities of the solution obtained by MOC at the transition zone in terms of overshooting. Even the shape of the interface in the middle of the model is not smooth. At the same time, TVD and FD have performed better than MOC in these situations. This is because of the larger transport step associated with the coarser cell size. Although the horizontal grid size is small, since the groundwater flow has a serious vertical component and the vertical cell size is coarse, the model creates larger transport steps. This error can be reduced but not overcome by changing the transport step size manually and force the model to adopt a smaller step. To some end, obeying the stability criteria is a good start, but experienced modellers know that extra information on the specific modelling processes need extra rigid parameter settings.

For Henry's case, the difference between the solvers was not significant due to the process of the saltwater intrusion is mainly a result from the (a very large) diffusion. As known from the MT3DMS manual, the solvers differ from each other only in the solution of the advection term, while the other terms (hydrodynamic dispersion and sources and sinks) are solved with the finite difference scheme. The reason for using Henry's case is because it is being used in a wide range as a benchmark for testing variable-density groundwater flow codes (Simpson and Clement, 2003).

In the case of the saltwater pocket, the difference between the solvers was noteworthy. Goswami, et al. (2012) talked about the unstable situation where the lower fluid density is not on top of the higher fluid density. They tested three solvers, FD, MOC and TVD, for two cases for rising plume and sinking plume and concluded that none of the solvers was able to produce satisfactory results under the same conditions for both experiments. However, FD has resulted in good results under the sinking experiments. In our case, FD managed to form the fingers but at the same time MOC could not form any fingers while TVD created some fingers to some extent, in order to be sure about it, a snadtank experiment can be carried out to be compared with. The sinking process of the saline groundwater under the gravity force and the upward counter flow of the fresh groundwater from below created a circular movement of flows with different velocities under the fingers while stagnations in other places. This mechanism created the difference between MOC and the other two solvers due to the discrete nature of the particle tracking approach. The difference between FD and TVD is related to the degree of numerical dispersion error, which is higher for the FD and in a very small degree at TVD.

In the DOW model, FD and TVD produced similar results. There is just some small difference in the degree numerical dispersion is created. On the other side, the results obtained from the MOC solution differs significantly from both previous solvers. The reason for the difference between MOC and the other two is related to the numerical scheme of these solvers. MOC uses particle tracking approach, by placing particles in each cell and then track these particles forward. The new location of each particle is defined with the travelled distance in x, y and z directions. The distance moved by the particle in each location is a function of the velocity in that direction and the transport step. The velocity in each direction is calculated with linear interpolation between the values of the cell two interfaces in that direction. While in TVD, the concentration at the cell is upstream biased. The concentration is brought from distance equivalent to the time step multiplied by the velocity at that cell.

73

In the DOW case, looking at cell by cell water flux for the flow in the z direction, the flow under the river is larger than the flow near the saline water block. Furthermore, the flow direction is changing between summer and winter due to the interaction with different surface water bodies as they are influent and effluent. Besides, some water bodies recharge the aquifer and others discharge the water from the aquifer, which also results in mixed directions at the same time. This can be seen when pathline simulation and tracking several particles forward is used to see the direction of particle movement. Particles are places in two different levels and tracked them forward to see the flow directions. In both, the movement is pretty serious in both ways, upwards and downwards, as can be seen in Figure 5-1. Furthermore, if we compared the two model layers, it can be seen that the particles in model layer 10 travelled longer distances downward from the starting line as the velocity in the area below the rivers is higher than the lower model layers which contain the saline water. Therefore, the particles placed at lower model layers containing saline groundwater will have smaller groundwater velocities. Therefore, the particles (given the discrete nature of the particle methods) distribute the chloride concentration around resulting in more brackish water as a result of distributing of the saline block.

Now comparing MOC with TVD, as stated above that the vertical velocities at the vicinity under the rivers are higher than in lower parts, for example comparing layer 8 (- 1m NAP) with layer 20 (-13m NAP), we can see the velocity in layer 8 is almost double the velocity in layer 20. So based on the concept of finite difference, which TVD used in solving the equation, with upstream what biased. The chloride concentration is being brought up from the areas with saline groundwater (layer 20) as the interface concentration of layer 8 is equal to the concentration at distance equal to velocity in the cells at that layer multiplied with the transport step. Therefore we can see the chloride is moving upward with the groundwater towards the river and in other direction the infiltration of freshwater increasing the freshwater lens.

In order to be 100 percent sure about which solver is accurate we need to check if the chloride concentration in the last 40 years. As we saw in TVD the concentration is quickly moving upward in the coming years. If it is the case of a Dutch polders and the concentration being moving up from the past then TVD is correct otherwise, maybe MOC is more accurate than both. Therefore, additional field tests need to be carried out to be certain about which one to choose.
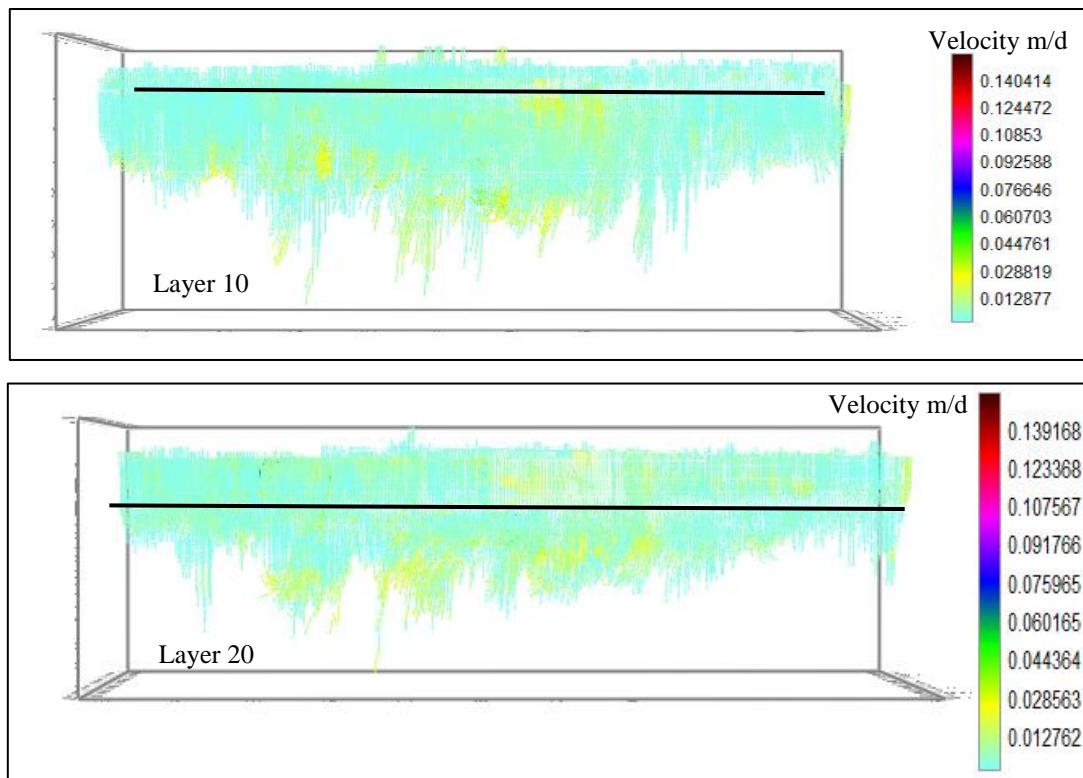
Figure 5-1: Pathlines for particles placed in two model layers, the level of starting point indicated by the black line.

Some of the solver's settings affected the results as can been seen in FD and MOC. For FD, switching between central in space weighting (CIS) and upstream weighting (UW) resulted in different results. The CIS method is affected by the artificial oscillation and can lead to overshooting and undershooting results as seen for the freshwater lens benchmark. This is because the concentration of the node is averaged between the older concentration of the cell and the new concentration of the upstream cell. In the case of the freshwater lens, the movement of water is controlled by the advection process and therefore this error is very big. On the other side, UW is free from the artificial oscillation because the concentration is taken as the upstream cell concentration but suffers from numerical dispersion. However, it can give reasonably accurate results by adopting the grid size to overcome the numerical dispersion.

For MOC, the number of particles placed per cell has great influence. There are situations in models where groundwater is moved such that it is in a stagnant situation, for example, the circular movement of groundwater in the saltwater pocket benchmark. In this situation, placing the same number of particles in each cell, making NPH equal to NPL, is significantly influencing and can improve the results (as seen in the modelling results of the saltwater pocket). This is because the cell of a small groundwater flow will not be considered in the

75

calculation, as in the default setting, the value of NPL is zero (as the manual of MT3DMS recommends for the normal situations). In DOW's case, the reduction of the Courant number has also reduced the scattering of the particles; in turn, the pattern of chloride distribution is quite different from the case with a large Courant number. This is because the Courant number restricts the movement of particles within one transport step.

However, is has been seen that each of these numerical settings influenced the results under different circumstances. Even so that the algorithm used in the particle tracking, Fourth-order Runge-Kutta, can give better results in the cases of higher converging and diverging flow, it does not have influence in our case study. Therefore, under different situations, solvers and solver's settings could lead to different results. Per case, only one suitable setting is ideal for that case, and so, we always need to test different solvers as well as settings of the solvers to reach the best solver configuration to be used.

5.3 Aquifer storage and recovery

The principle of Badon Ghijben-Herzberg, expressing the relation between the groundwater head and the freshwater lens thickness, is the main concept behind the idea of the adopted aquifer storage and recovery system. From the principle, increasing in groundwater head leads to an increase in the freshwater lens thickness. The groundwater table can fluctuate and influence much faster than the salinity, therefore we need to consider the average value of the groundwater head during the period, not the fluctuation, for the freshwater lens to develop. This system has been tested on a small scale in Walcheren, the Netherlands. It was found that an increase in the water table by 0.5 m is expected to increase the lens by 6-8 m within 10 years period (Pauw, et al., 2015). In our case study, the water head was increased by an averaged value of 0.106 m. This small increase in the water table has led to an increase in the freshwater volume available as shown in the cross-sections in the results and will be seen in the water volumes below (Figures 5-2 and Figure 5.3).

The amount of water available in the groundwater system can be estimated by counting the number of cells that have concentration under a certain threshold and then multiply the number of the cells by the cell volume. In this case, two thresholds have been considered, 0.15 g/l and 1 g/l. The first one is generally taken as the limit between the water is fresh and brackish. While the second one has been considered as up to this concentration of chloride the water can be used by the intended users (like farmers and industry) in the study area. Both thresholds are used to account for the available water under normal situation. Two cases are considered at the same

76

time: with recharge only and with both recharge and extraction at the same time. The results are shown in Figure 5-2 and Figure 5-3 using TVD.

Under the normal situation, the amount of fresh groundwater (both thresholds) is reducing with time and the volume of brackish groundwater starts to increase. As shown in the result section, this is due to the movement of the saline groundwater under the influence of the vertical movement of water resulted from the interaction between the aquifer and the rivers. Brackish groundwater is leaving the groundwater system through the rivers and drains.

When the recharge is doubled, the freshwater volume gets less in the beginning compared to the present situation. Afterwards, the volumes increases agian. The reason for the reduction in the fresh water volume at the beginning in all the simulations was that the model is correcting the initial salinity distribution created with the FRESHEM survey. After this correction, it can be seen that the groundwater system is pretty stable.

Under both recharge and extraction scenarios, it can be seen that at the beginning the amount of fresh groundwater volumeis lower than the other two situations; only later in time it increases. The extraction has led to a reduction in the outflow to rivers and in turn reduced the up-coning under the rivers, whereas the saline groundwater is mixed and more brackish groundwater is induced as the interface grows. At the same time by only extracting half of what comes in, additional fresh groundwater will accumulate and an increase the amount of available fresh groundwater volume. So, doubling the recharge during the winter and extraction during the summer has resulted in more fresh groundwater available in the system as the movement of saline groundwater from the bottom is reduced. Meanwhile, some spots under the extraction area start to up-cone and maybe under very long time can lead to higher up-coning.
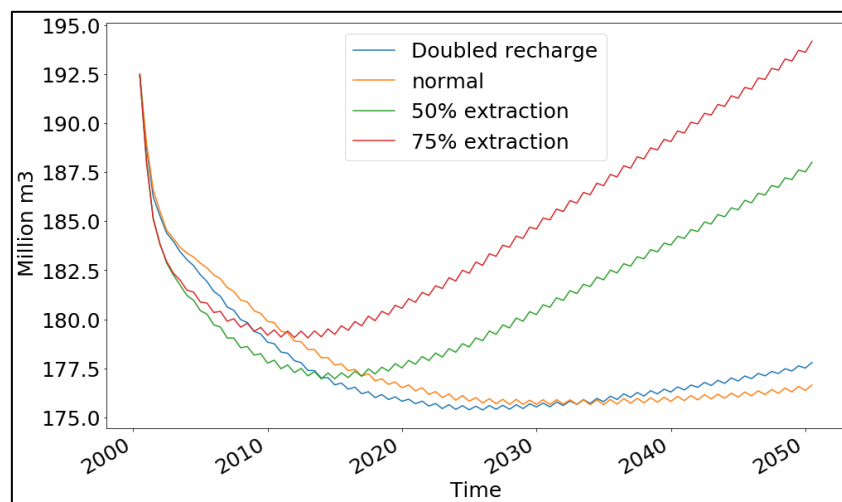
Figure 5-2: Evolution of the fresh groundwater volume before and after the recharge using 0.15 g Cl$^-$/l as a threshold.
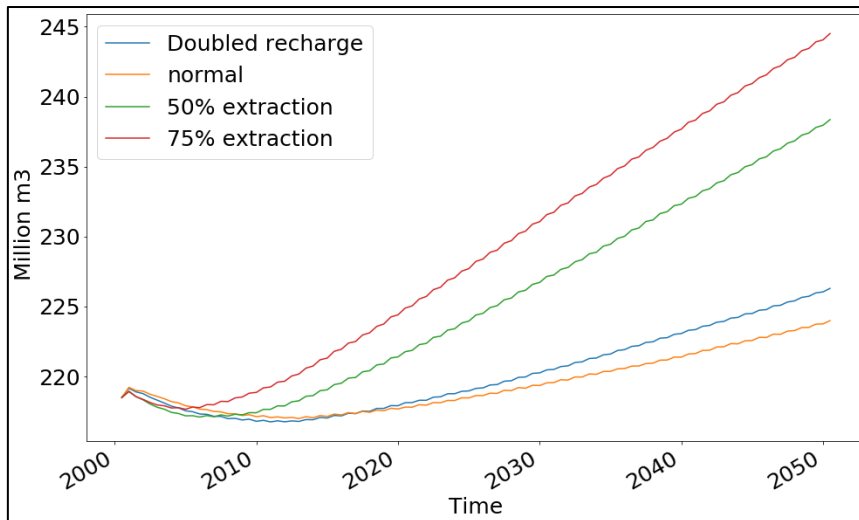
Figure 5-3: Evolution of the brackish groundwater volume before and after the recharge using 1.0 g/l as a threshold.

General limitations regarding the study area can be summarized in the following points. The average values for the recharge and the lack of recently observed groundwater heads made the correlation between the simulated and observed values not good enough. The high vertical velocities under the rivers induced by the values of the river conductance have added some uncertainties to the obtained model results. The groundwater flow patterns from the aquifer to the river are probably not simulated accurately, while the scale of the up-coning salinization process is small. This has locally led to higher vertical velocities under the rivers.

Chapter 6   Conclusion and Recommendations

First, the model discretization plays an important role in the degree of accuracy of the results. Adopting finer grids can eliminate numerical errors in terms of numerical dispersion and artificial oscillation. The discretization in the direction of the dominant groundwater flow direction has more influence on the accuracy of the results and to some degree in the length of the transport step. In general, we can see the finest grid can lead to accurate results but at the same time causes very long computational times. Therefore a relatively finer grid, especially in the preferential flow direction, can be used with adjusted transport step length for reliable results at the same time acceptable computational time. Of course, all depends on the purpose of the model and the degree of complexity required.

For each flow situation, one of the solvers will lead to better results. Comparing the results obtained with all solvers is important to identify the accurate one. Also linking the results to the groundwater flow characteristics is an important tool in understanding why each solver performed in a certain way and which one is better. Overall, TVD and MOC can lead to accurate results free of numerical errors. However, apart from the cell size, some other criteria need to be examined to select the good model for a certain case. For TVD, the Courant number is an important parameter. For MOC, the number of particles per cell is an important factor, besides, in some cases, the number of particles need to be the same in all cells where a weak groundwater flow occurs (making NPH equal to NPL). For both solvers, the mechanical dispersion is important as there are uncertainties about parametrizing the length of the longitudinal dispersivity from lab data into a real case study scale.

For DOW case, the groundwater flow regime in terms of the interaction between the groundwater flow system and the river has created flow regimes with mixed flow directions. This causes differences between MOC in one hand and TVD and FD in the other hand. TVD was adopted for carrying out the scenarios as it mimics the situation in the Netherlands whereas the groundwater system discharges saline groundwater to river systems. FD could also be considered but that solver creates a larger degree of numerical dispersion error then TVD. Reducing the transport step, using a larger number of particles all over the model and using

79

Fourth-order Runge-kutta algorithm for particle tracking and increasing the dispersivity has not changed the results obtained by MOC to be similar to the ones obtained by TVD and FD.

The degree of spatial discretization adopted in the existing model is used as a basis. When comparing different grid sizes (viz X Y Z) to each other, 25 m as cell size was found to give accurate results, and for the layer thickness (checking A B C), using 1 m and 2 m was found to give accurate results. However, using the small layer thickness will lead to serious longer computational time. Therefore, the existing discretization was adopted as a base case because it uses model layer thicknesses of 1 m and 2 m in the top layer where the interface is found and most of the groundwater dynamics is in the top model layers. The lower part of the model was discretized with 5 m as most of these layers have many inactive cells and have less influence on the top part. At the same time the shorter computational time can allow to perform numerous scenarios for the aquifer storage and recovery system.

The areas with higher elevation, which called the creek ridge, has a thicker freshwater lens in comparison to the other parts. Increasing the water table in this area has resulted in the growth of the freshwater lens underneath it. Adding more water without extraction led to more outflow through the rivers and the drainage system, and in turn, increased the up-coning and the movement of saline water in other areas.

The extraction of half of the water during the summer for the entire period is sustainable and has small negative effects on the salinity of the aquifer. Furthermore, the extraction process reduced the vertical velocity under the rivers by reducing the outflow, which resulted in more freshwater available as the movement of the saline water now is slower. Extraction of three-quarter of the water has less impacts as well but more up-coning is induced under the areas where the extraction took place. Worth to mention that this model is representing approximately a fifth of the actual study area of DOW case model, therefore from this area, this amount of water being extracted can help in covering the shortage. Recharging 3.6 million cubic meter and extracting half of it (1.8 MCM) will help covering the shortage during the summer period. Other larger projects in the whole study area will be examined as well but it out of the scope of this study.

Future recommendations regarding the case study model can be outlined as follow:

- Testing TVD and FD with more finer cell sizes and see if the same up-coning affect will remain or not.

- The values for the recharge should be modelled daily for better representation of the groundwater heads and examine the effects on the saline distribution and water budget.

- The values for the river's conductance can be adjusted to reduce the higher vertical velocities to see how the system will behave.

- To simulate the artificial recharge and extraction system more accurately we need to use river package instead of wells. So, the smaller rivers (which are simulated with river package) should be simulated using the general head boundary package (same as the larger rivers), then using the river package for simulating the aquifer storage and recovery.

- The influence of the drawdown and the reduction of the discharge to the rivers and drains has not been assessed in the case study yet. Therefore, assessing the impacts drawdowns and reduced discharges in the case study area need be carried out.

References

Al-Maktoumi A, Lockington DA, Volker RE (2007) SEAWAT 2000: modelling unstable flow and sensitivity to discretization levels and numerical schemes. Hydrogeology Journal 15: 1119-1129 DOI 10.1007/s10040-007-0164-2

Anderson MP, Woessner WW, Hunt RJ (2015) Applied groundwater modeling: simulation of flow and advective transport Academic press

Carrera J (1993) An overview of uncertainties in modelling groundwater solute transport. Journal of contaminant hydrology 13: 23-48

De Lange WJ, Prinsen GF, Hoogewoud JC, Veldhuizen AA, Verkaik J, Essink GHO, Van Walsum PE, Delsman JR, Hunink JC, Massop HTL (2014) An operational, multi-scale, multi-model system for consensus-based, integrated water management and policy analysis: The Netherlands Hydrological Instrument. Environmental Modelling & Software 59: 98-108

Delsman JR, Van Baaren ES, Siemon B, Dabekaussen W, Karaoulis MC, Pauw PS, Vermaas T, Bootsma H, De Louw PG, Gunnink JL (2018) Large-scale, probabilistic salinity mapping using airborne electromagnetics for groundwater management in Zeeland, the Netherlands. Environmental Research Letters 13: 084011

Deltares (2015) Geology of the Dutch coast

Deltares (2019) feasibilty study - subsurface fresh water storage in Braakman South region

Dillon P, Toze S, Page D, Vanderzalm J, Bekele E, Sidhu J, Rinck-Pfeiffer S (2010) Managed aquifer recharge: rediscovering nature as a leading edge technology. Water science and technology 62: 2338-2345

Goswami RR, Clement TP, Hayworth JH (2012) Comparison of Numerical Techniques Used for Simulating Variable-Density Flow and Transport Experiments. Journal of Hydrologic Engineering 17: 272-282 DOI 10.1061/(asce)he.1943-5584.0000428

Graf T, Degener L (2011) Grid convergence of variable-density flow simulations in discretely-fractured porous media. Advances in Water Resources 34: 760-769 DOI 10.1016/j.advwatres.2011.04.002

Guo W, Bennett GD (1998) Simulation of saline/fresh water flows using MODFLOWMODFLOW 98 Conference, Golden, CO In: Poeter, E et al(Ed), 1998 Proceedings (1), pp. 267-274.

Guo W, Langevin CD (2002) User's guide to SEAWAT; a computer program for simulation of three-dimensional variable-density ground-water flow.

Henry HR (1964) Effects of dispersion on salt encroachment in coastal aquifers, in" Seawater in Coastal Aquifers". US Geological Survey, Water Supply Paper 1613: C70-C80

Holzbecher E, Sorek S (2006) Numerical models of groundwater flow and transport. Encyclopedia of hydrological sciences

Ibaraki M (1998) A robust and efficient numerical model for analyses of density-dependent flow in porous media. Journal of Contaminant Hydrology 34: 235-246

Jha MK, Chowdhury A, Chowdary VM, Peiffer S (2006) Groundwater management and development by integrated remote sensing and geographic information systems: prospects and constraints. Water Resources Management 21: 427-467 DOI 10.1007/s11269-006-9024-4

Oude Essink G (2001) Density dependent groundwater flow: salt water intrusion and heat transport. Lecture Notes Utrecht University Interfaculty Centre of Hydrology Utrecht Institute of Earth Sciences Department of Geophysics

Oude Essink, Gualbert & Pauw, Pieter. (2018). Evaluatie en verdiepend onderzoek naar grondwateronttrekkingsregels in de provincie Zeeland. 10.13140/RG.2.2.21159.04004.

Park CH, Aral MM (2007) Sensitivity of the solution of the Elder problem to density, velocity and numerical perturbations. J Contam Hydrol 92: 33-49 DOI 10.1016/j.jconhyd.2006.11.008

Pauw PS, Van Baaren ES, Visser M, De Louw PG, Essink GHO (2015) Increasing a freshwater lens below a creek ridge using a controlled artificial recharge and drainage system: a case study in the Netherlands. Hydrogeology Journal 23: 1415-1430

Rahman MA, Rusteberg B, Uddin MS, Lutz A, Saada MA, Sauter M (2013) An integrated study of spatial multicriteria analysis and mathematical modelling for managed aquifer recharge site suitability mapping and site ranking at Northern Gaza coastal aquifer. Journal of environmental management 124: 25-39

Ramkumar M, Menier D, Kumaraswamy K (2019) Coastal Zone Management During Changing Climate and Rising Sea Level: Transcendence of Institutional, Geographic, and Subject Field Barriers Is the KeyCoastal Zone Management:1-12.

Reilly TE, Harbaugh AW (2004) Guidelines for evaluating ground-water flow models DIANE Publishing

Simpson M, Clement T (2003) Theoretical analysis of the worthiness of Henry and Elder problems as benchmarks of density-dependent groundwater flow models. Advances in Water Resources 26: 17-31

Simpson MJ, Clement TP (2004) Improving the worthiness of the Henry problem as a benchmark for density‐dependent groundwater flow models. Water Resources Research 40

Stafleu J, Maljers D, Gunnink JL, Menkovic A, Busschers FS (2014) 3D modelling of the shallow subsurface of Zeeland, the Netherlands. Netherlands Journal of Geosciences - Geologie en Mijnbouw 90: 293-310 DOI 10.1017/s0016774600000597

Stuyfzand PJ (2016) History of managed aquifer recharge in The Netherlands. Electronic Supplementary Material-Hydrogeology Journal Sixty years of global progress in managed aquifer recharge: 36

UNESCO I (2005) Strategies for Managed Aquifer Recharge (MAR) in Semi-arid Area UNESCO.

Van Baaren E, Oude Essink G, Janssen G, De Louw P, Heerdink R, Goes B (2016) Verzoeting en verzilting freatisch grondwater in de Provincie Zeeland. Rapportage 3D regionaal zoet-zout grondwater model (Utrecht: Deltares)

Ward JD, Simmons CT, Dillon PJ (2007) A theoretical analysis of mixed convection in aquifer storage and recovery: How important are density effects? Journal of Hydrology 343: 169-186

Braakman (2005) https://en.wikipedia.org/wiki/Braakman

Braakman (2011) https://nl.wikipedia.org/wiki/Braakman

Zheng C, Wang PP (1999) MT3DMS: a modular three-dimensional multispecies transport model for simulation of advection, dispersion, and chemical reactions of contaminants in groundwater systems; documentation and user's guide Alabama Univ University.

Zhou Y, Li W (2011) A review of regional groundwater flow modeling. Geoscience Frontiers 2: 205-214 DOI 10.1016/j.gsf.2011.03.003

Map of Zeeland fresh and salt groundwater (2017) https://www.zwdelta.nl/nieuws/zeeuws-zoet-en-zout-grondwater-in-kaart

Project GO-FRESH is entering a new phase (2018) https://www.zwdelta.nl/nieuws/project-go-fresh-nieuwe-fase-in

Zuurbier K (2016) Increasing freshwater recovery upon aquifer storage: a field and modelling study of dedicated aquifer storage and recovery configurations in brackish-saline aquifers

Appendix A. - Research Ethics Declaration Form

Date: 2020-03-16
To: Ali Ahmed Abdallah Obeid
MSc Programme: WSE- HWR
Approval Number: IHE-RECO 2020 -042

Subject: Exemption for further ethical review

Dear Ali Ahmed Abdallah Obeid

Based on your application for Ethical Approval, your proposal "Sensitivity Analysis of Density-variant Groundwater Models. case study of Braakman south region, the Netherlands has been exempted from further revision by the Research Ethics Committee (RECO), IHE Delft. You need to notify the RECO of any modifications to your research protocol.

Please keep this letter for your records and include a copy in the final version of MSc. Thesis.

On behalf of the Research Ethics Committee, I wish you success in the completion of your research.

Yours sincerely,

Angeles Mendoza
Acting Ethics Coordinator

Copy to: Academic VP.
Copy to: Reviewer

🏛️ **IHE**
DELFT

Part 1

1.1 General Information

Date:	08/11/2019		
Researcher	Ali Ahmed Abdallah Obeid		
Student number	1060099	E-mail	aob001@un-ihe.org
Department or MSc. Programme	Water Science and Engineering Department with specialization in Hydrology and Water Resources.		
Mentor	Yangxiao Zhou	E-mail	y.zhou@un-ihe.org
Supervisor	Michael McClain	E-mail	m.mcclain@un-ihe.org
Country where research will take place	Netherlands		
Project or funding source	Deltares		
Title of Research proposal	Sensitivity Analysis of Density-Variant Groundwater Model case study of braakman South region, the Netherlands		
Summary	Groundwater can be used as a big storage as it possesses many advantages, however sometimes saline water might be presence in the aquifer and can be of a complex distribution . This research aims to study the develop of fresh water lens in complex fresh/saline aquifer using density dependent groundwater models, in my case I will be using SEAWAT. The study will be carried out through assessment to the influence of the different numerical solutions, many model parameters and model discretization in the model results in order to obtain good assessment tool. Then the model will be used to investigate potential places for recharge and sustainable extraction mechanism.		
Signature of Student		Date:	08/11/2019
Signature of Mentor	Yangxiao Zhou	Date:	Nov. 8, 2019
Signature of Supervisor		Date:	18 Nov 2019

1.2 Screening checklist

These are common activities that may result in ethical issues. if not of them apply to your research, submit Part 1 of the application to IHE RECO. If one or more of the items apply to your research, you need to complete parts 1 and 2 and submit the application with the required documentation.

86

IHE DELFT

Answer yes or no to the questions that apply to your research.	Yes	No
Collecting personal information		
Will your research involve collecting, processing and/or reporting personal data obtained from primary or secondary sources?	☐	☑
Will you obtain information from individuals or groups of individuals through questionnaires, interviews, focus groups or other methods?	☐	☑
Debriefing and consent process		
Will you obtain information from individuals or groups through questionnaires, interviews, focus groups or other methods?	☐	☑
Will your research involve individuals or groups who need to give their voluntary consent to participate?	☐	☑
Will the participants include individuals belonging to groups that require special considerations, e.g. people under legal age of consent, immigrants, refugees, disable people, or other vulnerable groups in the country of the research?	☐	☑
Will your research involve participants for whom voluntary and informed consent may require special attention (e.g. children (under 18s), people with learning disabilities, undocumented migrants, patients, prisoners)?	☐	☑
Will your research include observation of individuals or groups of people without their explicit consent or knowledge?	☐	☑
Will your research require withholding information about the project or misleading participants?		☑
Will your research use the cooperation of a person or organization of influence or power (gatekeeper) in a community, organization, or other, to involve individuals or groups in your research?	☐	☑
Will you require the help of a translator to collect, process and/or report information from participants?	☐	☑
Will you use animals in your research?	☐	☑
Benefits and risks to participants and researchers		
Could the participation in the research, or the dissemination of its results cause -directly or indirectly- psychological stress, anxiety, harm or other negative consequences for participants or the researcher?	☐	☑
Could the involvement in the research contribute to any risk for participants or researchers because of the situation in the country or specific locations in which the research will take place?	☐	☑
Will you provide or offer any financial, material or other incentives for people to participate in your research?	☐	☑
Could any aspects of the research, or the communications related to, be perceived as inappropriate in the context of the culture, beliefs or practices of individuals or groups of informants, e.g. ethnic or religious groups, or could interfere with their culture, beliefs or practices?	☐	☑
Research context		
Will your research also require any research permits or ethical approval from national or local institutions or organizations?	☐	☑
Could any factors of the research - including design, funding, dissemination of results, or other - be associated to potential conflict of interest that would put at risk its integrity?	☐	☑

87

IHE
DELFT

If you are a student and answered *No* to all items, fill-in the declaration and submit it to your Program' Secretary and MSc Coordinators. Keep a copy for your records. Part 1, including the written personal declaration must be included in Annex 1 of the MSc. Thesis submitted for defence. Staff should contact RECO directly.

If you answered *Yes* to any of the questions, in addition to submitting the check list and declaration, you also need to answer the applicable questions in Part 2. Submit this part together with the check list and the declaration to your Program' Secretary and MSc Coordinators. They will submit it to the Research Ethics Committee. Staff should contact RECO directly.

Declaration

Check what applies to your research
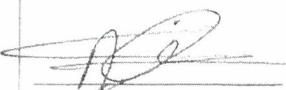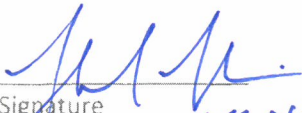
☒ I Ali Ahmed Abdallah Obeid   have read the Netherlands Code of Conduct for Research Integrity and IHE guidelines for Research Ethics.

☒ My research does not have any ethical implications because of the use of personal data or involvement of humans or animals as research subjects. I understand the Principles of Research Integrity and the Standards of Good Research Practices, and have considered them for my research in the following way:

[Write a short description, minimum 1,000 words, of how you have or will consider in your research the Principles and the Standards mentioned above]

☐ My research involves the collection of personal data and/or the involvement of human or animal subjects. I understand the principles that guide the use of personal data and/or involvement of human subjects or animals and have considered the ethical issues that may arise from my research. I have incorporated measures to prevent harm and/or ethical repercussions for research subjects (humans and/or animals), and the institutions or groups involved in the research and elaborate on them in the attached form (Part 2) that I submit for ethical clearance.

Signatures

Student/Researcher	Mentor
Signature	Yangxiao Zhou
Name: Ali Ahmed Abdallah Obeid	Signature Yangxiao Zhou
	Name:
Date: 08/11/2019	Date; Nov. 21 2019
Supervisor	
Signature ME McClain 18 Nov 2019	

Version 1.6

For comments or questions about this form, write to a.mendoza@un-ihe.org.

Appendix B. - Freshwater lens results

Horizontal cell size = 250 m
Vertical cell size = 10 m

Horizontal cell size = 100 m
Vertical cell size = 10 m

Horizontal cell size = 50 m
Vertical cell size = 10 m

Horizontal cell size = 25 m
Vertical cell size = 10 m

Horizontal cell size = 10 m
Vertical cell size = 10 m

Horizontal cell size = 250 m
Vertical cell size = 5 m

Horizontal cell size = 100 m
Vertical cell size = 5 m

Horizontal cell size = 50 m
Vertical cell size = 5 m

Horizontal cell size = 25 m
Vertical cell size = 5 m

Horizontal cell size = 10 m
Vertical cell size = 5 m

Horizontal cell size = 250 m
Vertical cell size = 1 m

Horizontal cell size = 100 m
Vertical cell size = 1 m

Horizontal cell size = 50 m
Vertical cell size = 1 m

Horizontal cell size = 25 m
Vertical cell size = 1 m

Horizontal cell size = 10 m
Vertical cell size = 1 m

Figure B-1: Freshwater lens interface for different spatial discretization using TVD

Numerical depth of TDS-0.5
Analytical Solution
Numerical depth of TDS-1.5
Numerical depth of TDS-8.75
Numerical depth of TDS-17.5
Numerical depth of TDS-26.25
Numerical depth of TDS-33.25
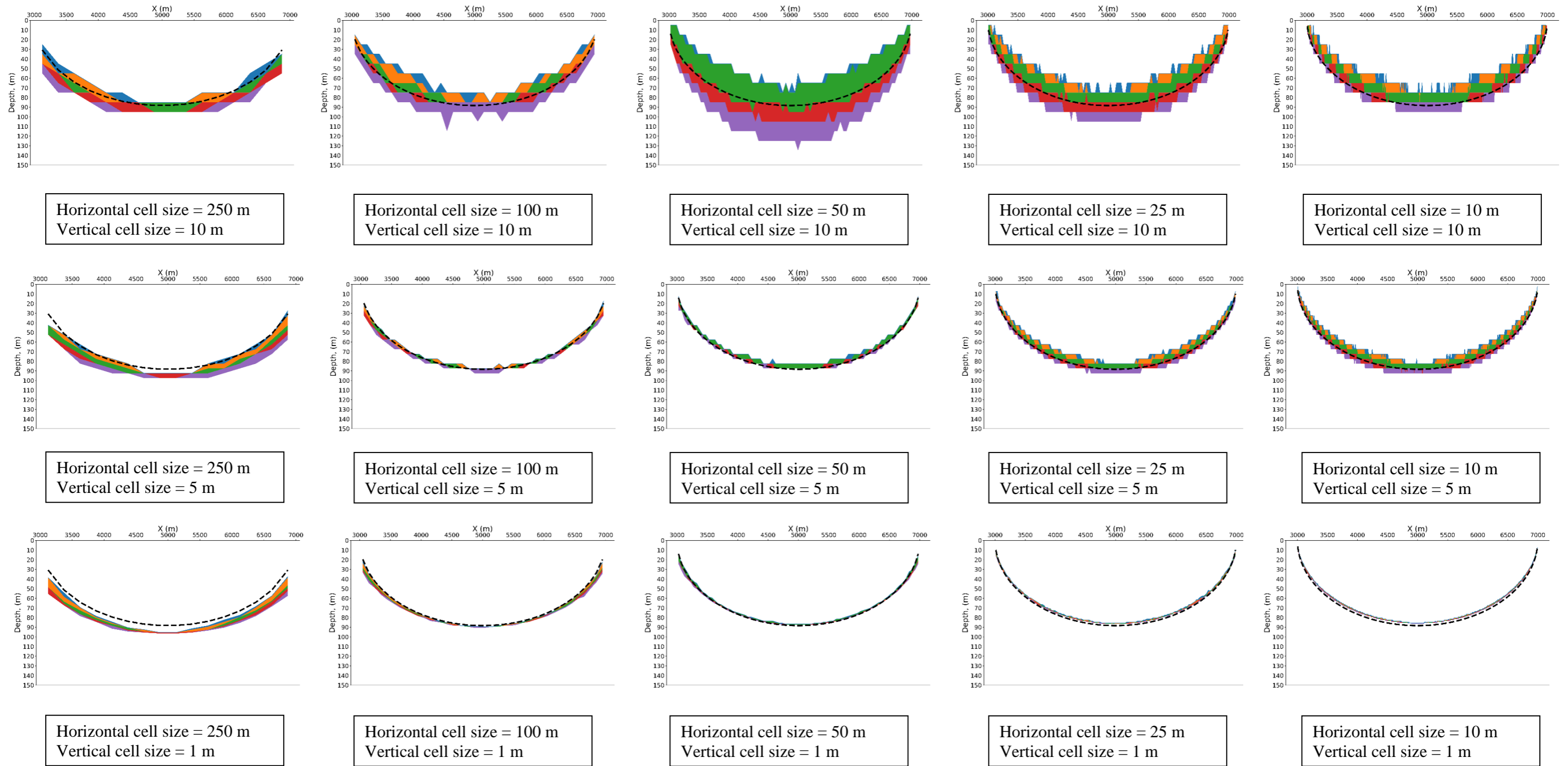
Figure B-2: Freshwater lens interface for different spatial discretization using MOC
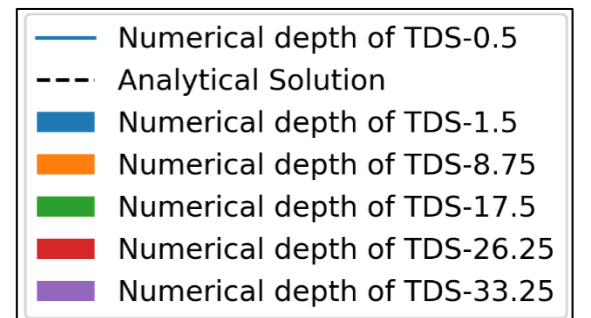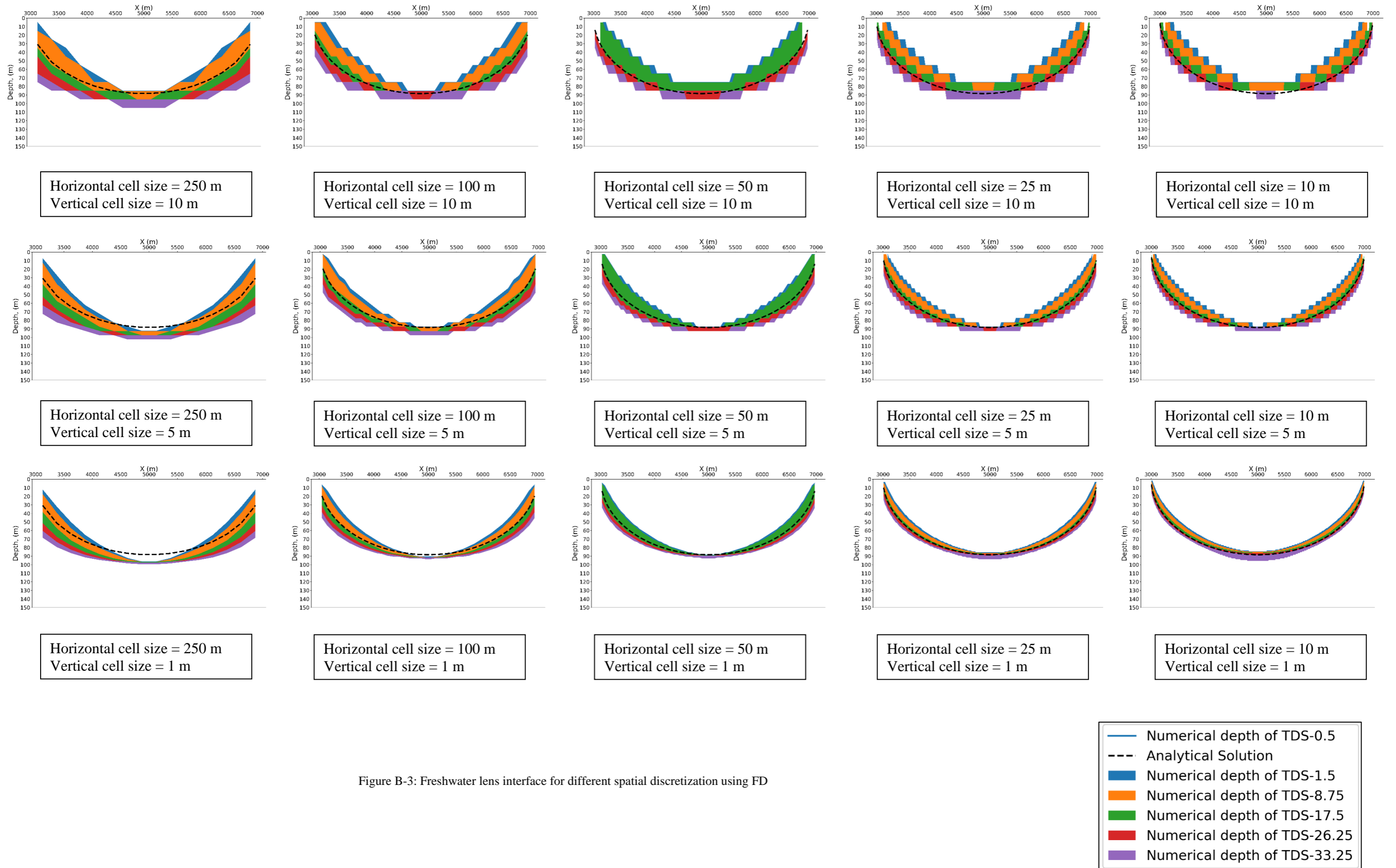
Figure B-3: Freshwater lens interface for different spatial discretization using FD
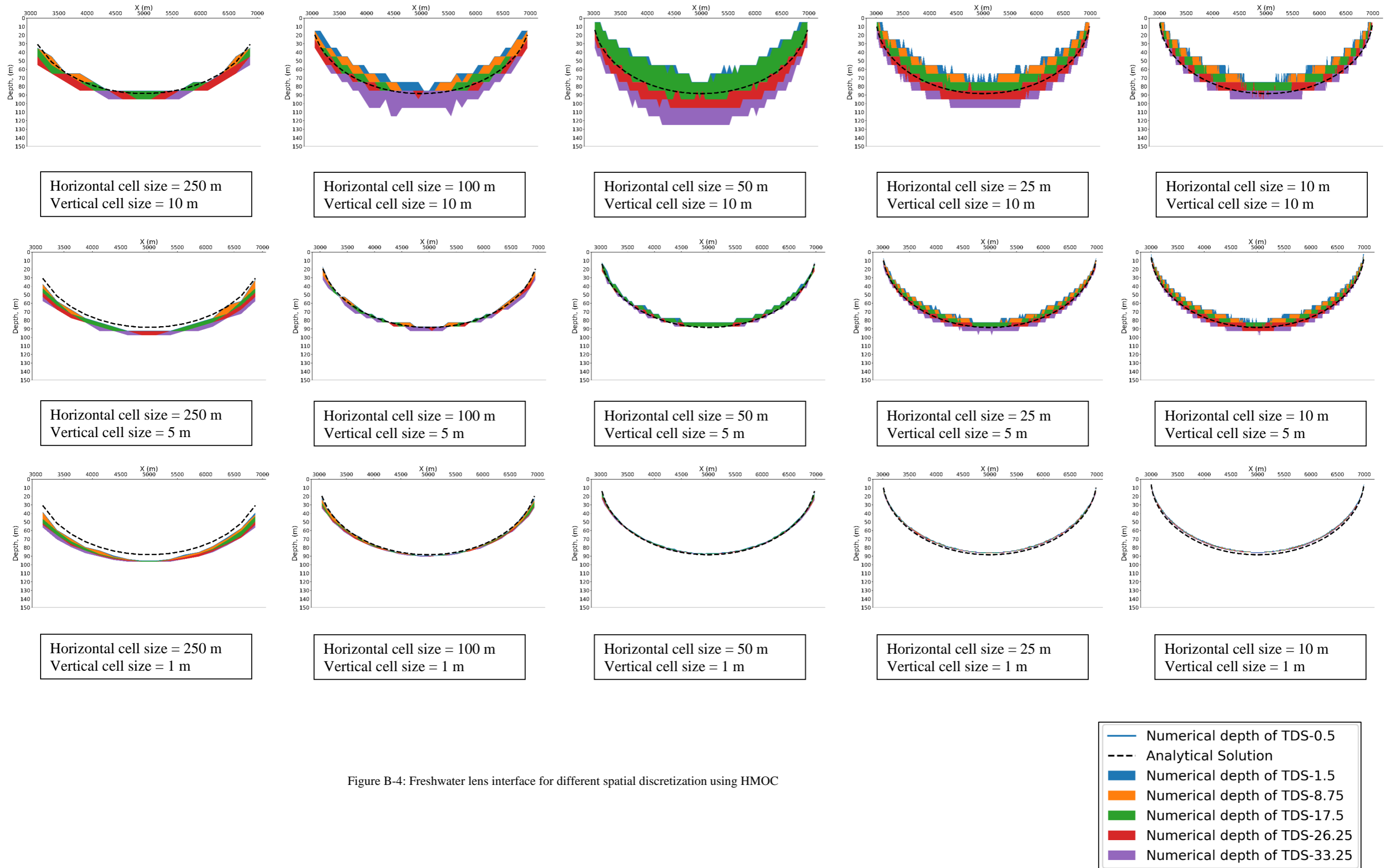
Figure B-4: Freshwater lens interface for different spatial discretization using HMOC

Figure B-5: Freshwater lens interface for different spatial discretization using MMOC
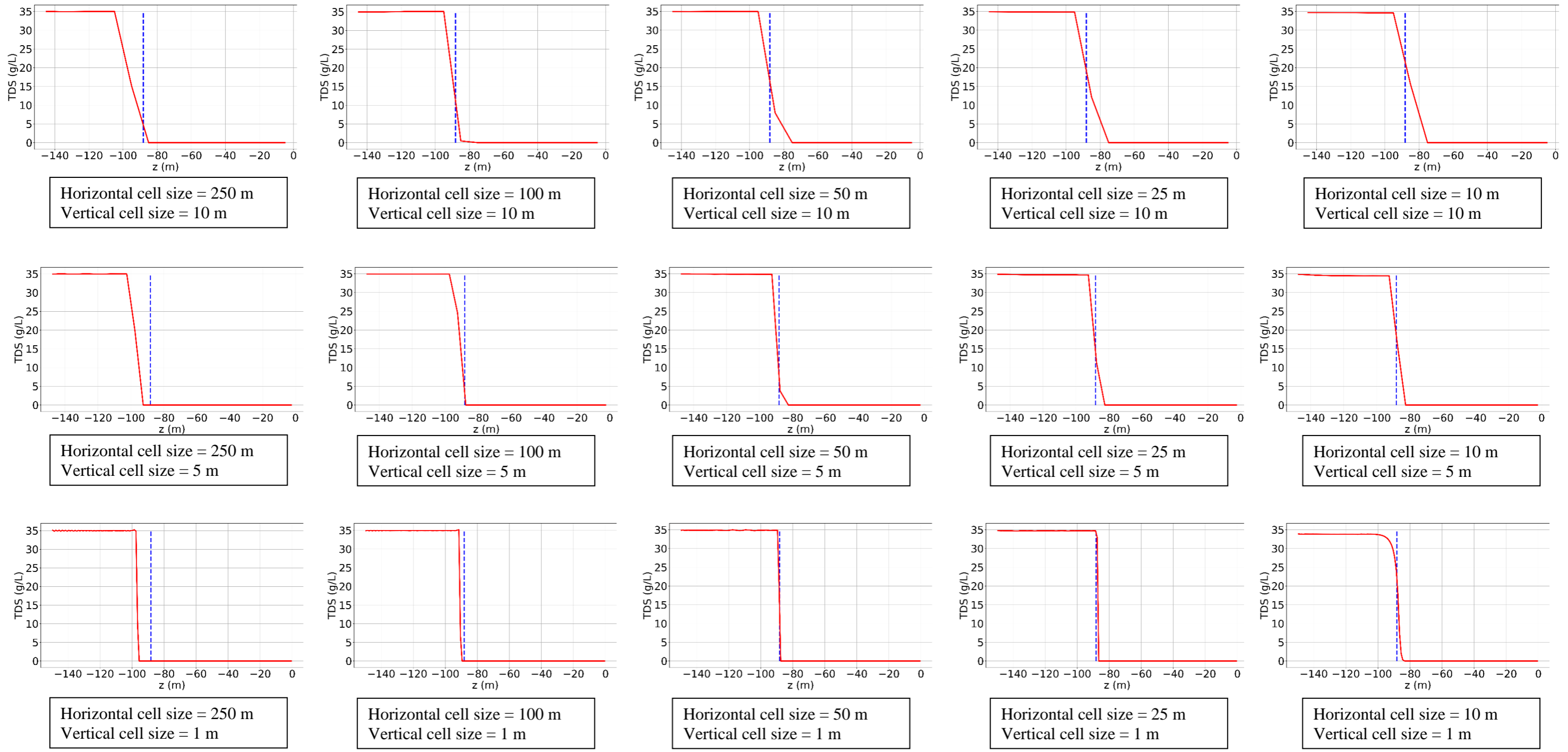
Figure B-6: Freshwater Lens interface shape at centre of the model using TVD
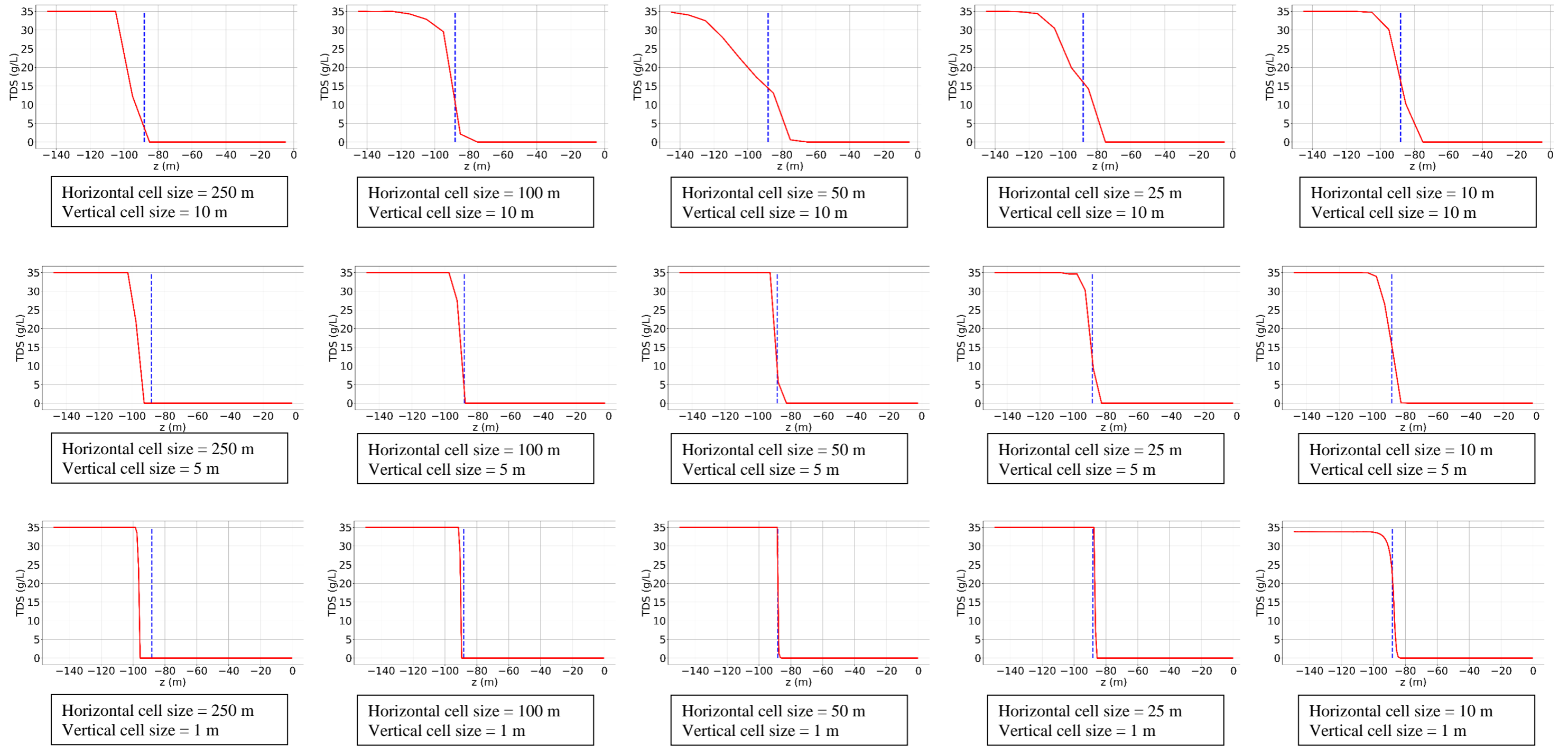
Figure B-7: Freshwater Lens interface shape at centre of the model using MOC
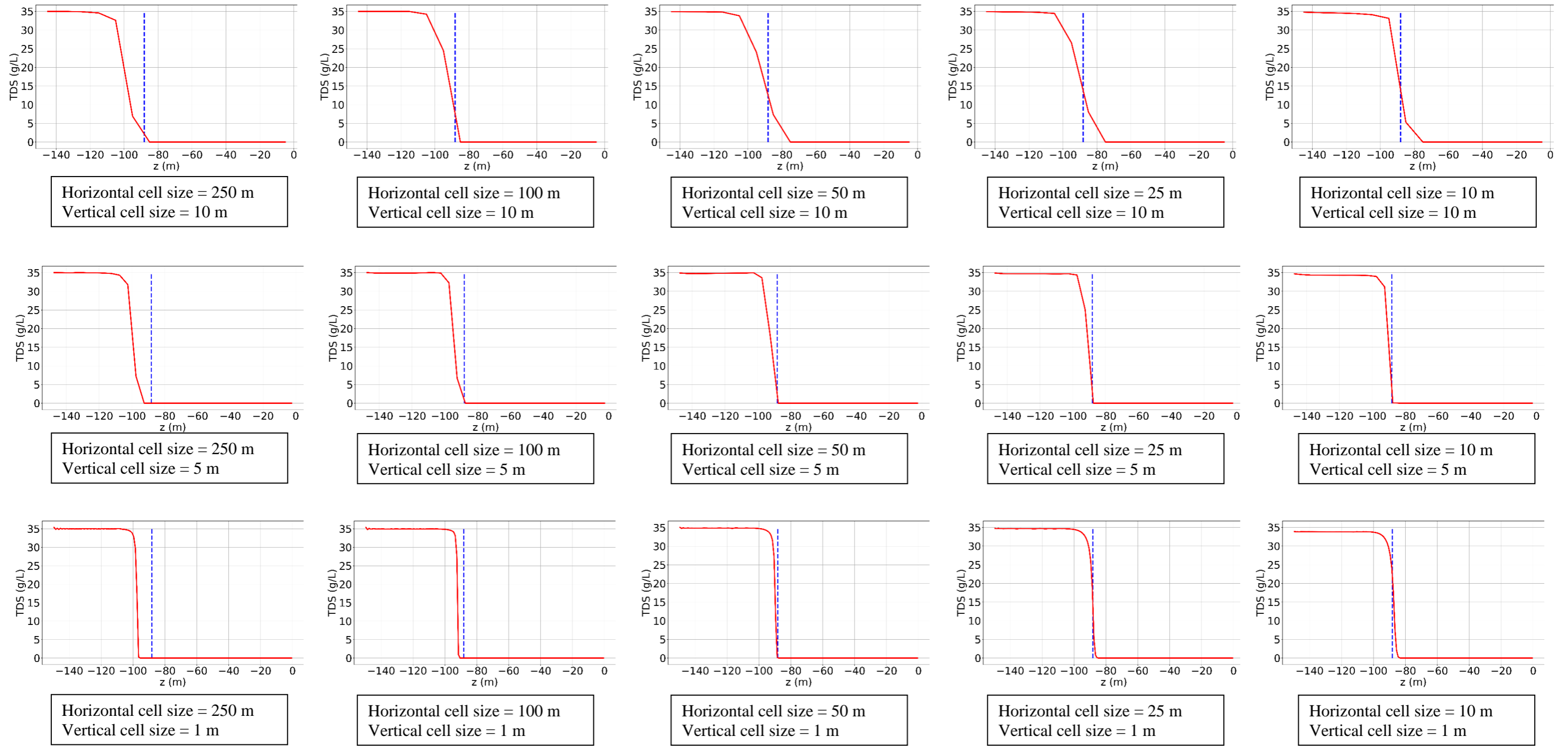
Figure B-8: Freshwater Lens interface shape at centre of the model using FD
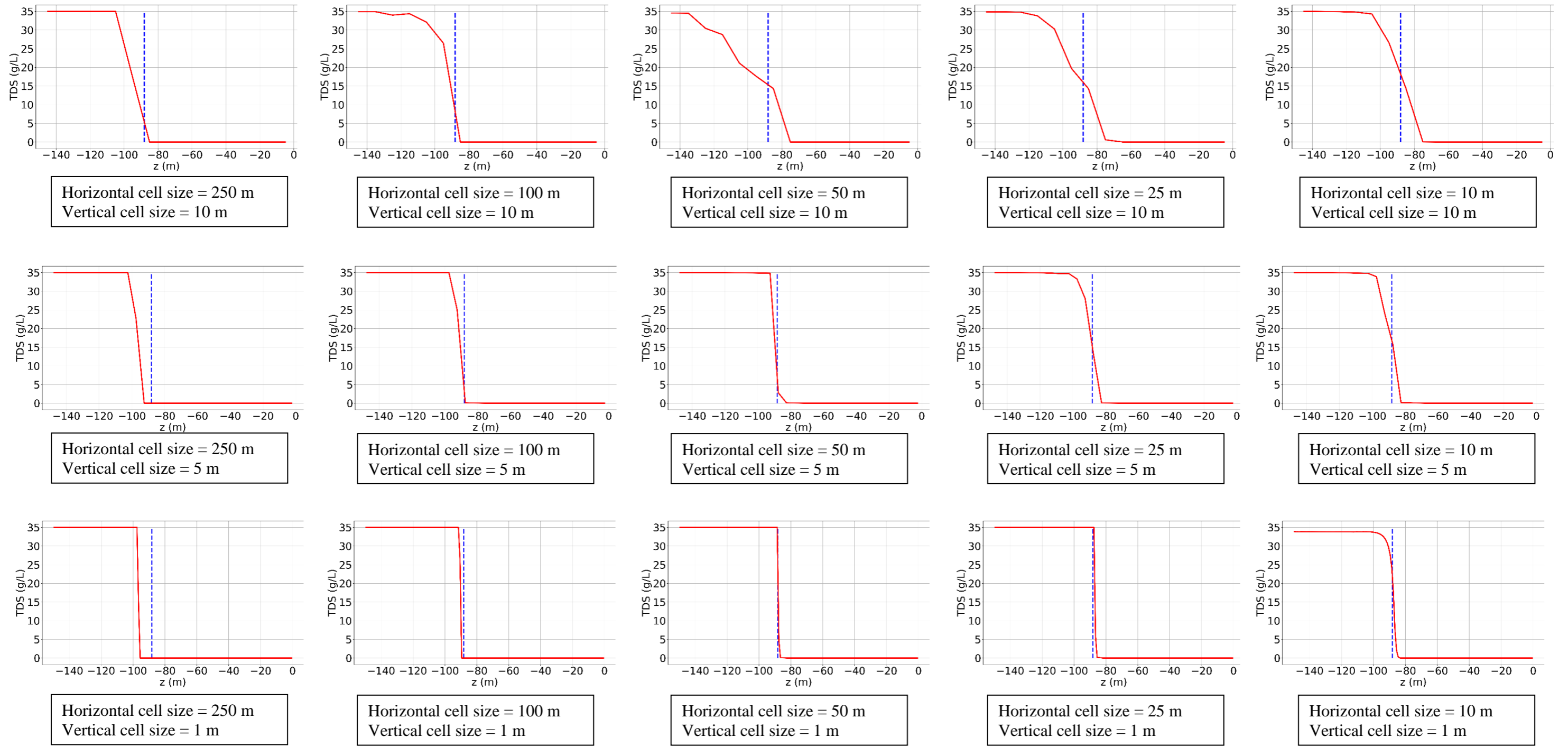
Figure B-9: Freshwater Lens interface shape at centre of the model using HMOC
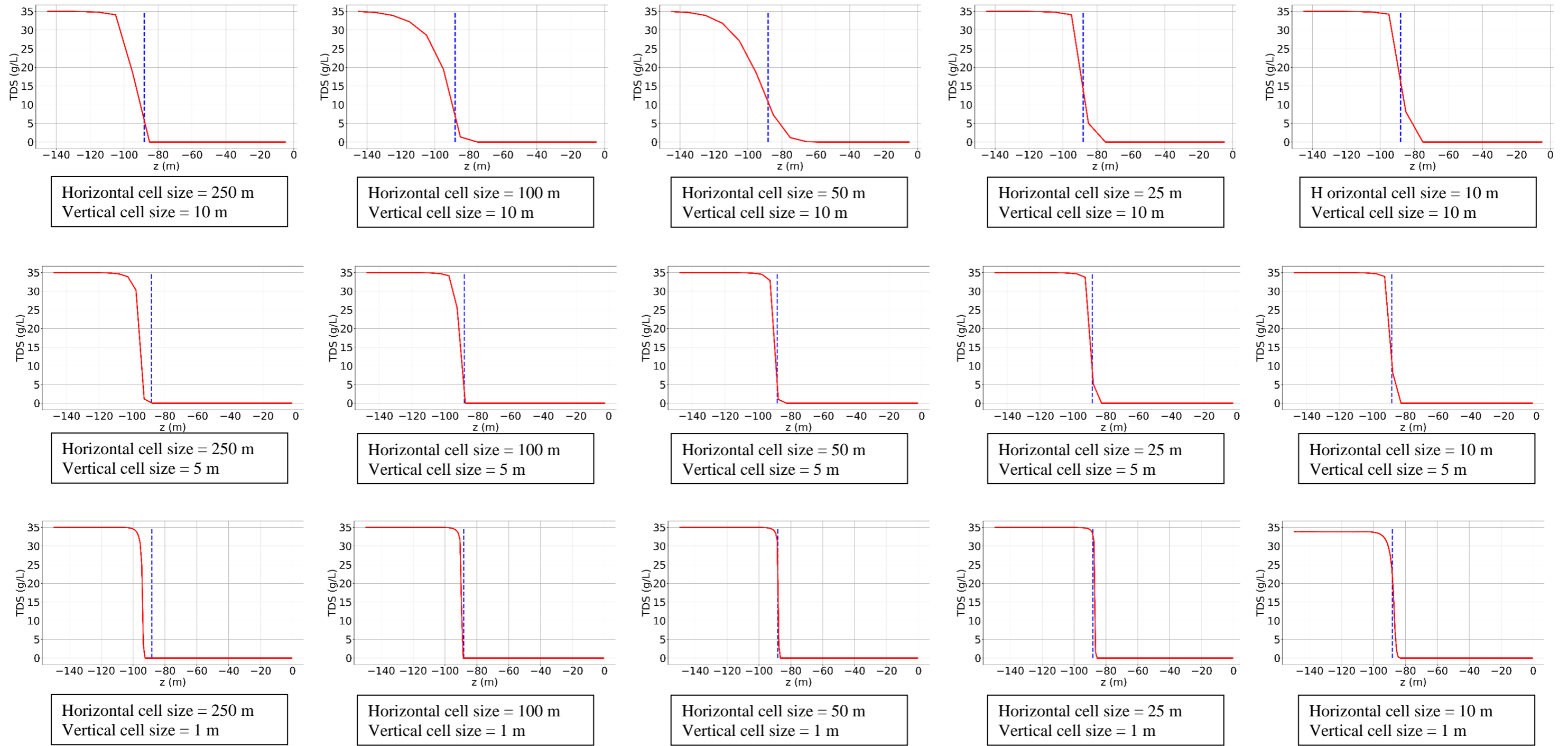
Figure B-10: Freshwater Lens interface shape at centre of the model using MMOC

Appendix C. - DOW model results
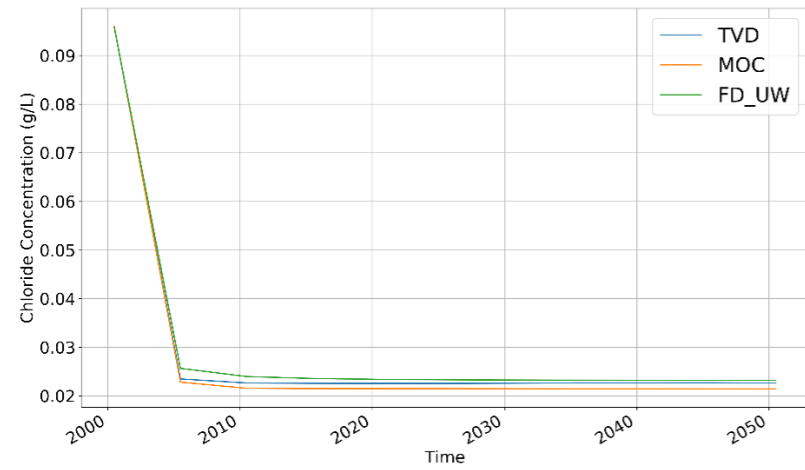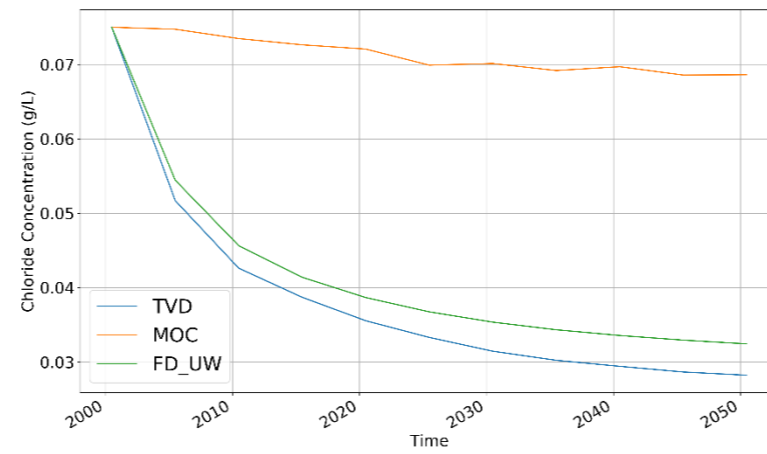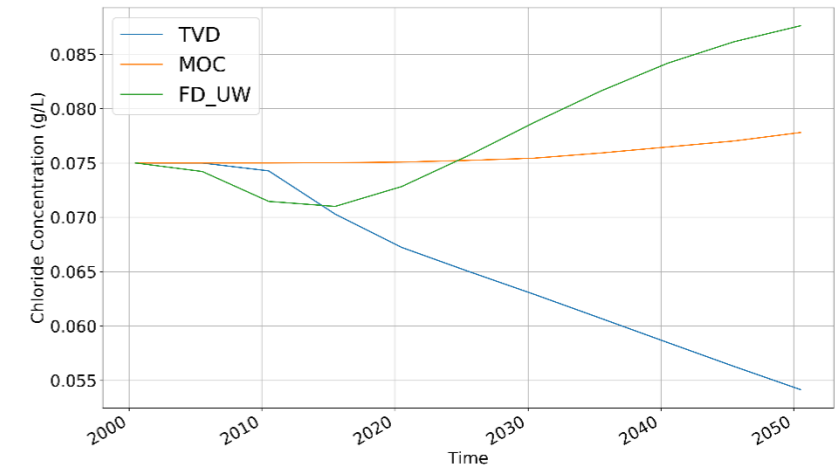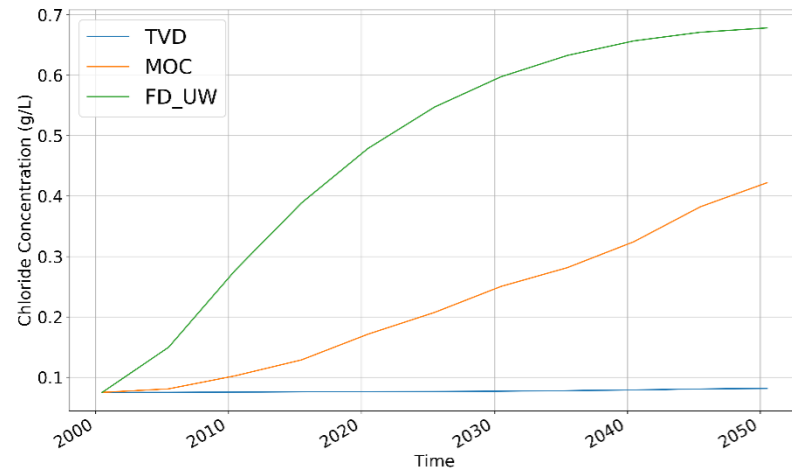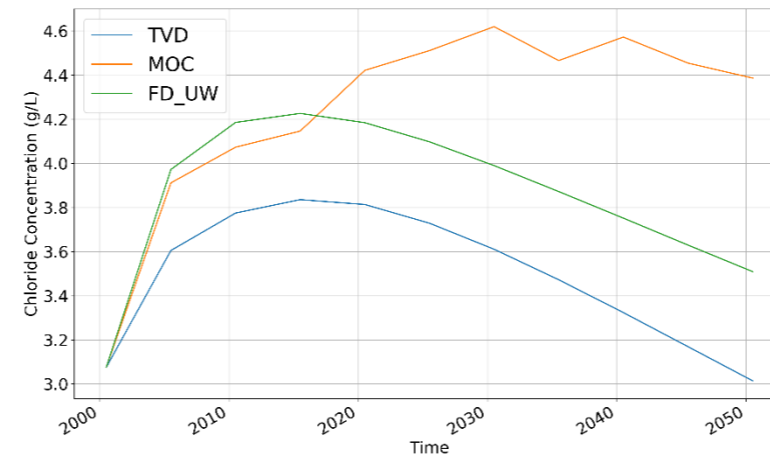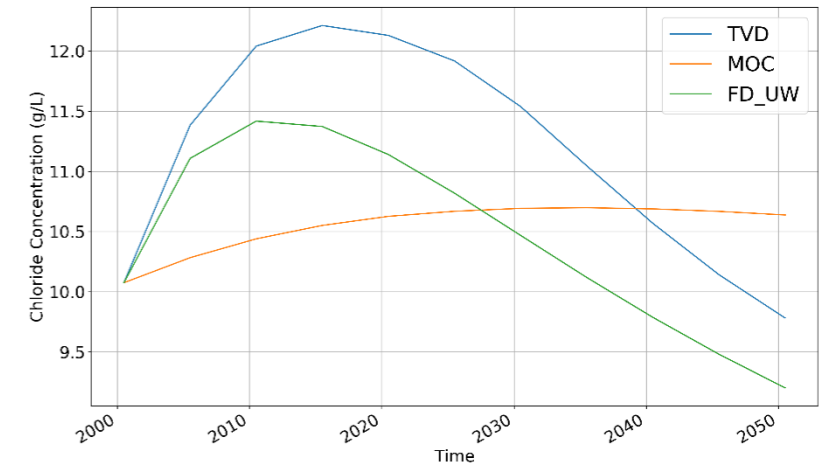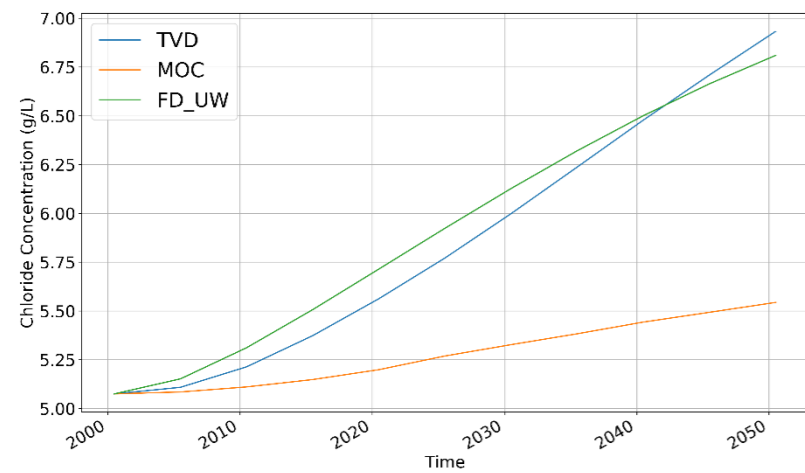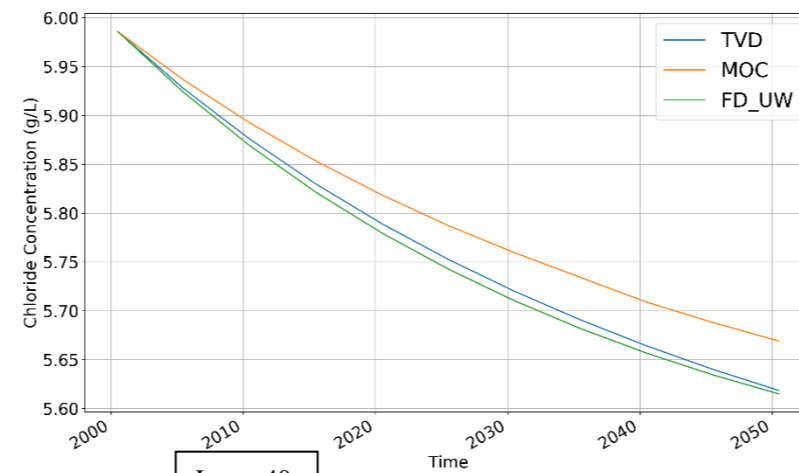
Figure C-1: breakthrough curves at x = 39050, y = 367856 for different layers
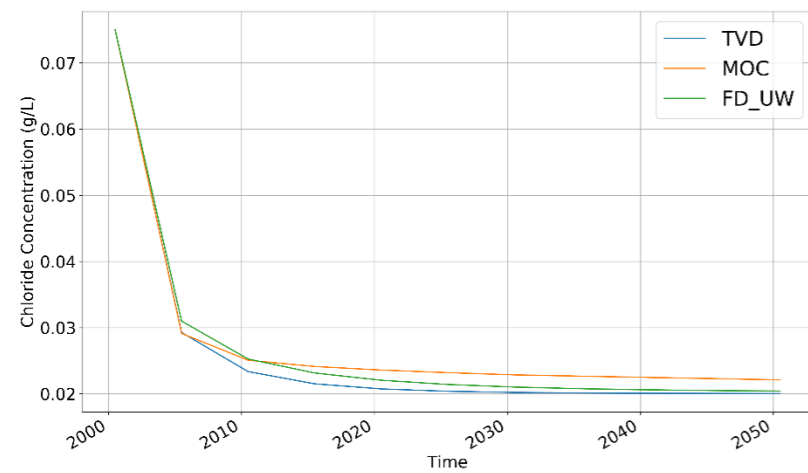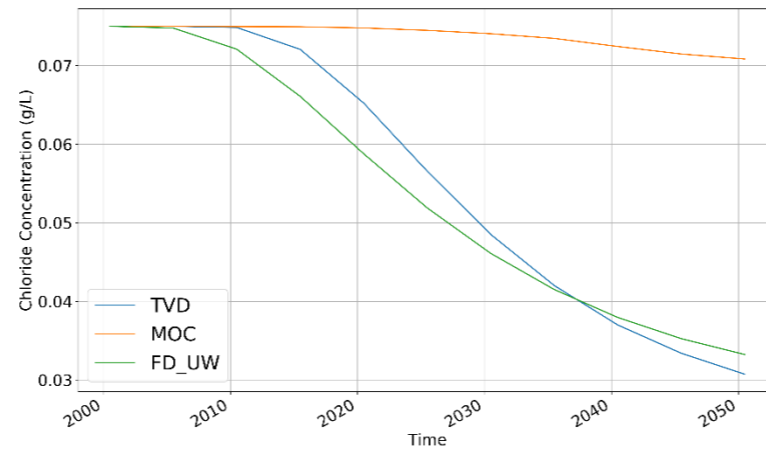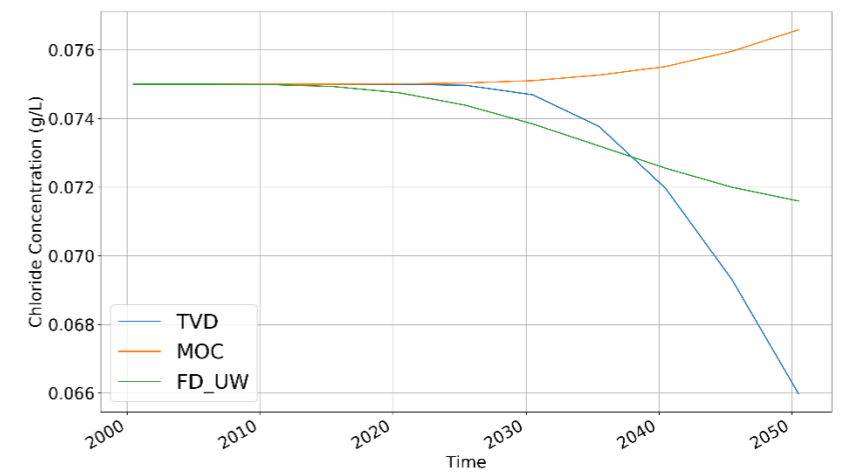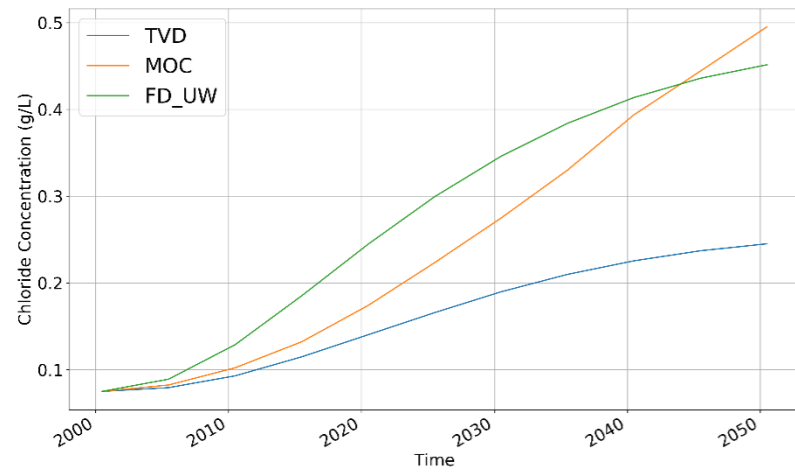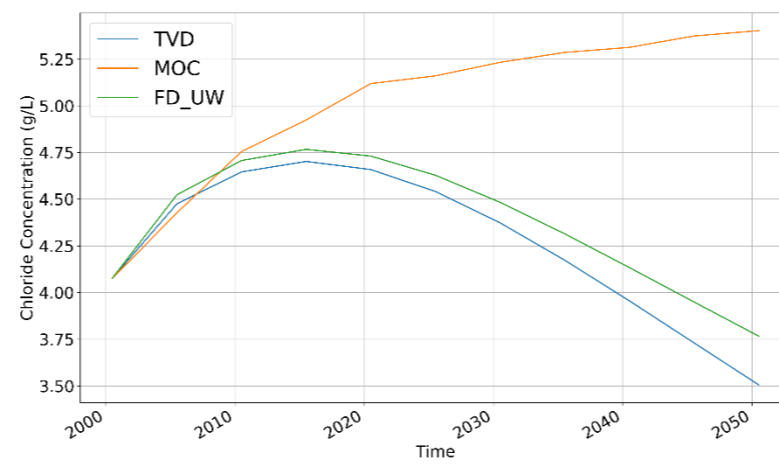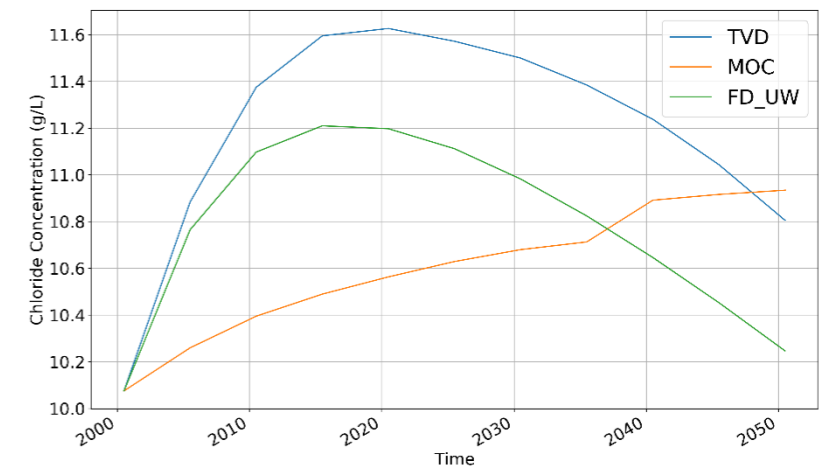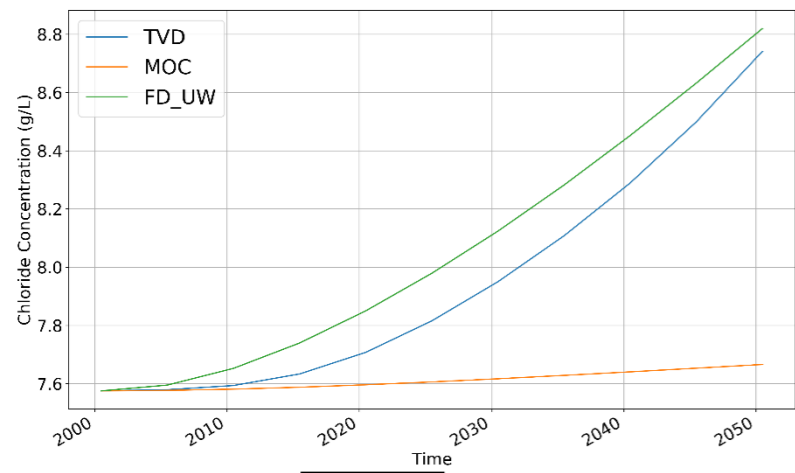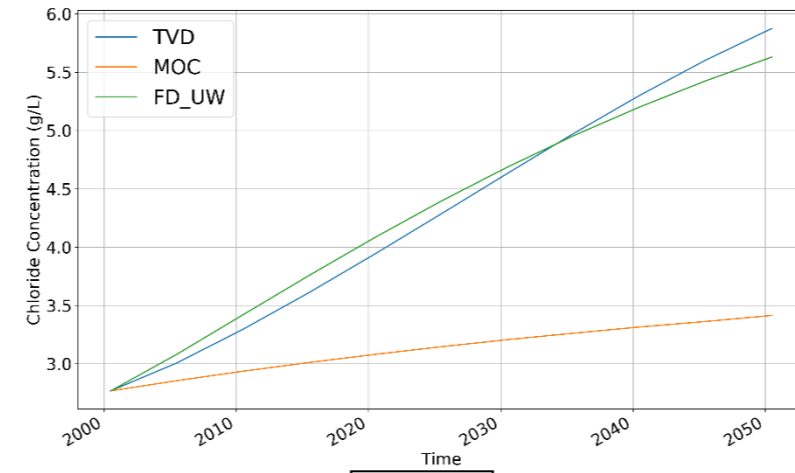
Figure C-2: breakthrough curves at x = 39050, y = 369350 for different layers
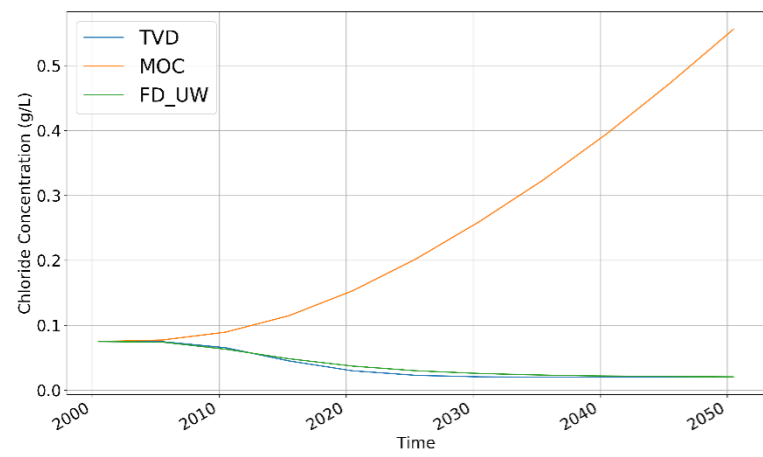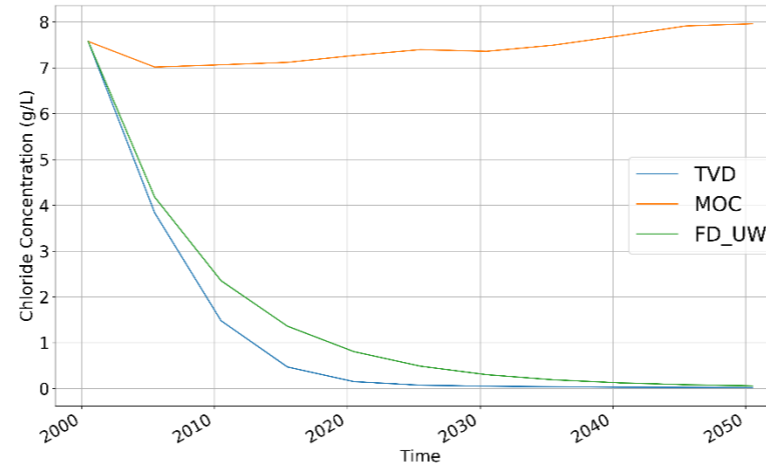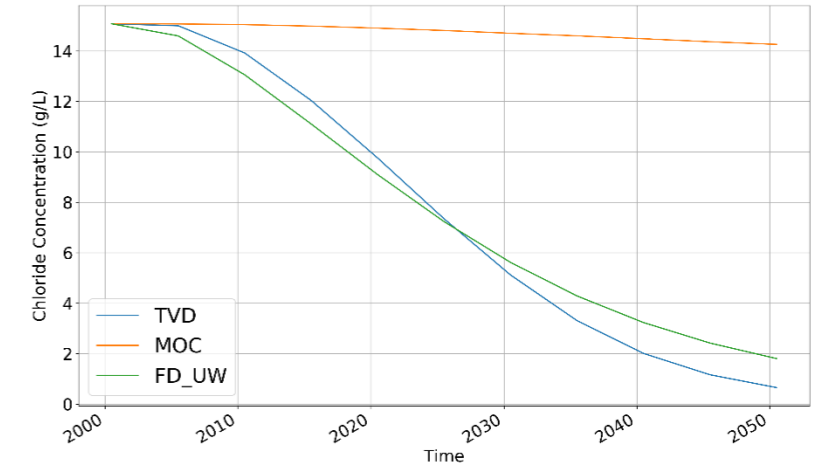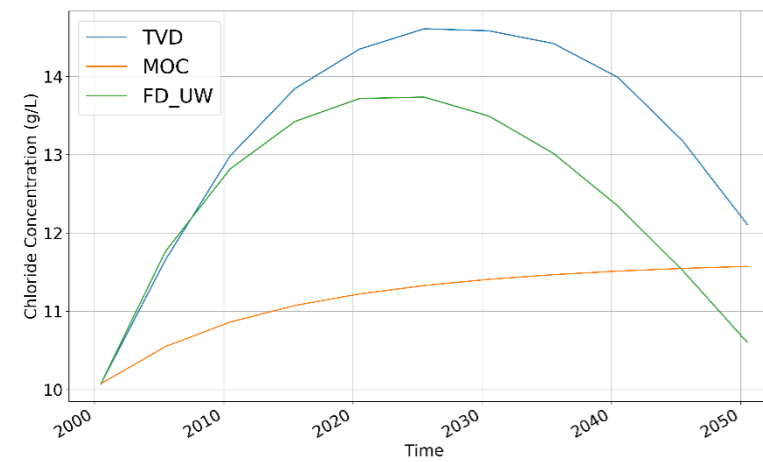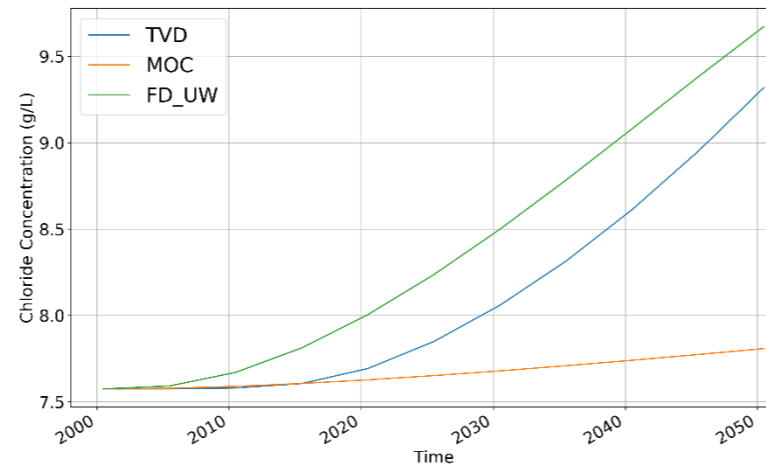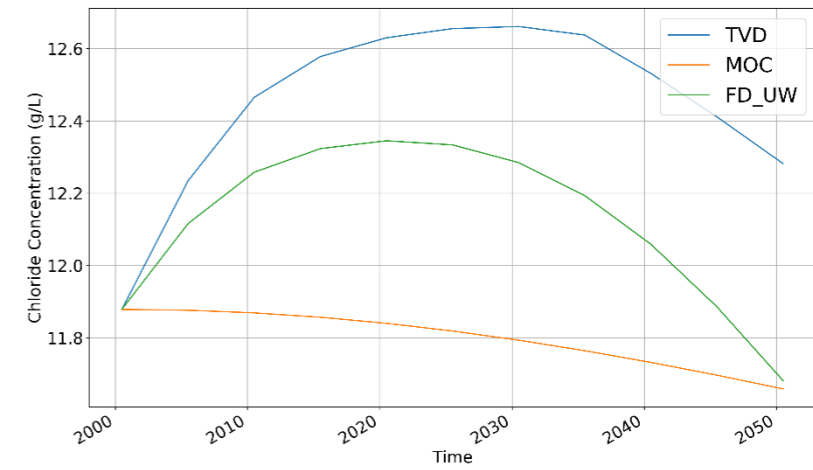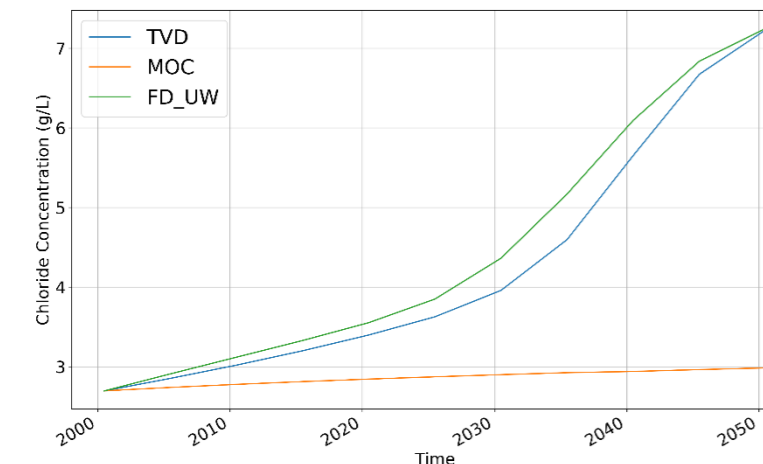
Figure C-3: breakthrough curves at x = 39050, y = 370875 for different layers
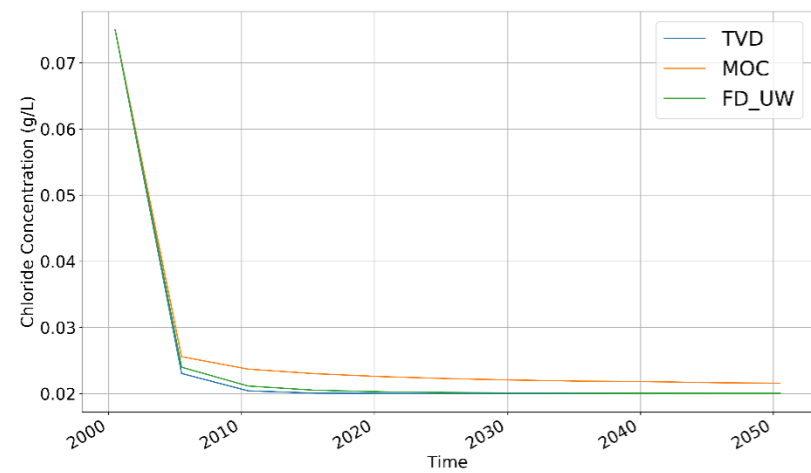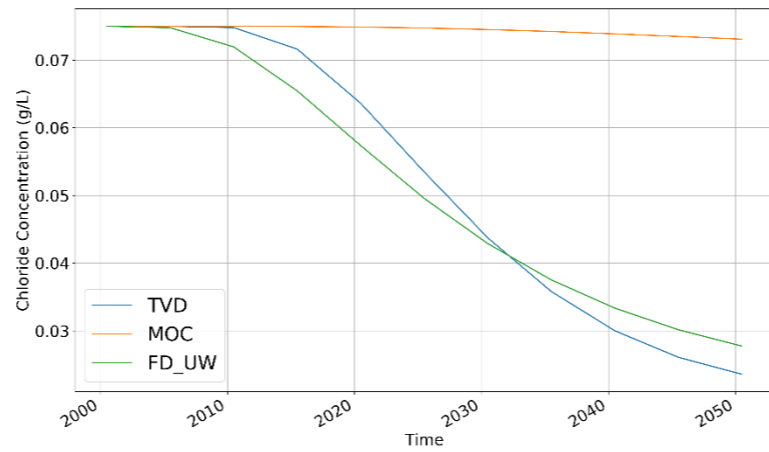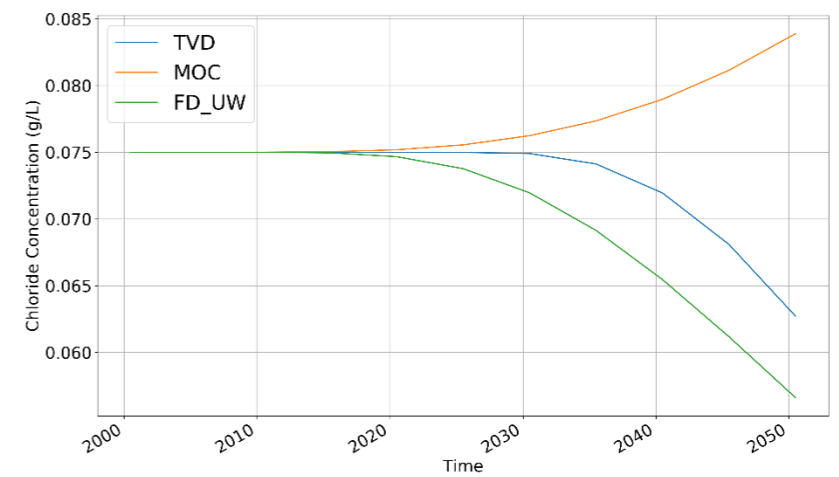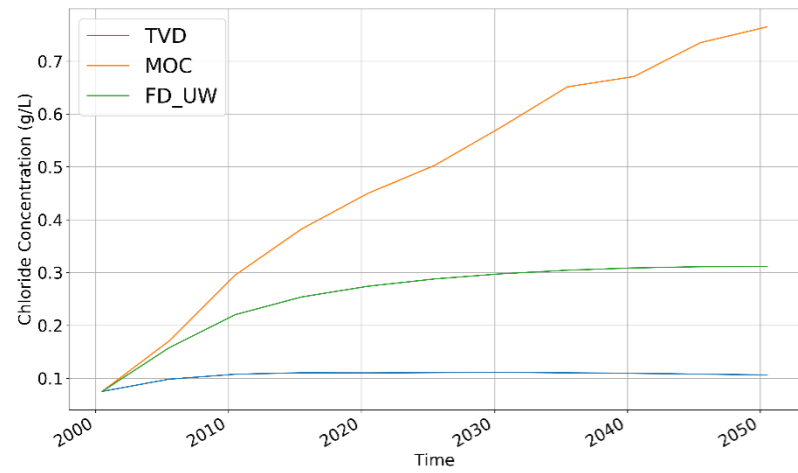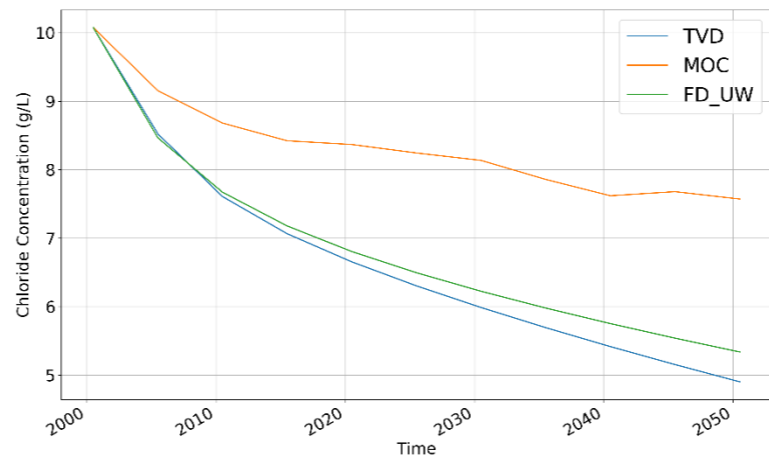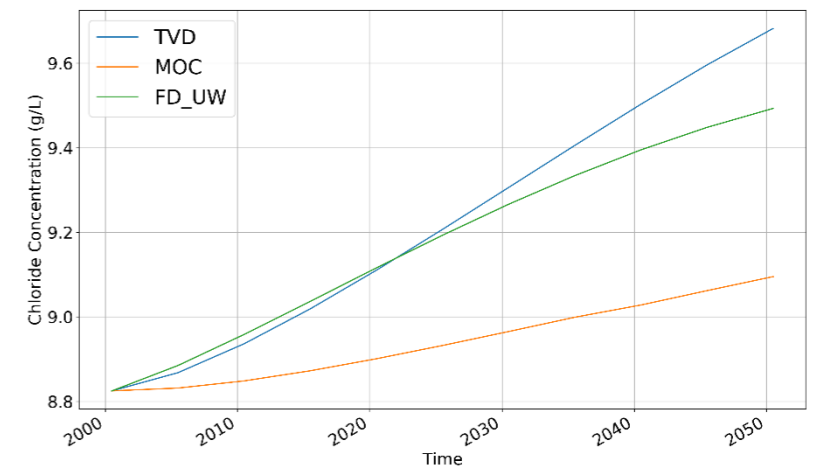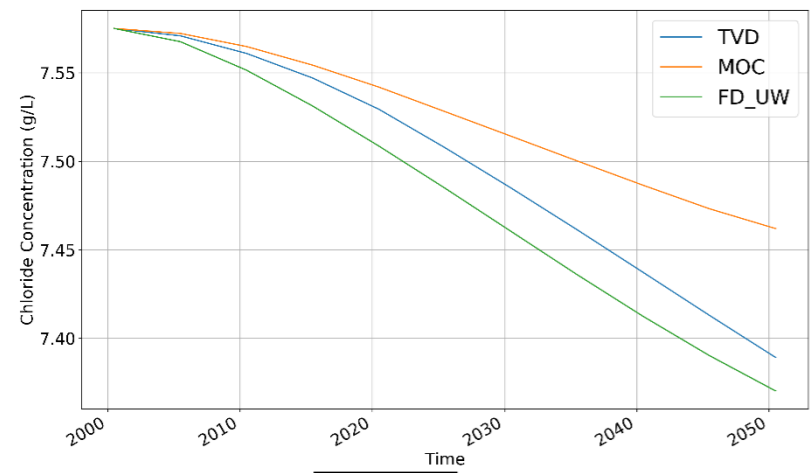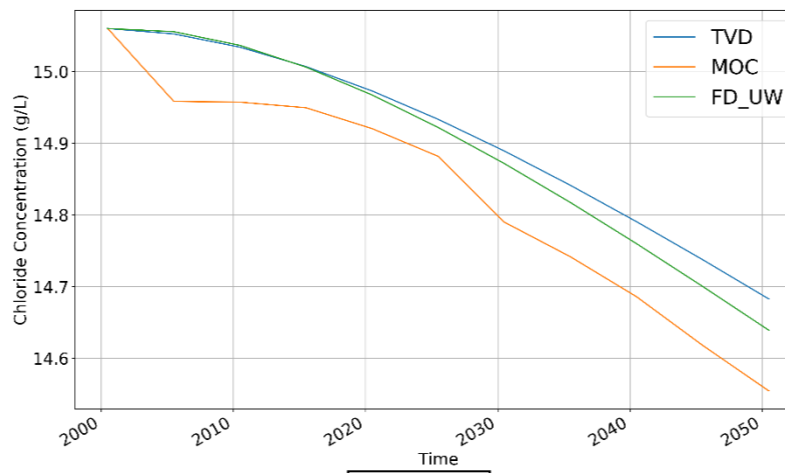
Figure C-4: breakthrough curves at x = 40700, y = 367825 for different layers
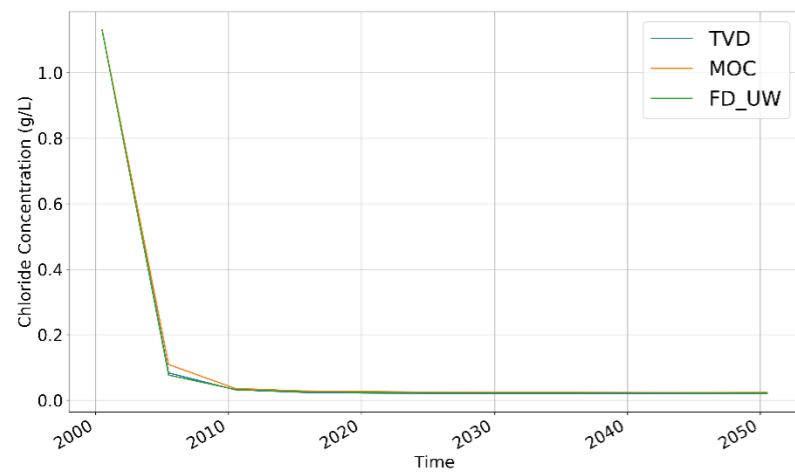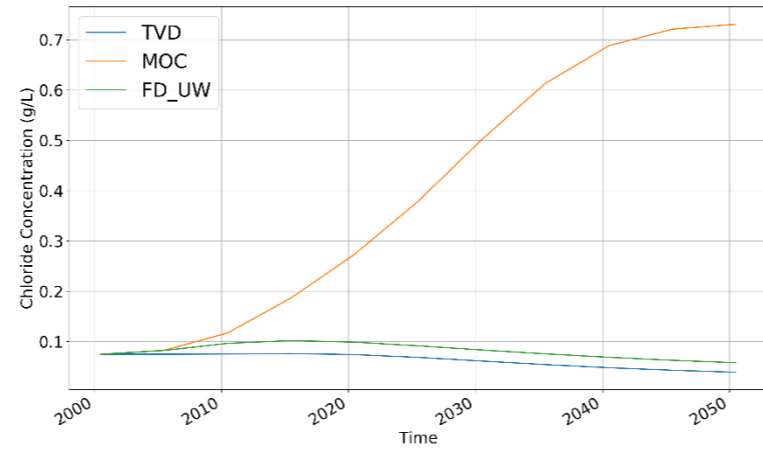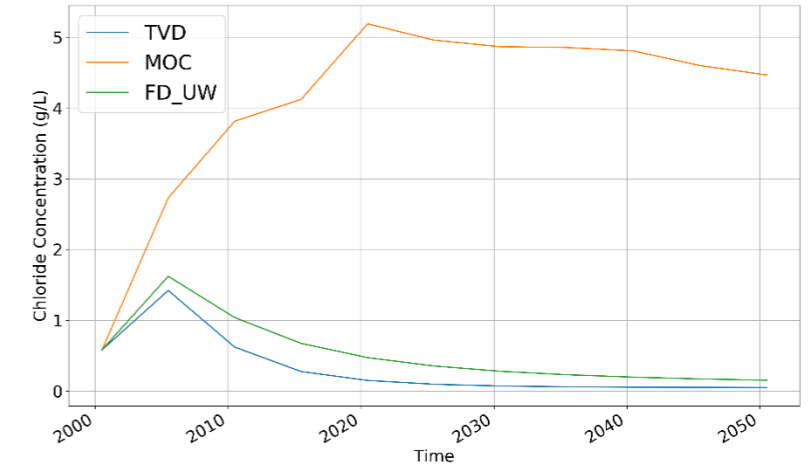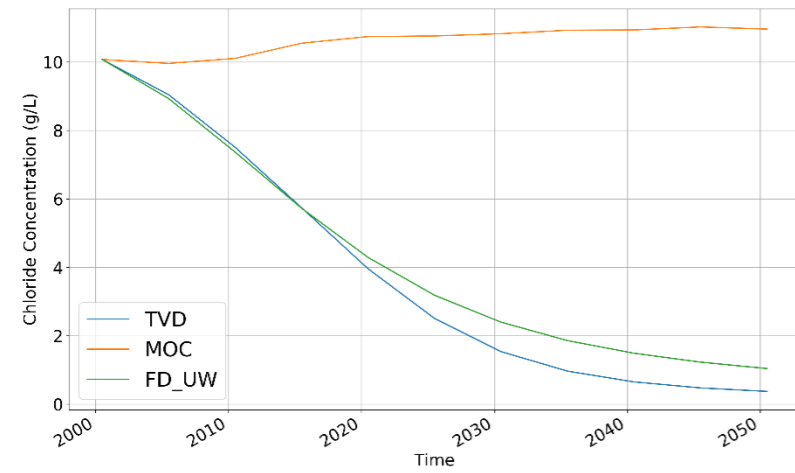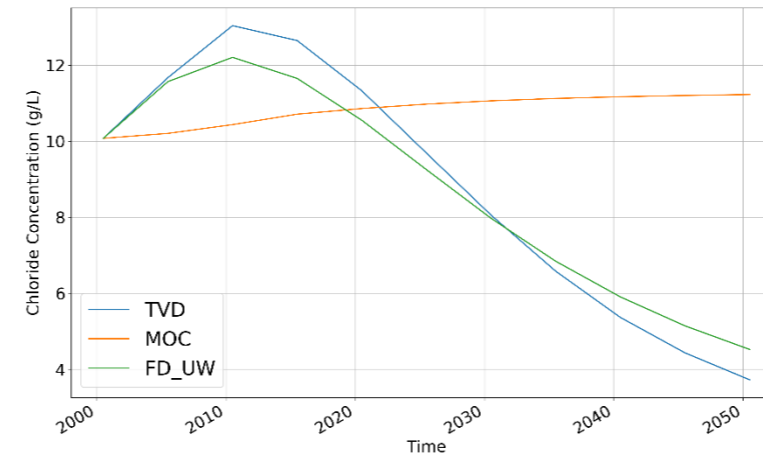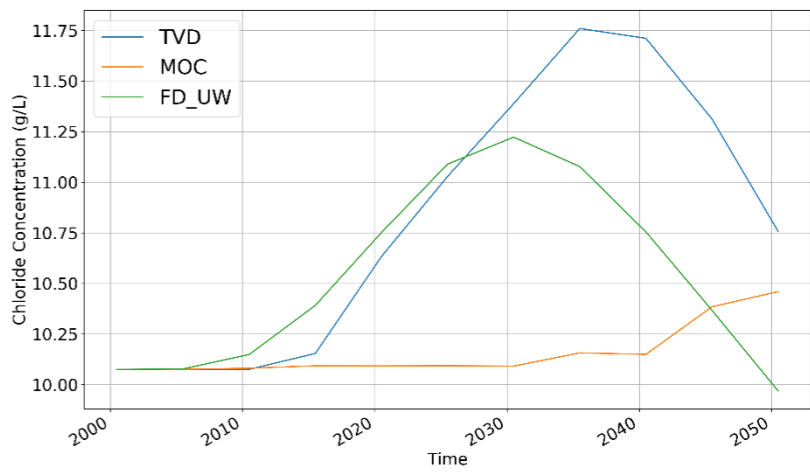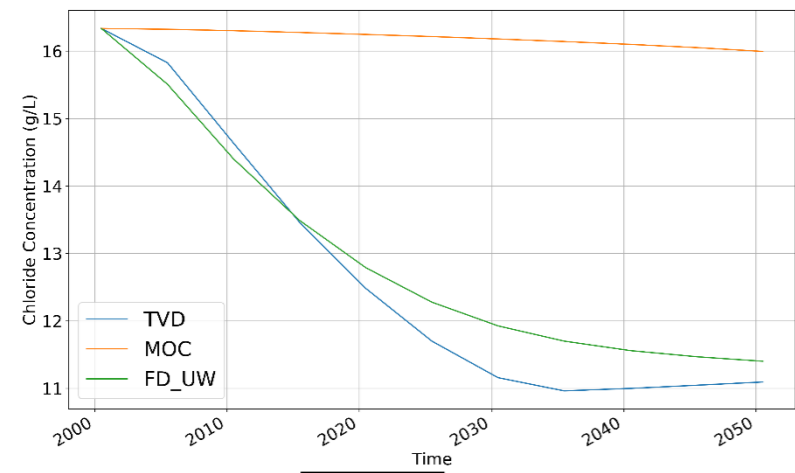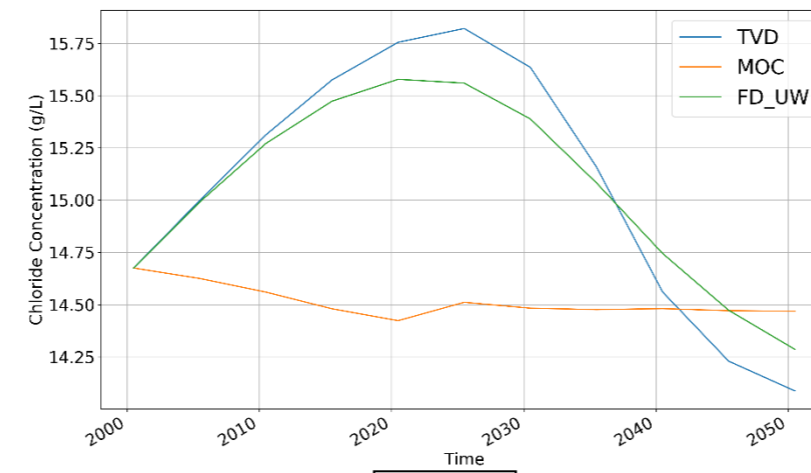
Figure C-5: breakthrough curves at x = 40700, y = 369350 for different layers
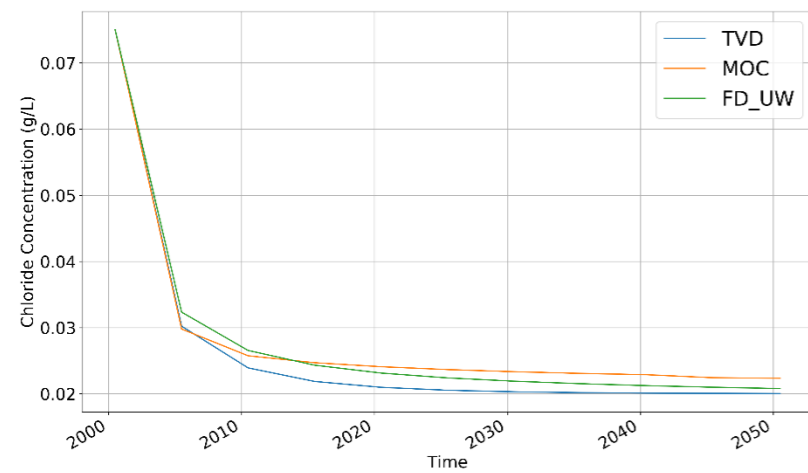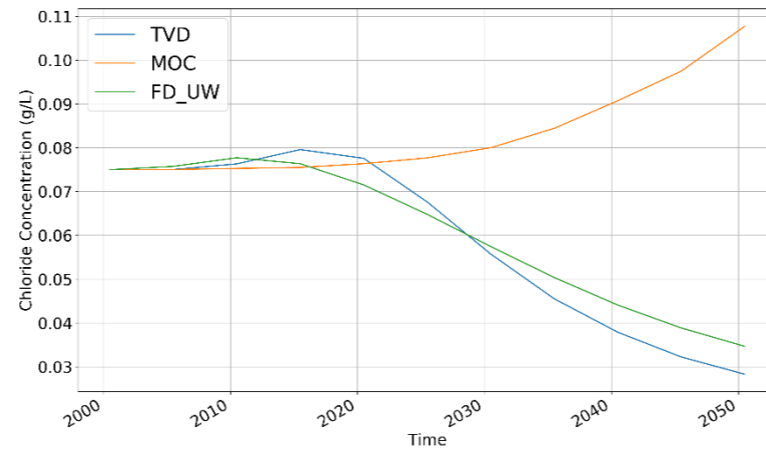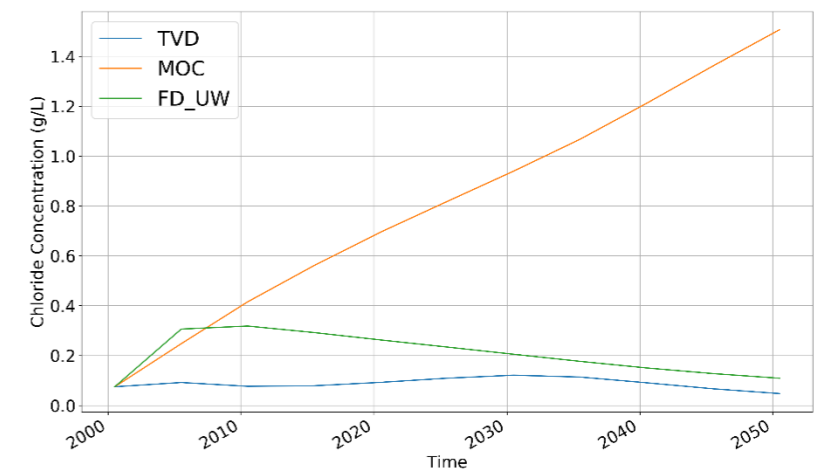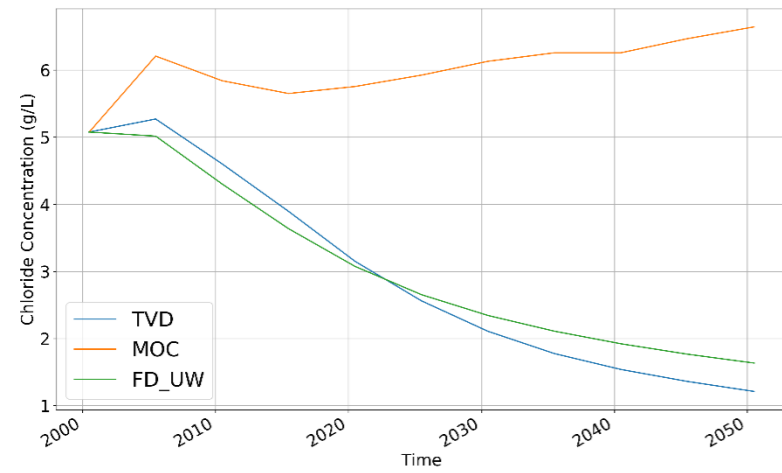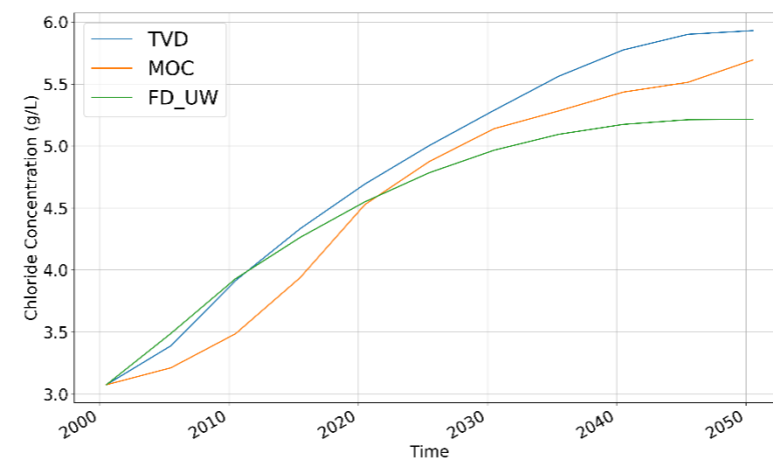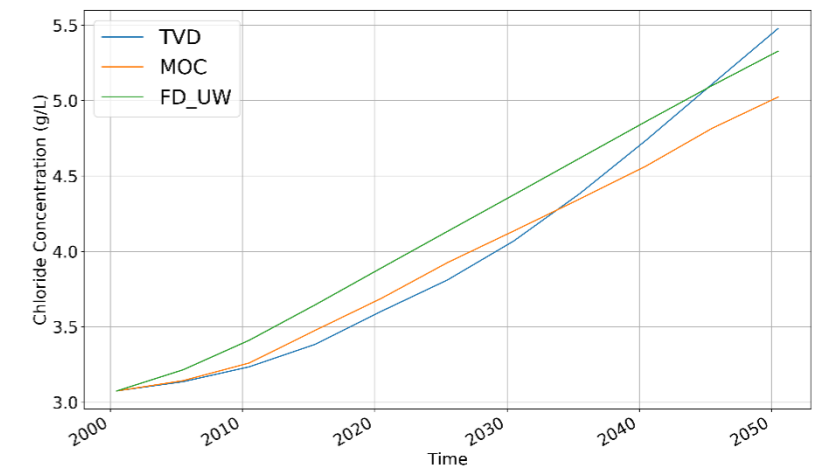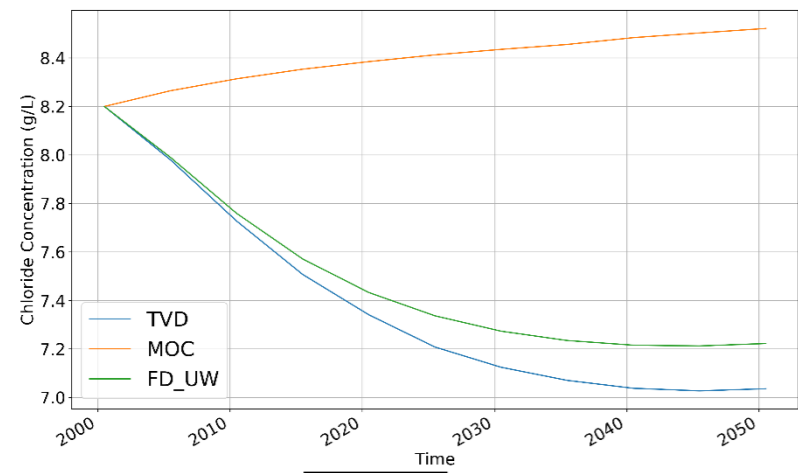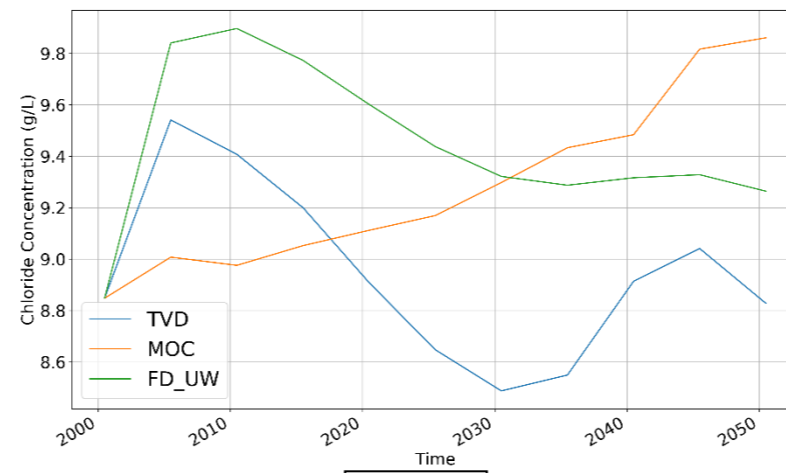
Figure C-6: breakthrough curves at x = 40700, y = 370875 for different layers
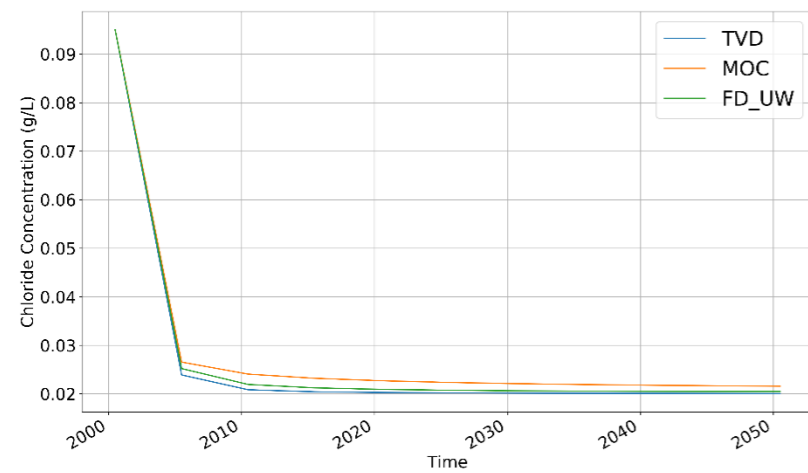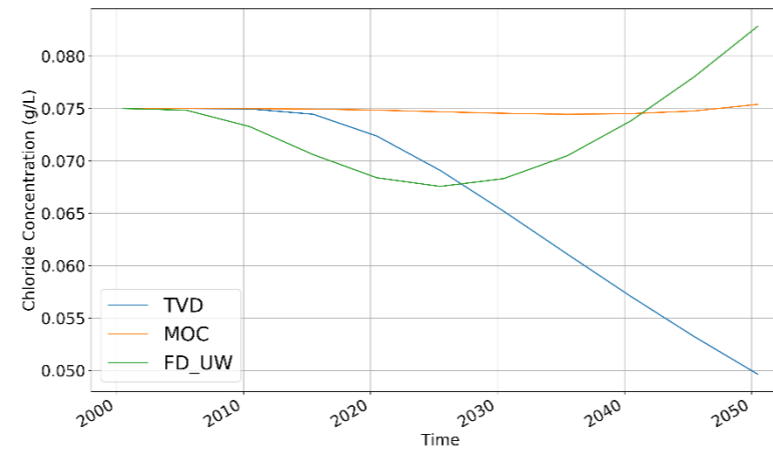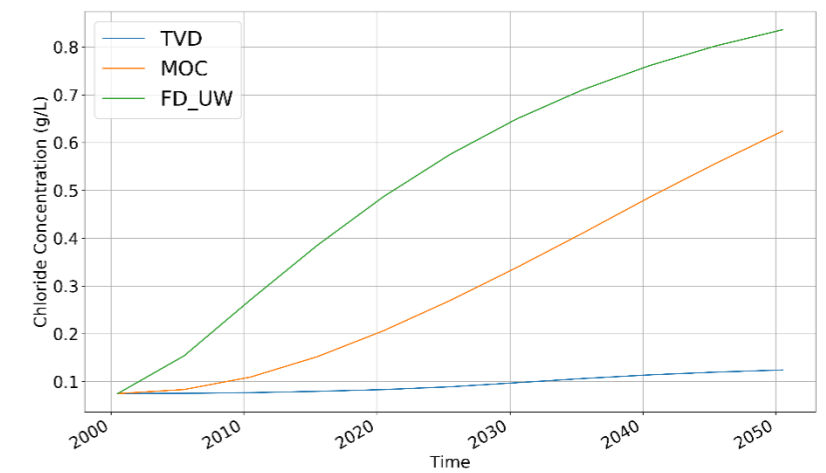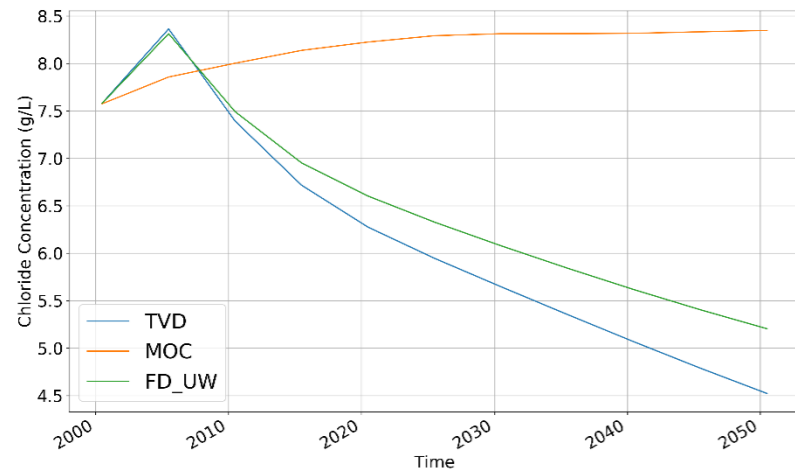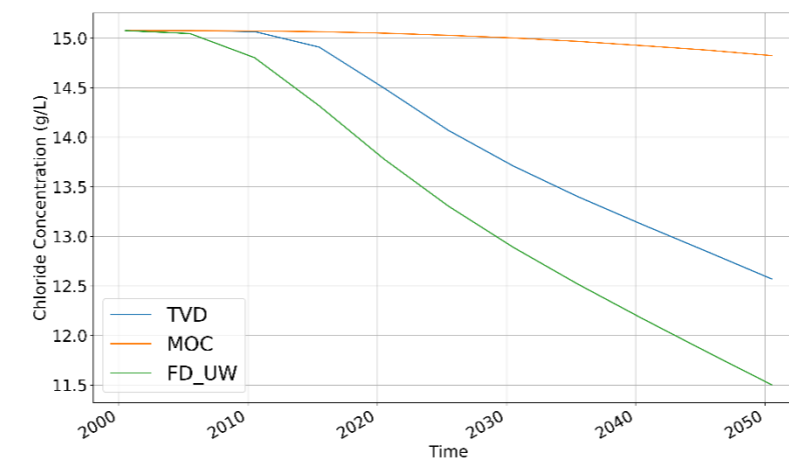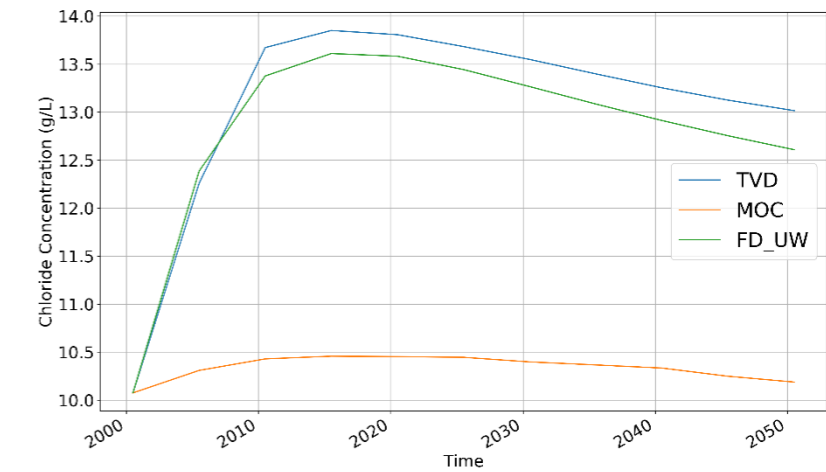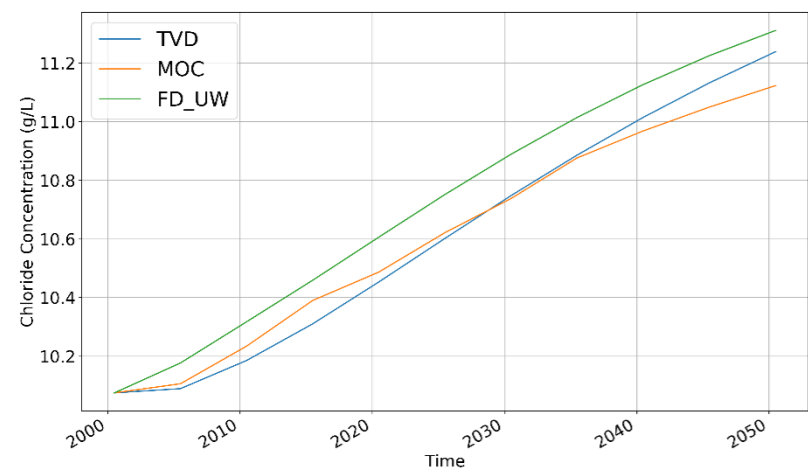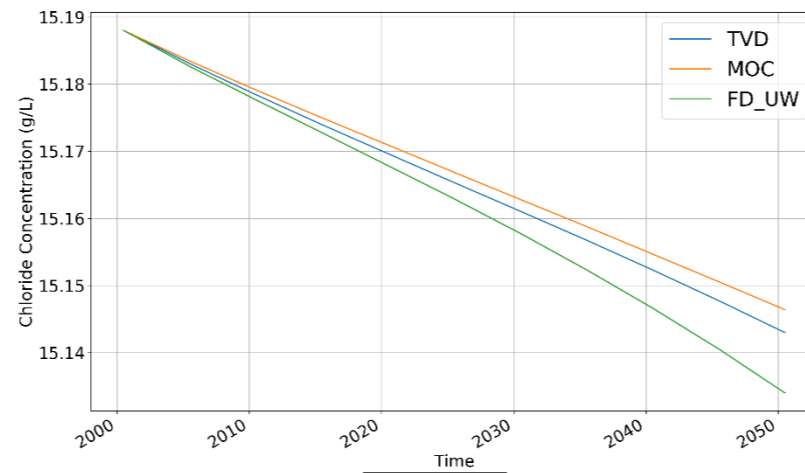
Figure C-7: breakthrough curves at x = 42350, y = 367825 for different layers
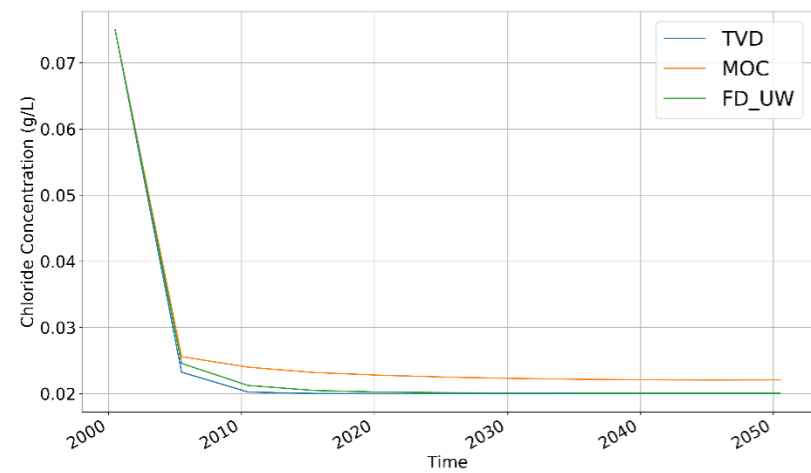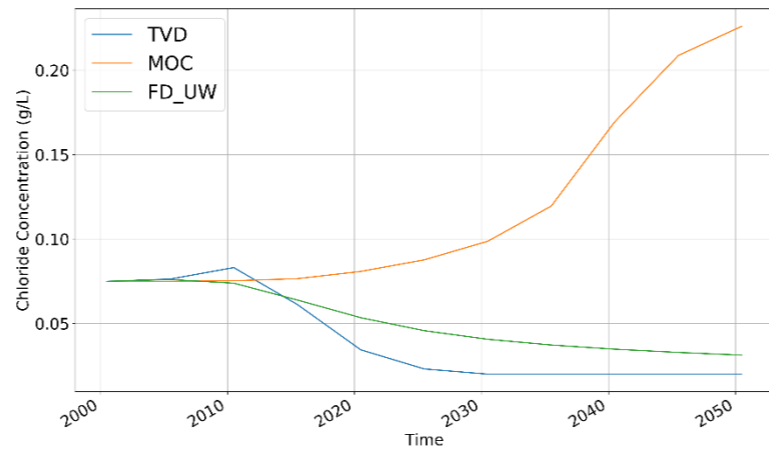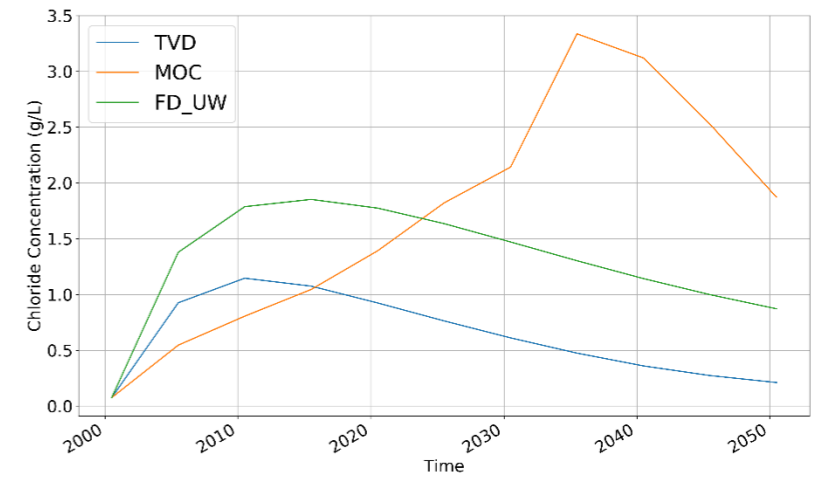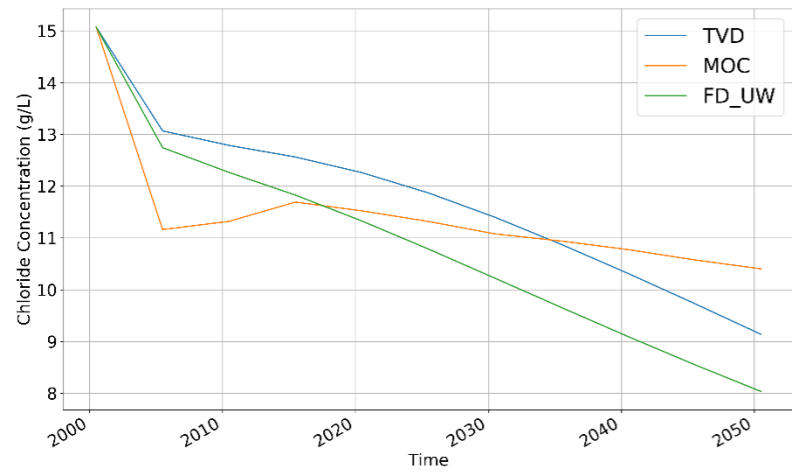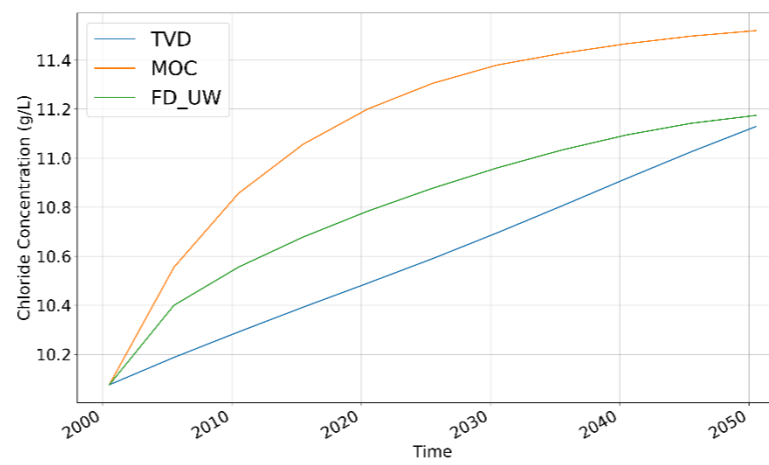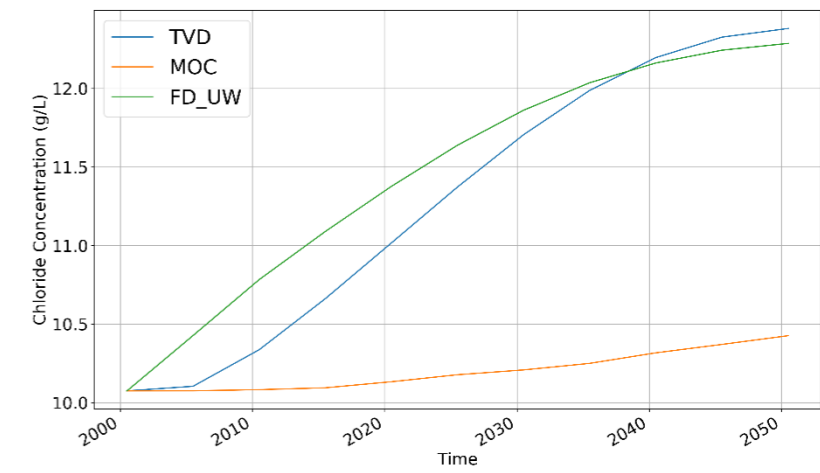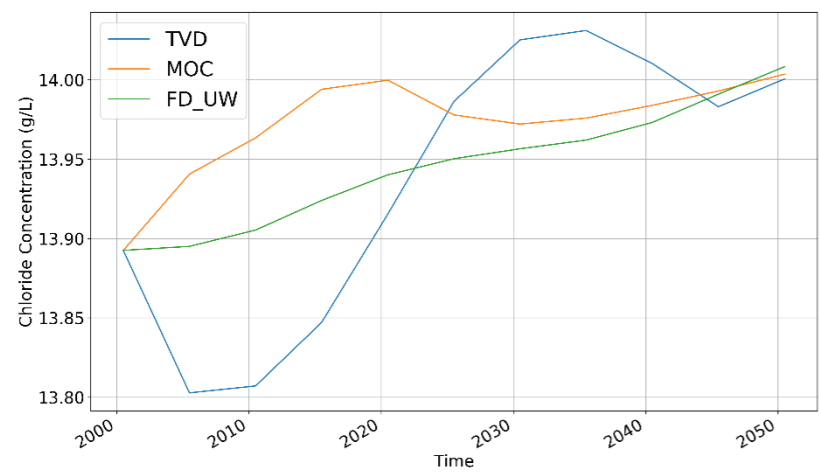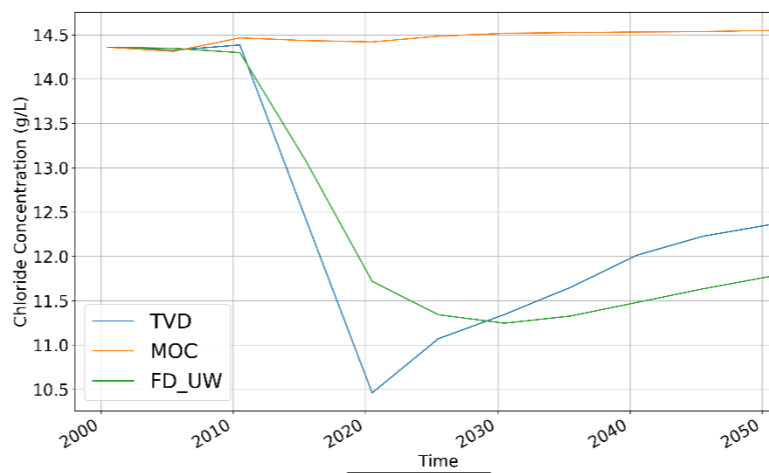
Figure C-8: breakthrough curves at x = 42350, y = 369350 for different layers
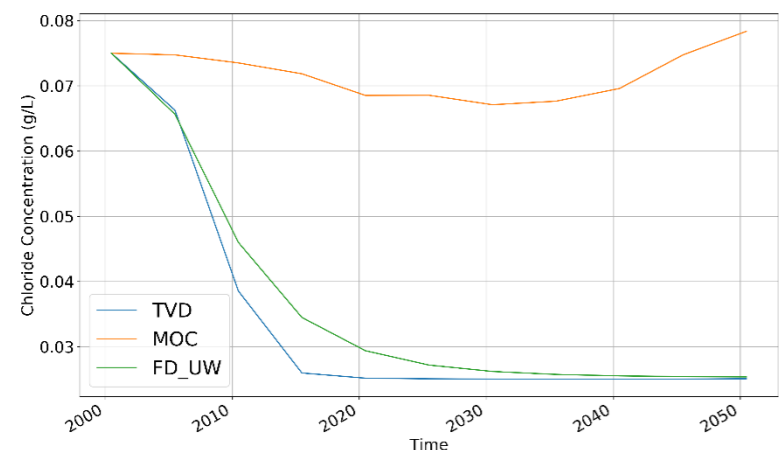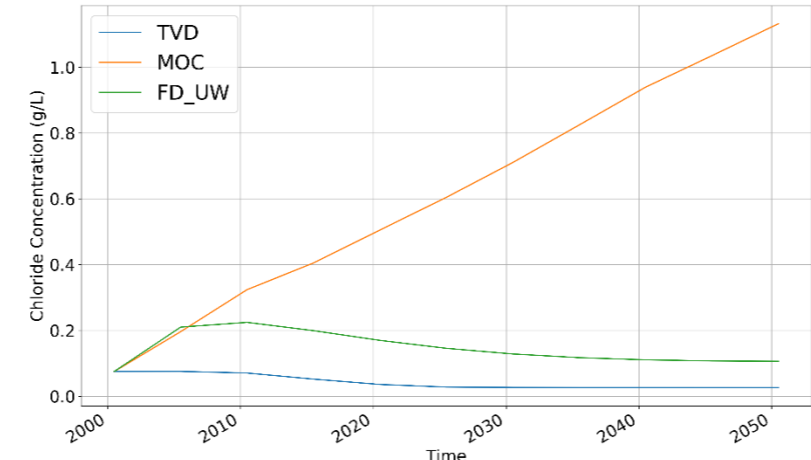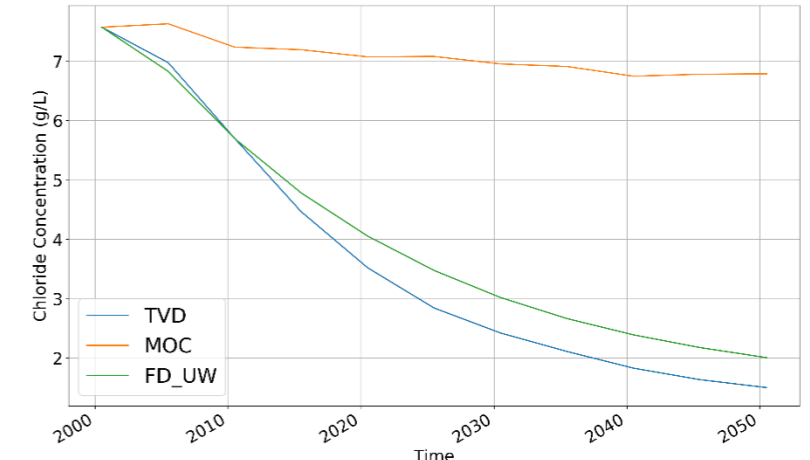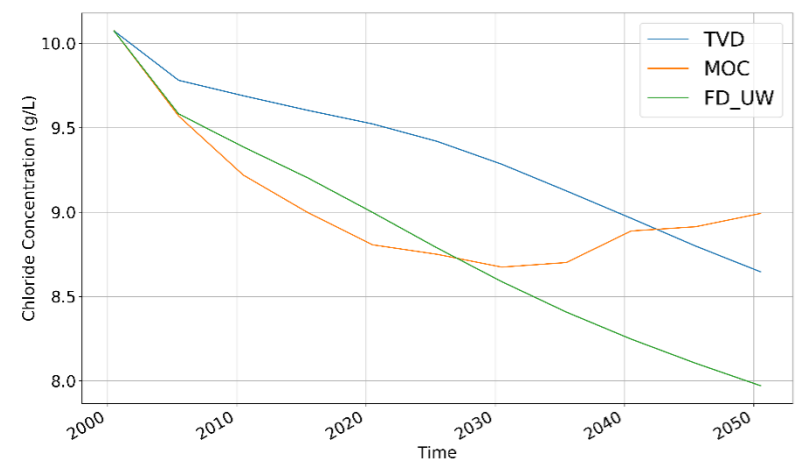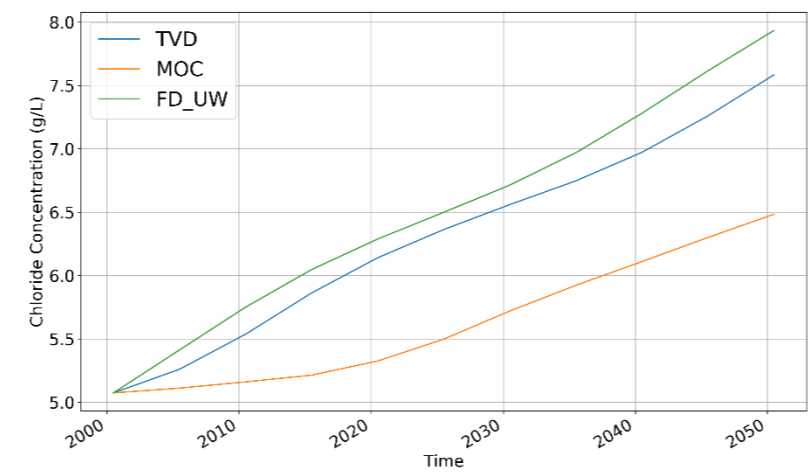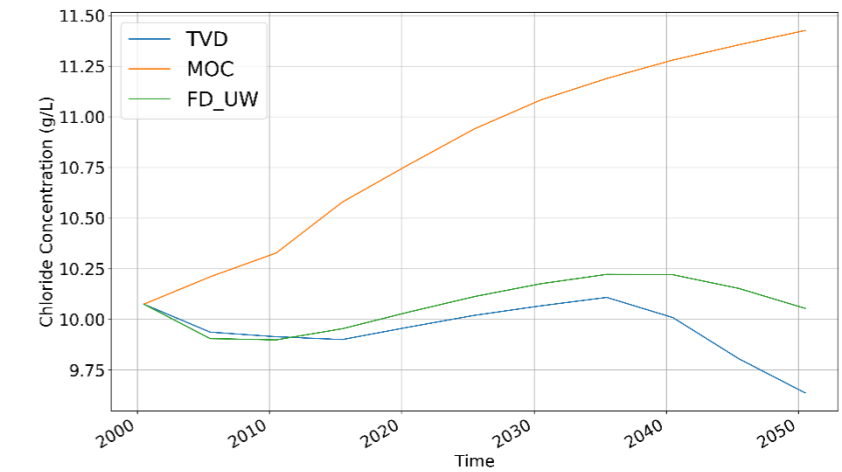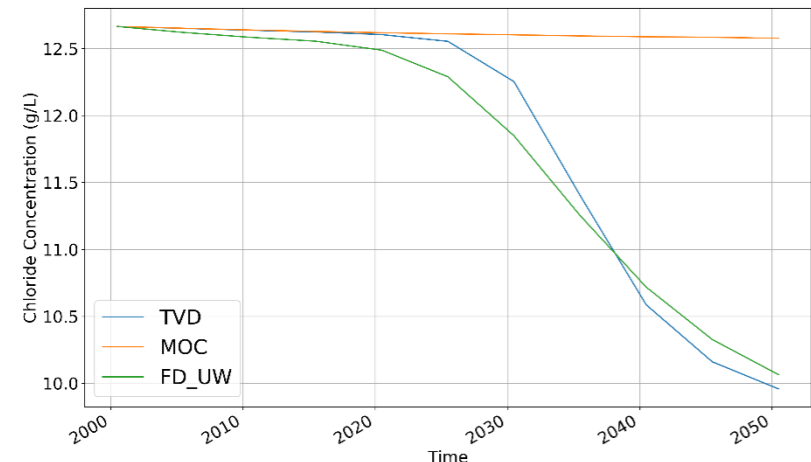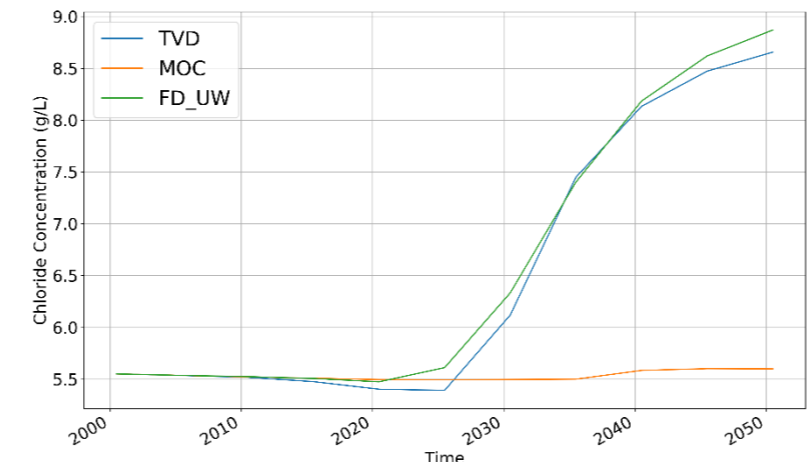
Figure C-9: breakthrough curves at x = 42350, y = 370875 for different layers

Appendix D. - Summary of All cases

Freshwater lens (simulation time: 1200 years):

Model ID	Discretization			Advection package	Dispersion package	Convergence criteria
	dx	dy	dz			
F_TVD001	250	1	10	TVD, PERCELL = 1.0	al = 0, DMCOEF = 0	Hclose = 0.0001, Rclose = 0.1
F_TVD002	100	1	10	TVD, PERCELL = 1.0	al = 0, DMCOEF = 0	Hclose = 0.0001, Rclose = 0.1
F_TVD003	50	1	10	TVD, PERCELL = 1.0	al = 0, DMCOEF = 0	Hclose = 0.0001, Rclose = 0.1
F_TVD004	25	1	10	TVD, PERCELL = 1.0	al = 0, DMCOEF = 0	Hclose = 0.0001, Rclose = 0.1
F_TVD005	10	1	10	TVD, PERCELL = 1.0	al = 0, DMCOEF = 0	Hclose = 0.0001, Rclose = 0.1
F_TVD006	250	1	5	TVD, PERCELL = 1.0	al = 0, DMCOEF = 0	Hclose = 0.0001, Rclose = 0.1
F_TVD007	100	1	5	TVD, PERCELL = 1.0	al = 0, DMCOEF = 0	Hclose = 0.0001, Rclose = 0.1
F_TVD008	50	1	5	TVD, PERCELL = 1.0	al = 0, DMCOEF = 0	Hclose = 0.0001, Rclose = 0.1
F_TVD009	25	1	5	TVD, PERCELL = 1.0	al = 0, DMCOEF = 0	Hclose = 0.0001, Rclose = 0.1
F_TVD010	10	1	5	TVD, PERCELL = 1.0	al = 0, DMCOEF = 0	Hclose = 0.0001, Rclose = 0.1
F_TVD011	250	1	1	TVD, PERCELL = 1.0	al = 0, DMCOEF = 0	Hclose = 0.0001, Rclose = 0.1
F_TVD012	100	1	1	TVD, PERCELL = 1.0	al = 0, DMCOEF = 0	Hclose = 0.0001, Rclose = 0.1
F_TVD013	50	1	1	TVD, PERCELL = 1.0	al = 0, DMCOEF = 0	Hclose = 0.0001, Rclose = 0.1
F_TVD014	25	1	1	TVD, PERCELL = 1.0	al = 0, DMCOEF = 0	Hclose = 0.0001, Rclose = 0.1
F_TVD015	10	1	1	TVD, PERCELL = 1.0	al = 0, DMCOEF = 0	Hclose = 0.0001, Rclose = 0.1
F_TVD016	100	1	1	TVD, PERCELL = 1.0	al = 0, DMCOEF = 0	Hclose = 0.01, Rclose = 1.0
F_TVD017	100	1	1	TVD, PERCELL = 1.0	al = 0, DMCOEF = 0	Hclose = 0.1, Rclose = 1.0
F_TVD018	100	1	1	TVD, PERCELL = 1.0	al = 0, DMCOEF = 0	Hclose = 0.001, Rclose = 1.0
F_TVD019	100	1	1	TVD, PERCELL = 1.0	al = 0, DMCOEF = 0	Hclose = 0.000001, Rclose = 1.0
F_TVD020	100	1	1	TVD, PERCELL = 1.0	al = 0, DMCOEF = 0	Hclose = 0.1, Rclose = 5.0
F_TVD021	100	1	1	TVD, PERCELL = 1.0	al = 0, DMCOEF = 0	Hclose = 0.1, Rclose = 10.0
F_TVD022	100	1	1	TVD, PERCELL = 1.0	al = 0, DMCOEF = 0	Hclose = 0.1, Rclose = 0.01
F_TVD023	100	1	1	TVD, PERCELL = 0.75	al = 0, DMCOEF = 0	Hclose = 0.0001, Rclose = 0.1
F_TVD024	100	1	1	TVD, PERCELL = 0.5	al = 0, DMCOEF = 0	Hclose = 0.0001, Rclose = 0.1
F_TVD025	100	1	1	TVD, PERCELL = 0.25	al = 0, DMCOEF = 0	Hclose = 0.0001, Rclose = 0.1

Model ID	Discretization			Advection package	Dispersion package	Convergence criteria
	dx	dy	dz			
F_MOC001	250	1	10	MOC, PERCELL = 1.0, MXPART = 10^6, WD = 0.5, ITRACK = 3, DCEPS = 1E-5, NPLANE = 0, NPL = 0, NPH = 16, NPMIN = 4, NPMAX = 32	al = 0, DMCOEF = 0	Hclose = 0.0001, Rclose = 0.1
F_MOC002	100	1	10	MOC, PERCELL = 1.0, MXPART = 10^6, WD = 0.5, ITRACK = 3, DCEPS = 1E-5, NPLANE = 0, NPL = 0, NPH = 16, NPMIN = 4, NPMAX = 32	al = 0, DMCOEF = 0	Hclose = 0.0001, Rclose = 0.1
F_MOC003	50	1	10	MOC, PERCELL = 1.0, MXPART = 10^6, WD = 0.5, ITRACK = 3, DCEPS = 1E-5, NPLANE = 0, NPL = 0, NPH = 16, NPMIN = 4, NPMAX = 32	al = 0, DMCOEF = 0	Hclose = 0.0001, Rclose = 0.1
F_MOC004	25	1	10	MOC, PERCELL = 1.0, MXPART = 10^6, WD = 0.5, ITRACK = 3, DCEPS = 1E-5, NPLANE = 0, NPL = 0, NPH = 16, NPMIN = 4, NPMAX = 32	al = 0, DMCOEF = 0	Hclose = 0.0001, Rclose = 0.1
F_MOC005	10	1	10	MOC, PERCELL = 1.0, MXPART = 10^6, WD = 0.5, ITRACK = 3, DCEPS = 1E-5, NPLANE = 0, NPL = 0, NPH = 16, NPMIN = 4, NPMAX = 32	al = 0, DMCOEF = 0	Hclose = 0.0001, Rclose = 0.1
F_MOC006	250	1	5	MOC, PERCELL = 1.0, MXPART = 10^6, WD = 0.5, ITRACK = 3, DCEPS = 1E-5, NPLANE = 0, NPL = 0, NPH = 16, NPMIN = 4, NPMAX = 32	al = 0, DMCOEF = 0	Hclose = 0.0001, Rclose = 0.1
F_MOC007	100	1	5	MOC, PERCELL = 1.0, MXPART = 10^6, WD = 0.5, ITRACK = 3, DCEPS = 1E-5, NPLANE = 0, NPL = 0, NPH = 16, NPMIN = 4, NPMAX = 32	al = 0, DMCOEF = 0	Hclose = 0.0001, Rclose = 0.1
F_MOC008	50	1	5	MOC, PERCELL = 1.0, MXPART = 10^6, WD = 0.5, ITRACK = 3, DCEPS = 1E-5, NPLANE = 0, NPL = 0, NPH = 16, NPMIN = 4, NPMAX = 32	al = 0, DMCOEF = 0	Hclose = 0.0001, Rclose = 0.1
F_MOC009	25	1	5	MOC, PERCELL = 1.0, MXPART = 10^6, WD = 0.5, ITRACK = 3, DCEPS = 1E-5, NPLANE = 0, NPL = 0, NPH = 16, NPMIN = 4, NPMAX = 32	al = 0, DMCOEF = 0	Hclose = 0.0001, Rclose = 0.1
F_MOC010	10	1	5	MOC, PERCELL = 1.0, MXPART = 10^6, WD = 0.5, ITRACK = 3, DCEPS = 1E-5, NPLANE = 0, NPL = 0, NPH = 16, NPMIN = 4, NPMAX = 32	al = 0, DMCOEF = 0	Hclose = 0.0001, Rclose = 0.1
F_MOC011	250	1	1	MOC, PERCELL = 1.0, MXPART = 10^6, WD = 0.5, ITRACK = 3, DCEPS = 1E-5, NPLANE = 0, NPL = 0, NPH = 16, NPMIN = 4, NPMAX = 32	al = 0, DMCOEF = 0	Hclose = 0.0001, Rclose = 0.1
F_MOC012	100	1	1	MOC, PERCELL = 1.0, MXPART = 10^6, WD = 0.5, ITRACK = 3, DCEPS = 1E-5, NPLANE = 0, NPL = 0, NPH = 16, NPMIN = 4, NPMAX = 32	al = 0, DMCOEF = 0	Hclose = 0.0001, Rclose = 0.1
F_MOC013	50	1	1	MOC, PERCELL = 1.0, MXPART = 10^6, WD = 0.5, ITRACK = 3, DCEPS = 1E-5, NPLANE = 0, NPL = 0, NPH = 16, NPMIN = 4, NPMAX = 32	al = 0, DMCOEF = 0	Hclose = 0.0001, Rclose = 0.1
F_MOC014	25	1	1	MOC, PERCELL = 1.0, MXPART = 10^6, WD = 0.5, ITRACK = 3, DCEPS = 1E-5, NPLANE = 0, NPL = 0, NPH = 16, NPMIN = 4, NPMAX = 32	al = 0, DMCOEF = 0	Hclose = 0.0001, Rclose = 0.1
F_MOC015	10	1	1	MOC, PERCELL = 1.0, MXPART = 10^6, WD = 0.5, ITRACK = 3, DCEPS = 1E-5, NPLANE = 0, NPL = 0, NPH = 16, NPMIN = 4, NPMAX = 32	al = 0, DMCOEF = 0	Hclose = 0.0001, Rclose = 0.1
F_MOC016	100	1	1	MOC, PERCELL = 1.0, MXPART = 10^6, WD = 0.5, ITRACK = 3, DCEPS = 1E-5, NPLANE = 0, NPL = 0, NPH = 16, NPMIN = 4, NPMAX = 32	al = 0, DMCOEF = 0	Hclose = 0.01, Rclose = 1.0
F_MOC017	100	1	1	MOC, PERCELL = 1.0, MXPART = 10^6, WD = 0.5, ITRACK = 3, DCEPS = 1E-5, NPLANE = 0, NPL = 0, NPH = 16, NPMIN = 4, NPMAX = 32	al = 0, DMCOEF = 0	Hclose = 0.1, Rclose = 1.0
F_MOC018	100	1	1	MOC, PERCELL = 1.0, MXPART = 10^6, WD = 0.5, ITRACK = 3, DCEPS = 1E-5, NPLANE = 0, NPL = 0, NPH = 16, NPMIN = 4, NPMAX = 32	al = 0, DMCOEF = 0	Hclose = 0.001, Rclose = 1.0
F_MOC019	100	1	1	MOC, PERCELL = 1.0, MXPART = 10^6, WD = 0.5, ITRACK = 3, DCEPS = 1E-5, NPLANE = 0, NPL = 0, NPH = 16, NPMIN = 4, NPMAX = 32	al = 0, DMCOEF = 0	Hclose = 0.000001, Rclose = 1.0
F_MOC020	100	1	1	MOC, PERCELL = 1.0, MXPART = 10^6, WD = 0.5, ITRACK = 3, DCEPS = 1E-5, NPLANE = 0, NPL = 0, NPH = 16, NPMIN = 4, NPMAX = 32	al = 0, DMCOEF = 0	Hclose = 0.1, Rclose = 5.0
F_MOC021	100	1	1	MOC, PERCELL = 1.0, MXPART = 10^6, WD = 0.5, ITRACK = 3, DCEPS = 1E-5, NPLANE = 0, NPL = 0, NPH = 16, NPMIN = 4, NPMAX = 32	al = 0, DMCOEF = 0	Hclose = 0.1, Rclose = 10.0
F_MOC022	100	1	1	MOC, PERCELL = 1.0, MXPART = 10^6, WD = 0.5, ITRACK = 3, DCEPS = 1E-5, NPLANE = 0, NPL = 0, NPH = 16, NPMIN = 4, NPMAX = 32	al = 0, DMCOEF = 0	Hclose = 0.1, Rclose = 0.01
F_MOC023	100	1	1	MOC, PERCELL = 0.75, MXPART = 10^6, WD = 0.5, ITRACK = 3, DCEPS = 1E-5, NPLANE = 0, NPL = 0, NPH = 16, NPMIN = 4, NPMAX = 32	al = 0, DMCOEF = 0	Hclose = 0.0001, Rclose = 0.1
F_MOC024	100	1	1	MOC, PERCELL = 0.5, MXPART = 10^6, WD = 0.5, ITRACK = 3, DCEPS = 1E-5, NPLANE = 0, NPL = 0, NPH = 16, NPMIN = 4, NPMAX = 32	al = 0, DMCOEF = 0	Hclose = 0.0001, Rclose = 0.1
F_MOC025	100	1	1	MOC, PERCELL = 0.25, MXPART = 10^6, WD = 0.5, ITRACK = 3, DCEPS = 1E-5, NPLANE = 0, NPL = 0, NPH = 16, NPMIN = 4, NPMAX = 32	al = 0, DMCOEF = 0	Hclose = 0.0001, Rclose = 0.1
F_MOC026	100	1	1	MOC, PERCELL = 1.0, MXPART = 10^6, WD = 0.75, ITRACK = 3, DCEPS = 1E-5, NPLANE = 0, NPL = 0, NPH = 16, NPMIN = 4, NPMAX = 32	al = 0, DMCOEF = 0	Hclose = 0.0001, Rclose = 0.1
F_MOC027	100	1	1	MOC, PERCELL = 1.0, MXPART = 10^6, WD = 1.0, ITRACK = 3, DCEPS = 1E-5, NPLANE = 0, NPL = 0, NPH = 16, NPMIN = 4, NPMAX = 32	al = 0, DMCOEF = 0	Hclose = 0.0001, Rclose = 0.1
F_MOC028	100	1	1	MOC, PERCELL = 1.0, MXPART = 10^6, WD = 0.5, ITRACK = 2, DCEPS = 1E-5, NPLANE = 0, NPL = 0, NPH = 16, NPMIN = 4, NPMAX = 32	al = 0, DMCOEF = 0	Hclose = 0.0001, Rclose = 0.1
F_MOC029	100	1	1	MOC, PERCELL = 1.0, MXPART = 10^6, WD = 0.5, ITRACK = 1, DCEPS = 1E-5, NPLANE = 0, NPL = 0, NPH = 16, NPMIN = 4, NPMAX = 32	al = 0, DMCOEF = 0	Hclose = 0.0001, Rclose = 0.1
F_MOC030	100	1	1	MOC, PERCELL = 1.0, MXPART = 10^6, WD = 0.5, ITRACK = 3, DCEPS = 1E-5, NPLANE = 8, NPL = 0, NPH = 16, NPMIN = 4, NPMAX = 32	al = 0, DMCOEF = 0	Hclose = 0.0001, Rclose = 0.1
F_MOC031	100	1	1	MOC, PERCELL = 1.0, MXPART = 10^6, WD = 0.5, ITRACK = 3, DCEPS = 1E-10, NPLANE = 0, NPL = 0, NPH = 16, NPMIN = 4, NPMAX = 32	al = 0, DMCOEF = 0	Hclose = 0.0001, Rclose = 0.1
F_MOC032	100	1	1	MOC, PERCELL = 1.0, MXPART = 10^6, WD = 0.5, ITRACK = 3, DCEPS = 1E-1, NPLANE = 0, NPL = 0, NPH = 16, NPMIN = 4, NPMAX = 32	al = 0, DMCOEF = 0	Hclose = 0.0001, Rclose = 0.1
F_MOC033	100	1	1	MOC, PERCELL = 1.0, MXPART = 10^6, WD = 0.5, ITRACK = 3, DCEPS = 1E-5, NPLANE = 0, NPL = 0, NPH = 32, NPMIN = 32, NPMAX = 64	al = 0, DMCOEF = 0	Hclose = 0.0001, Rclose = 0.1
F_MOC034	100	1	1	MOC, PERCELL = 1.0, MXPART = 10^6, WD = 0.5, ITRACK = 3, DCEPS = 1E-5, NPLANE = 0, NPL = 16, NPH = 16, NPMIN = 4, NPMAX = 32	al = 0, DMCOEF = 0	Hclose = 0.0001, Rclose = 0.1

Model ID	Discretization			Advection package	Dispersion package	Convergence criteria
	dx	dy	dz			
F_FD001	250	1	10	FD , PERCELL = 1.0, NADVFD = 0	al = 0, DMCOEF = 0	Hclose = 0.0001, Rclose = 0.1
F_FD002	100	1	10	FD , PERCELL = 1.0, NADVFD = 0	al = 0, DMCOEF = 0	Hclose = 0.0001, Rclose = 0.1
F_FD003	50	1	10	FD , PERCELL = 1.0, NADVFD = 0	al = 0, DMCOEF = 0	Hclose = 0.0001, Rclose = 0.1
F_FD004	25	1	10	FD , PERCELL = 1.0, NADVFD = 0	al = 0, DMCOEF = 0	Hclose = 0.0001, Rclose = 0.1
F_FD005	10	1	10	FD , PERCELL = 1.0, NADVFD = 0	al = 0, DMCOEF = 0	Hclose = 0.0001, Rclose = 0.1
F_FD006	250	1	5	FD , PERCELL = 1.0, NADVFD = 0	al = 0, DMCOEF = 0	Hclose = 0.0001, Rclose = 0.1
F_FD007	100	1	5	FD , PERCELL = 1.0, NADVFD = 0	al = 0, DMCOEF = 0	Hclose = 0.0001, Rclose = 0.1
F_FD008	50	1	5	FD , PERCELL = 1.0, NADVFD = 0	al = 0, DMCOEF = 0	Hclose = 0.0001, Rclose = 0.1
F_FD009	25	1	5	FD , PERCELL = 1.0, NADVFD = 0	al = 0, DMCOEF = 0	Hclose = 0.0001, Rclose = 0.1
F_FD010	10	1	5	FD , PERCELL = 1.0, NADVFD = 0	al = 0, DMCOEF = 0	Hclose = 0.0001, Rclose = 0.1
F_FD011	250	1	1	FD , PERCELL = 1.0, NADVFD = 0	al = 0, DMCOEF = 0	Hclose = 0.0001, Rclose = 0.1
F_FD012	100	1	1	FD , PERCELL = 1.0, NADVFD = 0	al = 0, DMCOEF = 0	Hclose = 0.0001, Rclose = 0.1
F_FD013	50	1	1	FD , PERCELL = 1.0, NADVFD = 0	al = 0, DMCOEF = 0	Hclose = 0.0001, Rclose = 0.1
F_FD014	25	1	1	FD , PERCELL = 1.0, NADVFD = 0	al = 0, DMCOEF = 0	Hclose = 0.0001, Rclose = 0.1
F_FD015	10	1	1	FD , PERCELL = 1.0, NADVFD = 0	al = 0, DMCOEF = 0	Hclose = 0.0001, Rclose = 0.1
F_FD016	100	1	1	FD , PERCELL = 1.0, NADVFD = 0	al = 0, DMCOEF = 0	Hclose = 0.01, Rclose = 1.0
F_FD017	100	1	1	FD , PERCELL = 1.0, NADVFD = 0	al = 0, DMCOEF = 0	Hclose = 0.1, Rclose = 1.0
F_FD018	100	1	1	FD , PERCELL = 1.0, NADVFD = 0	al = 0, DMCOEF = 0	Hclose = 0.001, Rclose = 1.0
F_FD019	100	1	1	FD , PERCELL = 1.0, NADVFD = 0	al = 0, DMCOEF = 0	Hclose = 0.000001, Rclose = 1.0
F_FD020	100	1	1	FD , PERCELL = 1.0, NADVFD = 0	al = 0, DMCOEF = 0	Hclose = 0.1, Rclose = 5.0
F_FD021	100	1	1	FD , PERCELL = 1.0, NADVFD = 0	al = 0, DMCOEF = 0	Hclose = 0.1, Rclose = 10.0
F_FD022	100	1	1	FD , PERCELL = 1.0, NADVFD = 0	al = 0, DMCOEF = 0	Hclose = 0.1, Rclose = 0.01
F_FD023	100	1	1	FD , PERCELL = 0.75, NADVFD = 0	al = 0, DMCOEF = 0	Hclose = 0.0001, Rclose = 0.1
F_FD024	100	1	1	FD , PERCELL = 0.5, NADVFD = 0	al = 0, DMCOEF = 0	Hclose = 0.0001, Rclose = 0.1
F_FD025	100	1	1	FD , PERCELL = 0.25, NADVFD = 0	al = 0, DMCOEF = 0	Hclose = 0.0001, Rclose = 0.1
F_FD026	100	1	1	FD , PERCELL = 1.0, NADVFD = 2	al = 0, DMCOEF = 0	Hclose = 0.0001, Rclose = 0.1

Model ID	Discretization			Advection package	Dispersion package	Convergence criteria
	dx	dy	dz			
F_HMOC001	250	1	10	HMOC, PERCELL = 1.0, MXPART = 10^6, WD = 0.5, ITRACK = 3, DCEPS = 1E-5, NPLANE = 0, NPL = 0, NPH = 16, NPMIN = 4, NPMAX = 32, INTERP = 1, NLSINK = 0, NPSINK = 16, DCHMOC = 0.0055	al = 0, DMCOEF = 0	Hclose = 0.0001, Rclose = 0.1
F_HMOC002	100	1	10	HMOC, PERCELL = 1.0, MXPART = 10^6, WD = 0.5, ITRACK = 3, DCEPS = 1E-5, NPLANE = 0, NPL = 0, NPH = 16, NPMIN = 4, NPMAX = 32, INTERP = 1, NLSINK = 0, NPSINK = 16, DCHMOC = 0.0055	al = 0, DMCOEF = 0	Hclose = 0.0001, Rclose = 0.1
F_HMOC003	50	1	10	HMOC, PERCELL = 1.0, MXPART = 10^6, WD = 0.5, ITRACK = 3, DCEPS = 1E-5, NPLANE = 0, NPL = 0, NPH = 16, NPMIN = 4, NPMAX = 32, INTERP = 1, NLSINK = 0, NPSINK = 16, DCHMOC = 0.0055	al = 0, DMCOEF = 0	Hclose = 0.0001, Rclose = 0.1
F_HMOC004	25	1	10	HMOC, PERCELL = 1.0, MXPART = 10^6, WD = 0.5, ITRACK = 3, DCEPS = 1E-5, NPLANE = 0, NPL = 0, NPH = 16, NPMIN = 4, NPMAX = 32, INTERP = 1, NLSINK = 0, NPSINK = 16, DCHMOC = 0.0055	al = 0, DMCOEF = 0	Hclose = 0.0001, Rclose = 0.1
F_HMOC005	10	1	10	HMOC, PERCELL = 1.0, MXPART = 10^6, WD = 0.5, ITRACK = 3, DCEPS = 1E-5, NPLANE = 0, NPL = 0, NPH = 16, NPMIN = 4, NPMAX = 32, INTERP = 1, NLSINK = 0, NPSINK = 16, DCHMOC = 0.0055	al = 0, DMCOEF = 0	Hclose = 0.0001, Rclose = 0.1
F_HMOC006	250	1	5	HMOC, PERCELL = 1.0, MXPART = 10^6, WD = 0.5, ITRACK = 3, DCEPS = 1E-5, NPLANE = 0, NPL = 0, NPH = 16, NPMIN = 4, NPMAX = 32, INTERP = 1, NLSINK = 0, NPSINK = 16, DCHMOC = 0.0055	al = 0, DMCOEF = 0	Hclose = 0.0001, Rclose = 0.1
F_HMOC007	100	1	5	HMOC, PERCELL = 1.0, MXPART = 10^6, WD = 0.5, ITRACK = 3, DCEPS = 1E-5, NPLANE = 0, NPL = 0, NPH = 16, NPMIN = 4, NPMAX = 32, INTERP = 1, NLSINK = 0, NPSINK = 16, DCHMOC = 0.0055	al = 0, DMCOEF = 0	Hclose = 0.0001, Rclose = 0.1
F_HMOC008	50	1	5	HMOC, PERCELL = 1.0, MXPART = 10^6, WD = 0.5, ITRACK = 3, DCEPS = 1E-5, NPLANE = 0, NPL = 0, NPH = 16, NPMIN = 4, NPMAX = 32, INTERP = 1, NLSINK = 0, NPSINK = 16, DCHMOC = 0.0055	al = 0, DMCOEF = 0	Hclose = 0.0001, Rclose = 0.1
F_HMOC009	25	1	5	HMOC, PERCELL = 1.0, MXPART = 10^6, WD = 0.5, ITRACK = 3, DCEPS = 1E-5, NPLANE = 0, NPL = 0, NPH = 16, NPMIN = 4, NPMAX = 32, INTERP = 1, NLSINK = 0, NPSINK = 16, DCHMOC = 0.0055	al = 0, DMCOEF = 0	Hclose = 0.0001, Rclose = 0.1
F_HMOC010	10	1	5	HMOC, PERCELL = 1.0, MXPART = 10^6, WD = 0.5, ITRACK = 3, DCEPS = 1E-5, NPLANE = 0, NPL = 0, NPH = 16, NPMIN = 4, NPMAX = 32, INTERP = 1, NLSINK = 0, NPSINK = 16, DCHMOC = 0.0055	al = 0, DMCOEF = 0	Hclose = 0.0001, Rclose = 0.1
F_HMOC011	250	1	1	HMOC, PERCELL = 1.0, MXPART = 10^6, WD = 0.5, ITRACK = 3, DCEPS = 1E-5, NPLANE = 0, NPL = 0, NPH = 16, NPMIN = 4, NPMAX = 32, INTERP = 1, NLSINK = 0, NPSINK = 16, DCHMOC = 0.0055	al = 0, DMCOEF = 0	Hclose = 0.0001, Rclose = 0.1
F_HMOC012	100	1	1	HMOC, PERCELL = 1.0, MXPART = 10^6, WD = 0.5, ITRACK = 3, DCEPS = 1E-5, NPLANE = 0, NPL = 0, NPH = 16, NPMIN = 4, NPMAX = 32, INTERP = 1, NLSINK = 0, NPSINK = 16, DCHMOC = 0.0055	al = 0, DMCOEF = 0	Hclose = 0.0001, Rclose = 0.1
F_HMOC013	50	1	1	HMOC, PERCELL = 1.0, MXPART = 10^6, WD = 0.5, ITRACK = 3, DCEPS = 1E-5, NPLANE = 0, NPL = 0, NPH = 16, NPMIN = 4, NPMAX = 32, INTERP = 1, NLSINK = 0, NPSINK = 16, DCHMOC = 0.0055	al = 0, DMCOEF = 0	Hclose = 0.0001, Rclose = 0.1
F_HMOC014	25	1	1	HMOC, PERCELL = 1.0, MXPART = 10^6, WD = 0.5, ITRACK = 3, DCEPS = 1E-5, NPLANE = 0, NPL = 0, NPH = 16, NPMIN = 4, NPMAX = 32, INTERP = 1, NLSINK = 0, NPSINK = 16, DCHMOC = 0.0055	al = 0, DMCOEF = 0	Hclose = 0.0001, Rclose = 0.1
F_HMOC015	10	1	1	HMOC, PERCELL = 1.0, MXPART = 10^6, WD = 0.5, ITRACK = 3, DCEPS = 1E-5, NPLANE = 0, NPL = 0, NPH = 16, NPMIN = 4, NPMAX = 32, INTERP = 1, NLSINK = 0, NPSINK = 16, DCHMOC = 0.0055	al = 0, DMCOEF = 0	Hclose = 0.0001, Rclose = 0.1
F_HMOC016	100	1	1	HMOC, PERCELL = 1.0, MXPART = 10^6, WD = 0.5, ITRACK = 3, DCEPS = 1E-5, NPLANE = 0, NPL = 0, NPH = 16, NPMIN = 4, NPMAX = 32, INTERP = 1, NLSINK = 0, NPSINK = 16, DCHMOC = 0.0055	al = 0, DMCOEF = 0	Hclose = 0.01, Rclose = 1.0
F_HMOC017	100	1	1	HMOC, PERCELL = 1.0, MXPART = 10^6, WD = 0.5, ITRACK = 3, DCEPS = 1E-5, NPLANE = 0, NPL = 0, NPH = 16, NPMIN = 4, NPMAX = 32, INTERP = 1, NLSINK = 0, NPSINK = 16, DCHMOC = 0.0055	al = 0, DMCOEF = 0	Hclose = 0.1, Rclose = 1.0
F_HMOC018	100	1	1	HMOC, PERCELL = 1.0, MXPART = 10^6, WD = 0.5, ITRACK = 3, DCEPS = 1E-5, NPLANE = 0, NPL = 0, NPH = 16, NPMIN = 4, NPMAX = 32, INTERP = 1, NLSINK = 0, NPSINK = 16, DCHMOC = 0.0055	al = 0, DMCOEF = 0	Hclose = 0.001, Rclose = 1.0
F_HMOC019	100	1	1	HMOC, PERCELL = 1.0, MXPART = 10^6, WD = 0.5, ITRACK = 3, DCEPS = 1E-5, NPLANE = 0, NPL = 0, NPH = 16, NPMIN = 4, NPMAX = 32, INTERP = 1, NLSINK = 0, NPSINK = 16, DCHMOC = 0.0055	al = 0, DMCOEF = 0	Hclose = 0.000001, Rclose = 1.0
F_HMOC020	100	1	1	HMOC, PERCELL = 1.0, MXPART = 10^6, WD = 0.5, ITRACK = 3, DCEPS = 1E-5, NPLANE = 0, NPL = 0, NPH = 16, NPMIN = 4, NPMAX = 32, INTERP = 1, NLSINK = 0, NPSINK = 16, DCHMOC = 0.0055	al = 0, DMCOEF = 0	Hclose = 0.1, Rclose = 5.0
F_HMOC021	100	1	1	HMOC, PERCELL = 1.0, MXPART = 10^6, WD = 0.5, ITRACK = 3, DCEPS = 1E-5, NPLANE = 0, NPL = 0, NPH = 16, NPMIN = 4, NPMAX = 32, INTERP = 1, NLSINK = 0, NPSINK = 16, DCHMOC = 0.0055	al = 0, DMCOEF = 0	Hclose = 0.1, Rclose = 10.0
F_HMOC022	100	1	1	HMOC, PERCELL = 1.0, MXPART = 10^6, WD = 0.5, ITRACK = 3, DCEPS = 1E-5, NPLANE = 0, NPL = 0, NPH = 16, NPMIN = 4, NPMAX = 32, INTERP = 1, NLSINK = 0, NPSINK = 16, DCHMOC = 0.0055	al = 0, DMCOEF = 0	Hclose = 0.1, Rclose = 0.01
F_HMOC023	100	1	1	HMOC, PERCELL = 0.75, MXPART = 10^6, WD = 0.5, ITRACK = 3, DCEPS = 1E-5, NPLANE = 0, NPL = 0, NPH = 16, NPMIN = 4, NPMAX = 32, INTERP = 1, NLSINK = 0, NPSINK = 16, DCHMOC = 0.0055	al = 0, DMCOEF = 0	Hclose = 0.0001, Rclose = 0.1
F_HMOC024	100	1	1	HMOC, PERCELL = 0.5, MXPART = 10^6, WD = 0.5, ITRACK = 3, DCEPS = 1E-5, NPLANE = 0, NPL = 0, NPH = 16, NPMIN = 4, NPMAX = 32, INTERP = 1, NLSINK = 0, NPSINK = 16, DCHMOC = 0.0055	al = 0, DMCOEF = 0	Hclose = 0.0001, Rclose = 0.1
F_HMOC025	100	1	1	HMOC, PERCELL = 0.25, MXPART = 10^6, WD = 0.5, ITRACK = 3, DCEPS = 1E-5, NPLANE = 0, NPL = 0, NPH = 16, NPMIN = 4, NPMAX = 32, INTERP = 1, NLSINK = 0, NPSINK = 16, DCHMOC = 0.0055	al = 0, DMCOEF = 0	Hclose = 0.0001, Rclose = 0.1
F_HMOC026	100	1	1	HMOC, PERCELL = 1.0, MXPART = 10^6, WD = 0.5, ITRACK = 3, DCEPS = 1E-5, NPLANE = 0, NPL = 0, NPH = 16, NPMIN = 4, NPMAX = 32, INTERP = 1, NLSINK = 0, NPSINK = 16, DCHMOC = 0.1	al = 0, DMCOEF = 0	Hclose = 0.1, Rclose = 0.01
F_HMOC027	100	1	1	HMOC, PERCELL = 1.0, MXPART = 10^6, WD = 0.5, ITRACK = 3, DCEPS = 1E-5, NPLANE = 0, NPL = 0, NPH = 16, NPMIN = 4, NPMAX = 32, INTERP = 1, NLSINK = 0, NPSINK = 16, DCHMOC = 0.01	al = 0, DMCOEF = 0	Hclose = 0.1, Rclose = 0.01
F_HMOC028	100	1	1	HMOC, PERCELL = 1.0, MXPART = 10^6, WD = 0.5, ITRACK = 3, DCEPS = 1E-5, NPLANE = 0, NPL = 0, NPH = 16, NPMIN = 4, NPMAX = 32, INTERP = 1, NLSINK = 0, NPSINK = 16, DCHMOC = 0.0001	al = 0, DMCOEF = 0	Hclose = 0.1, Rclose = 0.01

Model ID	Discretization			Advection package	Dispersion package	Convergence criteria
	dx	dy	dz			
F_MMOC001	250	1	10	MMOC, PERCELL = 1.0, MXPART = 10^6, WD = 0.5, ITRACK = 3, INTERP = 1, NLSINK = 0, NPSINK = 16	al = 0, DMCOEF = 0	Hclose = 0.0001, Rclose = 0.1
F_MMOC002	100	1	10	MMOC, PERCELL = 1.0, MXPART = 10^6, WD = 0.5, ITRACK = 3, INTERP = 1, NLSINK = 0, NPSINK = 16	al = 0, DMCOEF = 0	Hclose = 0.0001, Rclose = 0.1
F_MMOC003	50	1	10	MMOC, PERCELL = 1.0, MXPART = 10^6, WD = 0.5, ITRACK = 3, INTERP = 1, NLSINK = 0, NPSINK = 16	al = 0, DMCOEF = 0	Hclose = 0.0001, Rclose = 0.1
F_MMOC004	25	1	10	MMOC, PERCELL = 1.0, MXPART = 10^6, WD = 0.5, ITRACK = 3, INTERP = 1, NLSINK = 0, NPSINK = 16	al = 0, DMCOEF = 0	Hclose = 0.0001, Rclose = 0.1
F_MMOC005	10	1	10	MMOC, PERCELL = 1.0, MXPART = 10^6, WD = 0.5, ITRACK = 3, INTERP = 1, NLSINK = 0, NPSINK = 16	al = 0, DMCOEF = 0	Hclose = 0.0001, Rclose = 0.1
F_MMOC006	250	1	5	MMOC, PERCELL = 1.0, MXPART = 10^6, WD = 0.5, ITRACK = 3, INTERP = 1, NLSINK = 0, NPSINK = 16	al = 0, DMCOEF = 0	Hclose = 0.0001, Rclose = 0.1
F_MMOC007	100	1	5	MMOC, PERCELL = 1.0, MXPART = 10^6, WD = 0.5, ITRACK = 3, INTERP = 1, NLSINK = 0, NPSINK = 16	al = 0, DMCOEF = 0	Hclose = 0.0001, Rclose = 0.1
F_MMOC008	50	1	5	MMOC, PERCELL = 1.0, MXPART = 10^6, WD = 0.5, ITRACK = 3, INTERP = 1, NLSINK = 0, NPSINK = 16	al = 0, DMCOEF = 0	Hclose = 0.0001, Rclose = 0.1
F_MMOC009	25	1	5	MMOC, PERCELL = 1.0, MXPART = 10^6, WD = 0.5, ITRACK = 3, INTERP = 1, NLSINK = 0, NPSINK = 16	al = 0, DMCOEF = 0	Hclose = 0.0001, Rclose = 0.1
F_MMOC010	10	1	5	MMOC, PERCELL = 1.0, MXPART = 10^6, WD = 0.5, ITRACK = 3, INTERP = 1, NLSINK = 0, NPSINK = 16	al = 0, DMCOEF = 0	Hclose = 0.0001, Rclose = 0.1
F_MMOC011	250	1	1	MMOC, PERCELL = 1.0, MXPART = 10^6, WD = 0.5, ITRACK = 3, INTERP = 1, NLSINK = 0, NPSINK = 16	al = 0, DMCOEF = 0	Hclose = 0.0001, Rclose = 0.1
F_MMOC012	100	1	1	MMOC, PERCELL = 1.0, MXPART = 10^6, WD = 0.5, ITRACK = 3, INTERP = 1, NLSINK = 0, NPSINK = 16	al = 0, DMCOEF = 0	Hclose = 0.0001, Rclose = 0.1
F_MMOC013	50	1	1	MMOC, PERCELL = 1.0, MXPART = 10^6, WD = 0.5, ITRACK = 3, INTERP = 1, NLSINK = 0, NPSINK = 16	al = 0, DMCOEF = 0	Hclose = 0.0001, Rclose = 0.1
F_MMOC014	25	1	1	MMOC, PERCELL = 1.0, MXPART = 10^6, WD = 0.5, ITRACK = 3, INTERP = 1, NLSINK = 0, NPSINK = 16	al = 0, DMCOEF = 0	Hclose = 0.0001, Rclose = 0.1
F_MMOC015	10	1	1	MMOC, PERCELL = 1.0, MXPART = 10^6, WD = 0.5, ITRACK = 3, INTERP = 1, NLSINK = 0, NPSINK = 16	al = 0, DMCOEF = 0	Hclose = 0.0001, Rclose = 0.1
F_MMOC016	100	1	1	MMOC, PERCELL = 1.0, MXPART = 10^6, WD = 0.5, ITRACK = 3, INTERP = 1, NLSINK = 0, NPSINK = 16	al = 0, DMCOEF = 0	Hclose = 0.01, Rclose = 1.0
F_MMOC017	100	1	1	MMOC, PERCELL = 1.0, MXPART = 10^6, WD = 0.5, ITRACK = 3, INTERP = 1, NLSINK = 0, NPSINK = 16	al = 0, DMCOEF = 0	Hclose = 0.1, Rclose = 1.0
F_MMOC018	100	1	1	MMOC, PERCELL = 1.0, MXPART = 10^6, WD = 0.5, ITRACK = 3, INTERP = 1, NLSINK = 0, NPSINK = 16	al = 0, DMCOEF = 0	Hclose = 0.001, Rclose = 1.0
F_MMOC019	100	1	1	MMOC, PERCELL = 1.0, MXPART = 10^6, WD = 0.5, ITRACK = 3, INTERP = 1, NLSINK = 0, NPSINK = 16	al = 0, DMCOEF = 0	Hclose = 0.000001, Rclose = 1.0
F_MMOC020	100	1	1	MMOC, PERCELL = 1.0, MXPART = 10^6, WD = 0.5, ITRACK = 3, INTERP = 1, NLSINK = 0, NPSINK = 16	al = 0, DMCOEF = 0	Hclose = 0.1, Rclose = 5.0
F_MMOC021	100	1	1	MMOC, PERCELL = 1.0, MXPART = 10^6, WD = 0.5, ITRACK = 3, INTERP = 1, NLSINK = 0, NPSINK = 16	al = 0, DMCOEF = 0	Hclose = 0.1, Rclose = 10.0
F_MMOC022	100	1	1	MMOC, PERCELL = 1.0, MXPART = 10^6, WD = 0.5, ITRACK = 3, INTERP = 1, NLSINK = 0, NPSINK = 16	al = 0, DMCOEF = 0	Hclose = 0.1, Rclose = 0.01
F_MMOC023	100	1	1	MMOC, PERCELL = 0.75, MXPART = 10^6, WD = 0.5, ITRACK = 3, INTERP = 1, NLSINK = 0, NPSINK = 16	al = 0, DMCOEF = 0	Hclose = 0.0001, Rclose = 0.1
F_MMOC024	100	1	1	MMOC, PERCELL = 0.5, MXPART = 10^6, WD = 0.5, ITRACK = 3, INTERP = 1, NLSINK = 0, NPSINK = 16	al = 0, DMCOEF = 0	Hclose = 0.0001, Rclose = 0.1
F_MMOC025	100	1	1	MMOC, PERCELL = 0.25, MXPART = 10^6, WD = 0.5, ITRACK = 3, INTERP = 1, NLSINK = 0, NPSINK = 16	al = 0, DMCOEF = 0	Hclose = 0.0001, Rclose = 0.1

Henry case (simulation time: 400 min):

Model ID	Discretization			Advection package	Dispersion package
	dx	dy	dz		
H_001	0.05	1	0.05	TVD, PERCELL = 1.0	al = 0, DMCOEF = 1.63
H_002	0.05	1	0.05	MOC, PERCELL = 1.0, MXPART = 10^6, WD = 0.5, ITRACK = 3, DCEPS = 1E-5, NPLANE = 0, NPL = 0, NPH = 16, NPMIN = 4, NPMAX = 32	al = 0, DMCOEF = 1.63
H_003	0.05	1	0.05	FD , PERCELL = 1.0, NADVFD = 0	al = 0, DMCOEF = 1.63
H_004	0.05	1	0.05	HMOC, PERCELL = 1.0, MXPART = 10^6, WD = 0.5, ITRACK = 3, DCEPS = 1E-5, NPLANE = 0, NPL = 0, NPH = 16, NPMIN = 4, NPMAX = 32, INTERP = 1, NLSINK = 0, NPSINK = 16, DCHMOC = 0.0055	al = 0, DMCOEF = 1.63
H_005	0.05	1	0.05	MMOC, PERCELL = 1.0, MXPART = 10^6, WD = 0.5, ITRACK = 3, INTERP = 1, NLSINK = 0, NPSINK = 16	al = 0, DMCOEF = 1.63
H_006	0.01	1	0.01	TVD, PERCELL = 1.0	al = 0, DMCOEF = 1.63
H_007	0.01	1	0.01	MOC, PERCELL = 1.0, MXPART = 10^6, WD = 0.5, ITRACK = 3, DCEPS = 1E-5, NPLANE = 0, NPL = 0, NPH = 16, NPMIN = 4, NPMAX = 32	al = 0, DMCOEF = 1.63
H_008	0.01	1	0.01	FD , PERCELL = 1.0, NADVFD = 0	al = 0, DMCOEF = 1.63
H_009	0.01	1	0.01	HMOC, PERCELL = 1.0, MXPART = 10^6, WD = 0.5, ITRACK = 3, DCEPS = 1E-5, NPLANE = 0, NPL = 0, NPH = 16, NPMIN = 4, NPMAX = 32, INTERP = 1, NLSINK = 0, NPSINK = 16, DCHMOC = 0.0055	al = 0, DMCOEF = 1.63
H_010	0.01	1	0.01	MMOC, PERCELL = 1.0, MXPART = 10^6, WD = 0.5, ITRACK = 3, INTERP = 1, NLSINK = 0, NPSINK = 16	al = 0, DMCOEF = 1.63

Saltwater pocket (simulation time: 3600 min):

Model ID	Discretization			Advection package	Dispersion package
	dx	dy	dz		
S_001	1	1	1	TVD, PERCELL = 1.0	al = 0.001, DMCOEF = 8.64E-5
S_002	1	1	1	MOC, PERCELL = 1.0, MXPART = 10^8, WD = 0.5, ITRACK = 3, DCEPS = 1E-5, NPLANE = 0, NPL = 0, NPH = 16, NPMIN = 4, NPMAX = 32	al = 0.001, DMCOEF = 8.64E-5
S_003	1	1	1	FD , PERCELL = 1.0, NADVFD = 0	al = 0.001, DMCOEF = 8.64E-5
S_004	1	1	1	HMOC, PERCELL = 1.0, MXPART = 10^6, WD = 0.5, ITRACK = 3, DCEPS = 1E-5, NPLANE = 0, NPL = 0, NPH = 16, NPMIN = 4, NPMAX = 32, INTERP = 1, NLSINK = 0, NPSINK = 16, DCHMOC = 0.0055	al = 0.001, DMCOEF = 8.64E-5
S_005	1	1	1	MMOC, PERCELL = 1.0, MXPART = 10^6, WD = 0.5, ITRACK = 3, INTERP = 1, NLSINK = 0, NPSINK = 16	al = 0.001, DMCOEF = 8.64E-5
S_006	0.5	1	0.5	TVD, PERCELL = 1.0	al = 0.001, DMCOEF = 8.64E-5
S_007	0.5	1	0.5	MOC, PERCELL = 1.0, MXPART = 10^8, WD = 0.5, ITRACK = 3, DCEPS = 1E-5, NPLANE = 0, NPL = 0, NPH = 16, NPMIN = 4, NPMAX = 32	al = 0.001, DMCOEF = 8.64E-5
S_008	0.5	1	0.5	FD , PERCELL = 1.0, NADVFD = 0	al = 0.001, DMCOEF = 8.64E-5
S_009	0.5	1	0.5	HMOC, PERCELL = 1.0, MXPART = 10^6, WD = 0.5, ITRACK = 3, DCEPS = 1E-5, NPLANE = 0, NPL = 0, NPH = 16, NPMIN = 4, NPMAX = 32, INTERP = 1, NLSINK = 0, NPSINK = 16, DCHMOC = 0.0055	al = 0.001, DMCOEF = 8.64E-5
S_010	0.5	1	0.5	MMOC, PERCELL = 1.0, MXPART = 10^6, WD = 0.5, ITRACK = 3, INTERP = 1, NLSINK = 0, NPSINK = 16	al = 0.001, DMCOEF = 8.64E-5
S_011	0.25	1	0.25	TVD, PERCELL = 1.0	al = 0.001, DMCOEF = 8.64E-5
S_012	0.25	1	0.25	MOC, PERCELL = 1.0, MXPART = 10^8, WD = 0.5, ITRACK = 3, DCEPS = 1E-5, NPLANE = 0, NPL = 0, NPH = 16, NPMIN = 4, NPMAX = 32	al = 0.001, DMCOEF = 8.64E-5
S_013	0.25	1	0.25	FD , PERCELL = 1.0, NADVFD = 0	al = 0.001, DMCOEF = 8.64E-5
S_014	0.25	1	0.25	HMOC, PERCELL = 1.0, MXPART = 10^6, WD = 0.5, ITRACK = 3, DCEPS = 1E-5, NPLANE = 0, NPL = 0, NPH = 16, NPMIN = 4, NPMAX = 32, INTERP = 1, NLSINK = 0, NPSINK = 16, DCHMOC = 0.0055	al = 0.001, DMCOEF = 8.64E-5
S_015	0.25	1	0.25	MMOC, PERCELL = 1.0, MXPART = 10^6, WD = 0.5, ITRACK = 3, INTERP = 1, NLSINK = 0, NPSINK = 16	al = 0.001, DMCOEF = 8.64E-5
S_016	0.125	1	0.125	TVD, PERCELL = 1.0	al = 0.001, DMCOEF = 8.64E-5
S_017	0.125	1	0.125	MOC, PERCELL = 1.0, MXPART = 10^8, WD = 0.5, ITRACK = 3, DCEPS = 1E-5, NPLANE = 0, NPL = 0, NPH = 16, NPMIN = 4, NPMAX = 32	al = 0.001, DMCOEF = 8.64E-5
S_018	0.125	1	0.125	FD , PERCELL = 1.0, NADVFD = 0	al = 0.001, DMCOEF = 8.64E-5
S_019	0.125	1	0.125	HMOC, PERCELL = 1.0, MXPART = 10^6, WD = 0.5, ITRACK = 3, DCEPS = 1E-5, NPLANE = 0, NPL = 0, NPH = 16, NPMIN = 4, NPMAX = 32, INTERP = 1, NLSINK = 0, NPSINK = 16, DCHMOC = 0.0055	al = 0.001, DMCOEF = 8.64E-5
S_020	0.125	1	0.125	MMOC, PERCELL = 1.0, MXPART = 10^6, WD = 0.5, ITRACK = 3, INTERP = 1, NLSINK = 0, NPSINK = 16	al = 0.001, DMCOEF = 8.64E-5
S_021	0.125	1	0.125	TVD, PERCELL = 1.0	al = 0.0001, DMCOEF = 8.64E-5
S_022	0.125	1	0.125	MOC, PERCELL = 1.0, MXPART = 10^8, WD = 0.5, ITRACK = 3, DCEPS = 1E-5, NPLANE = 0, NPL = 0, NPH = 16, NPMIN = 4, NPMAX = 32	al = 0.0001, DMCOEF = 8.64E-5
S_023	0.125	1	0.125	FD , PERCELL = 1.0, NADVFD = 0	al = 0.0001, DMCOEF = 8.64E-5
S_024	0.125	1	0.125	HMOC, PERCELL = 1.0, MXPART = 10^6, WD = 0.5, ITRACK = 3, DCEPS = 1E-5, NPLANE = 0, NPL = 0, NPH = 16, NPMIN = 4, NPMAX = 32, INTERP = 1, NLSINK = 0, NPSINK = 16, DCHMOC = 0.0055	al = 0.0001, DMCOEF = 8.64E-5
S_025	0.125	1	0.125	MMOC, PERCELL = 1.0, MXPART = 10^6, WD = 0.5, ITRACK = 3, INTERP = 1, NLSINK = 0, NPSINK = 16	al = 0.0001, DMCOEF = 8.64E-5
S_026	0.125	1	0.125	TVD, PERCELL = 1.0	al = 0.01, DMCOEF = 8.64E-5
S_027	0.125	1	0.125	MOC, PERCELL = 1.0, MXPART = 10^8, WD = 0.5, ITRACK = 3, DCEPS = 1E-5, NPLANE = 0, NPL = 0, NPH = 16, NPMIN = 4, NPMAX = 32	al = 0.01, DMCOEF = 8.64E-5
S_028	0.125	1	0.125	FD , PERCELL = 1.0, NADVFD = 0	al = 0.01, DMCOEF = 8.64E-5
S_029	0.125	1	0.125	HMOC, PERCELL = 1.0, MXPART = 10^6, WD = 0.5, ITRACK = 3, DCEPS = 1E-5, NPLANE = 0, NPL = 0, NPH = 16, NPMIN = 4, NPMAX = 32, INTERP = 1, NLSINK = 0, NPSINK = 16, DCHMOC = 0.0055	al = 0.01, DMCOEF = 8.64E-5
S_030	0.125	1	0.125	MMOC, PERCELL = 1.0, MXPART = 10^6, WD = 0.5, ITRACK = 3, INTERP = 1, NLSINK = 0, NPSINK = 16	al = 0.01, DMCOEF = 8.64E-5
S_031	0.125	1	0.125	TVD, PERCELL = 1.0	al = 0.1, DMCOEF = 8.64E-5
S_032	0.125	1	0.125	MOC, PERCELL = 1.0, MXPART = 10^8, WD = 0.5, ITRACK = 3, DCEPS = 1E-5, NPLANE = 0, NPL = 0, NPH = 16, NPMIN = 4, NPMAX = 32	al = 0.1, DMCOEF = 8.64E-5
S_033	0.125	1	0.125	FD , PERCELL = 1.0, NADVFD = 0	al = 0.1, DMCOEF = 8.64E-5
S_034	0.125	1	0.125	HMOC, PERCELL = 1.0, MXPART = 10^6, WD = 0.5, ITRACK = 3, DCEPS = 1E-5, NPLANE = 0, NPL = 0, NPH = 16, NPMIN = 4, NPMAX = 32, INTERP = 1, NLSINK = 0, NPSINK = 16, DCHMOC = 0.0055	al = 0.1, DMCOEF = 8.64E-5
S_035	0.125	1	0.125	MMOC, PERCELL = 1.0, MXPART = 10^6, WD = 0.5, ITRACK = 3, INTERP = 1, NLSINK = 0, NPSINK = 16	al = 0.1, DMCOEF = 8.64E-5
S_036	0.125	1	0.125	FD , PERCELL = 1.0, NADVFD = 2	al = 0.001, DMCOEF = 8.64E-5
S_037	0.125	1	0.125	MOC, PERCELL = 1.0, MXPART = 10^8, WD = 0.5, ITRACK = 3, DCEPS = 1E-5, NPLANE = 0, NPL = 16, NPH = 16, NPMIN = 16, NPMAX = 32	al = 0.001, DMCOEF = 8.64E-5
S_038	0.125	1	0.125	MOC, PERCELL = 1.0, MXPART = 10^8, WD = 0.5, ITRACK = 3, DCEPS = 1E-5, NPLANE = 0, NPL = 16, NPH = 16, NPMIN = 16, NPMAX = 32	al = 0.01, DMCOEF = 8.64E-5
S_039	0.125	1	0.125	MOC, PERCELL = 1.0, MXPART = 10^8, WD = 0.5, ITRACK = 2, DCEPS = 1E-5, NPLANE = 0, NPL = 0, NPH = 64, NPMIN = 32, NPMAX = 128	al = 0.1, DMCOEF = 8.64E-5
S_040	0.125	1	0.125	MOC, PERCELL = 1.0, MXPART = 10^8, WD = 0.5, ITRACK = 2, DCEPS = 1E-5, NPLANE = 0, NPL = 0, NPH = 64, NPMIN = 32, NPMAX = 128	al = 0.01, DMCOEF = 8.64E-5

DOW case study (simulation time: 50 years):

Model ID	Discretization			Advection package	Dispersion package
	dx	dy	dz		
D_001	25	25	1	TVD, PERCELL = 1.0	al = 0.1, DMCOEF = 0.0001
D_002	25	25	2	TVD, PERCELL = 1.0	al = 0.1, DMCOEF = 0.0001
D_003	25	25	5	TVD, PERCELL = 1.0	al = 0.1, DMCOEF = 0.0001
D_004	25	25	10	TVD, PERCELL = 1.0	al = 0.1, DMCOEF = 0.0001
D_005	50	50	2	TVD, PERCELL = 1.0	al = 0.1, DMCOEF = 0.0001
D_006	100	100	2	TVD, PERCELL = 1.0	al = 0.1, DMCOEF = 0.0001
D_007	25	25	1,2,5	TVD, PERCELL = 1.0	al = 0.1, DMCOEF = 0.0001
D_008	25	25	1,2,5	FD , PERCELL = 1.0, NADVFD = 0	al = 0.1, DMCOEF = 0.0001
D_009	25	25	1,2,5	MOC, PERCELL = 1.0, MXPART = 10^8, WD = 0.5, ITRACK = 3, DCEPS = 1E-5, NPLANE = 0, NPL = 0, NPH = 16, NPMIN = 4, NPMAX = 32	al = 0.1, DMCOEF = 0.0001
D_010	25	25	1,2,5	TVD, PERCELL = 1.0	al = 1.0, DMCOEF = 0.0001
D_011	25	25	1,2,5	FD , PERCELL = 1.0, NADVFD = 0	al = 1.0, DMCOEF = 0.0001
D_012	25	25	1,2,5	MOC, PERCELL = 1.0, MXPART = 10^8, WD = 0.5, ITRACK = 3, DCEPS = 1E-5, NPLANE = 0, NPL = 0, NPH = 16, NPMIN = 4, NPMAX = 32	al = 1.0, DMCOEF = 0.0001
D_013	25	25	1,2,5	TVD, PERCELL = 1.0	al = 10.0, DMCOEF = 0.0001
D_014	25	25	1,2,5	FD , PERCELL = 1.0, NADVFD = 0	al = 10.0, DMCOEF = 0.0001
D_015	25	25	1,2,5	MOC, PERCELL = 1.0, MXPART = 10^8, WD = 0.5, ITRACK = 3, DCEPS = 1E-5, NPLANE = 0, NPL = 0, NPH = 16, NPMIN = 4, NPMAX = 32	al = 10.0, DMCOEF = 0.0001
D_016	25	25	1,2,5	FD , PERCELL = 1.0, NADVFD = 2	al = 0.1, DMCOEF = 0.0001
D_017	25	25	1,2,5	TVD, PERCELL = 1.0 - Daily time step (forced Dt0 = 1)	al = 0.1, DMCOEF = 0.0001
D_018	25	25	1,2,5	MOC, PERCELL = 0.1, MXPART = 10^8, WD = 0.5, ITRACK = 3, DCEPS = 1E-5, NPLANE = 0, NPL = 0, NPH = 16, NPMIN = 4, NPMAX = 32	al = 0.1, DMCOEF = 0.0001
D_019	25	25	1,2,5	MOC, PERCELL = 1.0, MXPART = 10^8, WD = 0.5, ITRACK = 2, DCEPS = 1E-5, NPLANE = 0, NPL = 0, NPH = 16, NPMIN = 4, NPMAX = 32	al = 0.1, DMCOEF = 0.0001
D_020	25	25	1,2,5	MOC, PERCELL = 1.0, MXPART = 10^8, WD = 0.5, ITRACK = 2, DCEPS = 1E-5, NPLANE = 0, NPL = 16, NPH = 16, NPMIN = 8, NPMAX = 32	al = 0.1, DMCOEF = 0.0001
D_021	25	25	1,2,5	TVD, PERCELL = 0.75	al = 0.1, DMCOEF = 0.0001